TECHNICAL DIVISION
SAVANNAH RIVER LABORATORY

Key Words: Z Area
Hydrology
Geology
Saltstone

DPST-86-426

cc: J. L. Steele, SRP, 703-A
J. D. Heffner, 703-A
J. K. Okeson, SRL, 773-A
W. R. Stevens, III, 773-A
J. A. Stone, 773-43A
M. W. Grant, 773-43A
H. F. Sturm, 773-43A
E. L. Wilhite, 773-43A
C. A. Langton, 773-43A
B. G. Kitchen, 773-41A
V. Price, 773-42A
H. W. Bledsoe, 773-42A
D. E. Stephenson, 773-42A
B. B. Looney, 773-42A
SRL Records, (4), 773-A

May 8, 1986

TO: E. L. Albenesius, 773-A

FROM: James R. Cook, 773-43A JRC

SRL FILE COPY

Z AREA SITE ASSESSMENT

Introduction and Summary

Intera Technologies, Inc. has performed a detailed site assessment of Z Area under contract AX 0682022. This work involved compiling and evaluating the available geologic information, performing hydrologic tests at the SDS wells, and three-dimensional modeling of the site. The final report of this work is attached. The following is taken from the Executive Summary of the report.

This report presents the results of a quantitative evaluation of the effects on ground water and surface water quality from the near-surface disposal of decontaminated nitrate salts which will result from the operation of the Defense Waste Processing Facility. The salt solution will be mixed with Portland cement and flyash. The resulting mixture will be solidified into saltstone monoliths and disposed using either above-ground or below ground disposal concepts. In either case the waste material will be placed in the unsaturated zone at least 3 meters above the historical maximum elevation of the water table.[1] The proposed disposal site is referred to as Z Area, which is located about 2 km. northeast of H Area.

Possible ground water contamination could result due to nitrate diffusion from the relatively impermeable saltstone to the surrounding backfill and natural materials, or by direct leaching of the soluble nitrates by infiltrating precipitation. The disposal designs focus on minimization of infiltration which comes in contact with the saltstone. Ground water originating as recharge at Z Area discharges primarily to McQueens Branch and Upper Three Runs Creek, which in turn drain to the Savannah River.

Following a complete review of the existing field and laboratory data, a number of field tests (single well slug tests) were conducted in piezometers installed at Z Area to obtain site-specific hydraulic conductivity data. The local geology and hydrology were interpreted and reconciled to the results of previous regional investigations. A three dimensional conceptual model of the Z Area hydrogeologic system was then developed.

The site was mathematically modeled using a three-dimensional model of ground water flow and solute transport. The model employed finite difference techniques to solve for the steady-state flow field and the method of characteristics (point tracking) to solve for solute transport.

The results of the study are summarized below. They are presented in the context of whether of not the disposal system will result in the ground water quality at the Z Area site boundary and the water in the creeks meeting water quality standards. Concentrations are calculated relative to a source-term concentration of 1.0.

Ground Water Quality

The modeling study included a base case with 30% of rainfall infiltrating throughout the modeled area, as well as infiltration rates at Z Area of 0.3%, 3% and 90% of precipitation (with 30% throughout the remainder of the modeled area). The variation of the infiltration rate was performed in order to account for the alternative designs under consideration. The evaluation focuses on two general design types for the disposal site: (i) a clay cap over the entire Z Area (in both above and below ground designs) diverting precipitation directly to surface runoff and resulting in a low percentage of infiltration, and (ii) a gravel cover and permeable backfill (below ground design) with individual clay caps over each monolith and gravel drains beside each monolith. The dry wells collect the diverted rainwater and recharge the underlying ground water with uncontaminated infiltration. This recharge would dilute the small remaining amount of contaminated infiltration resulting from either direct (advective flow through the monolith) or indirect (diffusive nitrate flux) contact of the infiltration with the saltstone.

In no instance does the nitrate concentration in any of the underlying formations beneath Z Area exceed 50% of the source concentration at the Z Area boundary over periods up to 200 years after disposal.

Surface Water Quality

Surface water nitrate concentrations in McQueens Branch will not likely exceed a relative concentration of 0.1, even after 200 years with a constant concentration source term. Nitrate relative concentrations of 0.01 or less are calculated for Upper Three Runs Creek. Contaminated ground water originating in Z Area will not discharge directly to Upper Three Runs Creek with the modeled 200 year period under any of the modeled scenarios.

If the performance criterion is to meet water quality standards of 44 mg/L nitrate at the site boundary, it is concluded that the concentration of nitrate in infiltration recharge at Z Area (i.e., the sum of contaminated and uncontaminated infiltration) should not exceed 90 mg/L. Thus, if the contaminant concentrations of the recharge at Z Area can be maintained below 90 mg/L, Z Area is suitable for saltstone disposal.

Related Work

Z Area was selected for saltstone disposal from among six candidate sites in 1979.[2] Two dimensional modeling of Z Area hydrology was done previously be Woodward-Clyde Consultants. Their report has been analyzed by Looney.[3] Looney estimates the ratio of nitrate concentration in the ground water at the Z Area boundary versus the source concentration from saltstone to be 0.5, in good agreement with Intera.

Hydrologic data used in Intera's work as well as additional data from Z Area are documented in reference 4. Unsaturated flow properties of Z Area soil were determined by Dr. V. Quisenberry of Clemson University and are documented in reference 5.

References

1. J. R. Cook, Estimation of High Water Table Levels at the Saltstone Disposal Site (Z Area), DPST-83-607.

2. J. R. Cook, Site Selection for Saltstone Disposal, DPST-84-502.

3. B. B. Looney, Assessment of Current Groundwater Flow and Contaminant Transport Modeling of the Proposed Z Area Saltstone Disposal Site, DPST-85-794.

4. J. R. Cook, Hydrogeologic Data form Z Area, DPST-86-320.

5. J. R. Cook, C. A. Langton, E. L. Wilhite, Hydraulic Properties of Saltstone and Z Area Soil, DPST-86-268.

Z-AREA

SITE ASSESSMENT

to

INTERA

Z-AREA
SITE ASSESSMENT

to

E. I. du Pont de Nemours & Company
Building 773-A
Savannah Research Labs.
Aiken, SC 29808

from

INTERA Technologies, Inc.
6850 Austin Center Blvd., Suite 300
Austin, Texas 78731

FINAL REPORT
MARCH 1986

H01201R008

EXECUTIVE SUMMARY

This report presents the results of a quantitative evaluation of the effects on ground water and surface water quality from the shallow disposal of decontaminated nitrate salts which result from the processing of high level radioactive wastes at the Savannah River Plant. The salt solutions will be mixed with Portland cement and flyash. The resulting mixture will be solidified into 'saltstone' monoliths and disposed using either above-ground or below-ground disposal design concepts. In either case the waste material will be disposed in the unsaturated zone of the Barnwell Formation at least 3 meters above the historical maximum elevation of the water table. The proposed disposal site is referred to as Z-Area, a local topographic high about 2 km northeast of the Savannah River Plant Separation Areas.

Possible ground water contamination could result due to nitrate diffusion from the relatively impermeable saltstone to the surrounding backfill and natural materials, or by direct leaching of the soluble nitrates by infiltrating precipitation. The disposal designs focus on minimization of infiltration which comes into contact with the saltstone. Ground water originating as recharge at Z-Area discharges primarily to McQueen Creek and Upper Three Runs Creek, which in turn drains to the Savannah River.

Following a complete review of the existing field and laboratory data a number of field tests (single well slug tests) were conducted in wells installed at Z-Area for the purpose of obtaining site-specific hydraulic conductivity data. The local geology and hydrogeology were interpreted and reconciled to the results of previous regional investigations. A three dimensional conceptualization of the Z-Area hydrogeologic system was developed using a representative hydrostratigraphy as indicated by the geologic and hydrogeologic data.

The site was modeled using a three-dimensional numerical model of ground water flow and solute transport. The model employed finite difference techniques to solve for the steady-state flow field and the method of characteristics ('point tracking') to solve for solute transport.

The results of the study are summarized below. They are presented in the context of whether or not the disposal system will result in the ground water quality at the Z-Area site boundary and the water in the creeks meeting water quality standards (and recalling that a final design has not been selected and that concentrations are calculated relative to a source-term concentration of 1.0).

- Ground Water Quality

The modeling study included a base case with 30% of rainfall infiltrating throughout the modeled area, including Z-Area, as well as infiltration rates at Z-Area of 0.3%, 3% and 90% of infiltration (with 30% throughout the remainder of the model). The variations of the infiltration rate was performed in order to account for the alternative designs currently under consideration. In actual fact, the evaluation focuses on two general design types for the disposal site: (i) a clay cap over the entire area (in both above-ground and below-ground designs) diverting precipitation directly to surface runoff and resulting in a low percentage of rainfall infiltrating, and (ii) a gravel cover and permeable backfill (below-ground design) with individual clay caps over each monolith and gravel drains (dry wells) beside each monolith. The dry wells collect the diverted infiltration and recharge uncontaminated infiltration to the underlying ground water. The dry-well recharge would serve to dilute the small remaining amount of contaminated recharge resulting from direct (advective flow through the monolith) or indirect (diffusive nitrate flux) contact of the infiltration with the saltstone.

In no instance does the nitrate concentration in any of the underlying formations beneath Z-Area exceed 50% of the source concentration at the Z-Area boundary over periods up to 200 years after disposal.

- Surface Water Quality

Surface water nitrate concentrations in McQueen Creek will not likely exceed a relative concentration of 0.1, even after 200 years with a con-

stant concentration source term. Nitrate relative concentrations of 0.01 or less are calculated for Upper Three Runs Creek, to which McQueen Creek is a tributary. Contaminated ground water originating in Z-Area will not discharge directly to Upper Three Runs Creek within the modeled 200 year period under any of the modeled scenarios.

If the performance criterion is to meet water quality standards of 45 mg/L nitrate at the site boundary, it is concluded that the concentration of nitrates in infiltration recharge at Z-Area (i.e., the sum of contaminated and uncontaminated infiltration) should not exceed 90 mg/L. Thus, if the contaminant concentrations of the recharge at Z-Area can be maintained below 90 mg/L, Z-Area is suitable for saltstone disposal.

TABLE OF CONTENTS

TABLE OF CONTENTS (continued)

TABLE OF CONTENTS FOR APPENDICES

TABLE OF CONTENTS FOR APPENDICES
(continued)

LIST OF FIGURES

LIST OF FIGURES (continued)

LIST OF FIGURES (continued)

LIST OF FIGURES FOR APPENDICES

LIST OF TABLES

LIST OF TABLES FOR APPENDICES

1.0 INTRODUCTION

The Savannah River Plant (SRP), operated by E.I. du Pont de Nemours & Company, is developing a system for disposal, in the unsaturated zone, of the by product of high level radioactive waste processing. The system consists of incorporating decontaminated waste salt solution (comprising primarily nitrate and nitrite salts) into a cement and flyash mixture termed saltstone. Du Pont has proposed placing the saltstone, as solid monoliths, in an area of SRP referred to as Z-Area, which is situated about 2 km northeast of the SRP Separation Areas (Figure 1-1). The saltstone monoliths will be placed in either above ground storage facilities, bounded by cement liners and earthworks, or in excavated trenches below the present ground surface. The proposed disposal options are discussed in more detail in Section 2.1.

1.1 Purpose and Scope

The purpose of this report is to evaluate the potential impact of the proposed saltstone disposal on the ground water and surface water quality at Z-Area and vicinity, specifically with respect to ground water quality at the boundary of Z-Area and surface water quality in Upper Three Runs Creek and its tributary McQueen Creek. Upper Three Runs Creek drains to the Savannah River, some 15 km to the southwest of Z-Area (Figure 1-1). The objectives were accomplished by employing a three-dimensional mathematical model of ground water flow and solute transport. The modeling study was initiated after (i) performance and interpretation of single well tests on the existing Z-Area wells and piezometers for the purpose of obtaining hydraulic conductivity data specific to Z-Area, and (ii) interpretation of the hydrogeologic system within which Z-Area is situated, including assignment of hydrostratigraphic units, development of a three dimensional conceptualization of the ground water flow patterns, and selection of appropriate boundaries to be used in the modeling study.

This report presents a complete evaluation of Z-Area as a disposal site, commencing with a review of the regional geology and an interpretation of the local geology in the regional context. The site specific geologic and hydrologic data are evaluated as to their internal consistency (e.g., are the fluid logs consistent with the laboratory sieve analyses, and are these in turn consistent with the field tests for hydraulic conductivity) as well as to their external consistency (e.g., are the local geologic and hydrostratigraphic interpretations consistent with the regional picture and with the interpretations of previous investigators).

Once the site specific data are reconciled with local and regional interpretations, the report proceeds to develop the rationale for the model conceptualization and to present the specifics of the model selection criteria and of the model implementation. Separate analyses are presented for three-dimensional ground water flow and solute transport, although in the model itself they are fully coupled. The model solves the flow equation using finite difference techniques and uses either the finite difference method or the method-of-characteristics (point tracking) for solute transport.

The solute transport characteristics of the site are evaluated by using 'relative' concentrations, i.e., the potential 'input' or 'source' concentration to the ground water system resulting from saltstone leaching is considered to have a concentration of 1.0 (or 100%). This approach was used because the actual concentration depends on the final design of the disposal system. The final design is as yet unselected from the general design types discussed in Section 2.1. Alternative designs were evaluated by varying the recharge rate, considered to be passing through the saltstone disposal area (the recharge rate is directly related to the final design selected).

The report concludes with an assessment of the suitability of Z-Area as a disposal site.

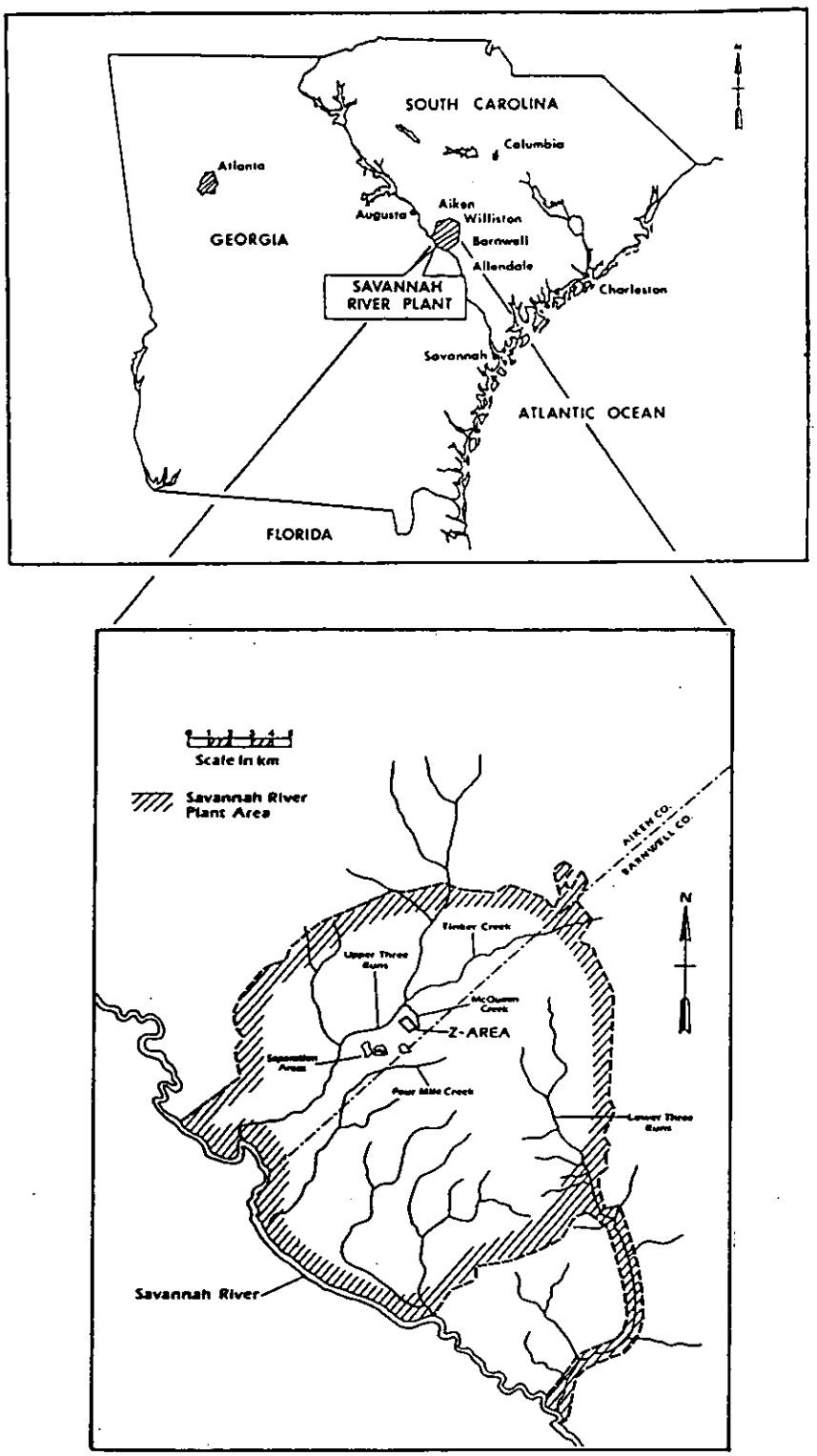

Figure 1-1: Location Map

2.0 SITE DESCRIPTION

Z-Area is located on a local topographic high bounded by McQueen Creek in the northeast and Upper Three Runs Creek in the northwest (Figure 1-1). McQueen Creek is a tributary of Upper Three Runs Creek. Upper Three Runs Creek drains to the Savannah River. The local relief is about 50 m. Branches of McQueen Creek and Upper Three Runs Creek are incised into the topographic high on the southwest and southeast of Z-Area; to the extent that the headwaters of the branches nearly meet about 1 km south of Z-Area.

2.1 Saltstone Disposal

The saltstone disposal concept has been under consideration for several years by du Pont. Recent studies by INTERA on behalf of du Pont have quantitatively evaluated the SRP 1/10 scale lysimeter experiment (INTERA, Aug. 1985); quantified the relative importance of nitrate leaching by advective ground water flow through the unsaturated saltstone and diffusion of nitrates from the saltstone to the backfill (INTERA, Aug. 1985); and evaluated flow and transport by modeling the Tank 24 lysimeter data (INTERA, Jan. 1986).

There are several potential designs for the saltstone disposal system which are currently under consideration. These designs include: (i) above ground disposal in concrete-lined facilities with a clay cap and overburden recasting (Figure 2-1); (ii) below ground disposal with either (a) a complete clay cover and diversion of Z-Area rainfall to surface water discharge (Figure 2-2a), or (b) local clay covers over each monolith with collection of virtually all direct precipitation and recharge to the ground water system beneath Z-Area using gravel drains (dry wells) (Figure 2-2b).

The saltstone monoliths comprise a mixture of cement, flyash and waste nitrate salts. The various designs result in different monolith geometry and sizes, however in general the monoliths are considered to be

of the order of 25 to 50 meters wide, 100 to 200 meters in length, and 5 to 10 meters in thickness. The saltstone has a relatively low saturated hydraulic conductivity of 2.5×10^{-11} m/s and a porosity of about 46% (INTERA, Aug. 1985, and Quisenberry, 1985). Although the hydraulic conductivity of the saltstone is very low it is expected that the nitrate salts, which are highly soluble, will release nitrate to the ground water system. The nitrate release mechanisms include direct leaching of the saltstone by infiltrating precipitation as well as diffusion of nitrate from the low permeability saltstone, through any shotcrete or concrete lining, to the backfill or natural materials surrounding the saltstone. Previous studies by INTERA (op. cit.) have evaluated these mechanisms in detail and the results have been used in designing possible disposal systems such as those shown in Figures 2-1 and 2-2.

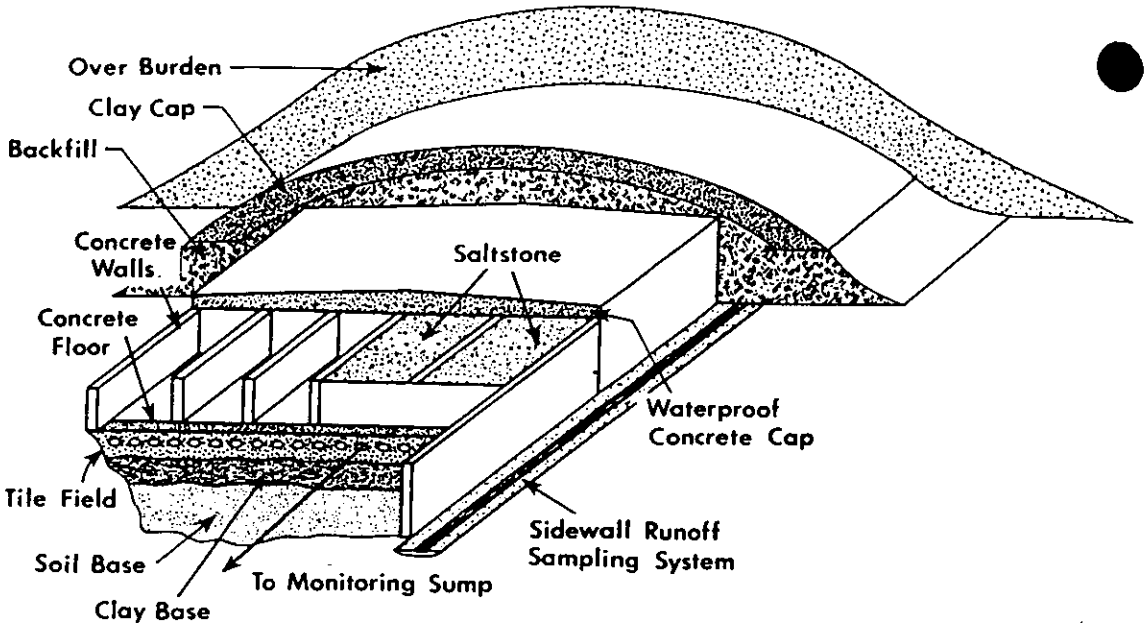

Scale(m)-Approx.

0 25 50

Bottom of monolith approximately 3m below natural ground surface

Each monolith = saltstone production of approximately one year

Figure 2-1 Saltstone Above Ground Disposal Design After SRP

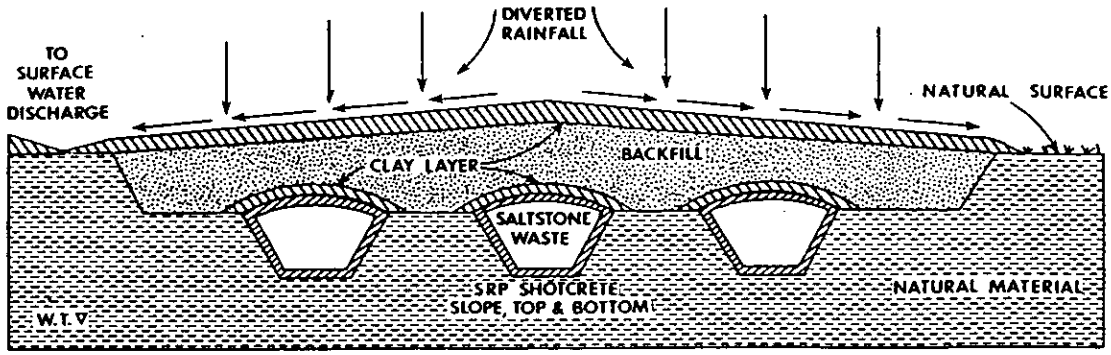

a) With overall claycap (cross section)

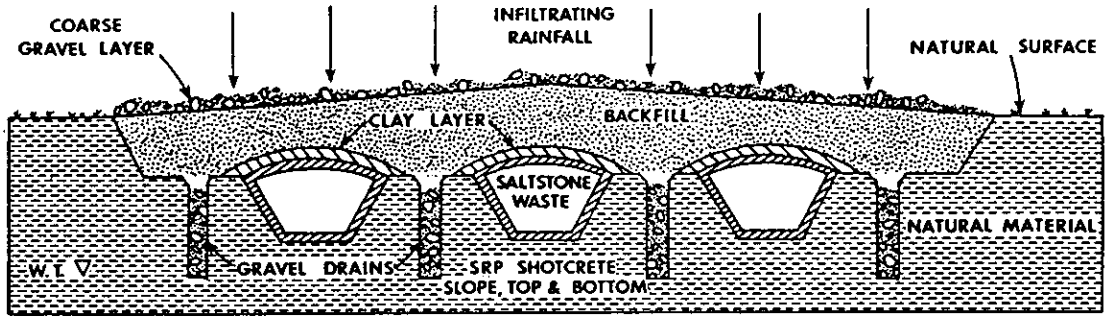

b) no overall claycap (cross section)

Figure 2-2 Possible Alternative Below Ground Saltstone Disposal Designs (After SRP)

3.0 GENERAL GEOLOGY AT THE SAVANNAH RIVER PLANT

3.1 Regional Stratigraphy

The Savannah River Plant is located in the Upper Atlantic Coastal Plain, about 30 km southeast of the Fall Line, which separates the Piedmont and Coastal Plain provinces (Figure 3-1). The Coastal Plain is underlain by a wedge of seaward-dipping unconsolidated and semiconsolidated sediments which increase in thickness from zero at the Fall Line to greater than 1000 m near the coast of South Carolina (Rankin, 1977). This sedimentary wedge, which ranges in age from Late Cretaceous to Holocene, continues to the seaward edge of the Continental Shelf. These Late Cretaceous sediments rest either directly on a crystalline basement of Precambrian and Paleozoic age or on Triassic sedimentary rock (Newark Series) embedded in basins within the crystalline basement.

Several attempts have been made to set up a lithostratigraphic and hydrostratigraphic system for the sediments of the Coastal Plain, but to date there is no overall accepted terminology for the numerous lithostratigraphic units (Marine, 1976; Huddleston, 1982; Mittwede, 1982).

For consistency with other work being done by or for E.I. du Pont de Nemours & Co., the stratigraphic terminology used in this report is taken from Christensen and Gordon (1983). This terminology is based on Siple (1967) and was modified by Christensen and Gordon in order to match the special needs when describing hydrostratigraphic units (rather than biostratigraphic or mappable units).

Consequently the following description of the regional stratigraphy is based primarily on Christensen and Gordon (1983).

3.1.1 Crystalline Basement

The crystalline basement rocks consist of chlorite-hornblende schist, hornblende gneiss and lesser amounts of quartzites (Table 3-1). Their

age ranges from Precambrian to Paleozoic. The surface of the crystalline basement dips at about 7.5 m per km to the southeast. The crystalline rock outcrops at the Fall Line (Figure 3-1) about 30 km northwest of the Savannah River Plant. At the Savannah River Plant the crystalline basement is buried beneath about 280 m of unconsolidated and semiconsolidated sediments.

Immediately overlying the crystalline rock is a layer of clay (saprolite) which is the residual product of weathering of the crystalline rock.

3.1.2 Triassic Sedimentary Rock

In the southern part of the Savannah River Plant Area a basin of mudstone is embedded within the crystalline basement rocks. This basin has been called the Dunbarton Basin (Marine and Siple, 1974). Based on gravity and ground magnetic surveys as well as on several drilling investigations, the Dunbarton Basin appears to be about 50 km long and at least 11 km wide (Figure 3-2). The depth of the basin was found to be 490 m in one well near the northwest boundary, and more than 1300 m in a well near the center of the basin.

Based on the drilling results, the Triassic sedimentary rocks consist of poorly sorted consolidated gravel, sand, silt and clay. The coarser material is found near the northwest margin where fanglomerates are abundant. Nearer the center, sand, silt and clay predominate; however, the sorting is always extremely poor which causes an extremely low primary permeability in the Triassic sedimentary rocks. The mineralogy of the clays in the sedimentary rock indicate that they were derived from the crystalline rock to the northwest of the Dunbarton Basin.

The Triassic sediments are unconformably overlain by sediments of the Tuscaloosa Formation (Late Cretaceous).

3.1.3 Tuscaloosa Formation

In the northern part of the Savannah River Plant the Tuscaloosa Formation (Upper Cretaceous) rests directly on the residual clay (saprolite), a weathering product of the crystalline metamorphic rock. No Triassic Sedimentary rocks were deposited in the northern part of the plant. In the southern part of the Savannah River Plant the Tuscaloosa Formation overlies the Triassic sedimentary rocks of the Dunbarton Basin.

The Tuscaloosa Formation consists generally of fluvial and estuarine deposits of cross-bedded sand and gravel with lenses of silt and clay.

Like the surface of the crystalline basement, the Tuscaloosa Formation dips to the southeast at about 6 to 7 m per km. At the Savannah River Plant the Tuscaloosa Formation outcrops only in the extreme upper part of the Upper Three Runs Creek valley. The thickness of the Tuscaloosa Formation ranges from zero at the Fall Line to about 180 m beneath the Savannah River Plant. The thickness remains fairly constant within the Savannah River Plant Area.

The Tuscaloosa Formation is the thickest (180 m) of the Coastal Plain formations in this area. Near the center of the Savannah River Plant site, the subunits of the Tuscaloosa Formation from top to bottom are: (1) a unit of clay, sandy clay, or clayey sand about 18 m thick (2) an aquifer unit of well-sorted medium to coarse sand about 46 m thick (3) a unit about 12 m thick, in which one or more clay lenses occur (4) an aquifer unit of well-sorted medium to coarse sand about 90 m thick, and (5) a basal unit of sandy clay about 12 m thick.

At the Savannah River Plant the Tuscaloosa Formation is overlain conformably by the Ellenton Formation.

3.1.4 Ellenton Formation

The Ellenton Formation consists of dark lignitic clay with coarse sand units. It is considered Late Cretaceous or Paleocene in age. The lignitic clay is dark gray to black, sandy, and micaceous. It is interbedded with medium quartz sand. The clay contains pyrite and gypsum. The upper part of the formation is characterized by gray silty to sandy clay with associated gypsum. The lower part consists generally of medium to coarse clayey quartz sand, which is very coarse and gravelly in some areas.

The Ellenton sediments are entirely within the subsurface (i.e., there are no known outcrops of Ellenton sediments). They range in thickness from zero near the northwest boundary of the Savannah River Plant to about 30 m southeast of the Savannah River Plant. Just inside the northwest boundary of the Savannah River Plant the thickness of the Ellenton is about 12 m.

The Ellenton Formation was described and named by Siple (1967) from subsurface studies on the Savannah River Plant. The formation was not correlated beyond the Savannah River Plant Area, but Siple (1967) speculated that it might be equivalent to the Black Creek Formation of Late Cretaceous age or the Black Mingo Formation of Paleocene or early Eocene age.

The Ellenton Formation is unconformably overlain by the Congaree Formation (of the Eocene Epoch).

3.1.5 Congaree Formation

Originally the Congaree Formation was included in the McBean Formation (Eocene Epoch) by Cooke (1936). Later the lower part of the original McBean Formation was raised to formational status and called the Congaree Formation (Cooke and MacNeil, 1952).

Although the Congaree Formation cannot be distinguished from the remaining upper part of the original McBean Formation, either where exposed or in well logs, for hydrologic studies it is advantageous to treat them as separate stratigraphic units. The reasons are, that in the central part of the Savannah River Plant the hydraulic head in the Congaree Formation is about 25 m lower than in the McBean Formation, and the Congaree Formation is about ten times more permeable. The head differential between these units is clearly maintained by a clay layer informally called the "Green Clay" in studies at the Savannah River Plant. This clay occupies the same stratigraphic position as the Warley Hill Marl of Cooke and MacNeil (1952) and separates the Congaree and McBean Formations.

In the central Savannah River Plant Area, the Congaree Formation consists of gray, green, and tan sand with some layers of gray, green, or tan clay. In the northwest Savannah River Plant Area, it consists primarily of tan clayey sand. It is slightly glauconitic in some places, slightly calcareous in others.

At the Savannah River Plant the Congaree Formation is exposed only where Upper Three River Runs Creek cuts into it, which is at the northern extreme of the Savannah River Plant Area.

The Congaree Formation dips at about 2 m per km to the southeast. Its thickness ranges from zero near the Fall Line to about 45 m in southeastern Allendale county. In the Savannah River Plant Area the Congaree Formation is 30-35 m thick.

3.1.6 Green Clay

The Green Clay layer at the top of the Congaree Formation consists of gray to green, dense, occasionally indurated clay. The indurated nature of the clay is caused by dense compaction and siliceous cement. Calcareous cement is usually absent.

The Green Clay appears to be continuous in the central Savannah River Plant Area where the thickness is about 3 to 10 m. This clay is hydrologically significant because it supports a relatively large head differential between the McBean Formation above and the Congaree Formation below.

In the northwest Savannah River Plant Area, the Green Clay becomes discontinuous, and concomitantly the vertical hydraulic gradient between the Congaree and McBean Formation is also less. To the south the Green Clay thickens to about 20 m and becomes what is referred to in Georgia as the Blue Bluff Marl of the Lisbon Formation.

3.1.7 McBean Formation

The McBean Formation (above the Green Clay) has a thickness ranging from zero near the Fall Line to 30 m in the southeast. At the Savannah River Plant it is about 20 to 25 m in thickness. The dip is about 2 m per km to the southeast.

The McBean Formation may be divided into two subunits; an upper unit consisting of tan clayey sands and occasionally red sand, and a lower unit consisting of light tan to white calcareous clayey sand. The lower unit is locally referred to as the "calcareous zone". In some places it contains void spaces that result in "rod drops" or lost circulation during drilling operations. To the northwest these void spaces appear to decrease to the extent that no calcareous zone appears to exist in the northwest part of the Savannah River Plant (M-Area). However, to the southeast the lime content of the zone increases as do the void spaces. Southeast of the Savannah River Plant the zone becomes limestone with only small amounts of sand.

The McBean Formation is considered to be the shoreward facies of the Santee limestone, which occurs to the southeast. In the Savannah River Plant Area, the calcareous zone may represent a tongue of the Santee limestone.

At the Savannah River Plant the McBean Formation is frequently exposed in the creek valleys.

A clay layer informally called the "Tan Clay" in studies at the Savannah River Plant overlies the McBean Formation.

3.1.8 Tan Clay

The Tan Clay can be considered to be the bottom of the overlying Barnwell Formation. It is less continuous than the Green Clay and has a higher hydraulic conductivity. Its thickness ranges from zero to 5 m. The Tan Clay commonly consists of two thin clay layers separated by a sandy zone. In many studies the Tan Clay is used as a marker horizon.

3.1.9 Barnwell Formation

The Barnwell Formation is reported to be Jackson (uppermost Eocene) in age (Siple, 1967). Its lowermost layer, the Tan Clay, directly overlies the McBean Formation.

The Barnwell Formation is exposed over a considerable area in the uplands of Aiken and Barnwell Counties. The formation thickens from zero in the northeastern part of Aiken county to about 30 m at the southeastern boundary of Barnwell County. The Barnwell Formation is overlain by the Hawthorn Formation, from which it is usually difficult to distinguish.

The Barnwell Formation consists mainly of deep red fine to coarse clayey sand and compact sandy clay. Other parts of the formation contain beds of mottled gray or greenish gray sandy clay and layers of ferruginous sandstone that range in thickness from 1 cm to 3 cm. Although fossils at some places indicate a marine origin, material identified as Barnwell may have been deposited in other places as alluvium during Pliocene to Pleistocene time. Beds of limestone occur

in the Barnwell Formation in Georgia, but none have been recognized in South Carolina.

These factors indicate that a considerable part of the Barnwell Formation was deposited as an arenaceous limestone in a near-shore or estuarine environment. Some evidence of the remnant calcareous nature of the formation is indicated by the comparatively high proportion of calcium carbonate found in ground water circulating in this unit.

3.1.10 Hawthorn Formation

The Hawthorn Formation outcrops over a very large area of the Atlantic Coastal Plain and is perhaps the most extensive surficial deposit of Tertiary age in this region. It is bounded on top and bottom by erosional unconformities, and is present at the surface in the higher areas of Aiken County. It ranges in thickness from zero in northwestern Aiken County to about 20 m near the Barnwell-Allendale County line.

Typical Hawthorn Formation is fine, sandy, phosphatic marl or soft limestone and brittle shale resembling silicified fuller's earth. Updip, however, in the vicinity of Aiken and Barnwell Counties, it is characterized by tan, reddish-purple, and gray sandy dense clay that contains coarse gravel, limonitic nodules, and disseminated flecks of kaolinitic material.

3.1.11 Surficial Formations

3.1.11.1 Tertiary Alluvium

Alluvial deposits of late Tertiary age occur irregularly and discontinuously on the interstream divides or plateaus. They are composed of coarse gravel and poorly sorted sand and were tentatively classified by Siple (1967) as Pliocene in age. Their thickness ranges from 2 to 6 meters.

3.1.11.2 Terrace Deposits

Cooke recognized seven marine terraces of Pleistocene age on the Atlantic Coastal Plain of South Carolina. He indicated that the four highest terraces are present in the Savannah River Valley. These features are not universally recognizable and have therefore been the subject of discussion. The deposits that may be associated with these terraces are not more than 10 m thick.

3.1.11.3 Holocene Alluvium

Alluvium of Holocene age occurs in the tributary and main channels of the Savannah River. These deposits, which are generally cross-bedded and heterogeneous in composition, consist of poorly sorted sand, clay and gravel. The thickness ranges from 0 to 10 m.

3.2 Local Stratigraphy at Z-Area

In the previous sections the regional stratigraphy is summarized. But in the area of interest, Z-Area and vicinity, not all of the stratigraphic units described above exist or are exposed.

The lowermost layer exposed near Z-Area is the Green Clay. The Green Clay at Z-Area occurs at elevations between 42 and 46 m a.s.l. and appears to be relatively continuous in the wells throughout the area (Parizek and Root, 1984). It forms the bottom of the Upper Three Runs Creek valley.

Thus the Congaree Formation is not exposed at Z-Area. However it is included in the modeling study as discussed in Chapter 4.

The hill at Z-Area itself consists of the sediments of the McBean and the Barnwell Formation. The Tan Clay, separating the McBean and the Barnwell Formations, can be recognized in several borehole logs. The elevation of the Tan Clay is between 60 and 69 m a.s.l. (Parizek and

Root, 1984). It appears that the Tan Clay is thinner and less continuous than the Green Clay. The Hawthorn Formation either does not exist at Z-Area or is indistinguishable from the Barnwell Formation. Also no surficial formations of significant thickness are known to exist at Z-Area.

A detailed local stratigraphy (i.e., for modeling purposes) can be derived from the results of numerous drilling investigations at Z-Area (see Section 6.5).

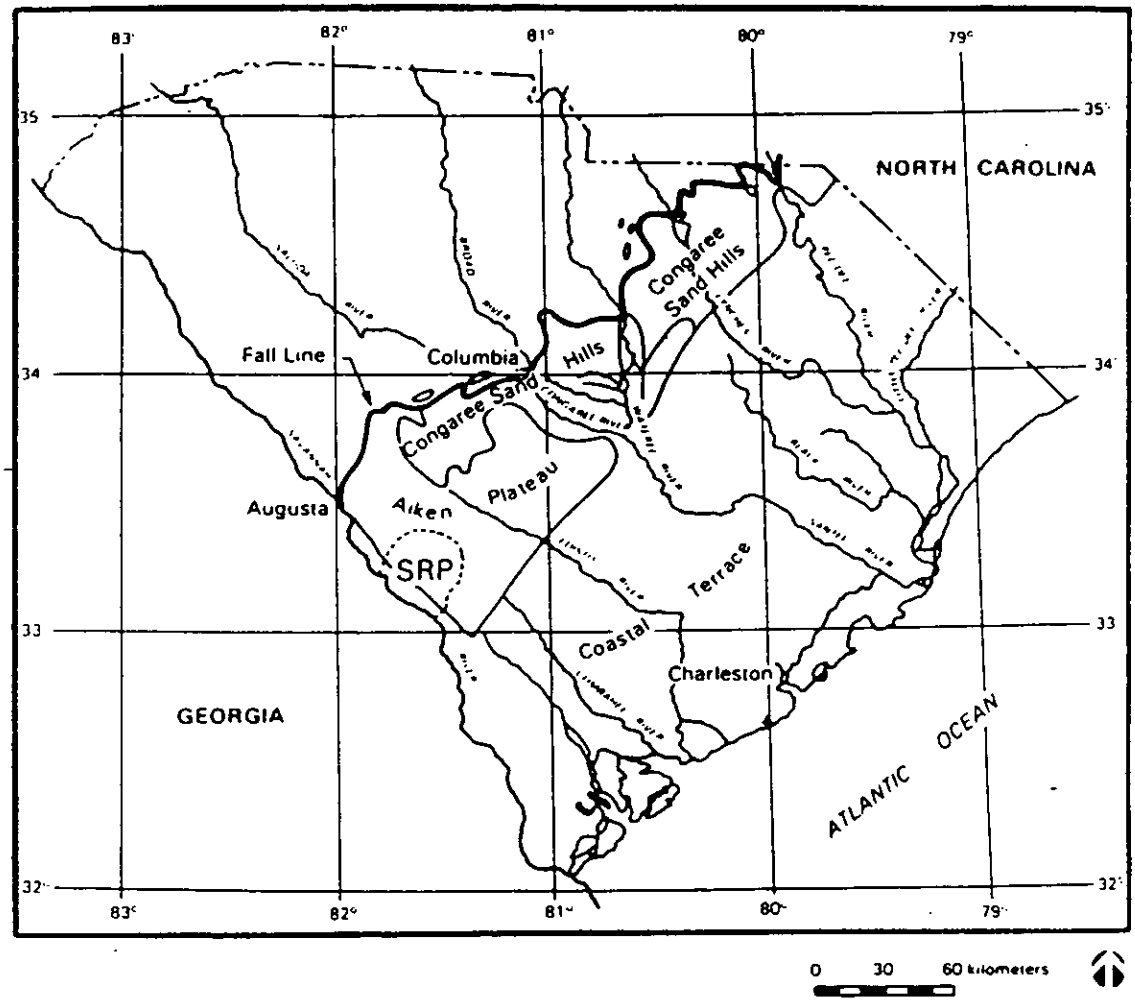

Figure 3-1 Physiography of the Savannah River Region (from Christensen and Gordon, 1983)

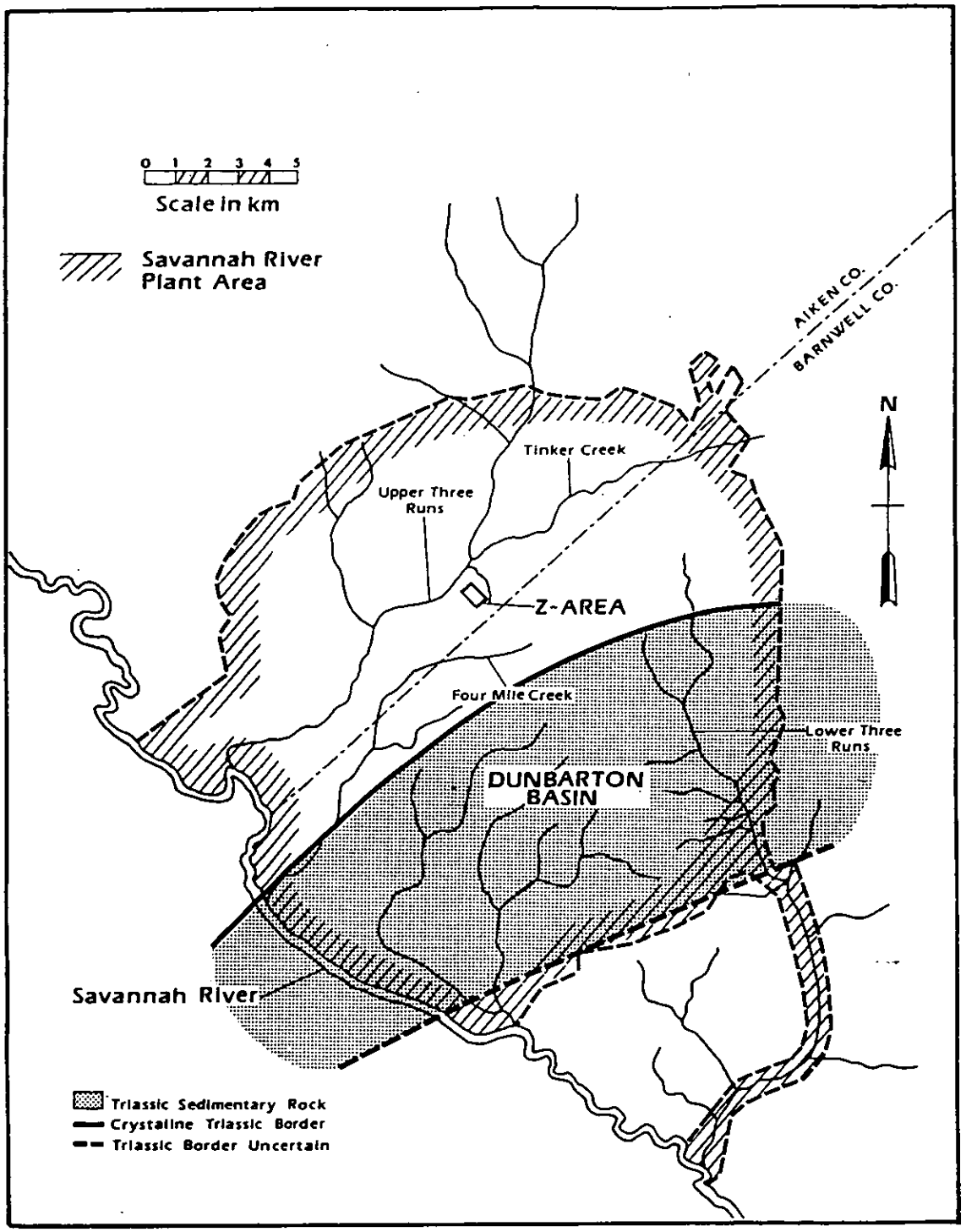

Figure 3-2 Outline of the buried Triassic basin at Savannah River Plant (modified from Marine, 1974)

Hydro-Stratigraphic Unit	Geologic Age	Outcrop	Description	Thickness (m at SRP)
Alluvium	Recent Epoch	River and creek bottoms	Fine to coarse sand, silt and clay	0 - 3
Terrace	Pleistocene Epoch	In flood plains and terraces of stream valleys	Tan to gray sand, clay, silt, and gravel on higher terraces	0
Alluvium	Pliocene Epoch	Surface of Aiken Plateau	Gravel and sandy clay	0
Hawthorn	Miocene Epoch	Large part of ground surface	Tan, red, and purple sandy clay with numerous clastic dikes	0 - 20
Barnwell	Eocene Epoch	Large part of ground surface near streams	Red, brown, yellow, and buff, fine to coarse sand and sandy clay	20 - 30
'Tan Clay'	Eocene Epoch		Dark silt, sandy clay	0 - 5
McBean	Eocene Epoch	In banks of larger streams	Yellow-brown to green, fine to coarse, glauconite quartz sand, intercalated with green, red, yellow, and tan clay, sandy marl, and lenses of siliceous limestone	20 - 25
'Green Clay'	Eocene Epoch		Grey, green, dense, indurated clay	3 - 20
Congaree	Eocene Epoch	In banks of larger streams	Yellow-brown to green, fine to coarse, glauconite quartz sand, intercalated with green, red, yellow, and tan clay, sandy marl, and lenses of siliceous limestone	30 - 35
Ellenton	Upper Cretaceous Epoch	None on plant	Dark gray to black sandy lignitic micaceous clay containing disseminate crystalline gypsum and coarse quartz sand	12- 30
Tuscaloosa	Upper Cretaceous Epoch	None on plant except the extreme upper part of Upper Three Runs Creek Valley	Tan, buff, red, and white; crossbedded, micaceous quartzitic and arkosic sand and gravel imbedded with red, brown, and purple clay and white kaolin	180
Newark Series "Red Beds"	Triassic Period	None on plant	Dark-brown and brick-red sandstone, siltstone, and claystone containing gray calareous patches. Fanglomerates near border.	0 or 1000
Basement rocks of the Slate Belt and Charlotte Group	Precambrian and Paleozoic Eras	None on plant	Hornblende gneiss, chlorite-hornblende schist, lesser amounts of quartzite. Covered by saprolite layer derived from basement rock	> 1000

Table 3-1 The Hydrostratigraphic Units Underlying the Savannah River Plant (modified from Christensen and Gordon, 1983)

4.0 GENERAL HYDROGEOLOGY AT THE SAVANNAH RIVER PLANT

4.1 General

The Coastal Plain sediments, as described in Chapter 3, constitute a multilayer hydrogeologic system characterized by lateral continuity (in most circumstances) of the formations. Hydraulic properties vary for each of the (hydro)stratigraphic units, depending on their lithology. Ground water flow paths and flow velocities within these units are governed by the hydraulic properties, the geometry of the units, and the distribution of recharge and discharge.

The Savannah River Plant lies completely within the drainage area of the Savannah River. The direction of flow in the shallow aquifers is governed by small tributaries, in deeper aquifers by major tributaries, and in the deepest aquifers only by the Savannah River itself. Thus, the deepest ground water may be moving at angles or even in the opposite direction to the shallow ground water at a particular location.

In the following section the (hydro)stratigraphic units (described in Chapter 3) are hydrogeologically characterized, as far as they are of importance for the actual flow and transport modeling. Similar to the previous chapter, most sections of this chapter are derived from Christensen and Gordon (1983).

4.2 Hydrogeologic Characterization of the (Hydro)Stratigraphic Units

The crystalline basement rock is relatively impermeable (10^{-10} m/s) except in certain fracture zones. The fracture zones have comparably higher but still relatively low absolute hydraulic conductivities (3×10^{-7} m/s). The Triassic Sedimentary rock in the Dunbarton Basin is characterized by extremely low permeability (from 10^{-11} to 10^{-14} m/s) and water movement within the Triassic Sedimentary Rock is considered to be almost nonexistent (Christensen and Gordon, 1983).

4.2.1 Tuscaloosa Formation

The Tuscaloosa Formation, stratigraphically overlying the Triassic Sedimentary Rock or the crystalline basement, is considered to be the lowermost aquifer at the Savannah River Plant Area. Its transmissivity, derived from field tests in boreholes in the Savannah River Plant Area, ranges from 7×10^{-3} m^2/s to 29×10^{-3} m^2/s with an average value of 16×10^{-3} m^2/s. Using a thickness of 180 m for the Tuscaloosa Formation (at the Savannah River Plant Area) a mean hydraulic conductivity of about 9×10^{-5} m/s can be calculated.

The Tuscaloosa Formation discharges to the Savannah River. Therefore at the Savannah River Plant the ground water in the Tuscaloosa Formation moves to the west or southwest (Figure 4-1). The piezometric head of the lower Tuscaloosa Formation at Z-Area is estimated at about 60 m a.s.l. Water level measurements in wells screened only at the bottom or at the top of the Tuscaloosa Formation indicate an increase of the piezometric head with depth. The measured head differences between upper and lower Tuscaloosa Formation range from 4 to 9 m (Christensen and Gordon, 1984). This indicates some upward movement of water in addition to its horizontal movement. The horizontal gradient within the Tuscaloosa Formation is generally about 0.002 m/m.

4.2.2 Ellenton Formation

The Ellenton Formation, which overlies the Tuscaloosa Formation, is not separated hydraulically from the Tuscaloosa Formation by an intervening confining bed. Therefore the Tuscaloosa and Ellenton Formation are considered to constitute a single aquifer. This is confirmed by water level measurements in boreholes in the Savannah River Plant Area. Based on these measurements the piezometric surface in the Ellenton Formation at Z-Area is at about 55 m a.s.l.

There are few hydrogeologic data for the Ellenton Formation, thus little is known about the lateral flow pattern of ground water within the formation. Because it is apparently connected to the Tuscaloosa Formation, its flow pattern is probably similar.

The water level data from the Ellenton Formation, measured in boreholes at the Savannah River Plant, indicate that the hydraulic head in the Ellenton Formation is consistently higher than that in the overlying Congaree Formation. This indicates that there is not a permeable hydraulic connection between these two formations. Although the clays that separate the Ellenton and the Congaree Formations are not thick, they are apparently extensive and continuous enough to impede the hydraulic connection. A pisolitic clay at the base of the Congaree Formation appears to be extensive and may constitute the principal confining bed that separates the Congaree Formation and the deeper hydrologic system. The upper part of the Ellenton Formation is a sandy clay, which may also function as a confining bed between the Ellenton and the Congaree Formations.

4.2.3 Congaree Formation

The sand beds of the Congaree Formation constitute an aquifer in this region, with a transmissivity of about 10^{-3} m^2/s. Using hydraulic tests in boreholes at the Savannah River Plant Area, the average hydraulic conductivity of the sandy zones of the Congaree Formation was determined to be about 2×10^{-5} m/s. At the central part of the Savannah River Plant Area, maximum values of 5×10^{-4} m/s were measured (Christensen and Gordon, 1983).

The Congaree Formation is drained by the Savannah River and its major tributaries. Thus, on a regional basis, the dissecting creeks divide the ground water in the Congaree Formation into discrete subunits. Depending on the depth of dissection, ground water is confined to its own subunits.

Within the Savannah River Plant Area, the Congaree Formation discharges into the Savannah River and Upper Three Runs Creek. Although springs occur, most of the discharge occurs along the valley bottoms in swamps and marshes, making it difficult to measure.

These discharges into the Savannah River and Upper Three Runs Creek govern the spatial variation of the piezometric surface of the ground water in the Congaree Formation (Figure 4-2). Thus, at the Savannah River Plant, the ground water generally moves to the southwest towards the Savannah River, but in the vicinity of Upper Three Runs Creek the ground water movement is directed towards Upper Three Runs Creek.

At Z-Area, the piezometric head in the Congaree Formation lies between 47 and 50 m above sea level (Figure 4-2). The flow is directed to the west or the northwest. Thus, at least a part of the Congaree ground water flowing beneath the Z-Area is discharged into Upper Three Runs Creek. The horizontal hydraulic gradient in the Congaree Formation at Z-Area is about .005 m/m.

As mentioned in the previous section, the hydraulic head in the Congaree Formation is generally lower than in the underlying Ellenton and Tuscaloosa Formations. The upward movement of water to the Congaree Formation is impeded by clay layers at the base of the Congaree Formation and at the top of the Ellenton Formation. Because of the different spatial flow pattern in the Congaree and the Ellenton-Tuscaloosa Formations, the head difference between these two formations is not constant in space (Figure 4-3). At Z-Area, the head difference is between 5 and 8 m. Similarly, the head in the Congaree Formation is also lower than in the McBean Formation above. This is caused by two factors: (1) the low permeability of the Green Clay above the Congaree Formation through which recharge from the McBean Formation must take place, and (2) the relatively high hydraulic conductivity of the Congaree sands below the Green Clay, which enhances lateral movement and discharge to the deeper creek valleys. Thus at Z-Area and its vicinity, the hydraulic head in the Congaree

Formation is the lowest of any (hydro)stratigraphic unit in the Coastal Plain system.

Laboratory tests indicated a median porosity value of 43% for the total porosity of the upper part of the Congaree Formation (Christensen and Gordon, 1983). Based on the lithology and degree of induration, it is estimated that an effective flow porosity of 20% is reasonable. A pumping test in the northwestern Savannah River Plant resulted in a value of 14% (Christensen and Gordon, 1983).

4.2.4 Green Clay

The Green Clay at the top of the Congaree Formation separates hydraulically the Congaree Formation below from the McBean Formation above. This separation appears to exist throughout the entire Savannah River Plant Area except in the far northwest, where the separation is less complete (Section 3.1.6).

Because of the different spatial flow patterns in the Congaree and McBean Formations (Section 4.2.5) the differential head through the Green Clay is not constant. At Z-Area the differential head ranges between 10 and 15 m.

4.2.5 McBean Formation

Ground water occurs in both the lower calcareous zone and the upper sandy zone of the McBean Formation. Some of the uppermost parts of the McBean Formation are unsaturated. As with the Congaree Formation, creeks in the region dissect the McBean Formation and divide this hydrogeologic unit into separate subunits, each having its own recharge and discharge area. Because the McBean Formation is a shallower formation than the Congaree Formation, smaller creeks with less deeply incised valleys make these divisions. The subunits of the McBean Formation are therefore smaller than those of the Congaree Formation.

The McBean Formation in the Z-Area hill can be considered to be an almost isolated hydrologic subunit (Figure 4-4). It is drained by Upper Three Runs Creek and small temporary tributaries in the north and west as well as by McQueen Creek in the east and southeast. Thus, the Z-Area hill is connected only in the south with the McBean Formation beneath the Separation Areas of the Savannah River Plant.

The piezometric surface of the McBean Formation at Z-Area itself ranges from 61 to 69 m a.s.l. at the time (August 1977) the data were collected. Near Upper Three Runs Creek the piezometric surface is 50 m a.s.l. and lower. Thus, taking into account the elevation of the top of the McBean Formation (Section 3.2) the piezometric surface in the McBean Formation is a free water table near the creeks (Parizek and Root, 1984). As Figure 4-4 shows, the flow pattern at the Z-Area hill is highly divergent. Although the general direction of flow is to the north, the individual flow vectors range from west to east.

The horizontal piezometric gradient ranges from 0.007 m/m at the center of Z-Area to 0.030 m/m at the western hill slope. The vertical head difference between upper and lower McBean Formation is about 0.6 m, indicating a downward component of ground water flow in addition to the horizontal flow component.

The median hydraulic conductivity in the upper part of the McBean Formation (sandy zone) is about 1.5×10^{-6} m/s based on hydraulic tests in boreholes (Christensen and Gordon, 1983). The variation of measured values is plus or minus one order of magnitude.

Fluid losses in the lower part of the McBean Formation (calcareous zone) during drilling operations make it appear very permeable. However, pumping tests on the calcareous zone indicate a lower hydraulic conductivity (0.5 to 1×10^{-6} m/s) than in the upper McBean Formation. Apparently zones of higher permeability in the lower McBean Formation do not connect over large distances, and the regional permeability of the calcareous zone is lower than it appears from drilling experience (Christensen and Gordon, 1983).

4.2.6 Tan Clay

As described previously, a clay layer called the "Tan Clay" overlies the McBean Formation. It is considered to be the lowermost part of the overlying Barnwell Formation. Similar to the Green Clay between the Congaree and McBean Formations, the Tan Clay impedes vertical movement of ground water between the Barnwell and the McBean Formations. The Tan Clay is not as continuous as the Green Clay and it has a somewhat higher hydraulic conductivity. The head differential between the Barnwell and the McBean Formations is generally smaller (5-10 m) than the head differential between the McBean and Congaree Formations (10-13 m at Z-Area). Nevertheless, the Tan Clay is an important hydrogeological unit because it supports a perched water table in the Barnwell Formation above the areas where the piezometric surface in the McBean Formation is below the Tan Clay.

4.2.7 Barnwell Formation

The Barnwell Formation is the uppermost hydrogeologic unit in Z-Area and vicinity (see Section 3.2). As with the McBean Formation below, the Barnwell Formation is divided into separate subunits by dissecting creeks but to an even greater extent due to its higher elevation. Therefore, the Barnwell Formation in the Z-Area hill can be considered to be an individual hydrologic subunit. As with the McBean Formation, this hydrologic unit is connected only in the south with the Barnwell Formation beneath the Separation Areas (Figure 4-5).

Like the McBean Formation, the Barnwell Formation at the Z-Area hill is drained by the creeks surrounding it, but most of the recharge that the Barnwell Formation receives, as infiltrated rainfall and from the south, migrates through the Tan Clay into the underlying McBean Formation.

The piezometric surface at Z-Area itself is a free water table ranging from 67 to 77 m a.s.l. at the time (Summer, 1986) when the data were

collected (Figure 4-5). Near the creeks, where the piezometric surface in the underlying McBean Formation is a free water table, the ground water in the Barnwell Formation must be considered to be perched ground water. As in the McBean Formation the horizontal component of ground water flow in the Barnwell Formation is highly divergent.

The horizontal hydraulic gradient ranges from 0.002 m/m at the southern part of Z-Area to 0.05 m/m at the northeastern Z-Area hill slope. Assuming a constant conductivity for the Barnwell Formation over the whole area, the large range for the horizontal hydraulic gradient indicates a corresponding variation of the ratio of the vertical and horizontal ground water flow components throughout the area.

Laboratory measurements of hydraulic conductivities on undisturbed Barnwell Formation samples, as well as results of field tests in boreholes, indicate conductivities of about 1×10^{-6} m/s with the measurements varying between 1×10^{-7} m/s and 1×10^{-5} m/s (Christensen and Gordon, 1983). Pumping tests in a sand lens in the upper Barnwell Formation resulted in even higher values (1×10^{-4} m/s). Thus the overall hydraulic conductivity of the Barnwell Formation probably does not differ significantly from the conductivity of the McBean Formation. However the Barnwell Formation is apparently more heterogeneous (see also Section 3.1.9). Low permeability clay lenses exist within the Barnwell Formation, which locally impede downward ground water movement, causing small perched ground water lenses above the general water table in the Barnwell Formation (Sargent, 1984).

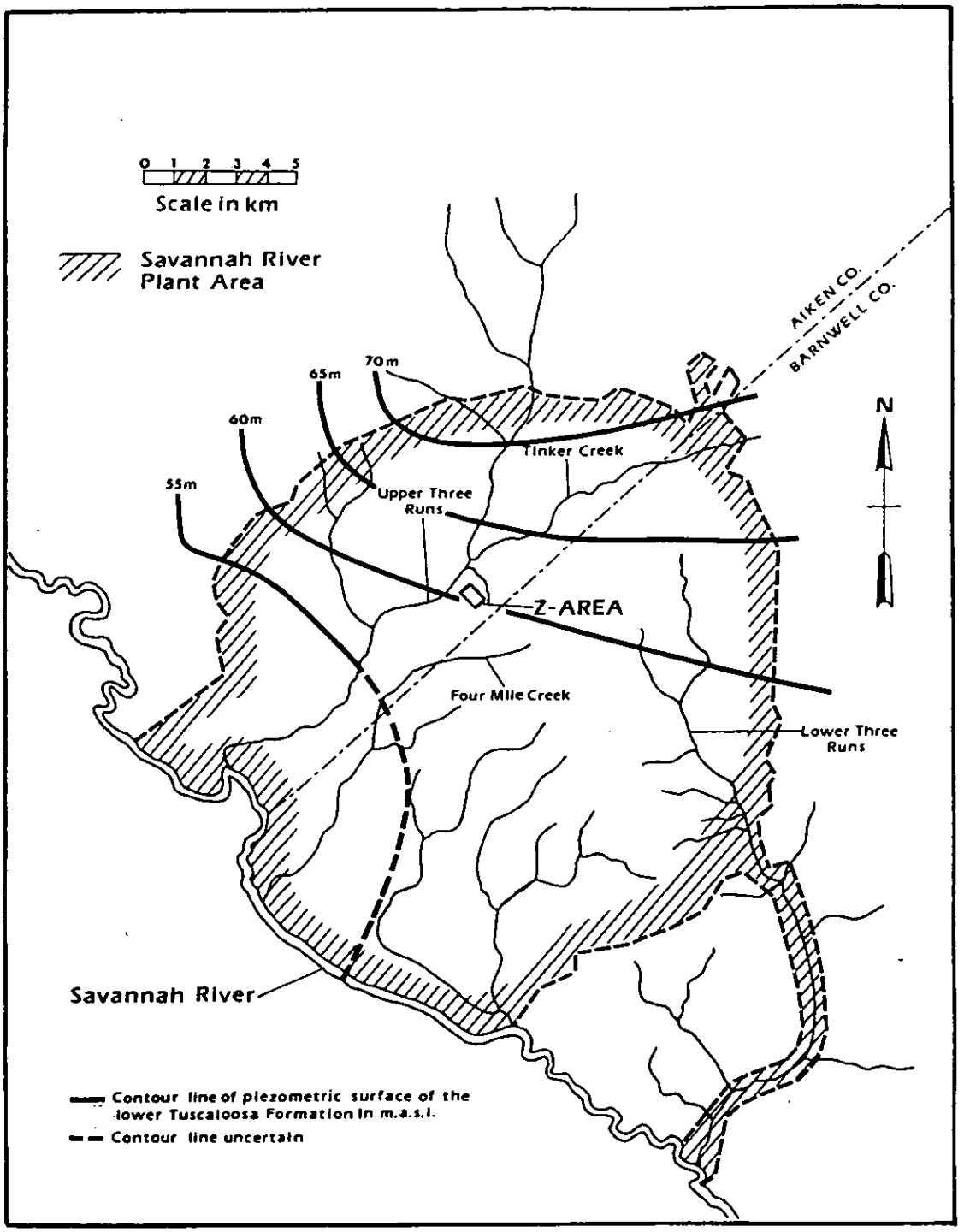

Figure 4-1 Piezometric Surface of the Lower Tuscaloosa Formation at the Savannah River Plant (modified from Christensen and Gordon, 1983)

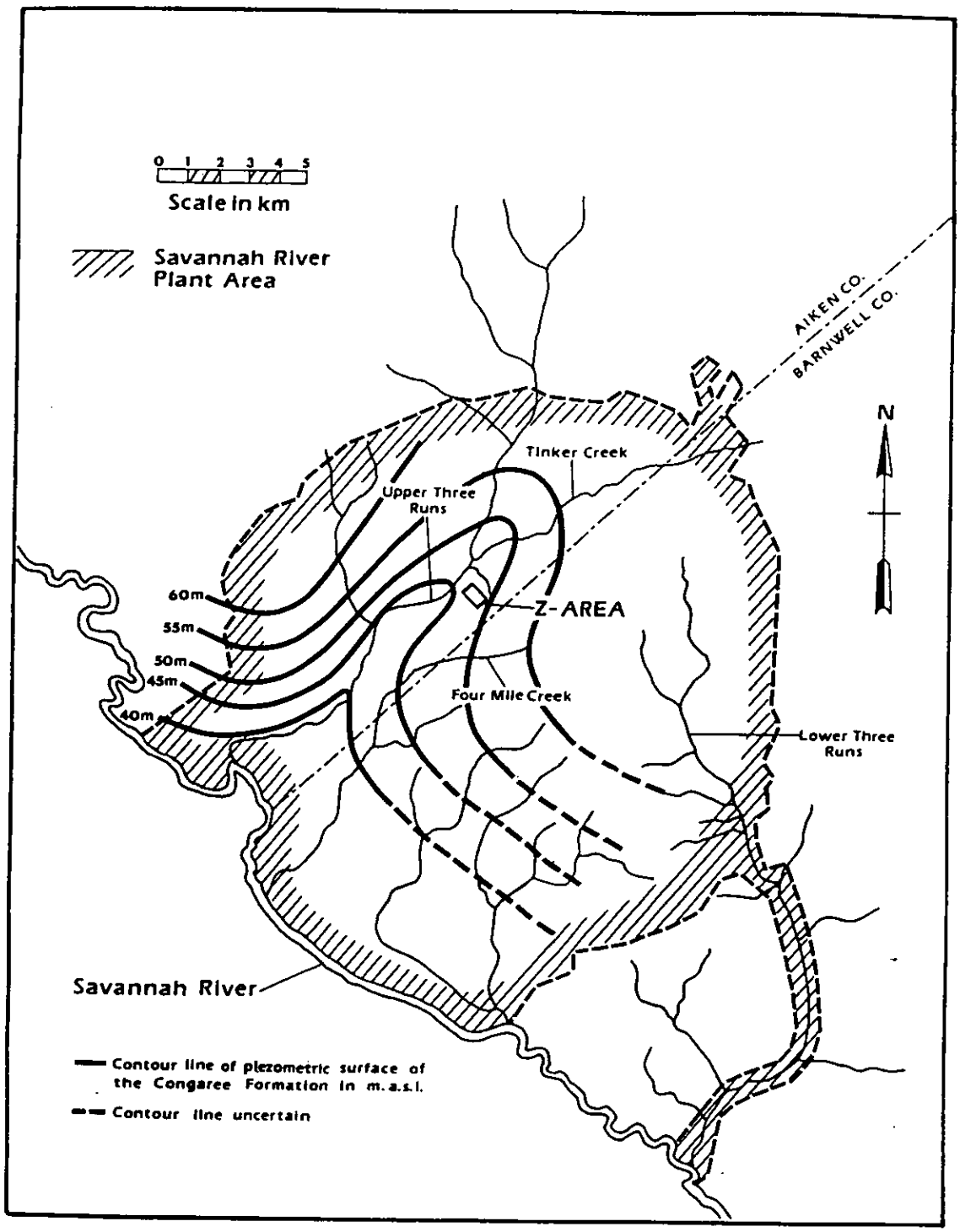

Figure 4-2 Piezometric Surface of the Congaree Formation at the Savannah River Plant (modified from Christensen and Gordon, 1983)

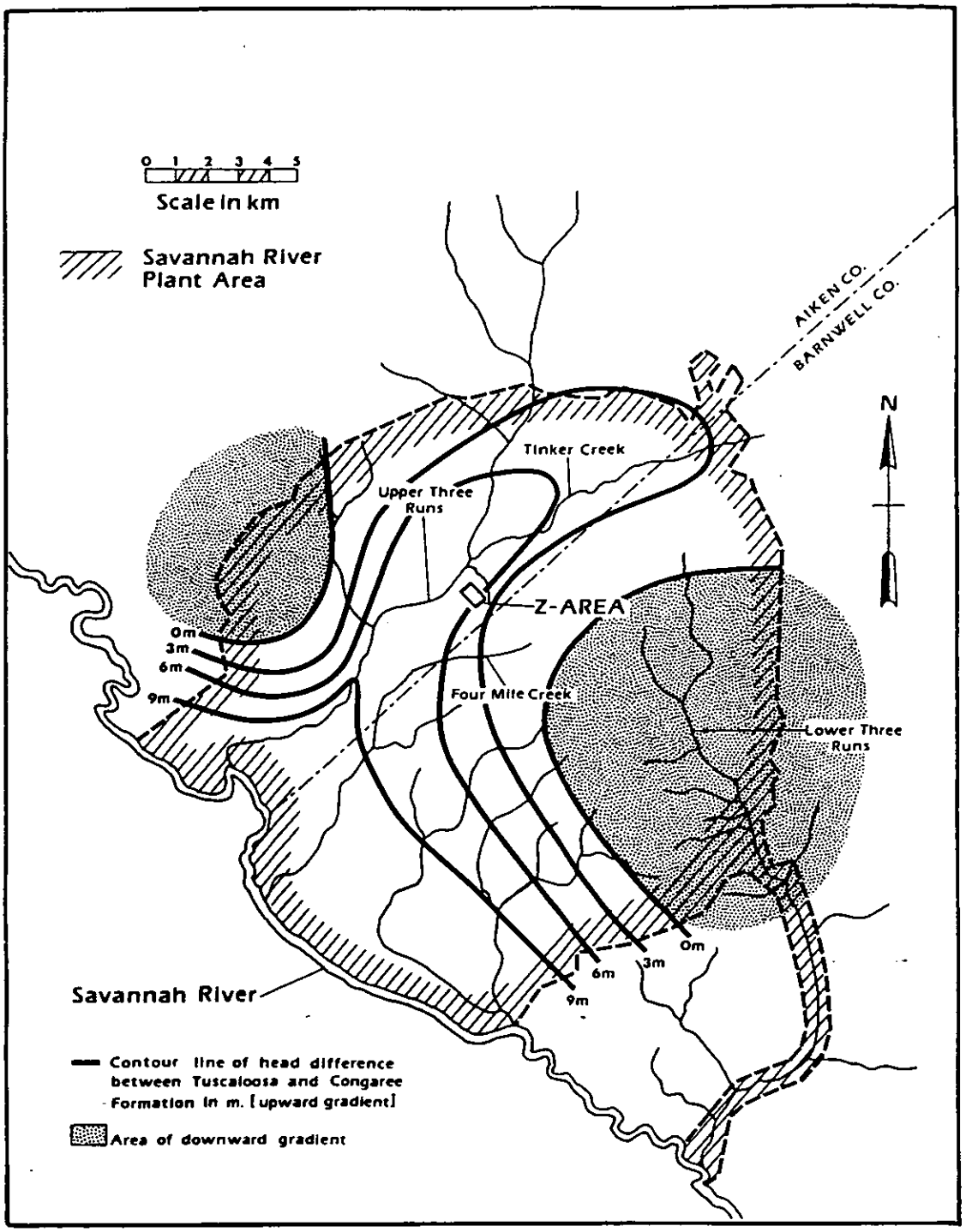

Figure 4-3 Head Difference Between the Tuscaloosa and Congaree Formations at the Savannah River Plant (modified from Christensen and Gordon, 1983)

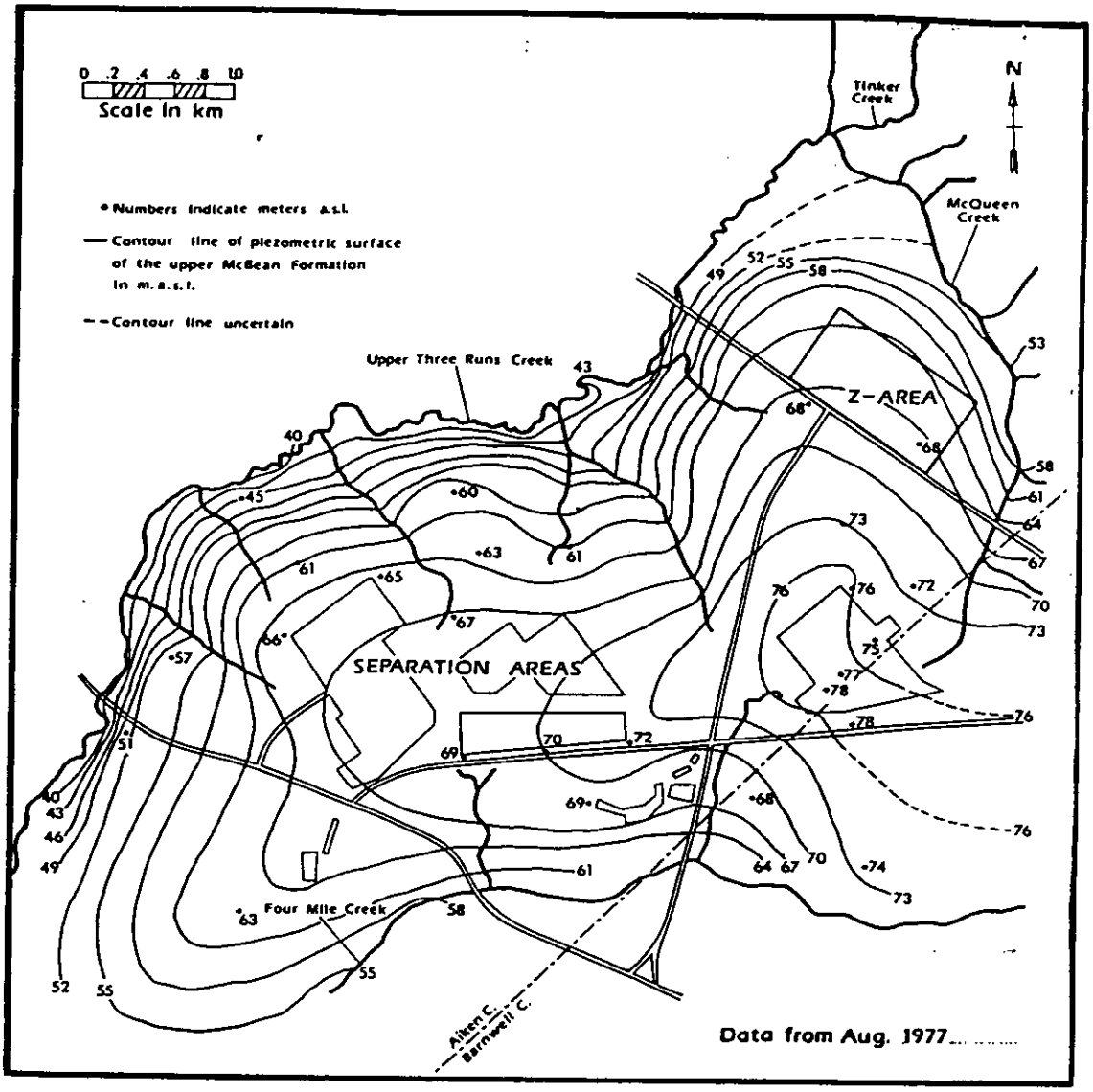

Figure 4-4 Piezometric Surface of the Upper McBean Formation at the Savannah River Plant Separation Areas (modified from Christensen and Gordon, 1983)

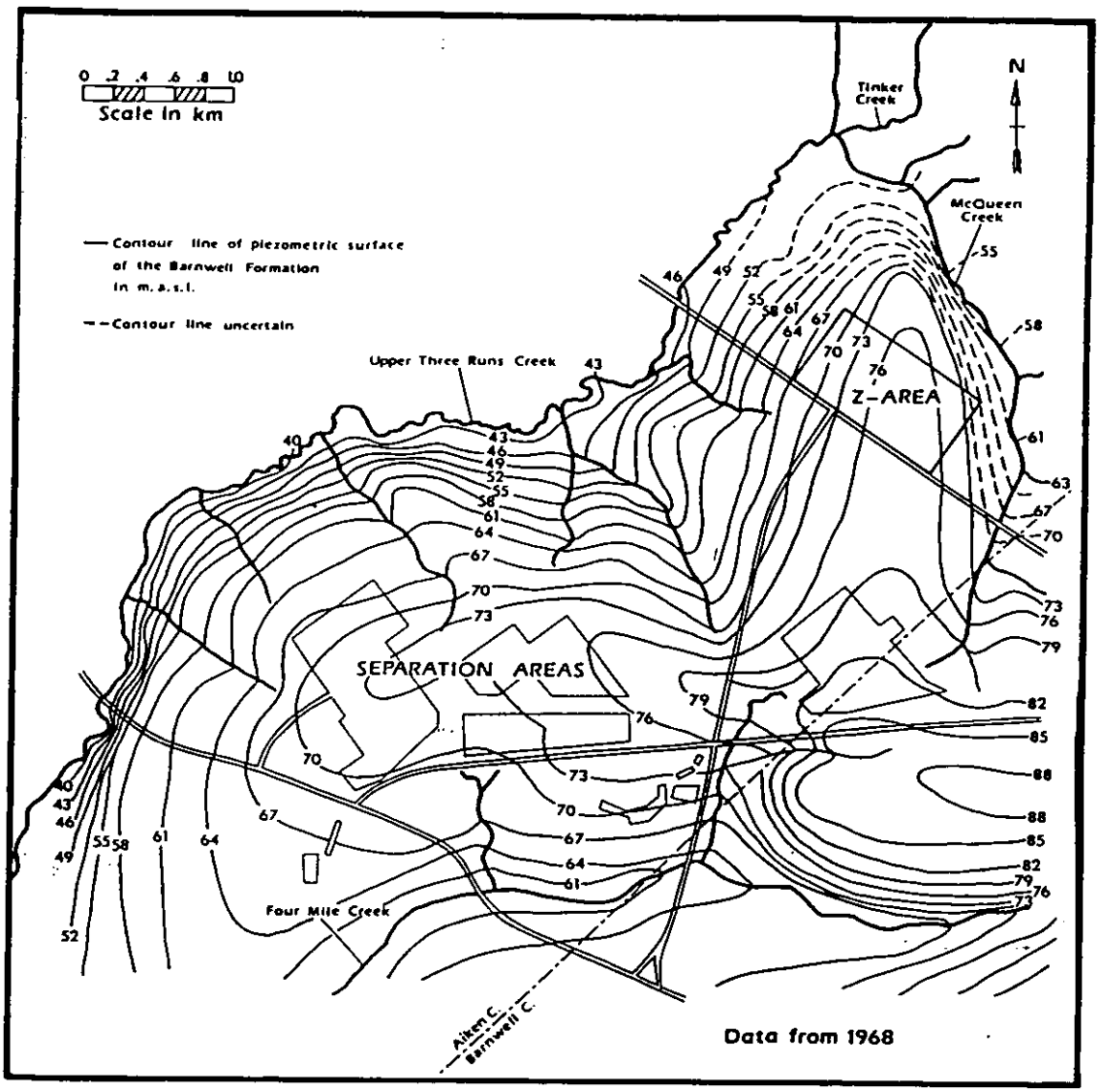

Figure 4-5 Piezometric Surface of the Barnwell Formation at the Savannah River Plant Separation Areas (modified from Christensen and Gordon, 1983)

5.0 GENERAL CLIMATOLOGY AT THE SAVANNAH RIVER PLANT

The climate at the Savannah River Plant Area is typical for the region. Average temperatures are 8-10°C in winter, 26-28°C in summer with extreme values of -16°C and 41°C (Fenimore and Hooker, 1977). The relative humidity generally lies between 70-80% at night and 50-60% at noon. The precipitation is relatively high, between 1000 and 2000 mm per year.

Rainfall measurements at Aiken near the Savannah River Plant, are available since 1854 (Figure 5-1). Precipitation data for the Savannah River Plant itself start in 1952 (Figure 5-2). The average annual rainfall at the Savannah River Plant was 1215 mm for the years 1952 through 1983 (Fenimore and Hooker, 1977). Within that time period, the recorded maximum and minimum annual rainfall were 1909 mm and 945 mm, respectively. During the period 1952-1972 the average rainfall is greatest in March (129.5 mm) and least in November (57.0 mm). Thus the rainfall is rather evenly distributed throughout the year (average monthly rainfall 992 mm). Further climatological details can be found in Fenimore and Hooker (1977).

Detailed analyses of the hydrologic budget for the recharge area of McQueen Creek have shown that about 67% of the average precipitation does not infiltrate but evaporates or runs off (Parizek and Root, 1984). Thus about 33% of the rainfall infiltrates as groundwater recharge. Using 1215 mm per year as annual average precipitation, the annual average recharge rate can be calculated to be about 400 mm per year.

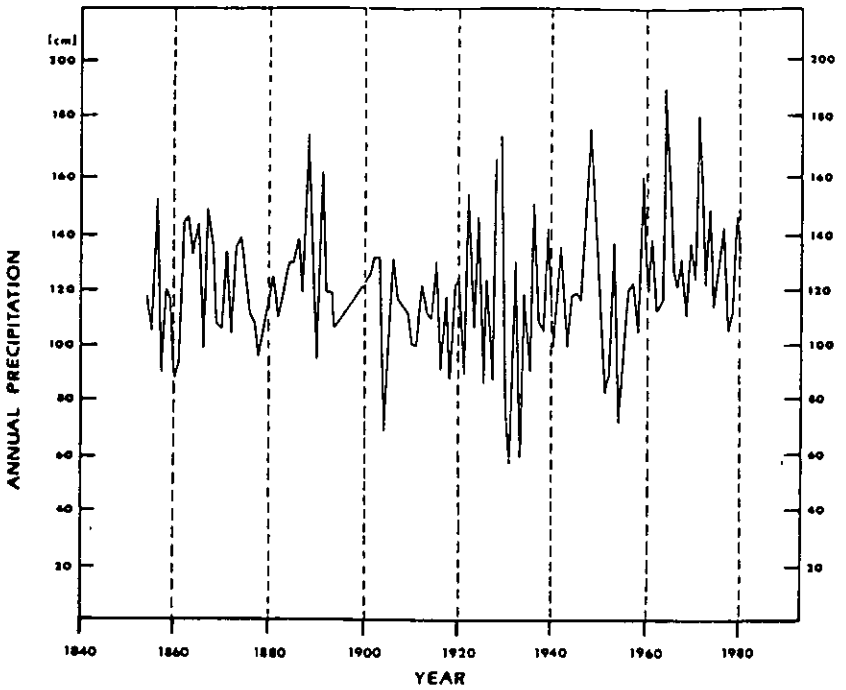

Figure 5-1 Annual Precipitation at Aiken 1854-1980 (modified from Cook, 1983)

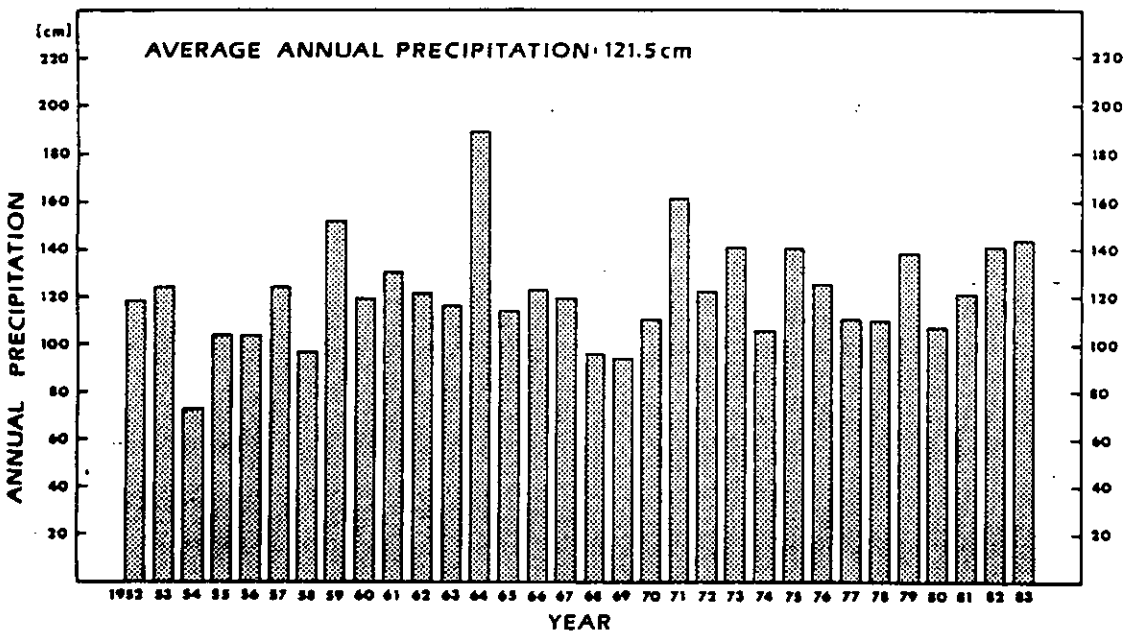

Figure 5-2 Annual Precipitation of the Savannah River Plant 1952-1983 (Data taken from Fenimore and Hooker, 1977 and Cook, 1983)

6.0 DATA REVIEW

6.1 Overview

Several studies have been conducted related to the geology and hydrogeology of the Savannah River Plant in general, and the Separation Areas in particular. However only a few of these are related directly to Z-Area itself. Most of the information concerning the geological conditions at Z-Area derives from the field exploration program performed by d'Apolonia (1981). This program included drilling (25 boreholes) sampling and geophysical borehole logging. The boreholes were completed with piezometers for the purpose of measuring ground water levels and for hydrochemical sampling.

Numerous laboratory tests were performed on Shelby Tube samples obtained during the drilling program. Estimates of the following formation properties were obtained: grain size distribution (sieve curves), horizontal and vertical permeabilities, total porosity and effective porosity.

Ground water levels were measured in the boreholes drilled and instrumented by d'Apolonia. Water level data are available for two time periods: (a) January 1982 - December 1982 and (b) March 1984 - August 1985. In 1984 and 1985 ground water samples were collected quarterly and the major ion concentrations were determined.

During 1983 and 1984 additional boreholes were drilled and piezometers installed. These additional boreholes form clusters, screened at different depths allowing measurements of the piezometric surface in the different hydrostratigraphic units at the same location. Thus it is possible to determine the horizontal component of ground water flow, using the water level measurements from boreholes at different locations, and also to determine the vertical component of ground water flow, using the water level measurements from the boreholes screened in the different hydrostratigraphic units at the same location. Periodic

water level measurements (monthly readings) started after completion of these wells.

In 1982 it was discovered that the water level measurements at one of the boreholes drilled by d'Apolonia (SDS-14) indicated an apparent depth of the uppermost water level of 3-4 m below surface (ca. 78 m a.s.l.), while in other wells the uppermost water level appeared to be about 15-20 m below surface (65 - 75 m a.s.l.). Subsequently 22 shallow wells (6.7 to 10.7 m deep) were augered in order to investigate in detail the shallow water table conditions. Samples were collected during drilling at 60 cm intervals using a split spoon sampler and grain size and mineralogic analyses were performed. Piezometers were installed in each borehole to a depth of 4.6 m. The results of this investigation program indicate that the Barnwell Formation is a rather heterogeneous hydrostratigraphic unit. Numerous low permeability clay lenses are intercalated in more sandy sedimentary rock, thus causing small perched ground water lenses above the general water table in the Barnwell Formation (Sargent, 1984). The general water table in the Barnwell Formation is of the order of 15 to 20 m below ground surface. Nearer the creeks where drainage of the underlying McBean occurs, this also becomes a perched water table.

Only a few hydraulic tests to determine the hydraulic conductivity had been conducted in wells located in or adjacent to Z-Area (Parizek and Root, 1984). Therefore INTERA Technologies performed a series of slug withdrawal tests in the deeper wells at Z-Area in June 1985. Prior to these conductivity tests the water levels in these boreholes were measured (Appendix A).

In 1982, a three dimensional finite difference model for the Separation Areas (about 2 km southwest of Z-Area) was developed to examine the ground water flow system in the saturated zone beneath the disposal areas (Root, 1982). This model simulated ground water movement in the Barnwell and McBean Formations.

In 1984 Parizek and Root submitted a quarterly report which attempts to establish the parameters necessary for the development of a hydrologic budget of the McQueen Creek drainage basin. The proposed disposal site (Z-Area) lies partly within the McQueen Creek drainage basin. In the hydrologic budget the following parameters were quantified: precipitation, surface runoff, ground water recharge, evapotranspiration and underflow (Parizek and Root, 1984).

The data obtained during the field and laboratory investigations outlined above were reviewed and interpreted prior to the modeling described in this report. The data review also included the results of the modeling work performed by Parizek and Root. In the following sections, the most important aspects of the data review and the results derived from it are summarized.

6.2 Geological and Geophysical Borehole Logs (d'Apolonia Report)

From 1980 to 1981 d'Apolonia performed a comprehensive drilling program (25 boreholes, SDS-2 to SDS-19) at Z-Area and vicinity (Figure 6-1). The results are presented as detailed lithological borehole profiles and as geophysical boring logs with a generalized material description (d'Apolonia, 1981). The latter are based on both the core logging during the drilling work and the geophysical logging in the boreholes (natural gamma log, self potential, single point resistance log and caliper log). No attempt was made in the d'Apolonia report (1981) to correlate the data with the regional stratigraphic units (e.g., McBean Formation or Barnwell Formation).

The review of the d'Apolonia data showed that the lithological borehole profiles are rather detailed on the one hand, but on the other hand they are insufficiently precise and discriminating to be used without further interpretation. For example, the geological description of borehole SDS-3 shown in Figure 6-2 appears rather detailed at first glance. However, the lithological description on which parameterization of a model can be based is:

0 - 40 ft	no information
40 - 66 ft	clayey sand (30-50% clay)
66 - 74 ft	sand with 5-30% clay
74 - 80 ft	sand (less than 5% clay)

This reduced information is almost the same as the generalized description presented in the geophysical boring log (Figure 6-2). Therefore the generalized descriptions were used as the primary base for further work.

The generalized descriptions contain four material categories:

- sand
- sand with a trace of clay
- clayey sand
- sandy clay

In order to check the suitability of the generalized description as a basis for the model input, its internal consistency was tested by comparison with the results of the laboratory grain size analyses (sieve curves) performed on samples taken from the boreholes during drilling.

6.3 Grain Size Analyses (d'Apolonia Report)

Grain size analyses were performed on 28 samples taken from different boreholes. The results are presented as sieve curves in d'Apolonia (1981). They show that no pure sand was found. Every sample had at least 4-5% silt or clay. Therefore the distinction between 'sand' and 'sand with a trace of clay' is not really obvious and was dropped for the further interpretative work.

Only one sample originates from a layer described as 'sandy clay' (SDS-8, 47.4 ft. depth, d'Apolonia, 1981). The sieve curve shows 40% clay and silt. There are several other samples, which were described as "clayey sand", and which show similar or even higher contents of clay

and silt; (e.g., SDS-3, 41.6 ft: 35% clay, SDS-5, 14.6 ft: 47% clay; SDS-14, 41.6 ft: 37% clay, d'Apolonia, 1981). Thus the samples 'sandy clay' and 'clayey sand' did not really represent different types of sediment. Therefore the distinction is not justified and was dropped.

After these simplifications only two types of sediments were left: 'sand' and 'clayey sand'. In order to check the consistency of this classification, the generalized descriptions from the geophysical boring logs were compared with the percentage of the silt and clay fraction from the grain size analyses. As Figure 6-3 shows, 17 samples originating from layers described as sand were analyzed. They have silt and clay contents between 4 and 20%. As already mentioned, the samples 'sand with trace of clay' are indistinguishable from the samples classified simply as sand. The percentage of the silt-clay content of the 11 'clayey sand' samples (incl. the 'sandy clay' sample) range over a relatively large interval, between 9 and 47%.

The diagrams in Figure 6-3 show the distribution of the silt and clay content in the two sedimentary types. The sand samples form a reasonably well defined group with a mean silt and clay content of about 10% (sample standard deviation 5%). However, the clayey sand samples are less uniform, with a mean silt and clay content of about 26% and a sample standard deviation of 11%.

Further attempts were made to characterize the two sample types by looking at the shape of the sieve curves. The only statement that can be made is that the 'sand' samples generally have steeper and less varying curves and therefore are somewhat better sorted.

As a result of the data review of the grain size analysis the following statements can be made:

- based on the data provided by d'Apolonia (1981) only two sedimentary rock types can be distinguished at Z-Area: 'sand' and 'clayey sand'.

- the differentiation between these two sediment types in the generalized geophysical boring logs is fairly consistent with the results of the grain size analyses.

- the generalized description in the geophysical logs possesses most of the existing information and therefore can be used for further data interpretation work. However the obvious heterogeneity of the two sample groups and the limited reliability of the boundaries between them must be taken into account.

6.4 Additional Borehole Logs (SDS-20, 21, 22)

Several years after the drilling conducted by d'Apolonia, additional boreholes were drilled at Z-Area and piezometers installed (J. Cook, pers. comm.). As discussed in Section 1.1, the additional boreholes form well clusters, each consisting of 3-4 boreholes. Geologic descriptions were available for the deepest of the three wells in each cluster (SDS-20A, SDS-21A, SDS-22A). As Table 6-1 shows, these logs provide the percentage of sand, silt and clay for finite depth intervals (60 m each).

In order to reconcile these data with d'Appolonia's generalized borehole logs, the computer logs were simplified by allowing only two types of sediments: 'sand' and 'clayey sand'. The criterion to discriminate between these two types was the percentage of the silt and clay content. Sand was defined to have generally less than 10% silt and clay. Consequently clayey sand has more than 10% silt and clay. As an exception it was found that in the boreholes SDS-20 (at 100 ft depth, or 49 m a.s.l.) and SDS-22 (at 130 ft depth = 47 m a.s.l.) calcareous sediments occur.

These simplified borehole logs were used together with d'Appolonia's generalized borehole logs for the further data evaluation.

6.5 Compilation of the Geological Data

In order to develop an understanding of the three-dimensional geological structure, the existing geological data were summarized in one diagram (Figure 6-4). For this, the topographic map and the generalized borehole logs (d'Apolonia, 1981) were used.

Figure 6-4 shows the borehole locations within the metric UTM-Grid. The grid (xy-plane) is assigned an elevation of 44 m a.s.l. The generalized borehole logs are drawn onto the plan, projecting the vertical dimension (z-direction) on the xy-plane. Thus the z-direction lies parallel to the x-direction (north-south).

Figure 6-4 reveals the extent of information available concerning the geology of the Z-Area hill. Also it discloses clearly the vertical and horizontal heterogeneity of the sedimentary rock. However, it is possible to correlate a clayey layer between elevations 60 and 70 m a.s.l., in most of the boreholes (Figure 6-5). In studies concerning the Savannah River Plant, this clayey layer is normally referred to as the "Tan Clay" (Parizek and Root, 1984).

Similarly a second clayey layer between 42 and 48 m can be recognized in the deeper wells (Figure 6-6). This clayey layer is called the "Green Clay" in studies at the Savannah River Plant (Parizek and Root, 1984).

Additionally a calcareous zone was logged in the well SDS-22, which represents the calcareous zone of the lower McBean Formation (Section 3.1.7).

Thus it is possible to correlate the geological data from the Z-Area hill with the regionally known lithology (or stratigraphy) and derive a representative lithologic (or stratigraphic) profile for the project area (Figure 6-7). It is obvious from Figure 6-4 that the thickness of the different lithologic units varies within Z-Area and vicinity, although some of the thickness variation is undoubtedly caused by the

imprecision inherent in field borehole logs. The representative lithological profile must therefore be interpreted as a typical profile with average thicknesses.

As far as the geological structure beneath Z-Area is concerned, Figures 6-5 and 6-6 reveal a relatively flat, layered system. There may be a slight dip to the south (ca. 5 m/km) in the southern part of the project area, but in the middle and northern part no uniform dip of the layers could be discerned.

6.6 Permeability and Porosity Data

The typical hydraulic conductivities of the hydrostratigraphic units at the Savannah River Plant on a regional scale are reported in Christensen and Gordon (1983). Because they were already discussed in Chapter 4, they are not repeated in this section, but Table 6-4 summarizes the data available.

D'Apolonia performed a series of permeability tests on the core samples within the context of the drilling program in 1980 and 1981. As Table 6-2 shows, 28 samples were taken from different boreholes and their permeability (in the horizontal and vertical directions) and their different porosities (total; effective; effective at 5 psi) were measured in a laboratory.

Table 6-3 shows the results of the laboratory permeability tests related to the hydrostratigraphic units as described in Section 6.5. Because of the heterogeneity of some of the hydrostratigraphic units, Table 6-3 differentiates between results derived from analyses of sample which represent sandy facies and from analyses on samples which represent clayey sandy facies.

Most of the tests (19 of 28) were performed on Barnwell samples. The results reveal the large heterogeneity within the Barnwell Formation. Sandy layers generally have permeabilities of 10^{-6} m/s, while in clayey sandy layers values between 10^{-8} and 10^{-9} m/s were measured.

On samples from the Tan Clay, values between 10^{-8} and 10^{-9} m/s were measured. However, the number of Tan Clay samples is relatively small (3).

Even fewer samples were analyzed from the McBean (2) and the Congaree (1) Formations. Because of the small sample number these values cannot be considered to be representative of the formations from which they were obtained. Therefore Table 6-4, which summarizes also the laboratory test results, shows the mean values only for the Barnwell Formation and the Tan Clay.

As reported by d'Appolonia (1981), the relationship between the horizontal and vertical permeability is somewhat erratic. No clear trend could be recognized (Table 6-3). Therefore these data were not used to estimate the ratio of the vertical and horizontal hydraulic conductivities.

Several years after the d'Appolonia work, some hydraulic tests were performed in the boreholes located at or near Z-Area (Parizek and Root, 1984). The results are also shown in Table 6-4.

In 1982 Root developed a three dimensional finite difference model of the Separation Areas (about 2 km southwest of Z-Area). This model was calibrated for steady state flow by matching the model-calculated heads to the water levels in the boreholes within the model area (Root, 1982). Root assumed a vertical to horizontal permeability anisotropy factor of 2:1 for the Barnwell and McBean Formations. The Tan Clay was implemented simply as low vertical permeability between the Barnwell and the McBean Formations. The Green Clay was considered to be impermeable, thus the McBean Formation was the lowermost aquifer included in Root's model. During the calibration, Root assigned the same hydraulic conductivities to the Barnwell and McBean Formations. Thus only two parameters remained to be varied, i.e., the hydraulic conductivity of the Barnwell and McBean Formations and the vertical hydraulic conductivity of the Tan Clay.

Root found the best match to the water level data was obtained using 2.1×10^{-5} m/s as the horizontal hydraulic conductivity for the Barnwell and McBean Formations, and 1.9×10^{-8} m/s as the vertical hydraulic conductivity for the Tan Clay (Figure 6-4).

In June 1985 INTERA performed additional hydraulic tests in some of the boreholes at Z-Area. The tests and their results are discussed in Appendix A. The final results (arithmetic mean values) are shown in Table 6-4.

Thus Table 6-4 summarizes 5 data groups (Christensen and Gordon, d'Appolonia, Parizek and Root, Root and INTERA). A comparison shows that the values usually range over two orders of magnitude for each hydrostratigraphic unit. This simply reflects the heterogeneity of the hydrostratigraphic units at Z-Area.

Although the hydraulic conductivities used for modeling Z-Area resulted from model calibration (matching the known water levels), it is useful to estimate the possible range in which the model hydraulic conductivities should fall.

The Barnwell data (sandy facies) lie fairly consistently between 1×10^{-6} m/s and 2.1×10^{-5} m/s. Thus the effective hydraulic conductivity used by the calibrated model should lie within this range.

For the Tan Clay few data are available. The existing data indicate a hydraulic conductivity of about 10^{-8} m/s. Therefore it can be expected that the model conductivity will be within the range of 0.5×10^{-8} to 5×10^{-8} m/s.

The most data are available for the McBean Formation. The mean values vary between 1×10^{-6} m/s and 3×10^{-5} m/s. Thus the effective hydraulic conductivity used by the calibrated model should fall in that range.

No data are available for the Green Clay. Based on the lithological description and on the fact that the Green Clay apparently acts as a confining bed between the McBean and Congaree Formations, a relatively low permeability can be assumed. Thus the hydraulic conductivity of the Green Clay likely lies between 10^{-10} m/s and 10^{-8} m/s.

Fewer data are available for the Congaree Formation than for the McBean Formation. Generally the hydraulic conductivities are higher in the Congaree than in the McBean Formation (Table 6-4). Christensen and Gordon (1983) report a factor of 10; which was one of the reasons to consider the Congaree Formation as a separate hydrostratigraphic unit (Section 3.1.5). Thus the expected range for the hydraulic conductivity of the Congaree Formation in the model is from 10^{-5} m/s to 5×10^{-4} m/s.

No data are available concerning the vertical anisotropy of the hydraulic conductivity of the Congaree Formation, i.e., the ratio of the vertical to horizontal hydraulic conductivity (see also Appendix A.3). Therefore these values were estimated for modeling Z-Area (Section 7.3).

The results of the porosity measurements by d'Appolonia are summarized in Table 6-2. The measured total porosities vary between 26% and 45.7%. The effective porosities (at 5 psi) range from 2.1% to 28.1%. This is fairly consistent with the existing literature. Christensen and Gordon (1983) reported an effective porosity value of 20% as being a reasonable estimate for both the McBean and Barnwell Formation. Root (1982) assumed a value of 25% for modeling the Separation Areas.

For transport modeling, the effective porosity for transport is somewhat higher than the effective flow porosity, but smaller than the total porosity. Thus a porosity of 30% is assumed for the transport modeling presented later in this report.

6.7 Piezometric Data

The piezometric surface of the ground water in the different hydrostratigraphic units at the Savannah River Plant is generally well known (Christensen and Gordon, 1983). An introductory overview is given in Chapter 4 of this report.

The ground water levels were periodically measured in boreholes at and adjacent to Z-Area beginning with January 1982. Water level data are available for two time periods: (1) January 1982 - December 1982 and (2) March 1984 - August 1985. As Table 6-5 shows, most of the wells drilled by d'Appolonia are screened in the Barnwell Formation. For the more recently drilled wells ("additional boreholes") no exact piezometer specifications were available, but according to the piezometer specifications (J. Cook, pers. comm.) they are open to the Congaree and the McBean Formations.

All available data are listed in Appendix A. Table 6-5 is a summary of piezometer readings only. Table 6-5 presents (for each borehole), the screened formation, the number of readings, the minimum and maximum and the mean value of all readings.

As Table 6-5 shows, the uppermost formation monitored is the Barnwell Formation. The mean water levels in the Barnwell Formation generally lie between 70 and 73 m a.s.l. Assuming 69 m a.s.l. as the elevation of the top of the Tan Clay, only the lowermost 4 m of the Barnwell Formation are fully saturated on the average. As an exception borehole SDS-14A shows comparably high water levels. Obviously a very local perched water table was measured there. As discussed in Section 6.1, this phenomenon was investigated by an additional drilling and investigation program (Sargent, 1984).

During the years, the water levels in the boreholes screened in the Barnwell Formation showed relatively strong fluctuations as compared to the thickness of the saturated zone. Except at borehole SDS-14A, the

fluctuations, i.e., the difference between the recorded maximum and the recorded minimum (INTERA's measurements not included), range from 1.63 to 3.26 m with an average of 2.2 m. Apparently the water table in the Barnwell Formation can also completely disappear in dry seasons (see Appendix A). Therefore it is difficult to determine representative "steady state" water levels as would be required for steady state modeling. Consequently the Barnwell water levels were not used as calibration data for the modeling study. Rather, a sensitivity analysis was performed for those parameters (permeability of the Tan Clay; infiltration rate) on which the water table in the Barnwell Formation depends most (see Section 9.2).

However, to set up correctly the boundary conditions for the model, at least an estimation of the piezometric surface within the Barnwell Formation is required. Because boundary conditions will be applied to the Barnwell Formation only at the southern edge of the model area (Section 7.1), it is there that the water levels must be known or estimated. The piezometric surface map, which covers the Savannah River Plant Separation Areas (Figure 4-5) was taken as the basis for that water table estimation at Z-Area. This map is based on data from 1968. As the meteorologic data (Figure 5-2) show, in 1966 and 1967 the precipitation was close to the long term average of 1215 mm. The year 1968 itself received less rainfall (ca. 1000 mm) than the average year. However taking into account the response time for hydrologic systems of that size, the water table elevations shown in Figure 4-5 can be considered to be representative.

The ground water contour lines from Figure 4-5 are shown in Figure 6-8 at an enlarged scale. Additionally the mean water levels from Table 6-5 are shown on Figure 6-8. A comparison reveals that although there is a fair general agreement between the more regional piezometric surface map and the local well measurements, the contour lines do not extend as far to the north as estimated in the more regional study. Therefore the contour lines were corrected on the local scale using the mean water level data from the Z-Area wells (Figure 6-8). This corrected piezo-

metric surface was later used for the definition of the boundary conditions applied to the Barnwell Formation at the southern edge of the model (Section 7.1).

The next aquifer below the Barnwell Formation is the McBean Formation. The water levels in the McBean Formation range from 61 to 71 m a.s.l. (mean values). Assuming 66 m as the elevation for the bottom of the Tan Clay, the ground water in the McBean is confined at the center and the southern part of the Z-Area and exhibits a free water surface near the slopes of the Z-Area hill, where the McBean Formation is drained by the creeks. The fluctuations of the water levels in the McBean Formation range from 0.4 to 3.4 m over the monitoring period. The average fluctuation is 2.4 m, which is comparable to the average fluctuation in the Barnwell Formation. Again borehole SDS-14 shows exceptionally high water tables and large fluctuations.

As in the Barnwell Formation, the water levels in the McBean Formation can fall below the bottom of the screened interval of the shallower boreholes (see Appendix A). Because of the difficulties in estimating a representative 'steady state' water table for these piezometers, only the deeper borehole data (SDS-7C, SDS-12B, SDS-20B, SDS-21B, SDS-22C) were used for the model calibration. In these boreholes, the water level measurements by INTERA (June 1985, Appendix H) are in very good agreement with the long term mean values. The deviation is 32 cm or less. Table 6-6 summarizes the water level data utilized for the model calibration.

As in the Barnwell Formation, an estimation of the piezometric surface in the McBean Formation is also required for definition of the southern boundary conditions of the model (Section 7.1). Again a more regional piezometric surface map for the McBean Formation was used as a basis for that estimation on a local scale. In this case, the regional piezometric surface map (Figure 4-4) is based on water level measurements taken in August 1977. The precipitation data (Figure 5-2) show that, although the precipitation in 1976 was above the average annual rainfall

(ca. 1250 mm) the precipitation in 1977 itself was below the average (ca. 1100 mm). Thus the contour map from 1977 can be considered to be representative.

The ground water contour lines from Figure 4-4 are shown in Figure 6-9 at an enlarged scale. Additionally the mean water levels (Table 6-5) in the deeper boreholes, which were also selected for the model calibration, are shown on the map. A comparison shows that the general agreement is good, although the local well data are somewhat higher than one would expect based on the contour lines only. Using the remaining borehole data from Table 6-5, the mean water levels in SDS-14 and SDS-13 are in excellent agreement with the contour lines, while on the other hand the values from SDS-18 and SDS-19 are comparably too high.

However, the data base was not considered to be sufficiently large and reliable to allow substantial improvement in the existing piezometric surface map for the McBean Formation by correcting the contour lines on the basis of the local well data. Thus the uncorrected map shown in Figure 6-9 was used for the definition of the boundary conditions applied to the Barnwell Formation at the southern edge of the model (Section 7.1).

The lowermost aquifer screened in the wells at Z-Area is the Congaree Formation. The Congaree water levels lie between 49 and 53 m a.s.l. This is consistent with the literature (e.g., Christensen and Gordon, 1983) where the large head differential between the McBean and the Congaree Formation is emphasized (Section 4.2.4). This head difference demonstrates that the two aquifers are relatively separated hydraulically by the Green Clay.

Compared to the McBean Formation above, the water levels in the Congaree Formation show relatively small fluctuations. The fluctuations over the monitoring period range from 0.2 to 0.8 m with an average of 0.5 m. The water level measurements performed by INTERA in June 1985 (see Appendix A) are in very good agreement with the long term mean (devi-

ation 20 cm or less). Therefore all mean water levels from the boreholes screened in the Congaree Formation (Table 6-6) were used for the model calibration.

Unlike the Barnwell and the McBean Formations, the information about the piezometric surface in the Congaree Formation that can be derived from regional studies (Figure 4-2) is not sufficiently detailed to be used in a local large scale map such as Figure 6-10. But as Figure 4-2 shows, there will be a need for defining boundary conditions in the southeast and the northwest of Z-Area in the later model. Like in the aquifers above, the definition of these boundary conditions must be based on an estimation of the local piezometric surface.

Because the regional piezometric surface map is too general, only the mean water levels from the wells at Z-Area (Table 6-5) are illustrated on the local map (Figure 6-10). Based on the regional information (Figure 4-2) two additional assumptions are justified: (1) the ground water flow at Z-Area is directed toward the northeast to Upper Three Runs Creek, and (2) the flow field is constant throughout the area of interest. Based on the well data and these two assumptions, the piezometric surface of the Congaree Formation was estimated (Figure 6-10) and used as the basis for definition of the boundary conditions applied to the Congaree Formation in the actual model (Section 7.1).

In summary the review of the piezometric data provided water level data for the McBean and the Congaree Formations, which can be used to calibrate the model. The piezometric surfaces in the three aquifers (Barnwell, McBean and Congaree Formations) were estimated from both the water level measurements in wells at Z-Area and the results of previous, more regional studies.

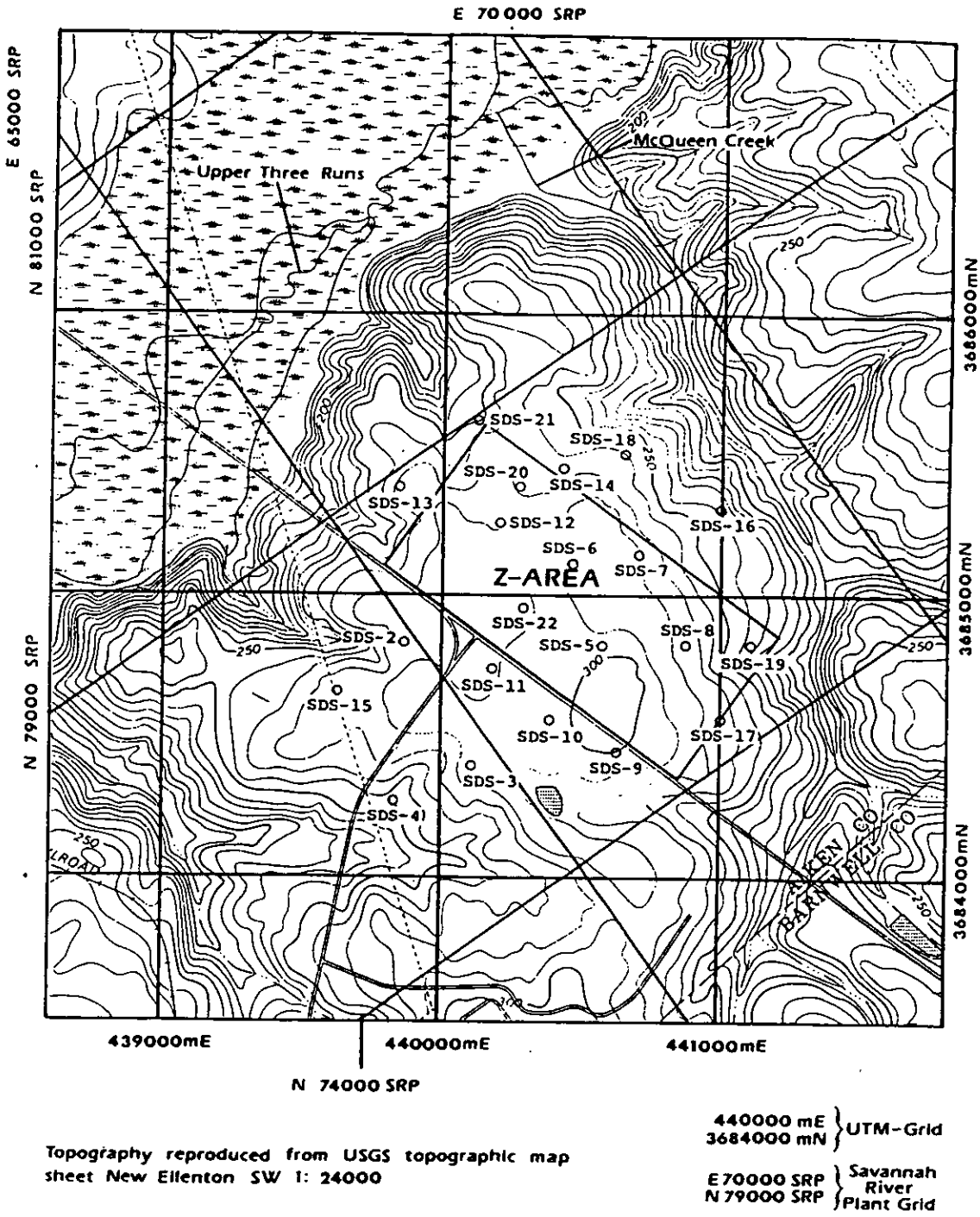

Figure 6-1 Borehole Locations at Z-Area

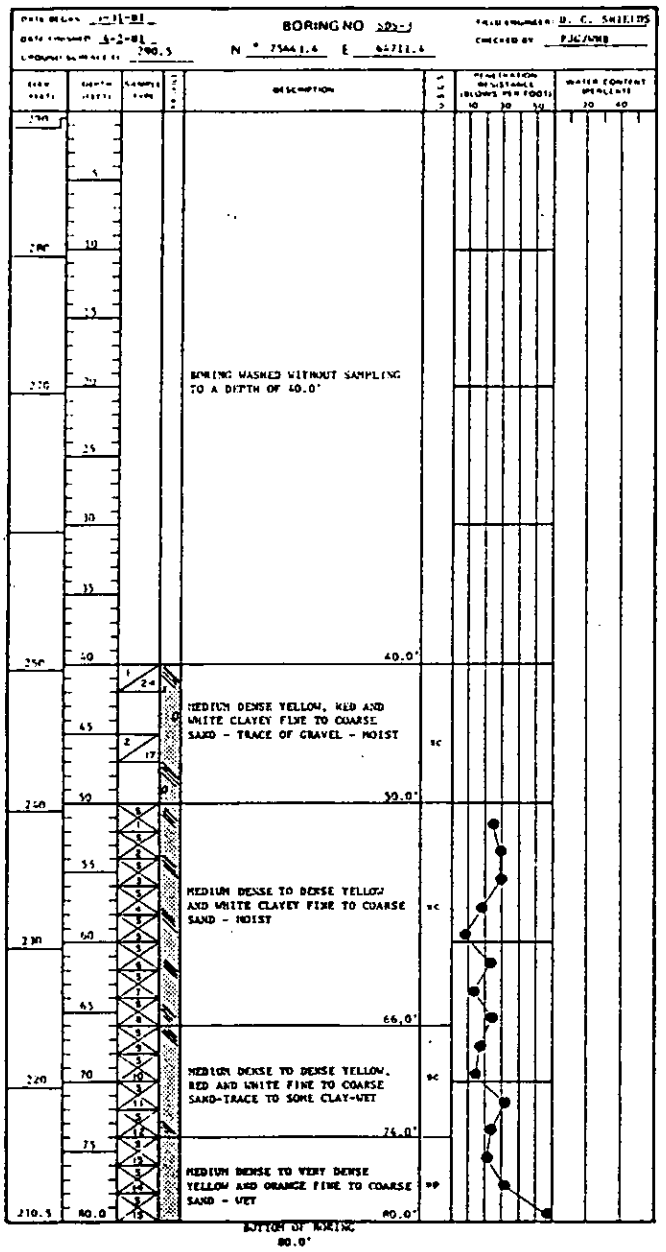

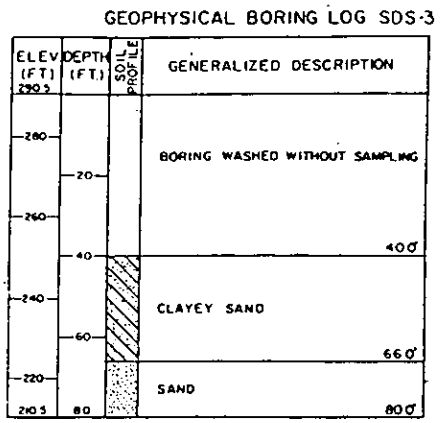

Figure 6-2 SDS-3 Borehole Log (from d'Appolonia, 1981)

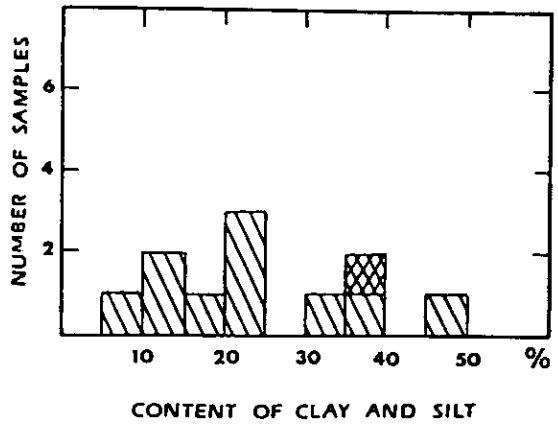

GENERAL DESCRIPTION

SANDY CLAY

CLAYEY SAND

NUMBER OF SAMPLES: 11
MEAN CLAY-SILT CONTENT: 26.3%
STANDARD DEVIATION: 11.3%

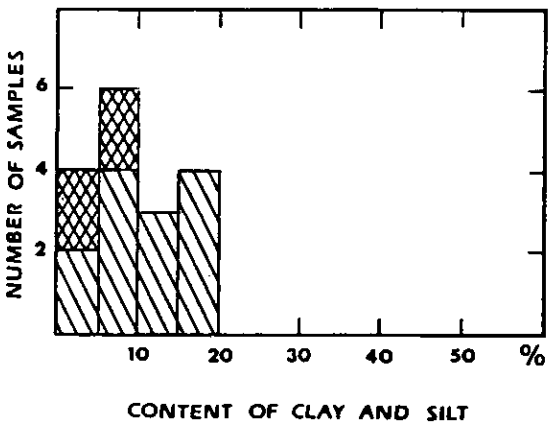

GENERAL DESCRIPTION

SAND

SAND WITH TRACE OF CLAY

NUMBER OF SAMPLES: 17
MEAN CLAY-SILT CONTENT: 10.2%
STANDARD DEVIATION: 5.2%

Figure 6-3 Grain Size Analyses: Contents of Clay and Silt (data from d'Appolonia, 1981)

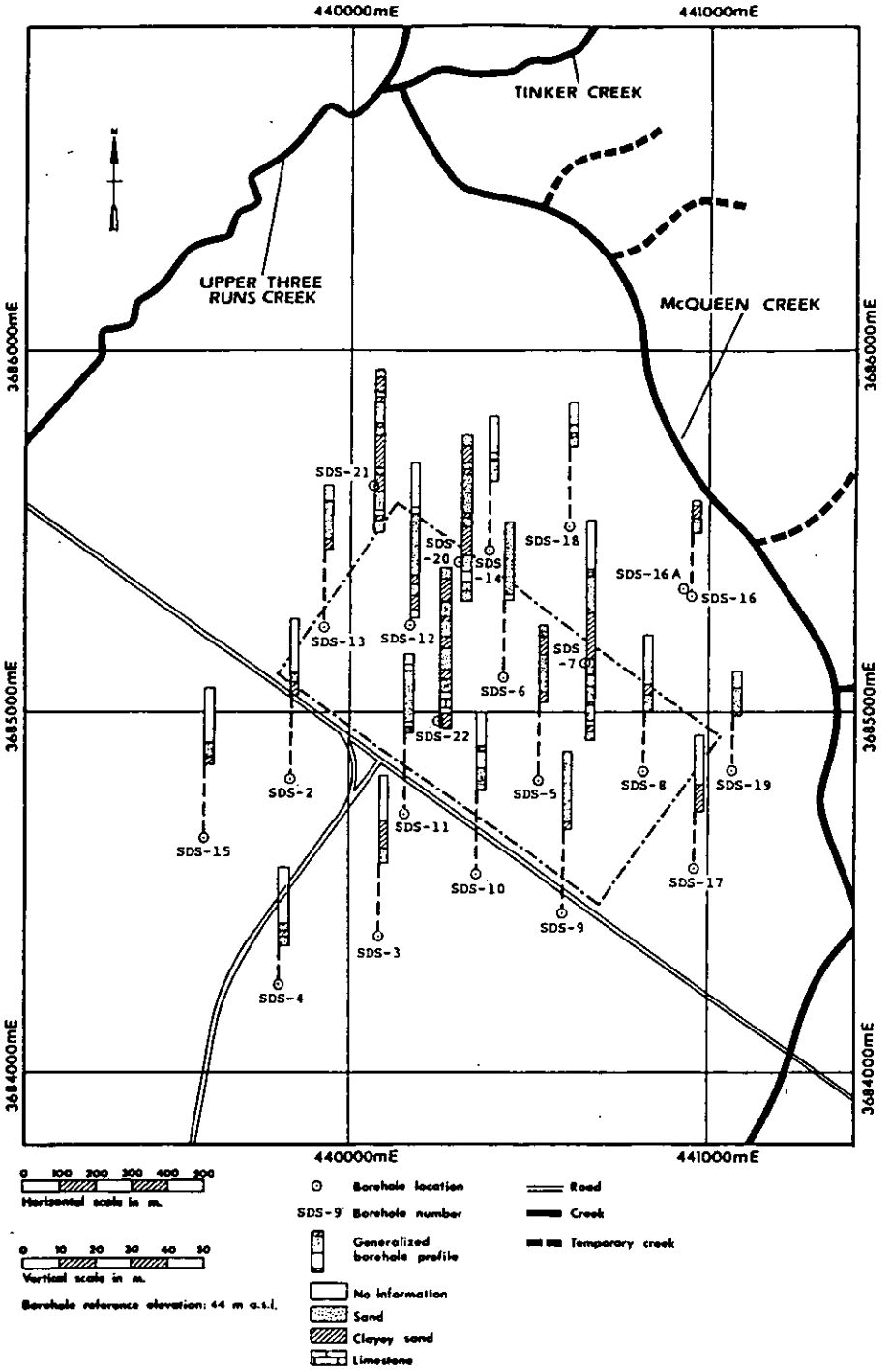

Figure 6-4 The Spatial Distribution of the Geological Data

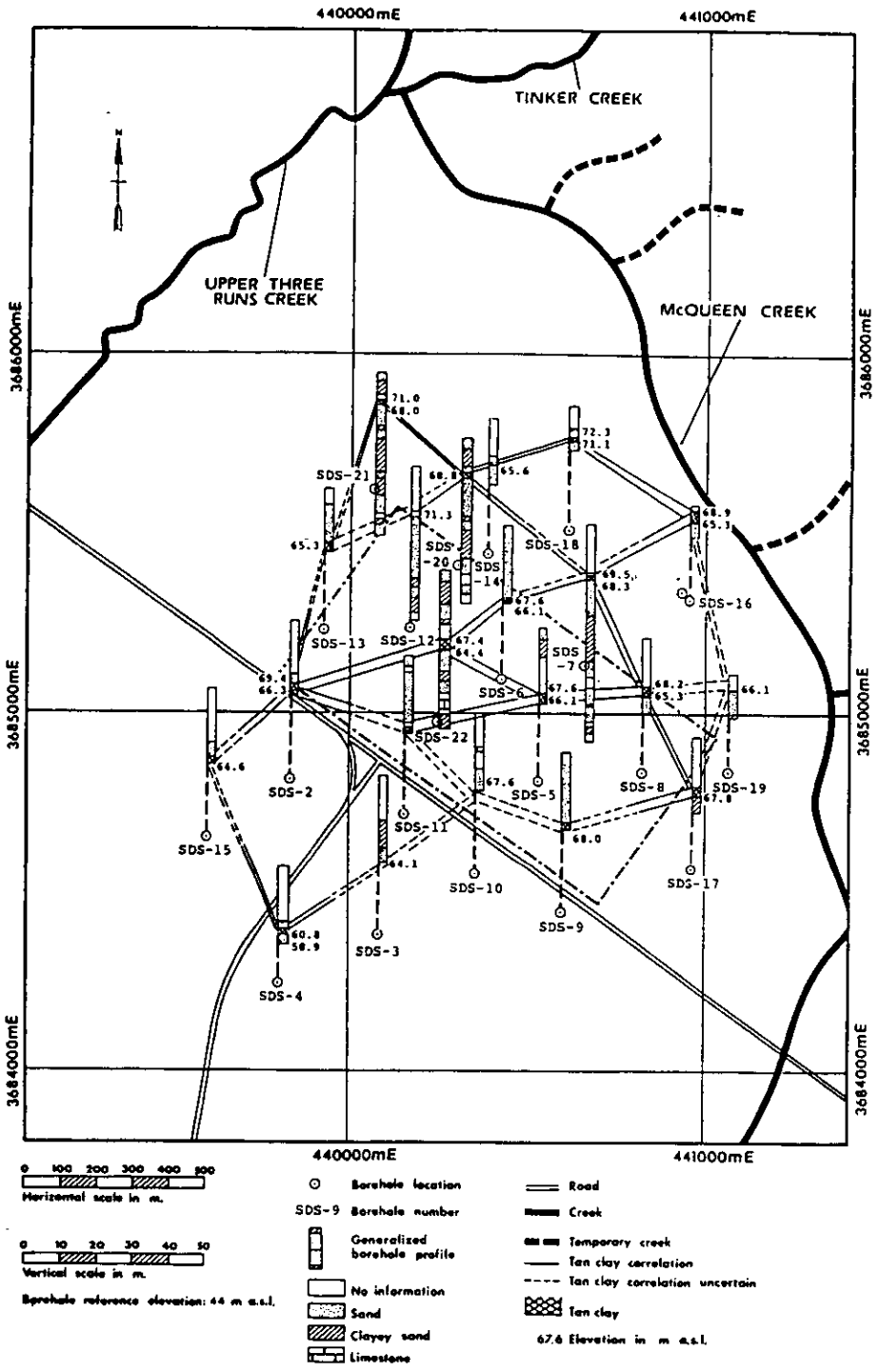

Figure 6-5 The Tan Clay at Z-Area

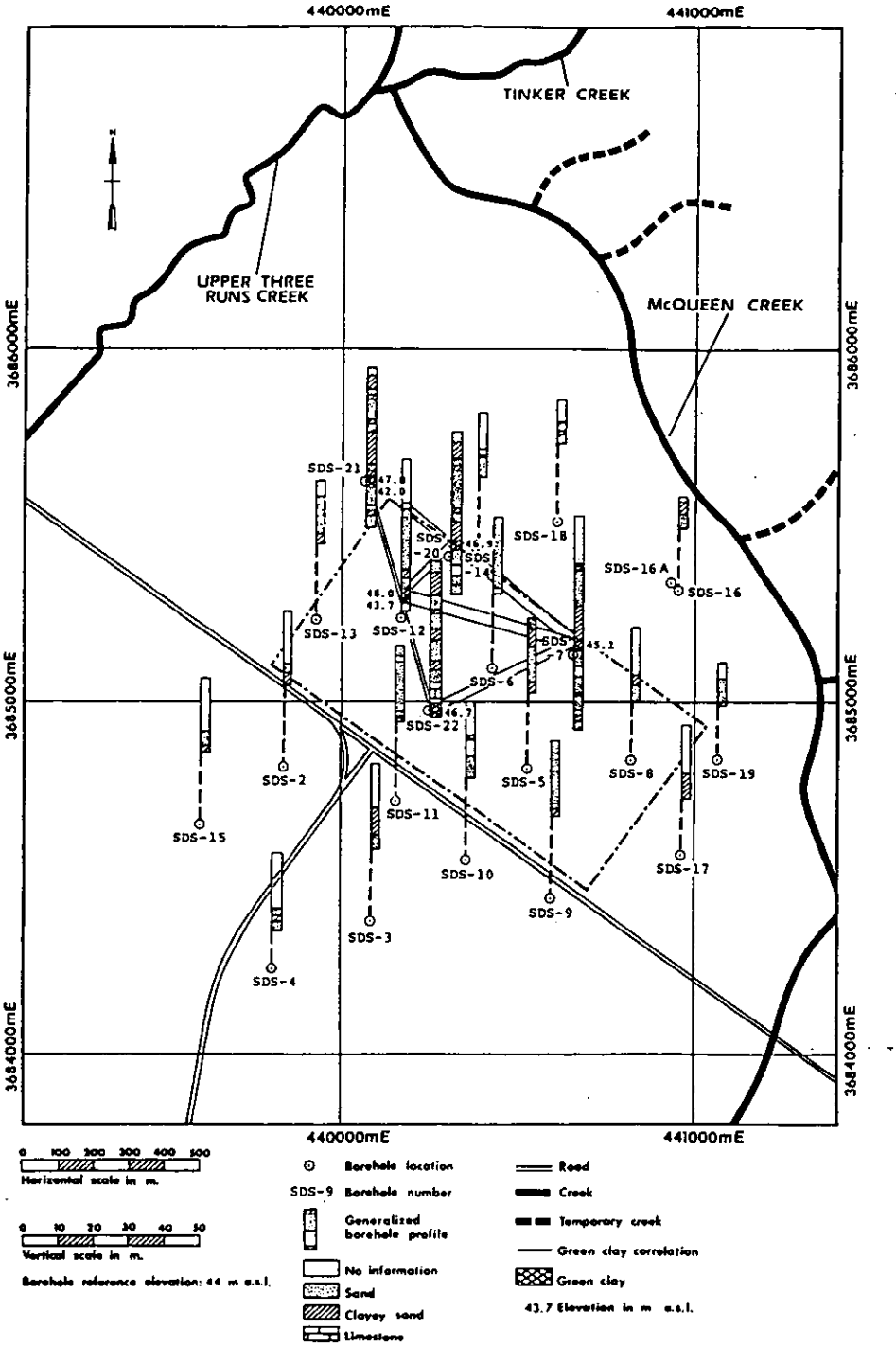

Figure 6-6 The Green Clay at Z-Area

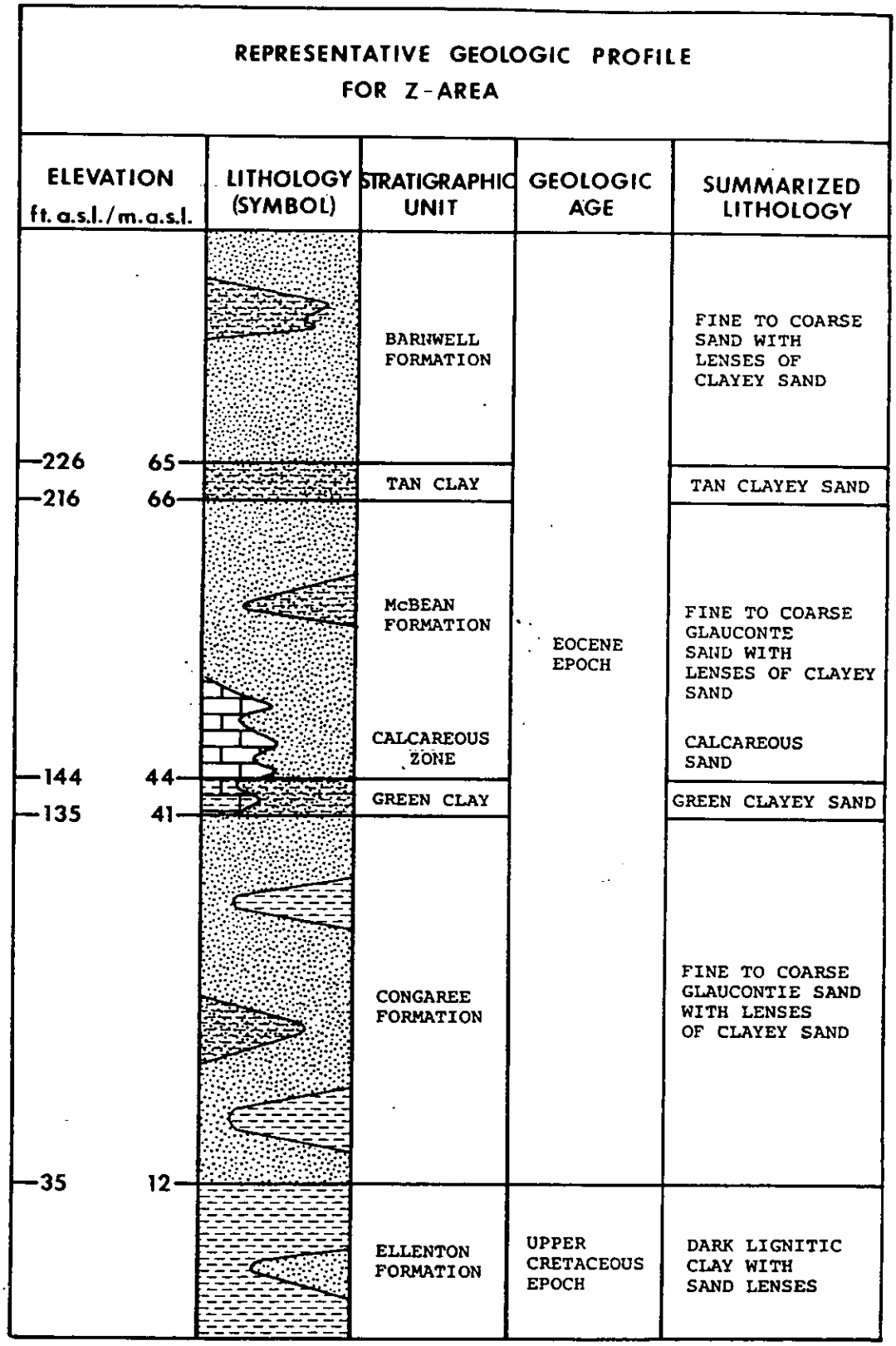

Figure 6-7 Representative Geologic Profile for Z-Area

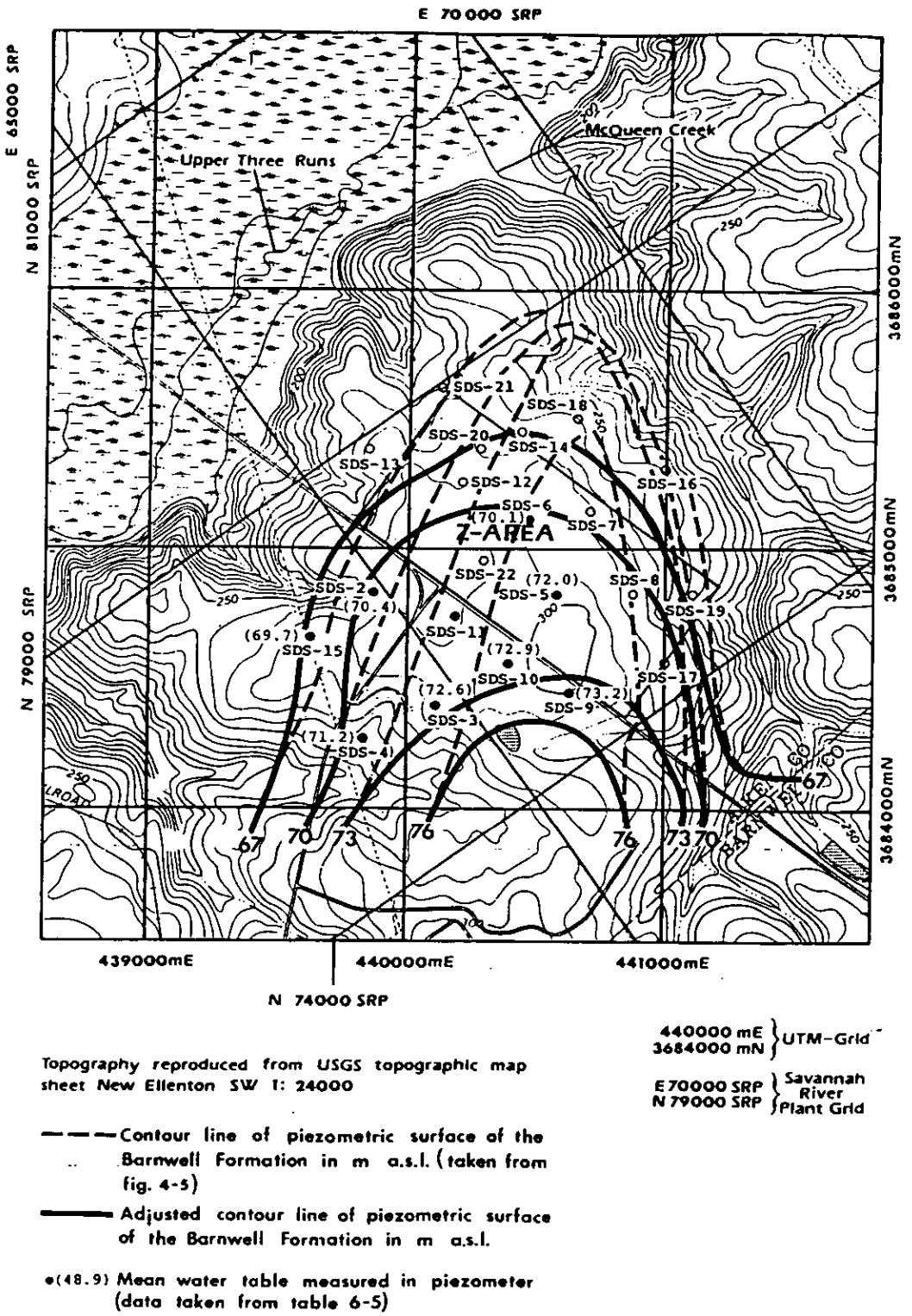

Topography reproduced from USGS topographic map sheet New Ellenton SW 1: 24000

——— Contour line of piezometric surface of the Barnwell Formation in m a.s.l. (taken from fig. 4-5)

——— Adjusted contour line of piezometric surface of the Barnwell Formation in m a.s.l.

•(48.9) Mean water table measured in piezometer (data taken from table 6-5)

Figure 6-8 The Estimated Piezometric Surface of the Barnwell Formation at Z-Area

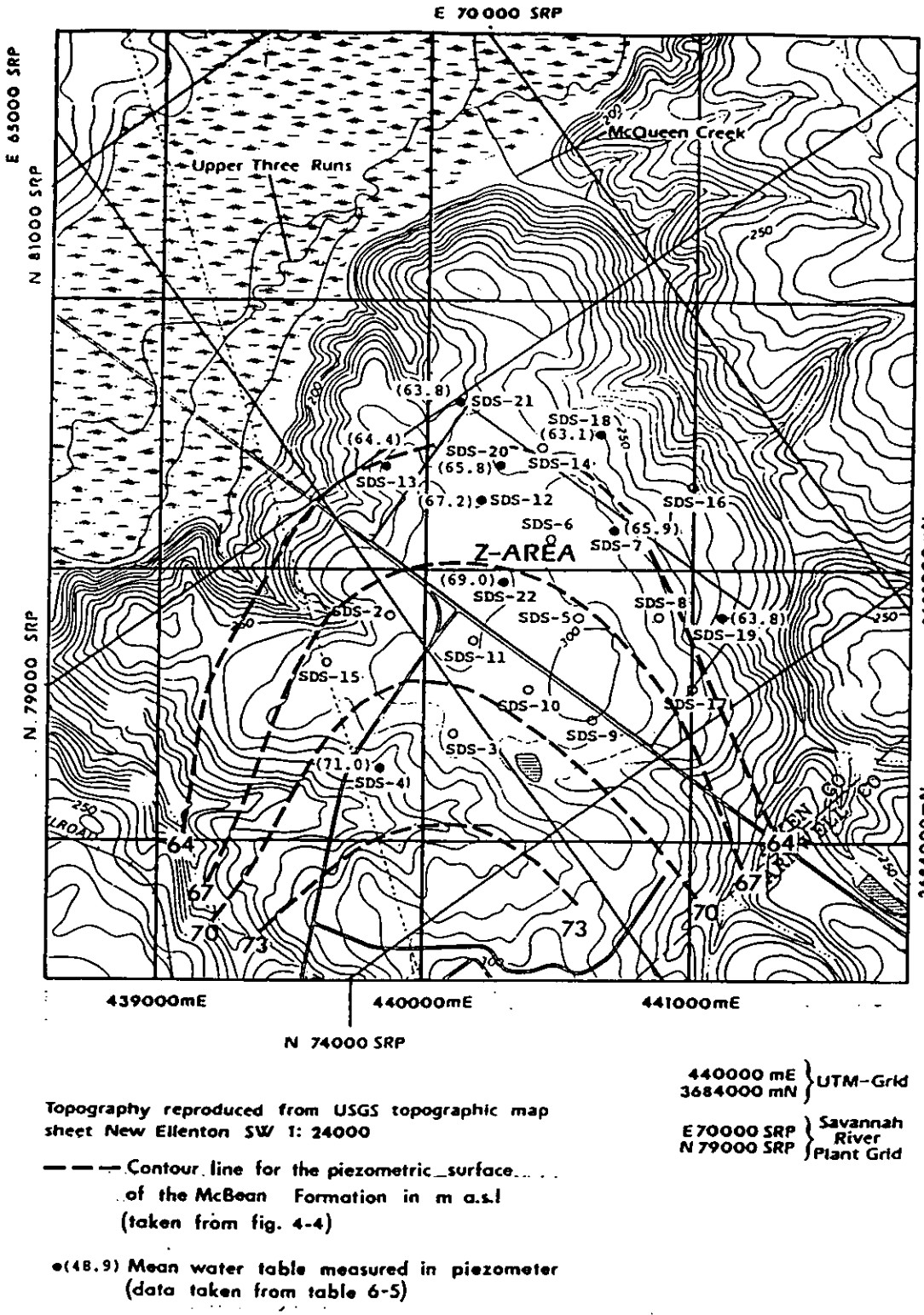

Figure 6-9 The Estimated Piezometric Surface of the McBean Formation at Z-Area

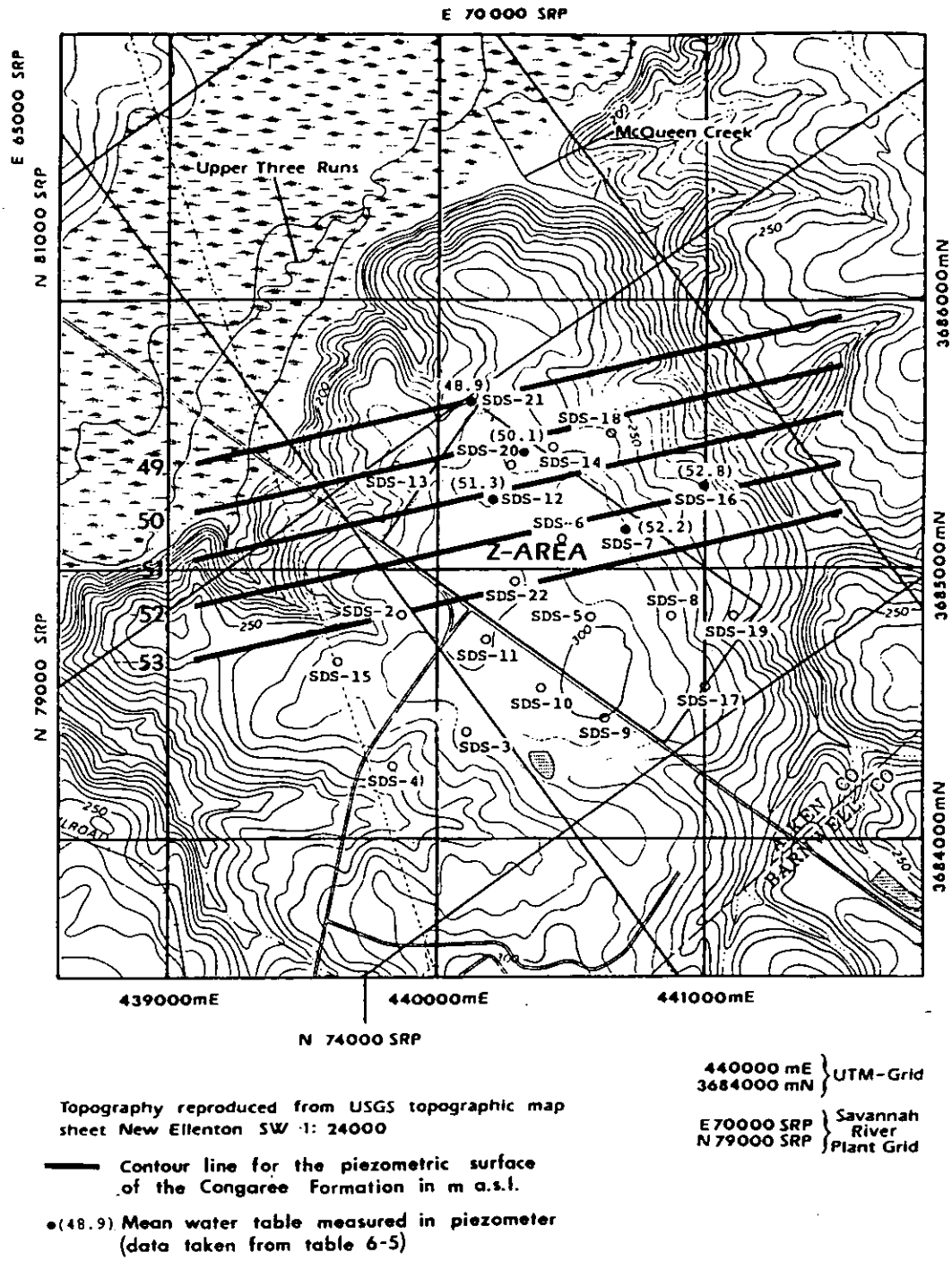

Figure 6-10 The Estimated Piezometric Surface of the Congaree Formation at Z-Area

Borehole	Depth (ft)	Color	Structure	Rock Name
SDS 20A	00	212TA	MA	9010 SD C M P1
SDS 20A	02	205GY YE	CLB	900505GY YE SD C M P1
SDS 20A	04	212YE	MA	97 03YE SD C M M1
SDS 20A	06	218OR YE	MA	93 07YE SD VCM V1
SDS 20A	08	217RE OR	MT	0203452525YE OR SDSTCL04M V1
SDS 20A	10	220RE	MA	0203602510RE STSD 04M V1
SDS 20A	12	221OR RE	MA	851005RE OR SD C F V1
SDS 20A	14	220OR RE	MA	801010OR RE SD VCM V1
SDS 20A	16	219OR	MA	950203OR SD M F P3
SDS 20A	18	215OR BR	MA	9505 SD VCM P2
SDS 20A	20	215OR BR	MA	50 50OR BR CLSD VCM V2
SDS 20A	22	213OR	MA	90 10OR SD C M P2
SDS 20A	24	218OR	MA	900505OR SD C M V1
SDS 20A	26	221OR	MA	950203OR SD C M W2 1Y
SDS 20A	28	218YE	MA	910504YE SD C M P2
SDS 20A	30	224YE	MA	030270 25YE CLSD 04M V1
SDS 20A	32	208YE	MA	85 15YE SD VCM V1
SDS 20A	34	207YE	MA	90 10YE SD VCM V1
SDS 20A	36	212L BR	MA	93 07L BR SD M F M3
SDS 20A	38	215M BR	MA	90 10M BR SD C F M2
SDS 20A	40	215M YE	MA	98 02M YE SD C M M2
SDS 20A	42	212M YE	MA	98 02M YE SD C M M2 02
SDS 20A	44	208M YE	MA	99 01M YE SD C M M2 2Y
SDS 20A	46	209L BR	MA	99 01L BR SD C M M2
SDS 20A	48	215M BR	MA	99 SD 08M M2
SDS 20A	50	212M BR	MA	98 02YE SD C M M2
SDS 20A	52	212M BR	MA	99 SD C M M2 3Y
SDS 20A	54	214D BR	MA	96 04BR SD C F M2
SDS 20A	56	222M BR	MA	01 95 04BR SD 06M M2
SDS 20A	58	218M BR	MA	01 970101M BR SD 04M M2
SDS 20A	60	221M YE BR	MA	99 SD VCF W3
SDS 20A	62	219M YE BL	MA	99 SD C M M2 1Y
SDS 20A	64	213D GY BR	MA	98 02TA SD C M M2 2Y
SDS 20A	66	210M YE BR	MA	99 SD VCC M2
SDS 20A	68	220M YE BR	MA	99 SD C C M2
SDS 20A	70	212M BR	MA	70 30TA CLSD C M P2 2Y
SDS 20A	72	212YE BR	MA	25 75TA SDCL F CL 2Y
SDS 20A	74	220M BR	MA	97 03TA SD C M M2 2Y
SDS 20A	76	210M YE	MA	99 SD C VFW3 1Y
SDS 20A	78	210M YE BR	MA	85 15TA SD C F M3 02
SDS 20A	80	213M YE	MA	93 07TA SD C M M3
SDS 20A	82	211L TA YE	MA	75 25TA CLSD F F M3
SDS 20A	84	207L TA	MA	030285 10TA 10SD 08VFM3 1Y
SDS 20A	86	207L TA	MA	02 631025TA 20CLSD 24VFP3 3Y
SDS 20A	88	212M BR	MA	99 01OR SD C M M2 2Y
SDS 20A	90	201M BR	02	88 10TA 50LSSD 24C P2
SDS 20A	92	200 NO RECOVERY		
SDS 20A	94	208TA	MA	75 25TA 05CLSD 12VFM3
SDS 20A	96	220L TA	MA	05 70 25TA 15CLSD 24F M3 3Y
SDS 20A	98	221L TA	MA	07 68 25 20CLSD 32F M3
SDS 20A	100	211L TA	MA	05 603005TA 50LSSTSD04VFM3 Y
SDS 20A	102	209D YE BRF	ICL	800515TA 05SD C F M3
SDS 20A	104	221D BK GN	MA	30 70GN SDCL C CL
SDS 20A	106	206GN	MA	55 45GN CLSD C M P2 0202
SDS 20A	108	212GN TA	MA	99 01YE SD VCC M2Y 02 1Y
SDS 20A	110	208GY TA GN	MA	98 02YE SD C M M3
SDS 20A	112	212GN	MA	90 10GN SD C M P2 10
SDS 20A	114	212D GN	MA	92 08GN SD C M P2 10 1Y
SDS 20A	116	209GY TA	MA	98 02GY TA 01SD VCM M2 1Y
SDS 20A	118	220GY GN	MA	020392 03GY GN SD 04C P2Y 05
SDS 20A	120	205GN TA	MA	010395 02GN TA SD 04C P2 2Y
SDS 20A	122	200 NO RECOVERY		
SDS 20A	124	200 NO RECOVERY		
SDS 20A	126	200 NO RECOVERY		
SDS 20A	128	223TA	MA	99 SD M F W3 2Y
SDS 20A	130	200 NO RECOVERY		
SDS 20A	132	206TA	MA	98 02TA SD C M M2
SDS 20A	134	203D TA	MA	97 03TA SD VCC M2Y 1Y
SDS 20A	136	207BR TA	MA	0395 02BR TA SD GRM M2
SDS 20A	138	206BR	MA	99 SD VCM M2 2Y
SDS 20A	140	209BR	MA	99 SD VCC W2 1Y
SDS 20A	142	208BR	MA	99 SD C M W2
SDS 20A	144	209L BR	MA	99 SD C F M2
SDS 20A	146	208GY	ICL	99 GY SD M F W3
SDS 20A	148	210TA	MA	99 SD C F W2 1Y

Table 6-1a Borehole Log SDS-20

(Legend see Table 6-1d)

Borehole	Depth (ft)	Color	Structure				Rock Name			
SDS 21	00	209BL OR	MA		98	02OR	SD	C F M2	03	1Y
SDS 21	02	219BR OR	MA		99		SD	VCF M2		1Y
SDS 21	04	213RE OR	MA		95	05OR	SD	C F M2		
SDS 21	06	212OR	MA		75	25OR	CLSD	C F P1		1Y
SDS 21	08	221OR	MA	02	78	20OR	SD	08M V1		
SDS 21	10	222OR	MA		75	25OR	CLSD	VCM V2		
SDS 21	12	220OR	MA		75	25OR	CLSD	VCM V2		
SDS 21	14	224OR	IPB CLB	05	70	25OR	CLSD	03M V2		1Y
SDS 21	16	220OR	ICL		75	25OR	CLSD	VCM M2		
SDS 21	18	220OR	MA		95	05OR	SD	C M M2		
SDS 21	20	218YE OR	MA		95	05OR	SD	VCF M2		
SDS 21	22	215YE OR	CLB ICL		85	15OR	SD	M F M2		
SDS 21	24	210YE TA	ISD		05	95TA	CL	C CL		
SDS 21	26	224TA YE	MA		020	395TA	CL	M CL		
SDS 21	28	212L YE TA	MA		80	10TA	SD	C F M2		
SDS 21	30	212L YE TA	MA		97	03OR	SD	M F W2		1Y
SDS 21	32	210BR	MA		98	02OR	SD	C F W3		
SDS 21	34	207BR	MA		98	02OR	SD	C F W3		
SDS 21	36	212BR	MA		98	02OR	SD	C F W3		
SDS 21	38	210OR BR	MA		98	02OR	SD	C M M3		
SDS 21	40	218OR BR	MA		95	05OR	SD	C M P1		
SDS 21	42	208YE OR	MA		97	03OR	SD	C M M2		
SDS 21	44	209BR YE	MA		98	02OR	SD	C M M2		
SDS 21	46	209BR YE	MA		99	01OR	SD	C M M2		
SDS 21	48	210YE	MA		60	40YE WH	CLSD	C M V1		
SDS 21	50	213GN BR	LAM		30	70GN TA	SDCL	M CL		
SDS 21	52	211YE	MA		99	01YE	SD	C M M2		
SDS 21	54	213YE	MA		99		SD	C M M2		3Y
SDS 21	56	210YE	ICL		95	05YE TA	SD	C M M3		
SDS 21	58	210GY YE	MA		90	10WH	SD	C M V1		
SDS 21	60	215YE	MA		75	25YE	05CLSD	M F P2		Y2Y
SDS 21	62	212GN PI	MA	01	64	25 10GN	07STSD	24VFW3		2Y
SDS 21	64	223L YE TA	MA	02	68	20 10L YE TA	07STSD	20VFM3		Y
SDS 21	66	210TA	MA		80	10 10TA	08SD	24F W3		
SDS 21	68	220TA	MA		75	25TA	05CLSD	10F M3		
SDS 21	70	209TA	MA	02	88	10TA	05SD	12F M3		
SDS 21	72	213TA	MA	05	80	15TA	05SD	20F M3		
SDS 21	74	215TA	MA	05	80	15TA	05SD	30F M3		Y
SDS 21	76	220TA	MA	60	15	25	60CLCO	24VCV1		Y
SDS 21	78	212TA	MA	50	10	10 20 10TA	70CO	20VCV1		
SDS 21	80	210YE TA	MA	05	05	50 40YE TA	10CLSD	12M V2		
SDS 21	82	209YE TA	MA	05	40	55YE TA	10SDCL	20CLV2		
SDS 21	84	218YE TA	MA	05	70	25	10CLSD	15VFV2		
SDS 21	86	222TA GN	MA	12	78	10TA GN	12SD	03VFW2		Y
SDS 21	88	210GY GN	MA		99		05SD	C F W3		
SDS 21	90	210GN	MA		95	05GN	SD	C F M3Y	03	01
SDS 21	92	209GN	MA		90	10GN	SD	M F M3Y		
SDS 21	94	218GN	ISD		05	10 85GN	CL	C CL Y		
SDS 21	96	212GN	MA		10	90GN	01CL	VCCL		
SDS 21	98	212GN	MA		25	75GN	SDCL	VCCL		
SDS 21	100	211GN	MA		05	95GN	CL	C CL	02	
SDS 21	102	215GN	MA			05 95GN	CL			
SDS 21	104	209GN	MA	01	30	69GN	SDCL	06CL		
SDS 21	106	203GN	MA		75	25GN	CLSD	VCC V1		
SDS 21	108	200 NO RECOVERY								
SDS 21	110	205GY GN	MA		95	05	03SD	C M V2		
SDS 21	112	200 NO RECOVERY								
SDS 21	114	208GY	MA		99		SD	C M M2		
SDS 21	116	203GN GY	MA		99		05SD	C F M2		3Y
SDS 21	118	203GY	MA		99		01SD	C M W2		3Y
SDS 21	120	210GY	MA		99		01SD	C M M3		3Y
SDS 21	122	204GY	MA		99		02SD	C M M3		2Y
SDS 21	124	203GY	MA		99		01SD	C M M3		2Y
SDS 21	126	208GY	MA		99		01SD	VCM M3		2Y
SDS 21	128	200 NO RECOVERY								
SDS 21	130	200 NO RECOVERY								
SDS 21	132	212TA GY	MA		99		01SD	VCC M3		2Y
SDS 21	134	210TA GY	MA		99		01SD	C M M2		2Y
SDS 21	136	200 NO RECOVERY								
SDS 21	138	210TA GY	MA		99		SD	C M M2		2Y
SDS 21	140	210TA GY	MA		99		SD	C M W2		2Y
SDS 21	142	210TA GY	MA		99		SD	C M W2		2Y
SDS 21	144	210GY GN	MA		99		SD	C M W2		2Y
SDS 21	146	200 NO RECOVERY								
SDS 21	148	212GY GN	MA		99		SD	C M W2		2Y

Table 6-1b Borehole Log SDS-21

(Legend see Table 6-1d)

Borehole	Depth (ft)	Color	Structure	Rock Name					
SDS 22	00	212YE	MA	9010		SD	M F W3		1Y
SDS 22	02	220YE	MA	871003YE		SD	M F M3		1Y
SDS 22	04	222BR YE	MA	851005YE		SD	C VFM3		1Y
SDS 22	06	221YE	MA	751015OR YE		SD	C VFV3		1Y
SDS 22	08	220L WH YE	CLB	700525GY		CLSD	C F V3		1Y
SDS 22	10	215L YE	MA	01 850510WH		SD	04F P4	04	1Y
SDS 22	12	218YE	MA	701515WH YE		SD	C M P3	03	
SDS 22	14	220L WH YE	MA	152560WH YE		STCL	C CL	05	
SDS 22	16	220L WH YE	MA	152560WH YE		STCL	C CL		
SDS 22	18	220D YE	MA	401050D BR YE		SDCL	VCCLP		
SDS 22	20	219OR YE	MA	75 25WH YE		CLSD	C M P3	02	
SDS 22	22	212D YE	MA	801010D BR		SD	C VFM3	01	
SDS 22	24	218OR WH	MA	851005WH		SD	C F M4	02	
SDS 22	26	218WH YE	MA	850510OR		SD	VCC P3		
SDS 22	28	218L WH YE	MA	900604YE WH		SD	C F M4		
SDS 22	30	215YE OR	MA	95 05OR		SD	C M M3		
SDS 22	32	215D OR YE	MA	90 10OR		SD	C M M3	01	2Y
SDS 22	34	220YE	ICL	90 10WH YE		SD	C F M3		
SDS 22	36	212PUBR	MA	95 05BR		SD	C F M3	01	
SDS 22	38	224YE	MA	95 05WH		SD	C F W3	01	1Y
SDS 22	40	206YE BR	MA	95 05BR		SD	M F W3		1Y
SDS 22	42	214RE BR	MA	95 05RE BR		SD	F F W4		1Y
SDS 22	44	211RE	MA	96 04RE		SD	M F W4		2Y
SDS 22	46	219RE BR	MA	95 05RE BR		SD	M F M4		1Y
SDS 22	48	211L YE BR	MA	831007YE		SD	C VFM4		
SDS 22	50	218BR	MA	95 05BR		SD	C F M4		
SDS 22	52	215BR	MA	95 05BR		SD	C F M4		
SDS 22	54	212L BR	MA	96 04BR		SD	C M W3		
SDS 22	56	215L BR	MA	900703YE		SD	C F W3		
SDS 22	58	219L BR	MA	99		SD	C M M3		
SDS 22	60	217L BR	MA	95 05L BR		SD	C M M3		3Y
SDS 22	62	218L YE BR	MA	881002YE		SD	C F M3		2Y
SDS 22	64	220L BR	MA	891001YE		SD	C F M3		2Y
SDS 22	66	220YE RE	MA	75 25RE YE		CLSD	C M P3		
SDS 22	68	222YE RE	MA	010183 15RE YE		SD	08M P3		
SDS 22	70	222D BR	MA	85 15D BR		SD	C M P3		
SDS 22	72	218YE RE	MA	90 10RE YE		SD	C M P3		
SDS 22	74	214BR	MA	900703BR OR		SD	C M M3		3Y
SDS 22	76	219BR	CLB	900703BR OR		SD	C F M3		3Y
SDS 22	78	215YE BR	CLB	97 03WH		SD	C F M3		
SDS 22	80	200 NO RECOVERY							
SDS 22	82	220YE	MA	97 03YE		SD	C M W3		2Y
SDS 22	84	212D BR	MA	900505D GY		SD	VCM M2		2Y
SDS 22	86	212D BR	MA	900505D GY		SD	C M M2		2Y
SDS 22	88	212D BK BR	MA	751015D BK GY		SD	VCM P2		
SDS 22	90	221L BR	MA	97 03YE BR		SD	C F W3		1Y
SDS 22	92	215M BR	MA	97 03YE BR		SD	C F W3		
SDS 22	94	215OR BR	MA	40 60OR BR		SDCL	VC		
SDS 22	96	215RE BR	MA	75 25RE		CLSD	C M P3	03	
SDS 22	98	200 NO RECOVERY							
SDS 22	100	215L BR	MA	8515		SD	F VFW4	01	3Y
SDS 22	102	219M BR	MA	9505		SD	C M W3		2Y
SDS 22	104	218M BR	MA	940501BR		SD	VCM W3		2Y
SDS 22	106	224L GN	MA	9505		SD	F F W4		
SDS 22	108	220M BR	MA	950401L BR		SD	C M W3		
SDS 22	110	204WH	MA	8515	25LSSD		C F		
SDS 22	112	200 NO RECOVERY							
SDS 22	114	215L GN	MA	9505	25LSSD		VCF W4		
SDS 22	116	206L GN	MA	721503	25LSSD		M F W4		
SDS 22	118	200 NO RECOVERY							
SDS 22	120	201L GN	MA	751510L GN	25LSSD		20F M4		
SDS 22	122	200 NO RECOVERY							
SDS 22	124	211L GN	MA	97 03L GN	25LSSD		24F W4		
SDS 22	126	212L GN	MA	404020L GN	25LSSD		20VFM4		
SDS 22	128	214L GN	MA	404020L GN	25LSSTSD		20VFM4		
SDS 22	130	216D GN	MA	20 80D GN	25LSCL		08CL		
SDS 22	132	218D GN	MA	25 75D GN	25LSSDCL		05CL		
SDS 22	134	200 NO RECOVERY							
SDS 22	136	218D GN	MA	051085D GN	CL		M CL		
SDS 22	138	215D GN	ILSSD	15 85D GN	10CL		F CL	Y	
SDS 22	140	215D GN	ISDST	050590D GN	CL		M CL		
SDS 22	142	212D GN	ISDST	050590D GN	CL		M CL		
SDS 22	144	224D GN	MA	701020D GN	SD		VCM P2		
SDS 22	146	214D GN	MA	10 90D GN	CL			Y10	
SDS 22	148	203M BR	MA	810504BR	10LSSD		05C M2		

Table 6-1c Borehole Log SDS-22

(Legend see Table 6-1d)

Table 6-1d Legend for Borehole Logs SDS-20,21,22

Depth to Top of Interval	Depth in feet to top of cored interval.		
Inches of Recovery	Inches of material recovered in core sample.	Maximum Size Modal Size	CL = clay ST = silt VF = very fine sand F = fine sand M = medium sand C = coarse sand VC = very coarse sand Larger than VC is size in millimeters
Color			
Overall	L = light M = medium D = dark		
Color	WH = white GY = gray GN = green YE = yellow OR = orange TA = tan RE = red PU = purple BR = brown BL, BK = black PI, PK = pink	Sorting	W = well sorted M = moderately sorted P = poorly sorted V = very poorly sorted
		Roundness	1 = very angular 2 = angular 3 = subangular 4 = subrounded 6 = rounded 8 = well rounded
	M, MT = mottled B = banded VAR = variegated	Sulphides	Y = yes
Structure	ISD = interbedded sand XB = cross-beds MT, M = mottled, patchy FS = fissile CLB = clay balls ICL = interbedded clay BU = burrows MA = massive IST = interbedded silt IPB = interbedded pebbles	% Muscovite, % Glauconite, % Organic (Lignite)	number = percentage TR = trace
		Fossils	Y = yes
		Fluoresence (Heavy Minerals)	1 = absent or few 2 = moderate 3 = abundant Y = yellow O = orange B = blue G = green R = red
Rock Name	LS = limestone SD = sand ST = silt CL = clay CO = conglomerate LG = lignite PY = pyrite CT = chert		

BORING NUMBER	SAMPLE NUMBER	DEPTH (feet)	SOIL DESCRIPTION	PERMEABILITY[1] (cm/sec)		POROSITY[1] (%)		
				VERTICAL k_v	HORIZONTAL k_h	TOTAL n	EFFECTIVE GRAVITY n_{eg}[2]	EFFECTIVE AT 5 psi n_{e5}[3]
SDS-3	ST-1	40.0-42.0	Brown silty fine to medium sand	3.3×10^{-7}	1.2×10^{-6}	39.5	2.4	3.8
SDS-3	ST-2	45.0-47.0	Brown fine to medium sand, some silt and clay	5.5×10^{-7}	1.6×10^{-6}	30.8	0.9	2.3
SDS-5	ST-1	5.0-7.0	Tan fine to medium sand, some clay	3.6×10^{-6}	1.7×10^{-5}	26.0	0.7	5.1
SDS-5	ST-2	13.0-15.0	Reddish brown and gray clayey fine to medium sand	1.1×10^{-7}	1.3×10^{-7}	31.2	1.5	3.4
SDS-5	ST-3	20.0-22.0	Red and tan fine to medium sand, some clay	1.5×10^{-6}	8.1×10^{-7}	31.2	3.3	7.1
SDS-5	ST-4	27.0-27.7	Red fine to medium sand, some silt	--- No testing, sample disturbance ---				
SDS-5	ST-5	31.0-35.0	Tan fine to medium sand, some silt	1.2×10^{-4}	5.3×10^{-5}	35.0	1.1	14.0
SDS-5	ST-6	42.0-43.7	Red and tan fine to medium sand, trace silt	2.4×10^{-4}	1.5×10^{-4}	37.8	1.4	24.7
SDS-6	ST-1	22.0-23.7	Reddish brown fine to medium sand, some silt and clay	4.0×10^{-6}	5.5×10^{-5}	33.5	3.3	10.7
SDS-6	ST-2	37.0-39.0	Tan fine to medium sand, some silt	1.6×10^{-4}	5.8×10^{-5}	42.7	2.0	16.3
SDS-6	ST-3	59.0-60.7	Tan fine sand, trace silt	6.3×10^{-5}	5.2×10^{-6}	44.5	1.2	15.8
SDS-6	ST-4	67.0-69.0	Tan fine sand, some silt	1.4×10^{-7}	7.5×10^{-6}	45.7	0.1	2.1
SDS-7A	ST-1	48.0-50.0	Red clayey sand interbedded with brown fine sand	--- No testing, sample disturbance ---				
SDS-7A	ST-2	78.0-80.0	Yellow fine to medium sand	2.3×10^{-5}	8.7×10^{-6}	38.9	2.7	10.4
SDS-7A	ST-3	120.0-122.0	Light tan and gray fine to coarse sand, some fine to coarse gravel, trace to some silt	--- No testing, insufficient quantity of trimmable undisturbed soil ---				
SDS-7A	ST-4	140.0-141.0	Dark greenish gray fine to coarse sand, some silt	8.5×10^{-8}	-[4]	34.7[5]	-[4]	-[4]
SDS-8	ST-1	67.0-69.0	Light yellow silty fine sand	1.1×10^{-7}	1.3×10^{-8}[6]	51.0[5]	-[7]	-[7]
SDS-9	ST-1	62.0-64.0	Red fine to medium sand, trace silt	9.9×10^{-5}	1.6×10^{-6}[6]	40.3	1.9	11.7
SDS-9	ST-2	68.0-69.5	Red and tan fine to medium sand	1.5×10^{-4}	4.4×10^{-5}	41.5	3.6	18.5
SDS-10	ST-1	30.0-32.0	Reddish brown fine to coarse sand, some silt	5.2×10^{-5}	-[8]	35.0	6.6	8.8
SDS-11	ST-1	30.0-32.0	Tan fine to medium sand, some silt	2.0×10^{-6}	1.3×10^{-5}	27.0	1.7	-[9]
SDS-11	ST-2	40.0-42.0	Red and tan fine to medium sand, trace silt	2.6×10^{-4}	4.9×10^{-5}	37.0	1.8	10.6
SDS-11	ST-3	45.0-47.0	Red fine to medium sand, trace silt	8.6×10^{-5}	1.9×10^{-4}	38.6	2.2	14.1
SDS-13	ST-1	15.0-17.0	Reddish brown fine to medium sand, trace silt	2.0×10^{-4}	2.6×10^{-4}	33.6	2.0	19.9
SDS-13	ST-2	25.0-27.0	Reddish brown fine to medium sand	8.0×10^{-4}	-[8]	41.8	3.1	28.1
SDS-14	ST-1	34.0-36.0	Tan fine to medium sand, trace silt	1.3×10^{-5}	2.6×10^{-6}	41.7	0.9	8.9
SDS-14	ST-2	40.0-42.0	Tan silty fine to medium sand	1.8×10^{-7}	3.1×10^{-7}	47.4[5]	-[7]	-[7]
SDS-14	ST-3	50.0-51.0	Tan fine to medium sand, trace silt	2.6×10^{-6}	5.9×10^{-5}	39.5	6.3	16.4

[1] Temperature corrected to 20°C.
[2] Effective porosity with gravity head.
[3] Effective porosity with 5 psi pressure head.
[4] Insufficient sample quantity for testing.
[5] Porosity computed from vertical permeability sample.
[6] Low k_h due to sample grading to finer grained soil than for k_v testing.
[7] Sample too fine-grained for effective porosity testing.
[8] Sample too sandy to trim.
[9] Test not performed.

Table 6-2 Permeability and Porosity Test Results (from d'Appolonia, 1981)

SUMMARY OF THE LABORATORY PERMEABILITY TESTS

Hydrostratigraphic Unit	Facies	Number of Samples	Vertical Permeability [m/s]			Horizontal Permeability [m/s]			Ratio	Mean
			Minimum	Maximum	Mean K_v	Minimum	Maximum	Mean K_h	K_v/K_h	0.5 x (K_v + K_h)
Barnwell Formation	Sand	15	0.2×10^{-7}	80×10^{-7}	18×10^{-7}	0.2×10^{-7}	24×10^{-7}	6.5×10^{-7}	2.8	1.2×10^{-6}
	clayey sand (lenses)	4	1.1×10^{-9}	18×10^{-9}	7.0×10^{-9}	1.3×10^{-9}	16×10^{-9}	9.4×10^{-9}	0.74	8.2×10^{-9}
Tan Clay	clayey sand	3	1.1×10^{-9}	1.8×10^{-9}	1.4×10^{-9}	0.1×10^{-9}	75×10^{-9}	26×10^{-9}	0.05	1.4×10^{-8}
McBean Formation	Sand	0	---	---	---	---	---	---	---	---
	clayey sand (lenses)	2	0.26×10^{-7}	2.3×10^{-7}	1.3×10^{-7}	0.87×10^{-7}	5.9×10^{-7}	3.4×10^{-7}	0.38	2.4×10^{-7}
Green Clay	Sandy clay clay	0	---	---	---	---	---	---	---	---
Congaree Formation	Sand	0	---	---	---	---	---	---	---	---
	clayey sand (lenses)	1	0.85×10^{-9}	---	---	---	---	---	---	---

Table 6-3 Summary of the Laboratory Permeability Tests (Data taken from d'Appolonia, 1981).

SUMMARY HYDRAULIC CONDUCTIVITY DATA

Hydrostratigraphic Unit	Regional Data (Christensen & Cordon, 1983) [m/s]	Laboratory Data (d'Appolonia, 1981) [m/s]	Field Data (Parizak & Root, 1984) [m/s]	Model Results (Root, 1982) [m/s]	Field Data (INTERA, 1985) [m/s]	Effective Hydraulic Conductivities (Possible Range)
Barnwell Formation	1×10^{-6} (10^{-7}-10^{-5})	1.2×10^{-6}(s) 8.2×10^{-9}(c)	7×10^{-6}	2.1×10^{-5} (h)		1×10^{-6}-1×10^{-5}(h)
Tan Clay		1.4×10^{-8}(c)		1.9×10^{-8}(v)		0.5×10^{-8}-5×10^{-8}(v)
McBean Formation	1×10^{-6} (10^{-7}-10^{-5})		3.9×10^{-6} (3×10^{-7}-1.2×10^{-5})	2.1×10^{-5}(h)	2.9×10^{-5} (10^{-8}-10^{-4})	1×10^{-6}-3×10^{-5}(h)
Green Clay						1×10^{-10}-1×10^{-8}
Congaree Formation	2×10^{-5} 5×10^{-4}(m)		1.1×10^{-5}		6.1×10^{-5} (2×10^{-4}-2×10^{-4})	1×10^{-5}-5×10^{-4}(h)

(v): vertical hydraulic conductivity
(h): horizontal hydraulic conductivity
(s): sandy facies
(c): clayey sandy facies
(m): maximum value of center of Savannah River Plant

Table 6-4 Summary of Hydraulic Conductivity Data.

BOREHOLE NUMBER	FORMATION SCREENED	ELEVATION TOP CASING [m asl]	SCREEN BOTTOM [m asl]	SCREEN LENGTH [m]	NUMBER OF READINGS	MINIMUM [ft bs]	MAXIMUM [ft bs]	MINIMUM [m asl]	MAXIMUM [m asl]	MEAN [m asl]	DIFFERENCE MAX.-MIN. [m]
SDS-1	Barnwell	90.00	63.7 ?	6.1	25	68.20	59.23	69.21	71.95	70.58	2.73
SDS-2	Barnwell	88.27	65.71	6.1	25	61.26	55.90	69.60	71.23	70.40	1.63
SDS-3	Barnwell	89.15	64.16	6.1	25	57.57	51.23	71.60	73.54	72.55	1.93
SDS-4	McBean	78.45	56.51	6.1	25	26.52	21.20	70.37	71.99	71.09	1.62
SDS-4A	Barnwell	78.52	69.62	1.5	25	26.70	21.05	70.38	72.10	71.16	1.72
SDS-5	Barnwell	88.33	66.51	6.1	25	56.17	50.87	71.21	72.82	71.98	1.62
SDS-6	Barnwell	88.39	66.11	6.1	25	63.36	57.00	69.08	71.02	70.11	1.94
SDS-7A	Congaree	84.99	22.86	1.5	26	108.55	106.25	51.90	52.60	52.22	0.70
SDS-7B	McBean	84.73	41.24	1.5	25	76.28	64.06	61.48	65.20	63.73	3.72
SDS-7C	McBean	84.48	56.14	1.5	26	64.68	56.82	64.77	67.16	65.93	2.40
SDS-7D	McBean	84.49	62.67	1.5	25	62.96	54.87	65.30	67.77	66.50	2.47
SDS-8	McBean	82.94	61.54	1.5	25	55.56	46.08	66.01	68.89	67.40	2.89
SDS-9	Barnwell	90.13	68.00	1.5	25	58.85	52.15	72.19	74.23	73.19	2.04
SDS-10	Barnwell	89.98	68.79	6.4	25	59.57	52.24	71.82	74.06	72.87	2.23
SDS-11	Barnwell	88.97	66.84	6.1	25	58.92	52.35	71.01	73.01	72.00	2.00
SDS-12A	Congaree	84.91	41.57	1.5	26	111.73	109.22	50.85	51.62	51.29	0.77
SDS-12B	McBean	84.94	56.91	1.5	26	65.42	54.03	65.00	68.47	67.23	3.47
SDS-12C	McBean	84.16	62.82	1.5	25	60.96	43.60	65.58	70.87	66.79	5.29
SDS-13	McBean ?	84.57	62.30	6.1	25	68.33	64.03	63.74	65.05	64.36	1.31
SDS-14	McBean ?	81.47	61.17	6.1	25	47.97	10.00	66.85	78.42	72.82	11.57
SDS-14A	Barnwell	82.60	77.05	6.1	25	18.70	8.00	76.90	80.16	78.68	3.26
SDS-15	Barnwell	86.84	64.62	6.1	25	60.31	15.58	68.46	82.09	69.71	13.63
SDS-16A	Congaree	71.41	?	1.5	8	61.20	59.80	52.76	53.18	53.04	0.43
SDS-16B	Congaree	71.41	?	1.5	8	63.30	62.20	52.12	52.45	52.35	0.34
SDS-16C	McBean	71.41	56.52	6.1	25	35.40	31.02	60.62	61.96	61.22	1.34
SDS-17	McB./Bw.	82.69	59.92	6.1	25	48.77	42.00	67.82	69.89	68.80	2.06
SDS-18	Barnwell	78.91	68.7 ?	6.1	0						
SDS-18A	McBean	78.91	62.79	6.1	7	54.24	50.90	62.38	63.40	63.05	1.02
SDS-19	McBean	71.96	58.77	6.1	25	29.22	23.78	63.05	64.71	63.78	1.66
SDS-20A	Congaree	79.80	?	?	8	98.22	97.25	49.86	50.16	50.07	0.30
SDS-20B	McBean	79.80	?	?	8	49.26	44.42	64.79	66.26	65.80	1.48
SDS-20C	McBean	79.83	?	?	8	47.95	45.20	65.21	66.05	65.58	0.84
SDS-21A	Congaree	76.50	?	?	8	91.22	90.35	48.70	48.96	48.86	0.27
SDS-21B	McBean	76.44	?	?	8	43.75	40.48	63.10	64.10	63.80	1.00
SDS-21C	McBean	76.44	?	?	8	42.82	41.38	63.39	63.83	63.65	0.44
SDS-22A	McBean ?	86.35	?	?	8	97.03	89.61	56.78	59.04	57.79	2.26
SDS-22B	McBean	86.32	?	?	7	60.22	50.85	67.96	70.82	70.17	2.86
SDS-22C	McBean	86.29	?	?	8	58.00	54.48	68.61	69.68	69.03	1.07

m asl = meters above sea level

ft bs = feet below ground surface

Table 6-5 Summary of Water Level Measurements at Z-Area.

Boreholes screened in the McBean Formation	Mean Water Level [m a.s.l.]
SDS-7C	65.9
SDS-12B	67.2
SDS-20B	65.8
SDS-21B	63.8
SDS-22C	69.0

Boreholes screened in the Congaree Formation	Mean Water Level [m a.s.l.]
SDS-7A	52.2
SDS-12A	51.3
SDS-16A/B	52.8
SDS-20A	50.1
SDS-21A	48.9

Table 6-6 Summary of Water Level Data Used for Model Calibration

7.0 CONCEPTUALIZATION OF THE MODEL

As discussed in Chapters 1 and 2, the purpose of the modeling study is to provide information required for the assessment of Z-Area as a disposal site. Thus the primary objectives of the modeling were:

- to develop an understanding of ground water flow in the different water bearing units at Z-Area and vicinity;
- to quantify the piezometric head distribution;
- to quantify the ground water flow field;
- to develop an understanding of how contaminants released by the planned disposal site will be transported by the ground water;
- to quantify the expected long term contaminant concentrations in the creeks surrounding the Z-Area hill as well as in the different aquifers.

Thus a numerical model with the capability of simulating both ground-water flow and contaminant transport must be developed. The first step of such a model development is usually the conceptualization of the model, which is based on the geologic and hydrogeologic data available.

Within the actual study, the model was conceptualized after completion of the data evaluation and data review (Chapter 6). The most important aspects of this model conceptualization are summarized in the following sections.

7.1 Model Area and Boundary Conditions

The evaluation of the piezometric data at Z-Area lead to the conclusion that the ground-water flow field is highly divergent in the upper aquifers in the area of interest (Section 6.7, Figures 6-8, and 6-9). Therefore, no completely representative cross-section can be established. This means, that the three dimensional ground water flow cannot be accurately modeled using only a two dimensional cross-section. Thus a complete three dimensional model must be developed.

First the vertical extent of the model and the area covered by the model must be defined, and the upper and lower boundaries as well as the boundaries around the model area must be selected.

7.1.1 Lower Model Boundary

According to the regional geologic and hydrologic data, the Congaree Formation is the lowermost hydrostratigraphic unit which would possibly be affected by the planned disposal site. This is due to two reasons: (1) The Congaree Formation is almost separated hydraulically from the underlying Ellenton Formation (Section 4.2.2) because confining clayey beds occur at the base of the Congaree Formation and the top of the Ellenton Formation, and (2) in the area of interest the hydraulic head in the Ellenton Formation is higher than in the Congaree Formation, resulting in an upward-directed vertical component of ground water flow from the Ellenton to the Congaree Formation (Figure 4-3). Therefore the Congaree Formation was selected as the lowermost hydrostratigraphic unit modeled in the actual study. The relatively small flux across the clayey layers from the Ellenton Formation into the Congaree Formation can be neglected for the actual investigation. Thus the bottom of the Congaree Formation (12 m a.s.l., Figure 6-7) is modeled as a no-flow boundary.

7.1.2 Upper Model Boundary

The waste material ('saltstone') will be disposed at surface or in trenches just below the surface. Because the final design for the disposal site did not exist when the model was developed, an arbitrary elevation of 78 m a.s.l. was chosen to be the upper boundary of the model. This elevation is most likely to be within 10 m of the bottom of the final landfill disposal site. This boundary lies within the Barnwell Formation (Figure 6-7). As Figure 7-1 shows, surface elevations occur above 78 m a.s.l. (256 feet) only in the central part of the Z-Area hill. In the surrounding valleys the surface elevations are as low as 45 m a.s.l. (150 feet). In the valleys the actual topographic surface was chosen to be the upper limit of the model.

In the model a recharge rate corresponding to the average annual infiltration rate was applied to the upper model boundary. About a third of the precipitation is assumed to infiltrate as recharge to the ground water system (Chapter 5). Based on the long term precipitation data, a recharge rate of 380 mm/year (15 inches/year) was selected. This recharge rate is consistent with previous studies performed for or by E.I. du Pont de Nemours and Co. (J. Cook, pers. comm.). Thus the upper model boundary is a prescribed flux boundary.

7.1.3 The Creeks as Model Boundaries

With the vertical extent of the model defined, it is possible to choose the lateral model boundaries. The upper two aquifers included in the model (Barnwell and McBean Formations) are drained by the creeks surrounding Z-Area. As stated in Sections 4.2.3 and 4.2.5, these dissecting creeks divide both formations into locally isolated, hydraulic subunits. Therefore, on the eastern, northern and western sides of Z-Area the creeks were selected as the model boundaries (Figure 7-1).

Although the McBean Formation is not completely dissected by McQueen Creek in the east, it was assumed that no ground water from the McBean Formation leaves the modeled area by flowing below McQueen Creek to the east. Ground water in the McBean and Barnwell Formations was considered to discharge into the creeks around the Z-Area hill (except for the small amount lost through the Green Clay into the underlying Congaree Formation). Assuming that the piezometric surface in the creek valleys corresponds to the local elevation of the creek, it is possible to define the creeks as constant head outflow boundaries.

Definition of the boundary conditions of the Congaree Formation below the creeks is more difficult. As Figure 6-10 shows, the ground water flow is directed to the northwest. Therefore most of the Congaree ground water likely leaves the model area below Upper Three Runs Creek and the lower part of McQueen Creek. Based on the piezometric data

(Figure 6-10) it is possible to estimate the piezometric head where the ground water leaves the model area. Thus it is possible to define the boundary of the Congaree Formation as a constant head outflow boundary.

Below the upper part of McQueen Creek, where the ground water in the Congaree Formation flows parallel to the creek, no ground water enters or leaves the model area. Therefore the boundary of the Congaree Formation below the upper part of McQueen Creek can be defined as a no-flow boundary.

Because the horizontal ground-water flux in the clayey layers (Green Clay, Tan Clay) is very small compared to the vertical flux through them and to the horizontal flux in the sandy layers, no-flow boundaries were generally selected for edges of these layers.

7.1.4 The Southern Model Boundaries

The southern (and southwestern) model boundary was selected using the piezometric well data (Figures 6-8 and 6-9). The aim was to minimize the effect of the boundary condition on the model. Therefore the southern boundary location was selected so as to allow as much as possible to be defined as a flow divide or no-flow boundary. The southern model boundary starts at Upper Three Runs Creek in the west and runs up the valley of an ephemeral tributary approximately to well SDS-2. From there it goes to the southeast to well SDS-3, crosses a small natural pond and goes down again in a small valley to McQueen Creek.

As Figure 6-8 shows, there is ground water inflow in the Barnwell Formation in the central part of the southern boundary. There the boundary must be defined as a constant head inflow boundary. In the western and eastern part of the southern boundary, the ground water flow in the Barnwell Formation is directed more or less parallel to the southern boundary. Thus the boundary there can be defined as a no-flow boundary.

As Figure 6-9 shows, the ground water flow field in the McBean Formation looks very similar to the flow field in the Barnwell Formation, but the inflow zone in the south is larger. Thus the central part of the southern boundary of the McBean Formation is defined as a constant head inflow boundary. The western and eastern parts were defined as no-flow boundaries or as flow divides corresponding to the creek cuts.

The ground water flow in the Congaree Formation is generally directed to the northwest (Figure 6-10). Thus ground water enters the modeled area primarily in the eastern part of the southern boundary. In the western part of the boundary (west of SDS-3) the inflow of ground water is much less, because the assumed ground water flow is almost parallel to the boundary. Therefore the eastern part of the southern model boundary was defined as a constant head inflow boundary, and the western part (west of SDS-3) as a no-flow boundary.

The southern boundary of the clayey layers (Tan Clay, Green Clay) was defined as an impermeable boundary because of the small possible inflow (comparably low transmissivity).

Thus the model area and the boundaries are defined. The required heads (in the formations) or elevations (at the creeks) can be derived from Figures 6-8, 6-9, 6-10. The implementation of the boundary conditions is discussed in more detail in Section 8.4.2.

7.2 Geological Structure

With the model area and the boundaries defined, the next step of the model conceptualization is to define the geological structure of the model. This structure must be representative of the area to be modeled. On the other hand, the structure must be simple enough to be implemented in a numerical model. Thus the geological structure of the model must be a balanced compromise between complexity and simplicity. From the data review the hydrostratigraphic units are (almost) horizontally layered at Z-Area (Section 6.5). As the data review resulted in a representative lithological profile for the model area; and assuming a horizontal layering, the geological structure of Z-Area can be simplified (Figures 7-2 and 7-3) into hydrostratigraphic units and incorporated in the numerical model.

7.3 Hydrogeologic Rock Properties

With the geological structure of the model defined, the initial hydrogeological rock properties (i.e., the hydraulic conductivity, the porosity and the compressibility) must be assigned.

The final hydraulic conductivities used by the model will result from model calibration. The calibration essentially means matching the model calculated hydraulic heads to the observed water levels at Z-Area by systematically varying the hydraulic conductivities of the hydrostratigraphic units. Nevertheless to start the calibration process, initial hydraulic conductivities are required. These initial values normally are estimated based on existing data.

The existing hydraulic conductivity data have been reviewed in Chapter 6. This review resulted in an estimation of the possible ranges of the hydraulic conductivities in the different hydrostratigraphic units (Table 6-4). The existing data base does not allow definition of the anisotropy of the hydraulic conductivity in the horizontal plane. Thus the horizontal hydraulic conductivity is considered isotropic. Based on

the data review, the initial horizontal hydraulic conductivities for the model were selected (Figure 7-6). The selected values lie within the ranges identified by the data review and represent the initial best estimate before modeling.

There are very little data available as far as the vertical hydraulic conductivity, or the vertical to horizontal anisotropy of the hydraulic conductivity is concerned. As mentioned in Section 6.6, laboratory measurements were conducted by d'Appolonia. However the results did not yield a clear indication of the ratio of vertical to horizontal hydraulic conductivity. In addition, the laboratory tests were not representative of the model scale.

Therefore the vertical to horizontal hydraulic conductivity anisotropy must be estimated using other criteria. The most important aspect is that the anisotropy is scale dependent. The two sizes or lengths involved are (1) the size of the model area, which covers about 2 km x 2 km (Figure 7-1) and (2) the size of the horizontally layered clay and sand lenses in the hydrostratigraphic units at Z-Area. These units are typical coastal plain sediments, in which the characteristic length of the clay or sand lenses ranges from 10 to 100 m. This is confirmed by the results of the drilling work at Z-Area, where many clayey or sandy layers cannot be correlated between boreholes approximately 100 m apart. Thus the clay or sand lenses (e.g., in the Barnwell Formation) are not continuous at a scale of several kilometers. Therefore the vertical hydraulic conductivities can be expected to be somewhat (but not an order of magnitude) lower than the horizontal hydraulic conductivities (see also Appendix A.3). Root (1982) assumed a vertical to horizontal hydraulic conductivity anisotropy ratio of 1:2. His model covered an area of about 6 km^2. In this report the model area is smaller (some 4 km^2). A hydraulic conductivity anisotropy ratio of 1:5 is considered a reasonable estimate (Figure 7-1).

The two clayey layers (Tan Clay and Green Clay) are considered to be homogeneous. Therefore no hydraulic conductivity anisotropy was assigned to them.

In addition to assigning the hydraulic conductivities, the porosity and compressibility of the hydrostratigraphic units must also be assigned. The porosity data have been reviewed in Chapter 6. An effective porosity of 30% was considered to be a reasonable estimate and was assigned to all hydrostratigraphic units for the transport modeling study.

The compressibility of the rock was derived from the literature (Touloukian and Ho, 1981). A value of 5.8×10^{-10} Pa^{-1} was selected, although this value is of importance only for transient flow modeling.

7.4 Contaminant Source Term and Contaminant Transport

The final design of the planned disposal site at Z-Area was not completed at the time of the model conceptualization (see Chapter 2). Thus the contaminant source term and the contaminant transport study had to be somewhat general in concept.

The following assumptions concerning the source term were made during the conceptualization of the model:

1. The waste material (saltstone) will be disposed in an area of 405,000 m^2 (100 acres). This assumption is based on the actual planning by E.I. du Pont de Nemours and Co. (J. Cook, pers. comm.).

2. The waste material will be disposed at surface or in trenches just below the surface. This surface is planned to be derived by removing some of the uppermost soil. The exact elevation of this artificial surface is not yet known, but the waste material will be disposed above the historic high of the ground water table in the Barnwell Formation (ca. 75 m a.s.l., Cook, 1983). Thus the distance between the disposed material and the long term ground water table in the Barnwell Formation is not yet known. Therefore it was assumed that the disposal site lies at the upper boundary of the model (78 m a.s.l., see Section 7.1.2).

3. The contaminant release rate from the disposal site and the actual contaminant concentrations reaching the ground water surface in the Barnwell Formation were not known. Therefore it was assumed for the base case of the transport modeling that the same percentage of the average annual precipitation infiltrates at Z-Area as elsewhere in the model area and that the infiltration passes through the upper model boundary. A dimensionless concentration of 1.0 (or 100%) was assigned to the recharge passing through all parts of Z-Area.

4. No time dependence for the source term was known. Therefore the contaminant concentration of the recharge at Z-Area was defined to be constant in time, with a continuous input source relative concentration of 1.0 over the entire simulation period.

For the contaminant transport modeling the following basic assumptions were made:

1. The contaminants do not decay with time.
2. The contaminants do not sorb or react in the subsurface.
3. The contaminants are transported by advection and dispersion. The dispersion and diffusion coefficients are discussed in detail in Section 8.4.6.

Based on the above listed assumptions, the contaminant transport modeling could be performed using this normalized source term.

7.5 Time Dependence of Ground-Water Flow and Contaminant Transport

The period of interest for the environmental assessment modeling was considered to be between 50 and 200 years.

At this time scale, the individual annual precipitation is far less important than the average annual precipitation (Figure 5-1). Therefore the ground-water flow was modeled using the average annual precipitation and a steady state ground-water flow algorithm.

Contrary to the ground-water flow, the contaminant concentrations in the aquifers beneath Z-Area will not be constant in time over the time period of interest. Therefore transient contaminant transport modeling was required. However, the contaminant transport simulation employs the steady state ground-water flow field.

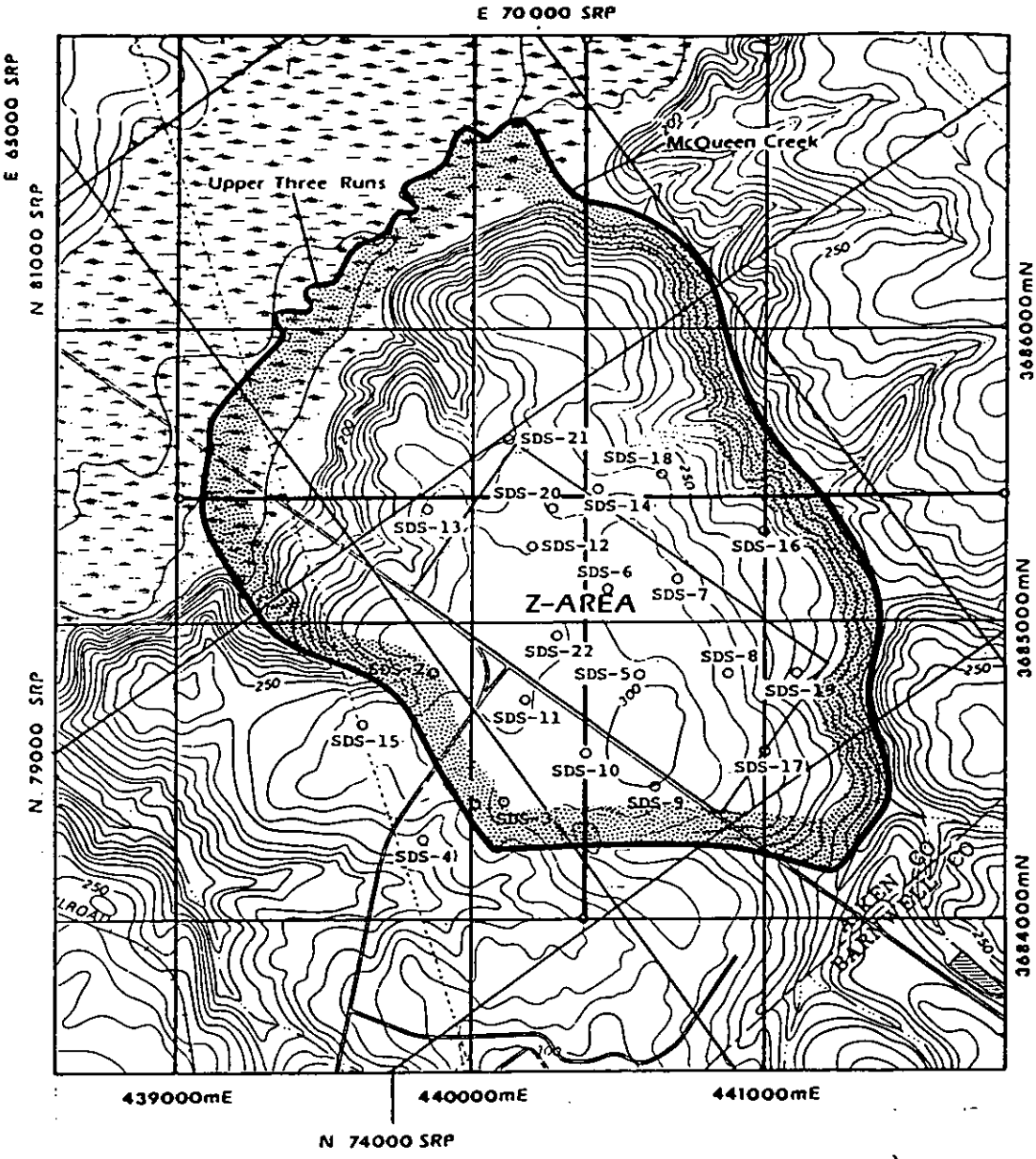

Figure 7-1 Model Area

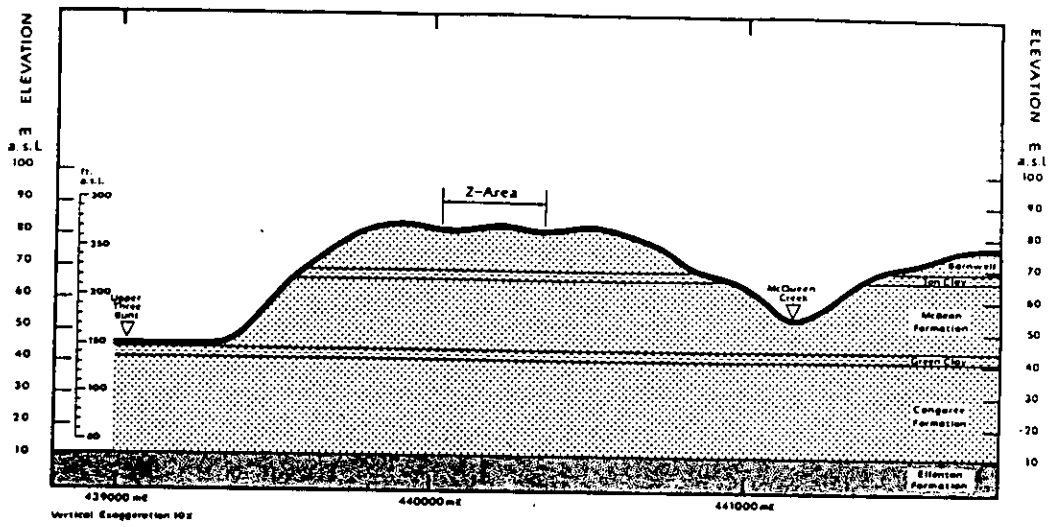

Figure 7-2 West-East Cross-Section Through the Model Area (Figure 7-1)

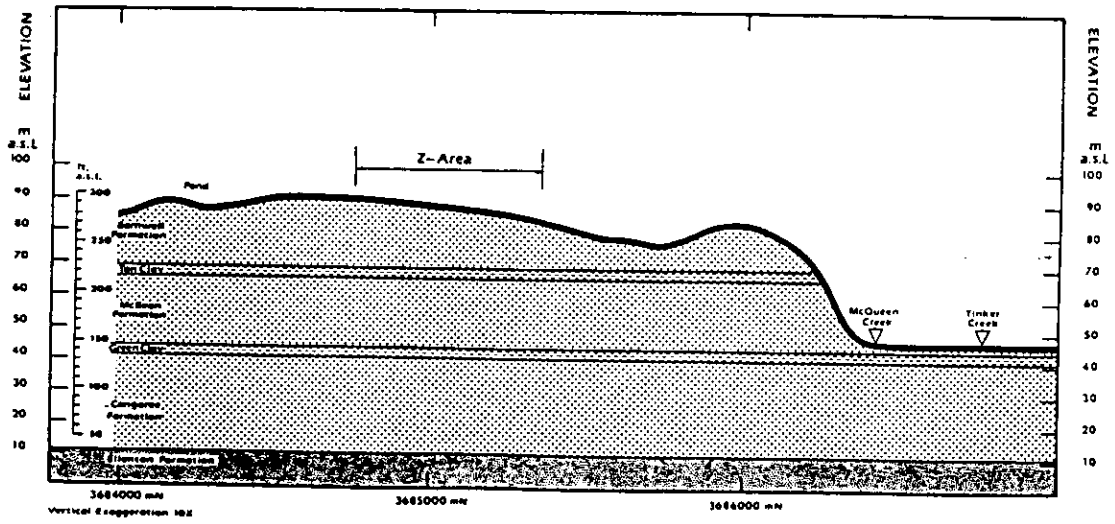

Figure 7-3 South-North Cross-Section Through the Model Area (Figure 7-1)

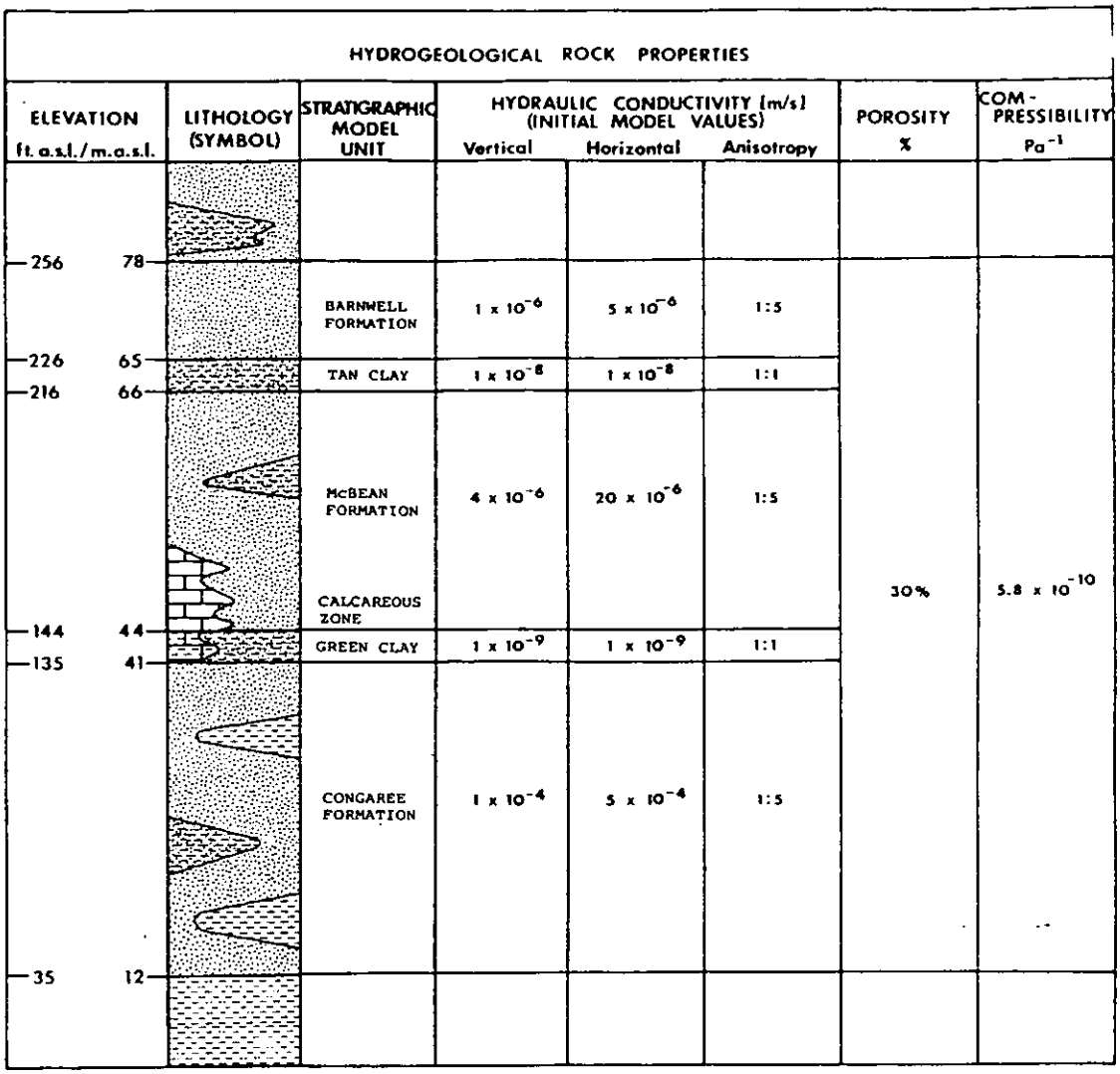

Figure 7-4 Rock Hydraulic Properties of the Model.

8.0 IMPLEMENTATION OF THE MODEL

For the assessment of the planned disposal site at Z-Area both the ground water flow beneath and around Z-Area and the transport of contaminants possibly released from the planned disposal site were simulated using a numerical model. The implementation of a numerical model normally comprises the computer code selection (or the code development), the adaptation of the selected computer code to the actual needs (if necessary) and the set-up of the input data or the parameter set.

Within the actual study, the model implementation was performed after completion of the model conceptualization (Chapter 7). The most important aspects of the model implementation are summarized in the following sections.

8.1 Computer Code Selection

Due to the expected highly divergent ground-water flow field, the model had to be fully three dimensional (Chapter 7.1). The area covered by the model has an extent of about 2 km x 2 km. This volume had to be discretized and handled by the selected computer code.

INTERA's in-house computer facilities (HARRIS 800 with optional Scientific Arithmetic Unit) can handle programs with up to 3 MByte memory allocation per user. Three dimensional models with maximally 1,000 to 10,000 grid blocks or grid elements can be implemented. The exact number obviously depends on the code actually used.

Assuming 3,000 as the maximum number of grid blocks or grid elements, each direction of a three dimensional model can be subdivided into about 14 grid blocks. Consequently, the expected grid block sizes (or distances between grid element centers) for the Z-Area model are about 100-200 m in the horizontal direction and about 3-6 m in the vertical direction.

The ground-water flow algorithm of most numerical models is relatively insensitive to the model discretization. However solute transport is very sensitive to numerical dispersion in most finite difference and finite element models (Lantz, 1971). Numerical dispersion can be minimized by using very small grid block sizes, resulting in a large number of blocks or alternatively a limited size of the modeled area. In transport modeling studies where the size of the modeled area and the number of grid blocks will likely result in excessive numerical dispersion, the method of characteristics or 'point tracking' (Garder et al., 1963) can be employed to simulate the solute transport. Point tracking simulates contaminant transport by moving 'points' representing the contaminants along the ground water stream lines through a finite difference grid. The method of characteristics is virtually free of numerical dispersion.

The INTERA code HCTM (INTERA, 1982) simulates three dimensional ground water flow using the finite difference method and uses either finite difference techniques or the method of characteristics for solute transport. HCTM consequently was chosen as the computer code for the Z-Area model.

8.2 Description of the Computer Code (HCTM)

The Hydrology Contaminant Transport Model (HCTM) is a three-dimensional numerical model that simulates fluid flow and transport of a contaminant in a porous medium. The contaminant transport includes advection; molecular diffusion; hydrodynamic dispersion; a first order decay chemical reaction term; and linear and non-linear, kinetic and equilibrium sorption.

The basic equations used in the model are conservation of total fluid mass and conservation of contaminant mass. Fluid velocities in the first equation are expressed in terms of spatial gradients of fluid potential through the use of Darcy's law in a porous medium. The fluid velocities calculated by solving the first equation are then used in the

second equation. The independent variables are the hydraulic head and contaminant concentration. User options have been provided to specify initial conditions and constant flux or constant potential and concentration boundary conditions along the edges of selected numerical grid blocks. In addition, the user may specify heterogeneities in the hydraulic conductivity and porosity values.

To facilitate efficient use of the model, the user has the option to use the code in any one of the following modes:

- Steady state flow solution, no contaminant transport;
- Transient flow solution, no contaminant transport;
- Steady state flow solution, transient contaminant transport;
- Transient flow and contaminant transport solutions.

The flow equation is always solved by a finite-difference method, whereas an option has been provided to solve the contaminant transport equation by a finite-difference or point-tracking (method of characteristics) method. In the point tracking option, the convection term is solved by the method of characteristics, the reaction or decay term is treated analytically and the dispersion term is included by finite-difference. For both methods, options have been provided to use several finite-difference approximations in space and time. The model includes two methods for solving both flow and contaminant transport finite-difference equations: direct Gaussian elimination and the iterative-line successive overrelaxation method. This gives the user an option to select the most appropriate finite-difference approximation and solution technique for the problem.

A detailed description of the HCTM code is provided in Appendix B. This documentation includes the basic partial differential equations, the finite-difference approximations, a description of the point tracking method, the contaminant transport equations and verification tests for both the flow and the contaminant transport.

The basic partial differential equations are derived in Section B-1 (Appendix B) and the major assumptions contained in the model are listed. The model is based upon generally accepted principles in the field of ground water modeling. The assumptions (such as the system being a continuum system and that average quantities over representative elementary volumes can accurately describe the system) are implied and not explicitly stated. Appendix B-1 also includes finite-difference approximations of the partial differential equations and the form in which they are internally used in the code. A description of the method of characteristics, as used in the model, is also provided.

Verification tests are described in Section B-2 (Appendix B). Objectives of verification testing are: (a) to test that the program has been coded properly and debugged, and (b) to test the adequacy of the numerical approximations and the solution technique. In any methodical code development, the developer verifies the coding by comparing code-calculated numbers against hand-calculated numbers in individual sections of the program. This was done extensively during the code development. The second type of verification is done by comparing model results against solutions obtained by using independent solution methods, such as analytical solutions. Since analytical solutions are available for simplified cases only (e.g., one-dimensional, homogeneous conditions), verification testing is generally restricted to simple cases. In Section B-2 (Appendix B), one flow verification and three contaminant transport verifications are presented.

Section B-3 (Appendix B) discusses the overall organization of the program, the dimensioning of various arrays and the numerical error as it is related to block size and time step restrictions.

Various user options provided in the model are described in Section B.4. A detailed input data description is not included in Appendix B, since it would exceed the scope of this report. However, a detailed input data description can be found in the original code documentation (INTERA, 1982).

8.3 Special Code Modifications for the Z-Area Model

At Z-Area the Congaree Formation is a confined aquifer (Sections 4.2.3, 6.7). The ground water in the McBean Formation is partly confined. Along the slopes of the Z-Area hill, where the McBean Formation is drained by the creeks, a free water table exists (Section 4.2.5), consequently this part of the McBean Formation is not fully saturated. In the Barnwell Formation there is a free water table (Section 4.2.7, 6.7). Consequently the ground water in the Barnwell Formation is perched where a free water table exists in the underlying McBean Formation. However, at the center of the Z-Area hill (i.e., immediately underlying most of Z-Area) there is no perched water table.

HCTM in general is a very flexible code. It can be used for confined as well as for unconfined aquifer systems (Appendix B-4.1.2). However the original version of the code was not able to simulate a perched water table. Thus it was necessary to modify the HCTM code for the Z-Area model.

The basic flow equation of HCTM (Appendix B-1) includes the flux q and the gradient of the hydraulic head (∇p) or the gradient of the hydraulic potential ($\nabla \Phi$); the flux and the hydraulic gradient are coupled by the hydraulic conductivity (i.e., essentially Darcy's law). The hydraulic conductivity in HCTM can vary in space (heterogeneous rock) but must be constant in time.

A correct simulation of unsaturated flow includes a moisture content dependent hydraulic conductivity and is normally a transient problem. Thus a code for unsaturated flow must have the capability of varying the hydraulic conductivity in time according to the moisture content. It is not possible to add this facility to HCTM without changing the code's principles which would be almost equivalent to the development of a new code. Therefore no attempt was made to model the physics of flow in the unsaturated zones. It was rather assumed that the flow in the unsaturated zones could be modeled using the same hydraulic conductivities as

in the saturated zones. This simplification causes no error for the steady state flow in the saturated zones because the accumulation term of the basic flow equation is zero at steady state (Appendix B). Given the capillary pressure curves for the Barnwell Formation presented in INTERA (January 1986) and given the similarity of the Barnwell and McBean Formations (Gruber, 1981) it is expected that the moisture content between the saturated zones will be very close to 100%, yielding an unsaturated hydraulic conductivity approximately the same as the saturated conductivity. The velocities calculated by the model in those areas that are unsaturated will therefore be virtually identical to those that actually occur under field conditions. The difference is likely less than a few percent. With respect to the site assessment this error is negligible.

As mentioned above (and derived in detail in Appendix B), the basic model equations comprise the flux (between the grid elements) and the hydraulic gradient (or the head difference between two grid elements) but no absolute hydraulic heads or hydraulic potentials. The absolute head values in the model are calculated using the hydraulic gradient and the hydraulic heads of the constant head boundaries (Appendix B-4.4.3). Without at least one constant pressure boundary the absolute hydraulic heads of the model are not defined. The calculation of the absolute hydraulic heads for each grid block center is possible without difficulty as long as a continuous saturated zone exists between the grid element for which the hydraulic head has to be calculated, and the constant head boundaries.

However, a lens of perched ground water in the middle of the model is virtually independent from the boundary conditions at the edges of the model. Therefore it was necessary to introduce a boundary condition specific for perched ground water. This new boundary condition simply implies that the perched ground water head at the inverted water table (i.e. the bottom of the perched zone of saturation) is equal to the elevation of that inverted water table. This condition is almost equivalent to the definition of a water table. However, it also allows the

calculation of absolute ground water heads for perched ground water using this boundary condition and the hydraulic gradient.

This additional feature is handled in several steps by the modified HCTM-Code:

1. The flow equations are solved as described in Appendix B-4.1 and provide the flow, the hydraulic heads in the (main) ground water system and the hydraulic gradient (head differences) in both the perched and the main ground water systems.

2. Then the unsaturated zones are identified. The criterion used is whether the hydraulic head is below the top of a grid element. For grid elements overlying unsaturated grid elements the head difference to the underlying grid element is compared with the elevation of the grid element itself. This algorithm also identifies saturated zones (perched ground water) within unsaturated areas.

3. In a third step, the correct hydraulic heads for the grid elements with perched ground water are calculated using the bottom elevation of the lowermost grid element of the perched ground water lens as the constant head boundary condition and the hydraulic gradient (or head differences between the grid elements).

Within the context of the code modifications the output and plot routines were also improved, thereby easing the interpretation of the results.

8.4 Model Parameters

With the appropriate computer code selected and modified to meet the special needs of the actual modeling study, the initial values of the model parameters were then assigned. These parameter values represent, in many cases, best estimates before the beginning of the modeling (e.g., the hydraulic conductivities). Some of these were changed or

varied during the model calibration or the sensitivity analysis (see Chapters 9 and 10).

A complete guide on preparation of the input data for the HCTM code is included in INTERA (1982). Therefore the description of the initial parameter values in the following sections does not include any model-specific notation or any code-specific input problems, except in those cases in which the actual parameter value is restricted or influenced by HCTM code specifics.

8.4.1. Model Grid

The model and the vertical model extent have been defined in Section 7.1. A code-specific restriction for the gridding is that the ratio of the thickness of two adjacent grid blocks should not exceed a factor of 2 because of the possible introduction of truncation errors (Appendix B-4.2.2). With these constraints in mind, the model area was discretized using a regular grid of 16 x 17 grid blocks (Figure 8-1). Each grid block measures 150 m x 150 m. On the vertical scale, for the steady state flow modeling, 14 grid layers with thicknesses between 1.5 m and 12 m were defined (Figures 8-2 and 8-3). With this grid almost 100% of the available computer memory was used.

The contaminant transport modeling requires some additional memory to store the 'points' of the point tracking method. Thus for the contaminant transport modeling the number of grid blocks had to be decreased in order to free some memory. Therefore the two grid layers (1.5 m thick) within the Tan Clay (Figures 8-2 and 8-3) were replaced by a single grid layer (3 m thick) for the contaminant transport modeling.

Grid blocks outside the defined model area (e.g., in the 'corners' of the horizontal grid or above the topographic surface) were eliminated (Figures 8-1, 8-2, and 8-3). There are two code specific ways to

eliminate grid blocks which occur outside the model area: (1) to assign a zero pore volume to a grid block, and (2) to assign a very low permeability (10^{-10} m/s or less) to a grid block. Grid blocks with a zero pore volume are considered to be nonexistent by the code's internal routines, while very low permeability blocks on the peripheries of the model are existent, but do not influence the model results. Generally the first method is the preferred one, because the nonexistent grid blocks do not require storage, and the flow equation is not solved for them. However, experience has shown that under certain geometric configurations the nonexistent grid blocks affect the convergence of the equation solving process. In these cases the alternate method to eliminate grid blocks must be used. For the actual study all grid blocks were eliminated by assigning a zero pore volume to them except the grid blocks in the southeastern corner of the model area (Figure 8-1), where the alternate method was used. The resulting model topography is shown in Figure 8-4. The numbers within the model area indicate the elevation of the top of the uppermost grid blocks in the model.

8.4.2 Constant Pressure Boundary Conditions

Based on the review of the piezometric data (Section 6.7) the general concept of the model boundaries was developed (Section 7.1). Using the estimated piezometric surfaces shown in Figures 6-8, 6-9 and 6-10, the appropriate hydraulic heads for the constant pressure boundaries were chosen (Figures 8-5, 8-6, and 8-7) and implemented.

Contaminant concentrations of zero were assigned to those constant head boundaries where a ground water inflow was expected to occur (southern boundary). The contaminant concentrations for the outflow constant head boundaries (e.g., the creeks) were left undefined. Thus the concentrations at these boundaries were calculated during the transport modeling.

8.4.3 Recharge

Based on long term precipitation data (Chapter 5) and on the estimated infiltration rate (30%), a general recharge of 380 mm/year (15 inches/year) was assumed for the model area (Section 7.1.2). This recharge was implemented as a prescribed flux boundary condition for all of the uppermost grid blocks in the model.

For the steady state flow modeling (Chapter 9) the recharge was constant over the entire area. For the transient transport modeling (Chapter 10), the recharge rate of the base case was also constant over the entire area. However during the parameter variation (Section 9.2.3) the recharge rate over Z-Area was varied in order to simulate on increased or reduced infiltration rate caused by the alternative disposal design concepts.

For the contaminant transport modeling, the contaminant concentration of the recharge was assigned a value of zero (simulating the infiltration of uncontaminated meteoric water) except at Z-Area, where a contaminant concentration of 1.0 (100%) was assigned to the recharge (see also Section 7.4) thereby simulating infiltration of rainfall and leaching within the landfill area. The number of grid blocks (18) with contaminated recharge was chosen such that the total 'contaminated area' (Figure 8-8) measures 405,000 m^2 (100 acres).

It was assumed for the contaminant transport modeling that the waste material will be disposed over the northern and central 100 acres of the identified Z-Area drawn on internal du Pont documents (pers. comm. J. Cook).

8.4.4 Hydrogeologic Rock Properties

Based on the existing literature (Chapter 4) and the data from various field and laboratory investigations (Chapter 6) the appropriate hydrogeologic rock properties or at least the initial values assigned to the model, were derived (Section 7.3). These (initial) values

(Figure 7-4) were assigned to the corresponding grid blocks as part of the model implementation.

8.4.5 Fluid Properties

In simulating ground-water flow, the HCTM code assumes a constant fluid viscosity and a fluid density, which is a function of fluid pressure only (Appendix B.1). Thus only three parameters for the model fluid (i.e., ground water) had to be defined: the compressibility of the fluid, the viscosity of the fluid and the specific weight of the fluid (although the compressibility of the fluid is irrelevant in the steady state flow modeling).

The compressibility of the fluid, 4.65×10^{-1} Pa^{-1} was derived from the literature (Kuchling, 1982). For the fluid viscosity and the specific weight, the model's default values were used (0.001 Pas and 9800 Pa/m).

8.4.6 Transport Parameters

For contaminant transport essentially three parameters must be defined for the HCTM code: the longitudinal dispersivity, the ratio of transverse to longitudinal dispersivity and the molecular diffusivity in the porous medium (Appendix B-1.2).

Based on the scale of the observed heterogeneity (i.e., the lenses of silt, clay, and sand), the screened intervals of the monitoring wells at Z-Area, and on the arguments concerning scale dependent dispersion presented in Pickens and Grisak (1981 a, b) a longitudinal dispersivity of 10 m was assigned. The ratio of transverse to longitudinal and porosity was assigned a value of 0.05 (Bear, 1972; Pickens and Grisak, 1981 a, b).

The molecular diffusivity of 10^{-10} m^2/s for nitrate in a porous medium derived from Lerman (1975) Dullien (1978) and Grisak and Pickens (1980) was selected.

8.4.7 Equation Solution Techniques

For ground-water flow modeling, HCTM provides two solution method options (Appendix B-4.1.4):

- direct-alternating diagonal direction Gaussian elimination method (ADGAUSS);
- iterative-line successive overrelaxation method (LSOR).

It was found that the LSOR method converges relatively slowly with the actual parameter set (grid, eliminated grid blocks, hydrogeologic rock properties, etc.). Therefore the ADGAUSS method was used, which proved to be several orders of magnitude faster, but required somewhat more computer memory (see also Appendix B.4.1.4).

For the contaminant transport modeling, there are also two options available: (1) a finite difference method, and (2) the method of characteristics (Appendix B.4.1.3). As discussed in Section 8.1, the expected numerical dispersion of the finite difference method was too large. Therefore the method of characteristics ('point tracking method') was selected for the contaminant transport.

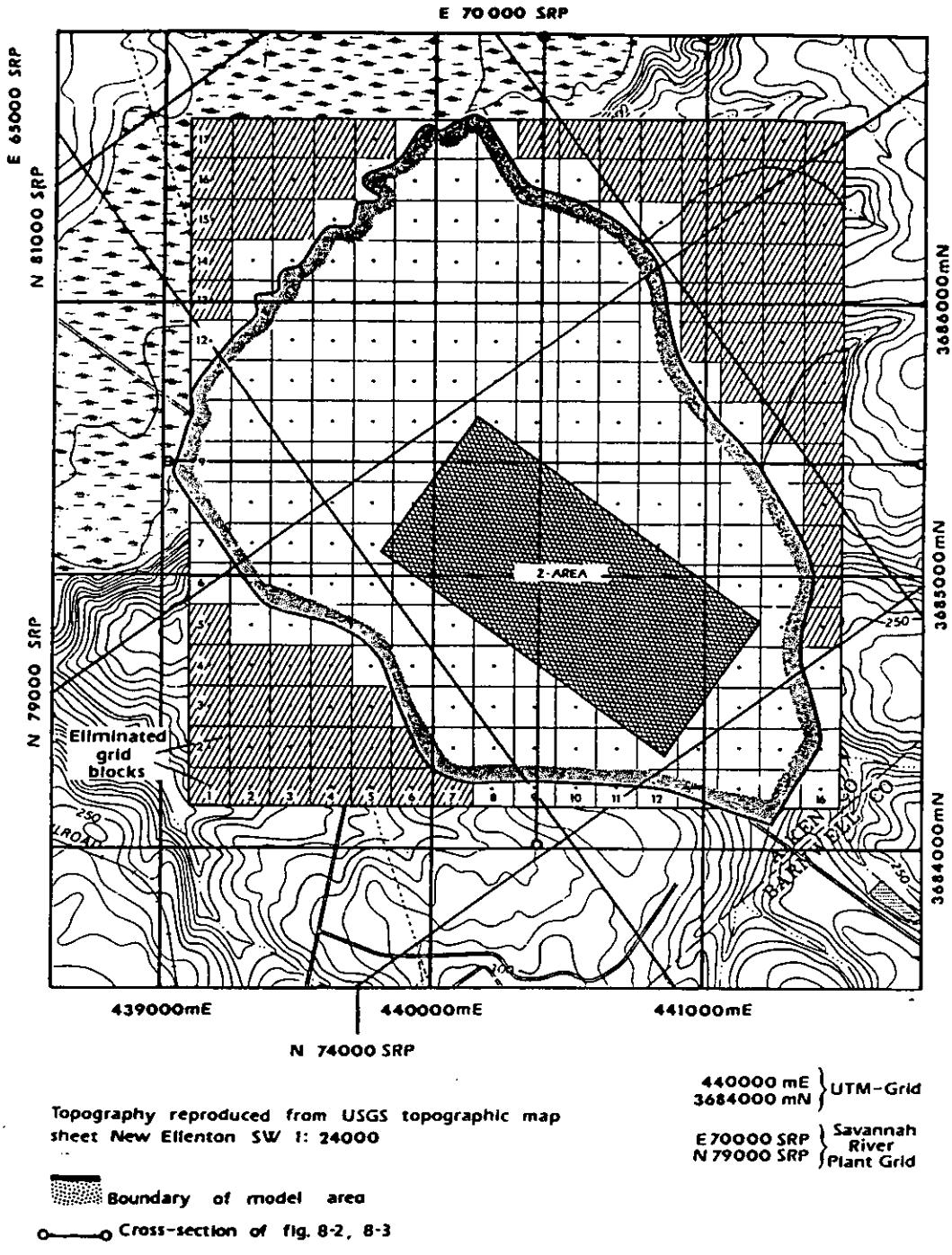

Figure 8-1 Model Area and Model Grid (lower most grid layer).

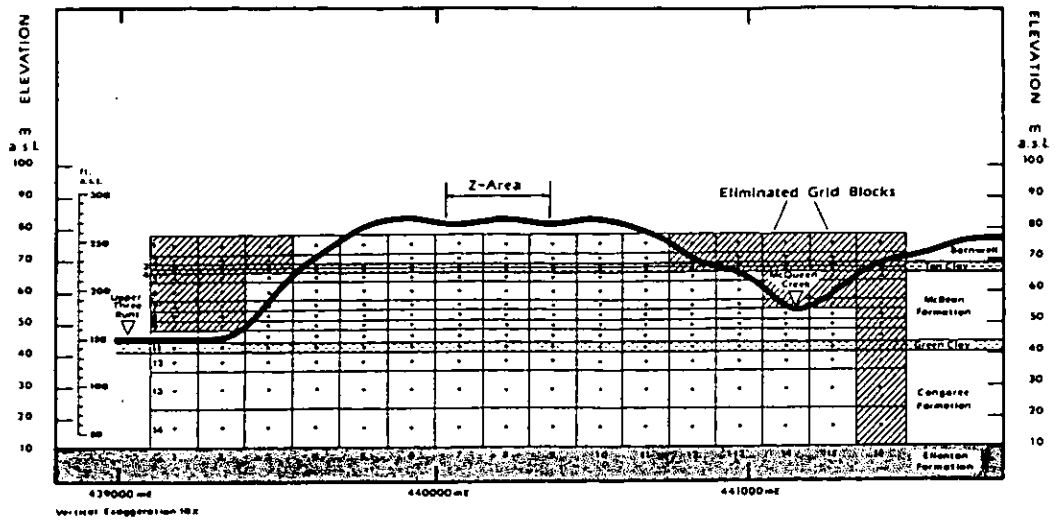

Figure 8-2 West-East Cross-Section Through the Model Area (Figure 8-1) and Model Grid.

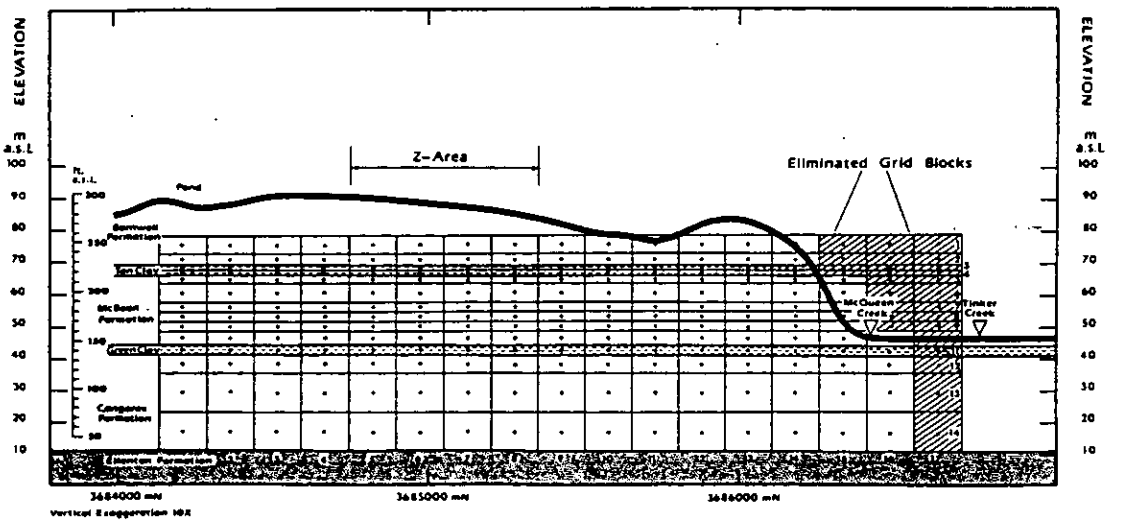

Figure 8-3 South-North Cross-Section Through the Model Area (Figure 8-3) and Model Grid.

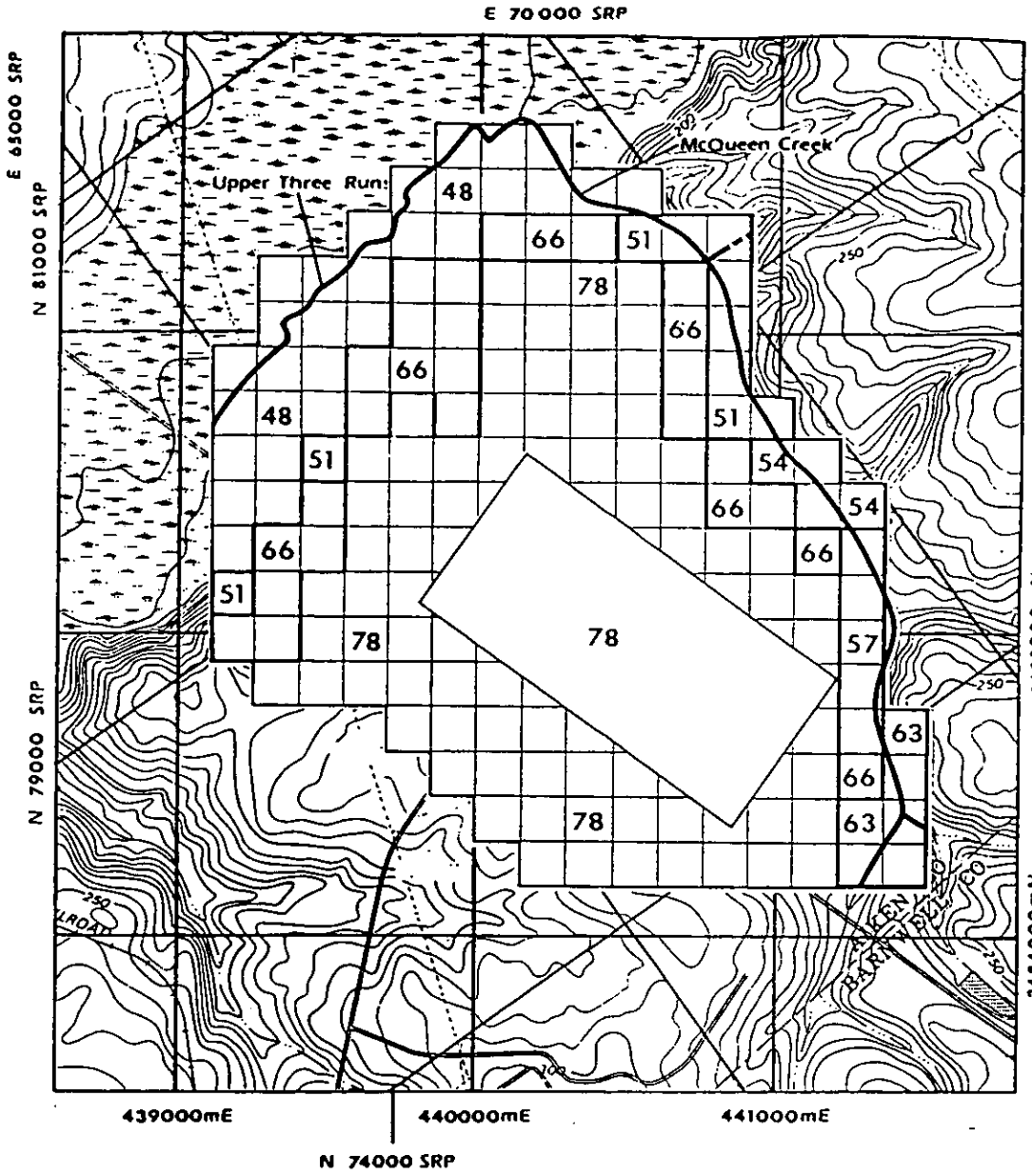

Figure 8-4 Model Topography.

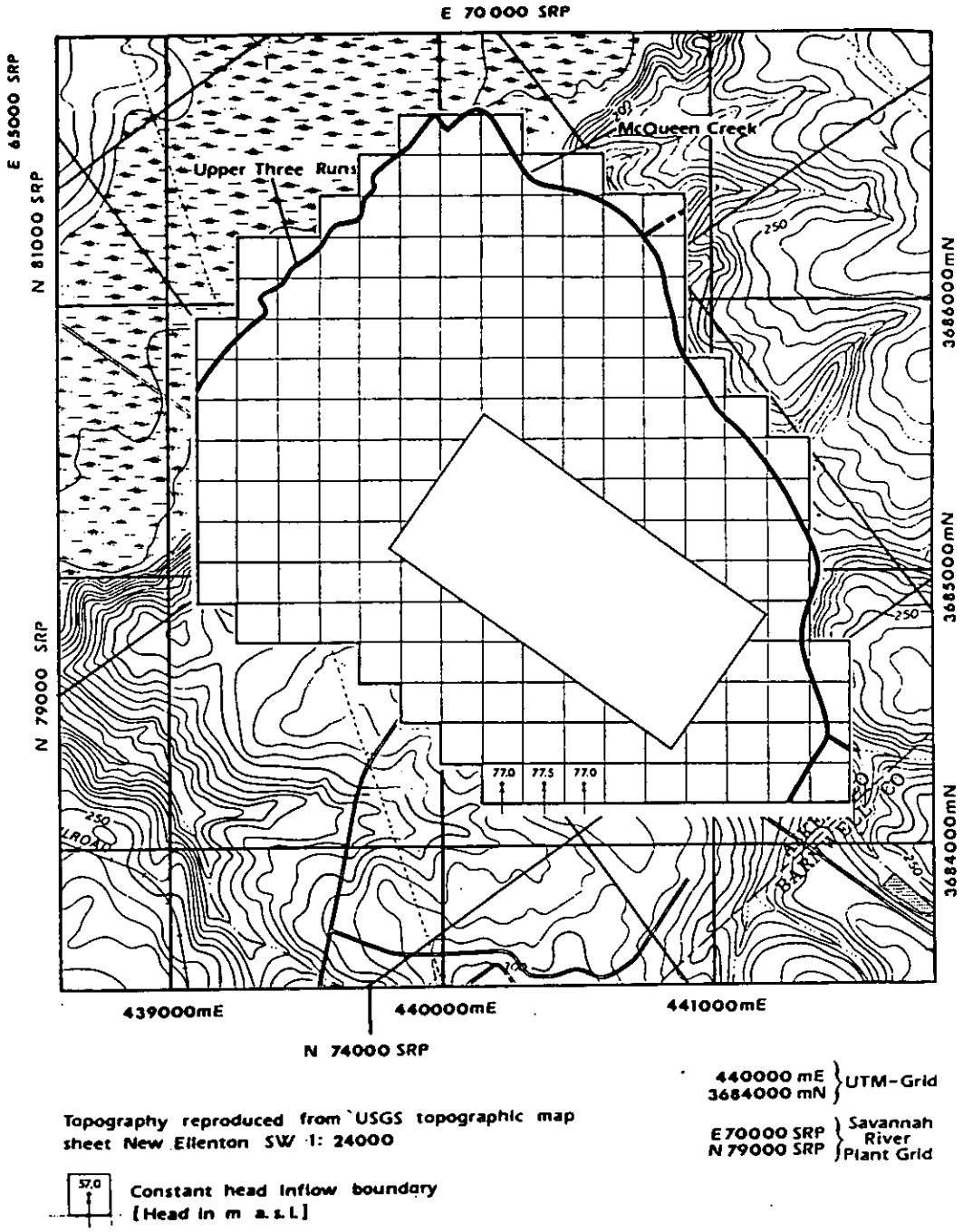

Figure 8-5 Constant Head Boundary Conditions in the Barnwell Formation.

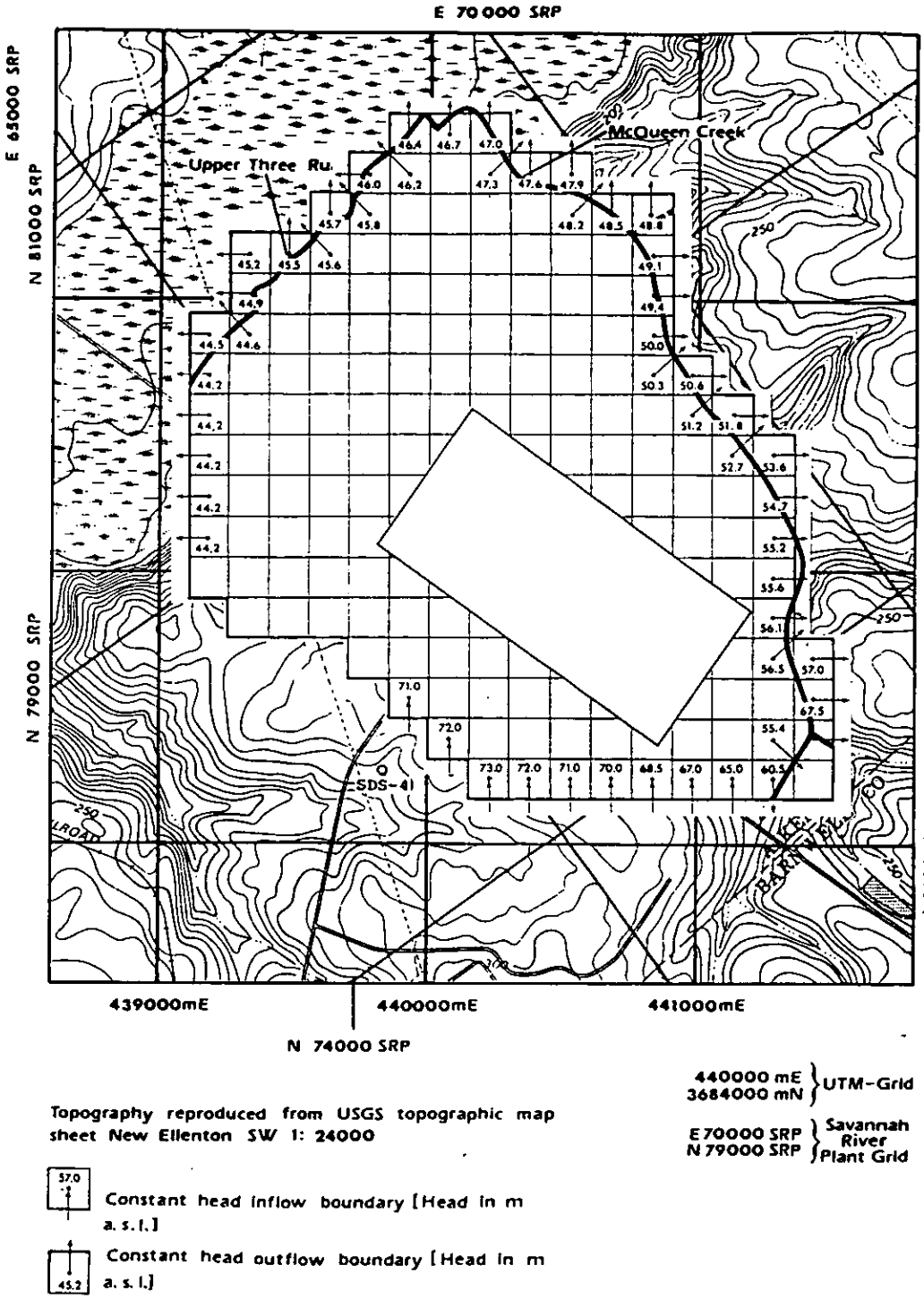

Figure 8-6 Constant Head Boundary Conditions in the McBean Formation.

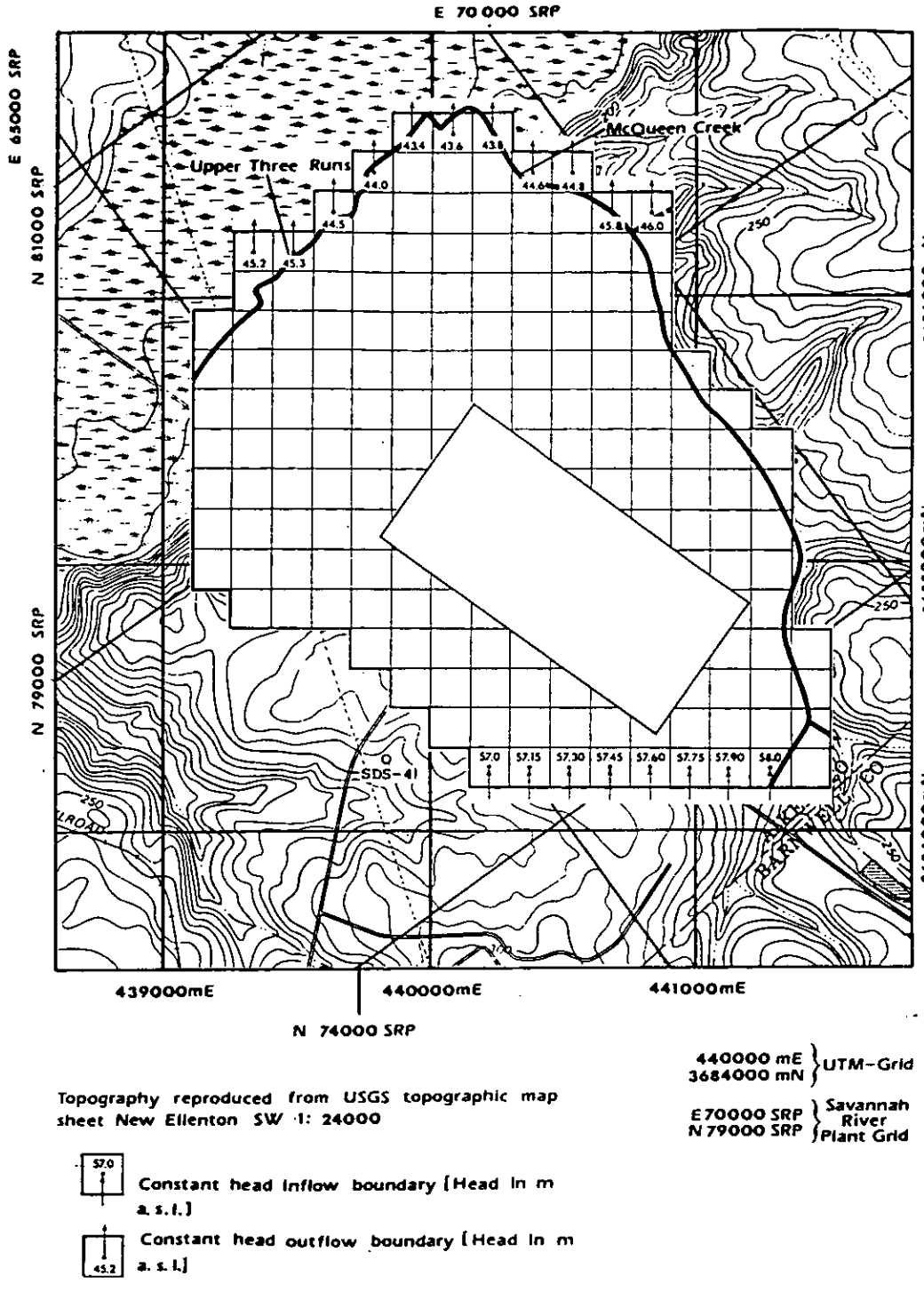

Figure 8-7 Constant Head Boundary Conditions in the Congaree Formation.

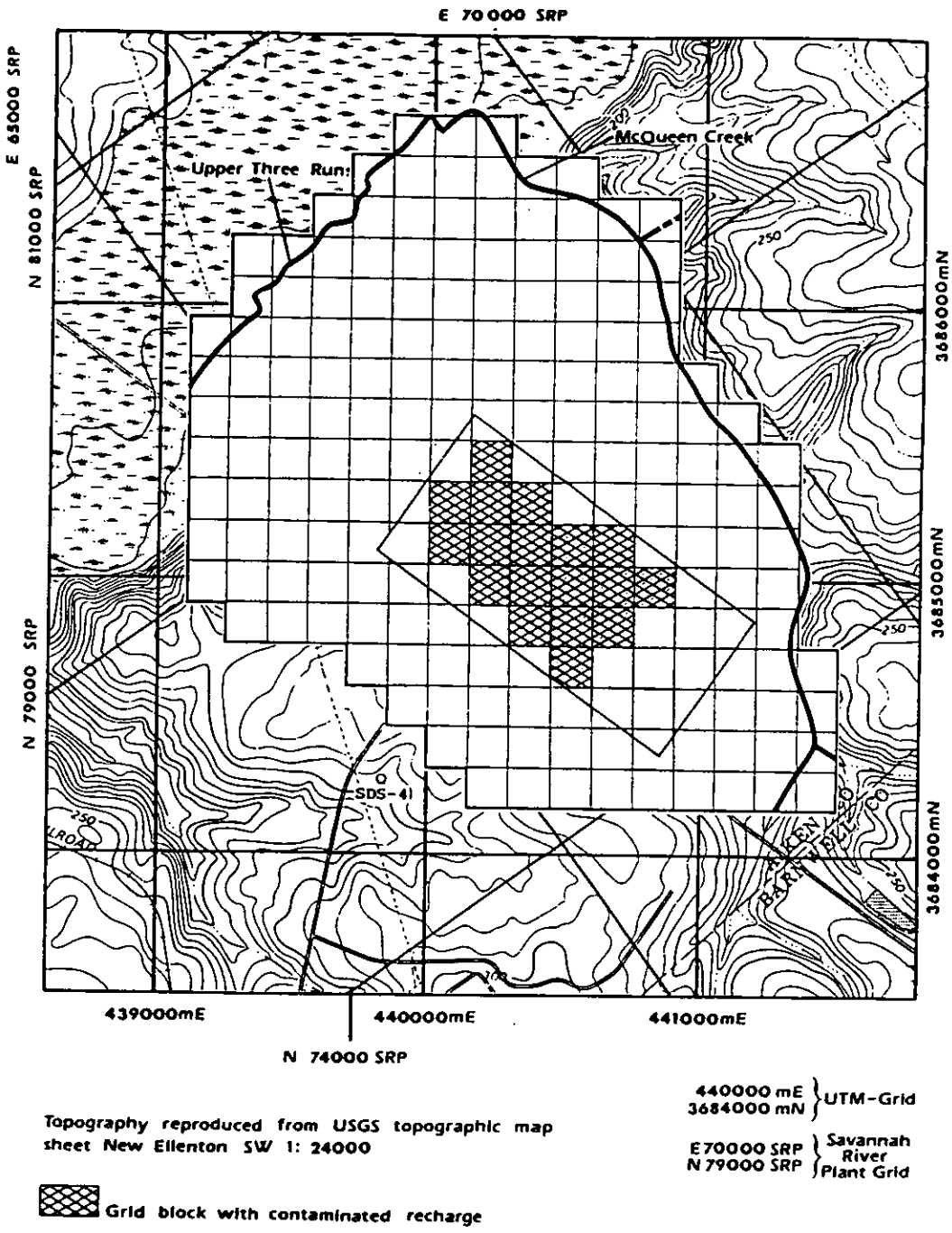

Figure 8-8 Contaminant Transport Modeling: Grid Blocks With Contaminant Recharge (Z-Area).

9.0 FLOW ANALYSIS

As discussed in Section 7.5, the ground water flow could be modeled as steady state flow, while the contaminant transport must be simulated as a transient process. However the contaminant transport simulation utilizes the steady state ground water flow field. Thus the contaminant transport modeling required a calibrated steady state ground water flow model. Within the actual study the steady state ground water flow model was conceptualized (Chapter 7), implemented (Chapter 8), and calibrated before any contaminant transport modeling was performed. Together with the calibration of the flow model, a sensitivity analysis for the most important model parameters was conducted. The most important steps of both the calibration process and the sensitivity analysis are summarized in the following sections.

9.1 Initial Flow Model

INTERA's computer code HCTM was selected as the code for the study (Section 8.1) and modified to meet the special requirements (Section 8.3). Then the input data or model parameters, as far as required for flow modeling, were assigned (Section 8.4)

Base case model parameters were best estimates (e.g., the hydraulic conductivity of the Green Clay, see Section 8.4.4) based on a limited data set. Employing the initial best estimates in the model implementation resulted in an initial uncalibrated flow model.

The calculated hydraulic heads of the initial flow model are shown in two cross-sections of the model (Figures 9-4 and 9-5). Although the model was not yet calibrated, the cross-sections demonstrate, in general terms, the site-specific head distribution resulting from the best-estimate parameter set. The head in the Congaree Formation is about 52 m a.s.l. beneath Z-Area. The ground water in the McBean Formation is confined in the central and southern part of the model area. The ground

water in the Barnwell Formation is part of the main ground water body where the McBean Formation is confined, and perched ground water, where there is a free water table in the underlying McBean Formation. The water table in the Barnwell Formation is generally several meters above the base of the Tan Clay (71-72 m a.s.l.).

Thus the general head distribution (particularly the "perched ground water tongue") fits very well to the expectations based on the data review (Chapter 6) and demonstrates the validity of the model's hydrostratigraphic conceptualization.

The calculated piezometric surfaces in the three aquifers are also displayed in Figures 9-3, 9-4, and 9-5. For comparison, the mean Congaree and McBean water levels from borehole measurements, which are considered to be sufficiently reliable (Section 6.7) are also shown (Figures 9-3 and 9-4). Figures 9-3, 9-4, and 9-5 can be also compared with Figures 6-8, 6-9 and 6-10, where the estimated piezometric surfaces (based on the existing data) are shown.

A comparison between the Congaree heads, calculated by the initial flow model, and the measured mean water levels shows a very good agreement as far as both the general flow pattern in the Congaree Formation and the heads (or water levels) at the borehole locations are concerned. This is also demonstrated by Table 9-1, where the calculated head and the measured water levels are listed. The average difference between these two data groups (Average Δ Head) is only 0.124 m. Considering the limited data base, any reduction of this difference would not make the model more representative of the actual Congaree ground water levels. Unlike the Congaree aquifer, the agreement between calculated heads and measured water levels in the McBean Formation was not yet satisfactory.

Although the general flow pattern looks similar to the expected flow pattern (Figures 6-9 and 9-4) the calculated heads are substantially lower than the observed values. The average difference is about 3 meters (Table 9-2).

Because the applied boundary conditions which affect the McBean and Congaree Formations are considered to be reasonably correct, and the Congaree aquifer exhibits satisfactory heads, the variables on which the McBean heads depend most and which can be used to calibrate the McBean aquifer are the hydraulic conductivities of the McBean Formation and the Green Clay. The calibration of the McBean aquifer is described in Section 9.2.

The calculated hydraulic heads in the Barnwell Formation (Figure 9-5) fit reasonably well to the estimated piezometric surface (Figure 6-8).

Because the Barnwell ground water discharges through the Tan Clay into the underlying McBean Formation, the water table in the Barnwell Formation depends primarily on two parameters: (1) the hydraulic conductivity of the Tan Clay and (2) the recharge. The conductivity of the Barnwell Formation itself is less important, because it is about two orders of magnitude higher than that of the Tan Clay. Thus the hydraulic conductivity of the Tan Clay is the dominant hydraulic conductivity for the water table calibration in the Barnwell Formation.

As pointed out in Section 9.7, it is difficult to establish a representative steady state piezometric surface in the Barnwell Formation based on the existing field data. Therefore it was not attempted to calibrate the Barnwell aquifer. Rather a sensitivity analysis for the hydraulic conductivity of the Tan Clay was conducted in order to establish the range for which the model results are consistent with the observed water levels (Section 9.2.2). In addition, a sensitivity analysis was performed for the recharge rate in order to evaluate the uncertainty as far as the actual infiltration rate is concerned and in order to demonstrate the effect of fluctuations in the annual precipitation on the Barnwell ground water table (Section 9.2.3).

9.2 Calibration and Sensitivity Analysis

9.2.1 McBean Formation and Green Clay

As pointed out in the previous section, the hydraulic heads in the McBean Formation, as calculated by the initial flow model, are about 3 meters too low. It was further indicated that the McBean heads depend primarily on the conductivity of both the McBean Formation and the Green Clay.

Therefore these two parameters were systematically varied in order to calibrate the McBean aquifer. During this parameter variation the evaluation criterion was how well the calculated hydraulic heads agreed with the measured mean water levels (Table 6-7). This agreement was quantified by using both the average head difference (between the calculated and the measured values) and the sum of squared differences (delta square sum). While the average head difference (Average Δ Head) indicates whether the calculated water levels are generally too high or too low, the delta square sum is a generally accepted discriminating indicator of the quality of agreement between two data sets.

In order to reduce the influence of the Congaree Formation during this parameter variation, the southern inflow boundary of the Congaree Formation was temporarily suspended and the northern boundary adjusted, such that the hydraulic head in the Congaree Formation was maintained at about 52 m a.s.l. within the entire model area. By this means, the principles of the hydraulics in the McBean Formation could be shown more clearly.

During the parameter variation the hydraulic conductivity of the McBean Formation was varied between 2×10^{-5} m/s and 5×10^{-7} m/s. It was found that for every conductivity value (for the McBean Formation) within that range a hydraulic conductivity can be found for the Green Clay with which the calculated head values and the measured water

levels in the McBean Formation are in good or at least fair agreement (Figures 9-6 and 9-7). Thus there exists no well defined calibration point for the McBean aquifer with definite conductivities for both the McBean Formation and the Green Clay. Rather there is an infinite number of conductivity pairs, for which the McBean aquifer can be considered to be calibrated. These conductivity pairs form the calibration line of the McBean aquifer in the McBean-Green Clay conductivity diagram (Figure 9-6 and 9-7). In Figure 9-6, the calibration line represents those conductivity pairs where the average head difference is zero. In Figure 9-7, the calibration line represents those conductivity pairs where the delta square sum is a minimum, when one conductivity is fixed and the other is varied.

As both Figures 9-6 and 9-7 reveal, the calibration line for the McBean Formation stretches between two situations: (1) where the conductivity of the Green Clay is zero and (2) where the conductivity of the Green Clay is the same as the conductivity of the McBean Formation. The first case is comparable to the model presented by Root (1982) in which an impermeable Green Clay was assumed. Root considered the model calibrated with a hydraulic conductivity of 2.1×10^{-5} m/s for the McBean Formation. This is in excellent agreement with the calibration line in Figures 9-6 and 9-7, which indicates that a McBean conductivity of 2×10^{-5} m/s corresponds to a completely impermeable Green Clay. The delta square sum at this point is 2.84 m^2.

On the other hand, the calibration line also approaches the point where the hydraulic conductivity of the McBean Formation is equal to the hydraulic conductivity of the Green Clay (equal conductivity line). At that point the Green Clay loses its hydrostratigraphic identity. The closest conductivity pair to the equal conductivity line which was utilized during the parameter variation is 2×10^{-8} m/s for the Green Clay and about 5.8×10^{-8} m/s for the McBean Formation. The delta square sum at this point is 83.6 m^2. Thus the agreement between calculated and measured values at this end of the calibration line is worse than at the other end.

Figure 9-8 displays the delta square sums along the calibration line as a function of the permeability of the Green Clay. It shows, that for Green Clay conductivity values below 6×10^{-10} m/s the square sum is relatively stable at about 3 m^2 . Above 6×10^{-10} m/s the delta square sum rises considerably, although there is a small local minimum at 2.99×10^{-9} m/s. This minimum is caused by the actual spatial distribution of the exiting data set and is of no importance for the general characteristics of the model. Thus the hydraulic situation within the McBean Formation stays relatively stable for Green Clay conductivities below 6×10^{-10} m/s, but changes dramatically above that value.

It is instructive to see the calculated head distributions, shown in south-north cross-sections, for the different conductivity pairs. (Figure 9-9). They show that the models with Green Clay conductivities below 2×10^{-9} show very similar head distributions and consequently very similar flow patterns. The general direction of flow in the McBean Formation is directed horizontally, thus most of the McBean ground water discharge into the creeks.

In contrast, when increasing the hydraulic conductivity of the Green Clay from 2×10^{-9} m/s to 5×10^{-9} m/s and reducing consequently the hydraulic conductivity of the McBean Formation from 6.4×10^{-6} m/s to 1.1×10^{-7} m/s, (in order to stay on the model's calibration line), the head distribution and the flow pattern change dramatically. The general direction of flow rotates from horizontal to vertically downwards. The unsaturated zone below the Tan Clay disappears and most of the McBean ground water discharges into the Congaree Formation.

This change is also shown in Figure 9-10. While the total flux into the model (due to infiltrating precipitation and inflow through the constant head boundaries in the south) stays more or less constant, the discharge of McBean ground water into the underlying Congaree Formation increases from 16% (when using 6×10^{-10} m/s for the Green Clay) to 82%, (when using 5×10^{-9} m/s.

It is obvious from Figure 9-8, that Green Clay conductivities greater than 6×10^{-10} m/s result in an increasingly less satisfactory agreement between calculated and measured heads. Below 6×10^{-10} m/s the agreement does not vary significantly. However, the lowest delta square sum was obtained for a very low Green Clay conductivity (5×10^{-11} m/s). While no hydraulic conductivity data for the Green Clay were available, the data review provided the possible range in which the hydraulic conductivity of the McBean Formation should lie (Section 6.6, Table 6-4). Accordingly the McBean conductivity should be between 1×10^{-6} and 3×10^{-5} m/s. The corresponding hydraulic conductivities for the Green Clay on the calibration line range from 0 to about 2.8×10^{-9} m/s.

Based on the lithological description of the Green Clay (Section 3.1.6), extremely low hydraulic conductivities did not appear to be realistic. Therefore the highest conductivity value that can be assigned to the Green Clay without increasing significantly the delta square sum (Figure 9-8), was selected as the model hydraulic conductivity (6×10^{-6} m/s). The corresponding hydraulic conductivity for the McBean Formation is 1.7×10^{-5} m/s. With these two conductivity values the delta square sum is about 3 m^2. Employing these two conductivity values resulted in what was considered to be a calibrated McBean aquifer. The selected hydraulic conductivities were used for the further parameter variations (Section 9.2.2 and 9.2.3) as well as in the calibrated flow model (Section 9.2.4.).

9.2.2 Tan Clay

As pointed out in Section 9.1, a calibration of the Barnwell aquifer was not performed. Rather a systematic variation of the hydraulic conductivity of the Tan Clay, which is the most important parameter with respect to the water table in the Barnwell aquifer, was conducted. The result of this parameter variation is shown in Figure 9-11.

The highest hydraulic conductivity assigned to the Tan Clay was 1×10^{-7} m/s. With this conductivity a perched water table above the Tan Clay is not developed. The Barnwell and McBean Formation form a common hydraulic system.

Using 5×10^{-8} m/s as the conductivity for the Tan Clay, a perched ground water 'tongue' occurs in the northern part of the model. As the Tan Clay conductivity is decreased, the perched ground water above the Tan Clay grows thicker. With 5×10^{-9} m/s, the perched ground water table reaches the upper boundary of the model (78 m a.s.l.) and with 2×10^{-9} m/s, the perched water table would be partly above land surface.

The existing water level data from the borehole show that there is a perched water table and that it's elevation should be between 70 and 72 m a.s.l. (see Section 6.7 Table 6-5). Although it is difficult to calculate a precise steady state water level for the Barnwell Formation (Section 6.7) at least this range (70-72 m a.s.l.) can be used as a criterion when assigning a hydraulic conductivity to the Tan Clay.

As the cross-sections in Figure 9-11 show, a Tan Clay conductivity value of 2×10^{-8} m/s results in water levels too low (i.e., < 70 m a.s.l.) except in the extreme southern part. A conductivity of 0.5×10^{-9} m/s causes a water table between 71 and 74 m a.s.l. which is somewhat too high. Thus the hydraulic conductivity of the Tan Clay

must lie between 0.5 x 10^{-9} m/s and 2 x 10^{-8} m/s. A conductivity of 1 x 10^{-8} m/s lies approximately in the middle of that interval. It results in a water table in the Barnwell Formation that lies between 70 and 72 m a.s.l. in a large part of the model area. Therefore 1 x 10^{-8} m/s was selected as the hydraulic conductivity of the Tan Clay for the calibrated flow model.

9.2.3 Recharge

In order to investigate the sensitivity of the model to variations in the recharge rate, a parameter variation about the recharge rate was performed.

As the cross-sections in Figure 9-12 show the applied recharge ranges from 127 mm/y to 760 mm/y. These values correspond either to different infiltration rates (between 10 to 60%) of the long-term average annual precipitation (about 1250 mm/y) or to different annual precipitation rates (423 mm/y to 2533 mm/y) with a fixed infiltration rate of 30%. Thus this parameter variation can be used to quantify both a variation of the infiltration rate and a variation of the precipitation. However this is possible only for short term variations of the infiltration or precipitation rates, because the model could be also calibrated for different steady state recharge values simply by applying different hydraulic conductivities to the hydrostratigraphic units.

When interpreting the results of this parameter variation, it must be recalled that the boundary conditions were not varied and that these boundary conditions were estimated for years with average recharge. Therefore the effect of the boundary conditions, especially the southern boundary with prescribed heads is not taken into account.

As Figure 9-12 displays, the model shows relatively stable heads around a 30% infiltration rate (20 to 40%). However, both water tables in the Barnwell and the McBean Formation would change according

to the infiltration rate. Also the size of the unsaturated zone would vary. However, the typical head distribution and the general flow pattern would remain the same.

According to the long-term rainfall data (Figure 5-1) the annual precipitation varies between 550 mm and 1900 mm. With a fixed infiltration rate, the corresponding recharge ranges between 165 mm/y and 570 mm/yr. Thus the first number represents an extremely dry year, while the second value stands for extremely wet years. As shown in Figure 9-12, this variation has drastic effects on the water tables. In very dry years, the perched ground water in the Barnwell Formation almost disappears. In very wet years, the perched water in the Barnwell Formation can reach about 78 m a.s.l. and the unsaturated zone in the McBean Formation almost disappears. As mentioned before, this very high water level for extremely wet years is based on a fixed infiltration rate. However, it is likely that in very wet years the run-off is higher, resulting in a somewhat lower infiltration rate. Thus the water table maximum for the Barnwell Formation is likely to be somewhat lower (see Cook, 1983).

9.3 Calibrated Flow Model

After completion of the parameter variation, the two grid layers representing the Tan Clay were replaced by a single grid layer in order to free some computer memory for the subsequent contaminant transport modeling (see Section 8.4.1). It was found that this grid simplification resulted only in a very minor loss of resolution of the ground water head distribution in the Tan Clay itself. The model in general was not affected by the change.

All initial model parameters were assigned to this slightly simplified grid except the hydraulic conductivities of the McBean Formation and the Green Clay (Figure 9-13). There the results of the calibration or parameter variation (Section 9.2.1) were used. The resulting flow model is shown in two cross-sections (Figures 9-14 and 9-15) and in three piezometric maps (Figures 9-16, 9-17 and 9-18).

The general head distribution and the ground water flow pattern is very similar to the initial flow model (Figure 9-1 through 9-5). The agreement between the calculated heads and the measured water levels is very good in both the Congaree and the McBean Formations (Tables 9-3 and 9-4). The delta square sum in the Congaree is 0.77 m^2 which is about the same as with the initial flow model. In the McBean Formation the delta square sum is 1.99 m^2 as compared to 46.4 m^2 with the initial flow model. The average head differences are 0.18 m (Congaree Formation) and 0.1 m (McBean Formation).

Compared to the initial flow model, the water table in the McBean Formation is generally 1-3 m higher. Therefore the unsaturated zone in the central part of the model area is very thin (Figure 9-4) or non-existent (Figure 9-5). The good agreement between calculated and measured data demonstrate that the model was successfully calibrated. The steady state flow field of this calibrated flow model was used for the contaminant transport modeling.

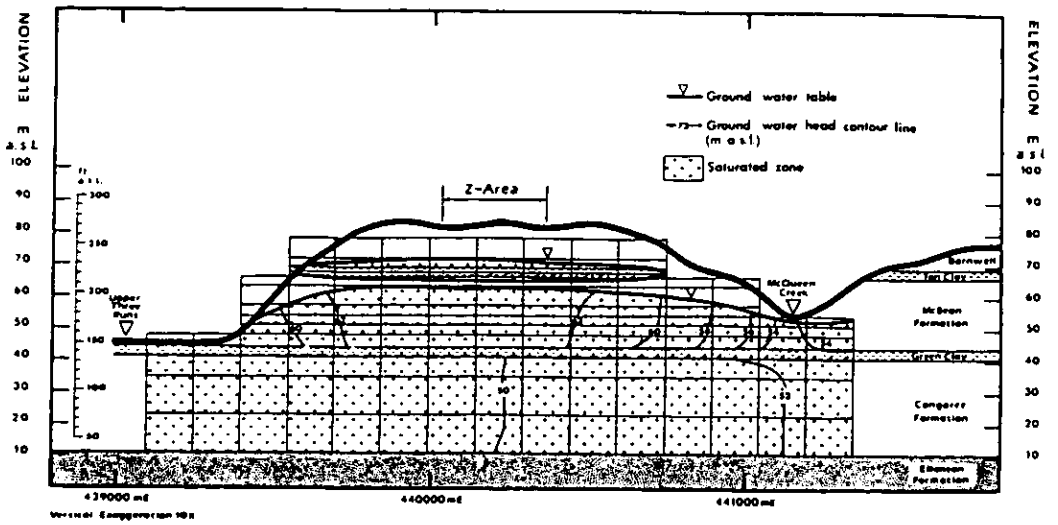

Figure 9-1 Initial Flow Model: West-East Cross-Section

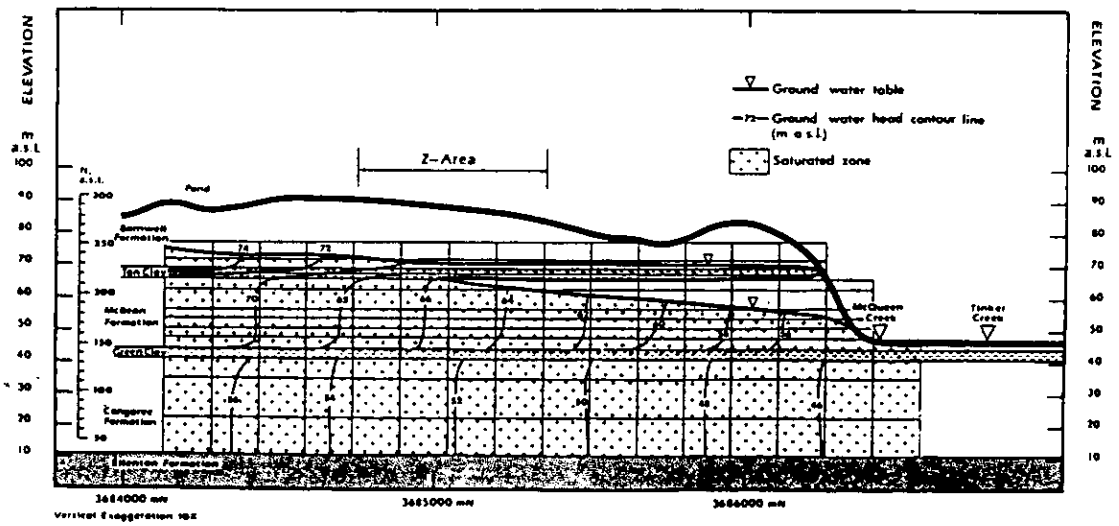

Figure 9-2 Initial Flow Model: South-North Cross-Section

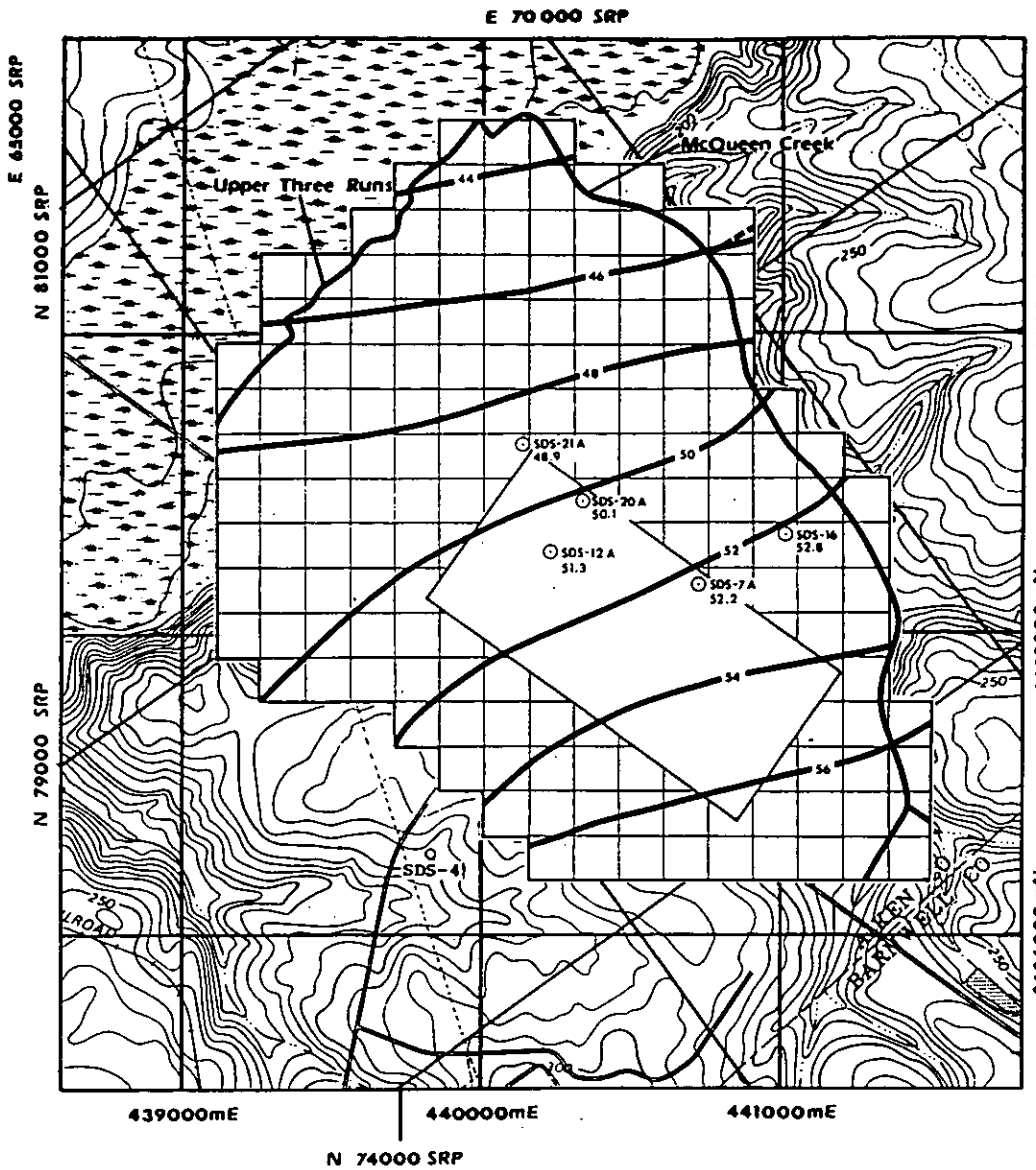

Figure 9-3 Initial Flow Model: Calculated Piezometric Surface in the Conagree Formation

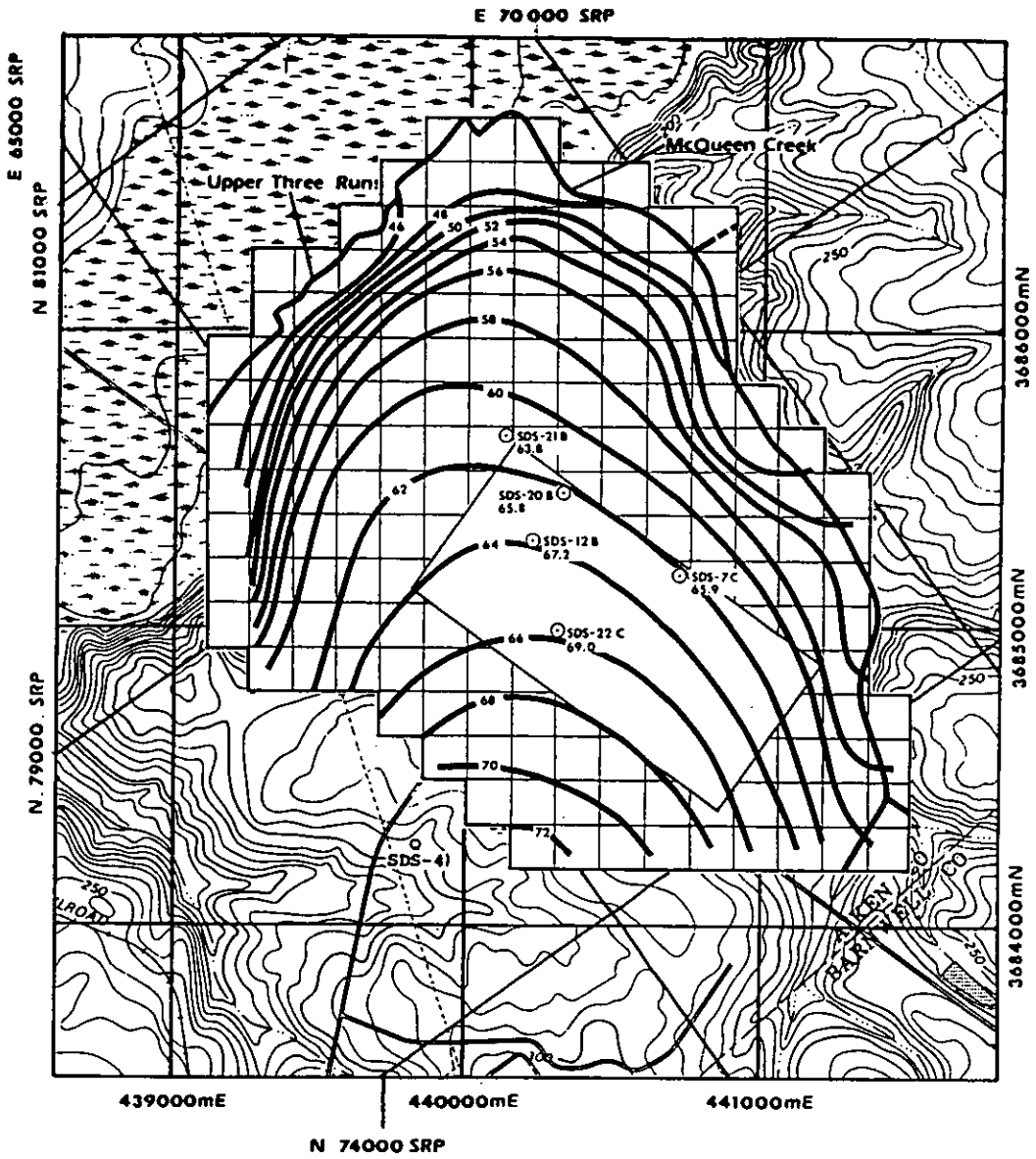

Figure 9-4 Initial Flow Model: Calculated Piezometric Suface in the McBean Formation

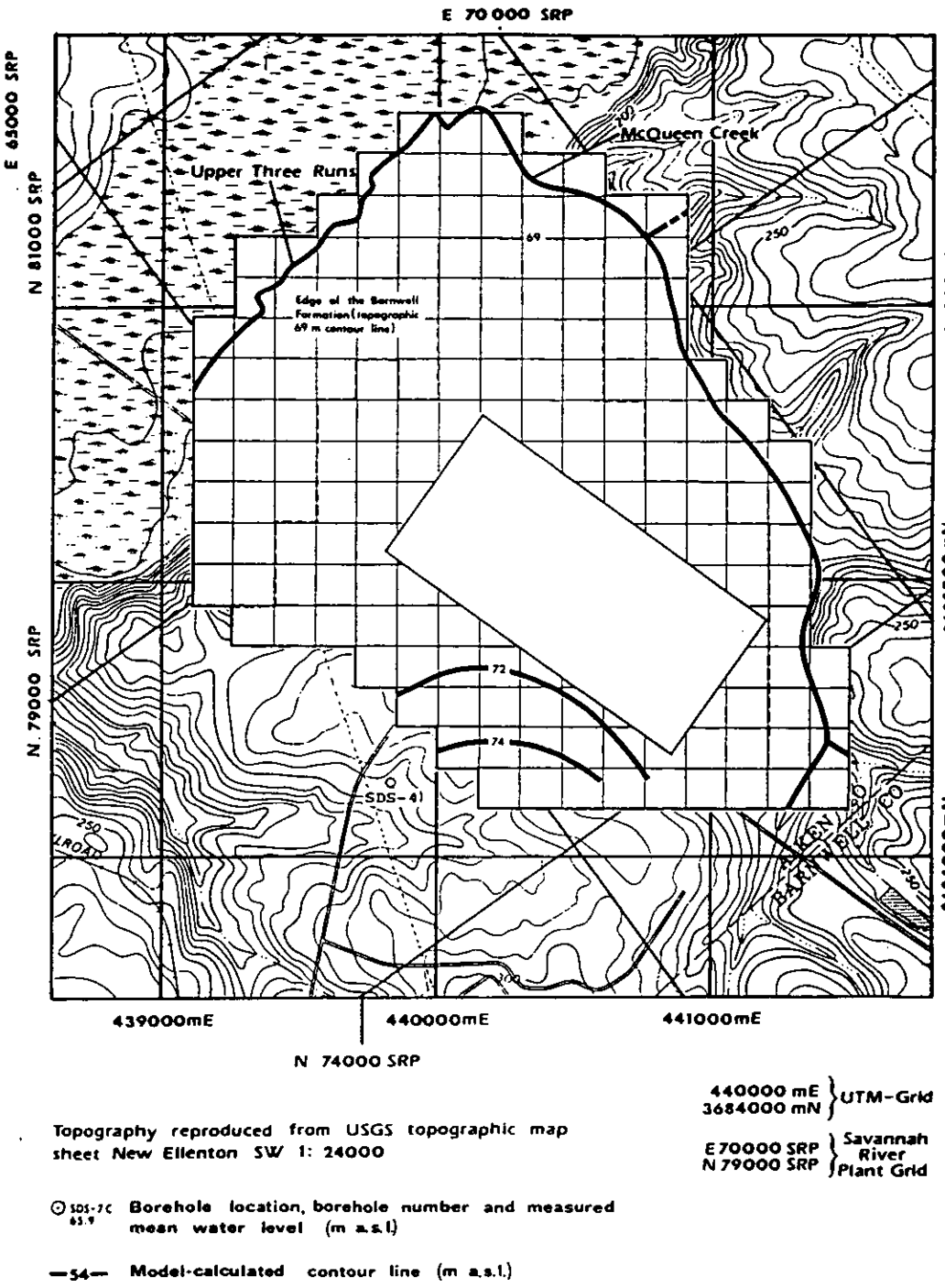

Figure 9-5 Initial Flow Model: Calculated Piezometric Surface in the Barnwell Formation

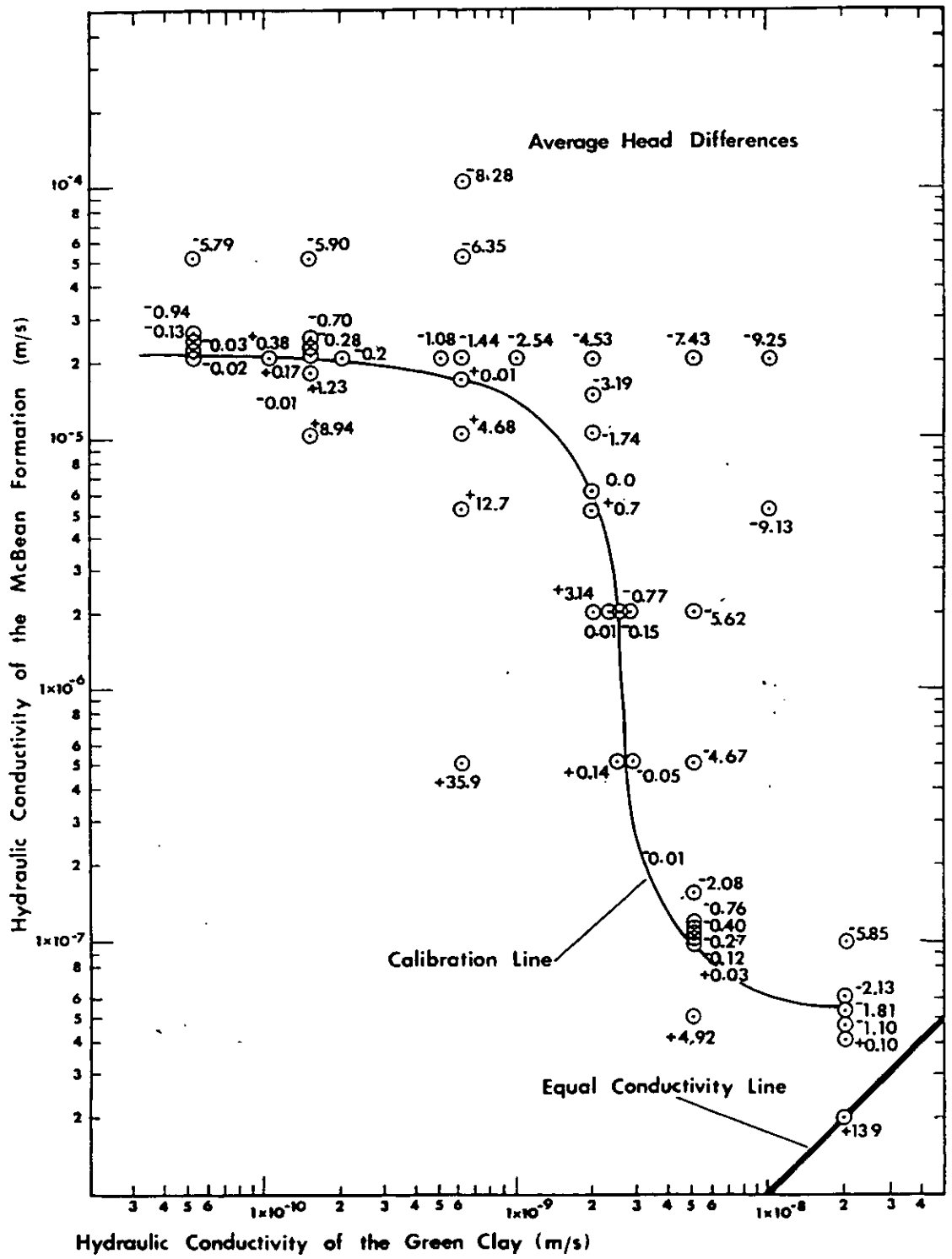

Figure 9-6 Parameter Variation McBean Formation - Green Clay: Average Head Difference.

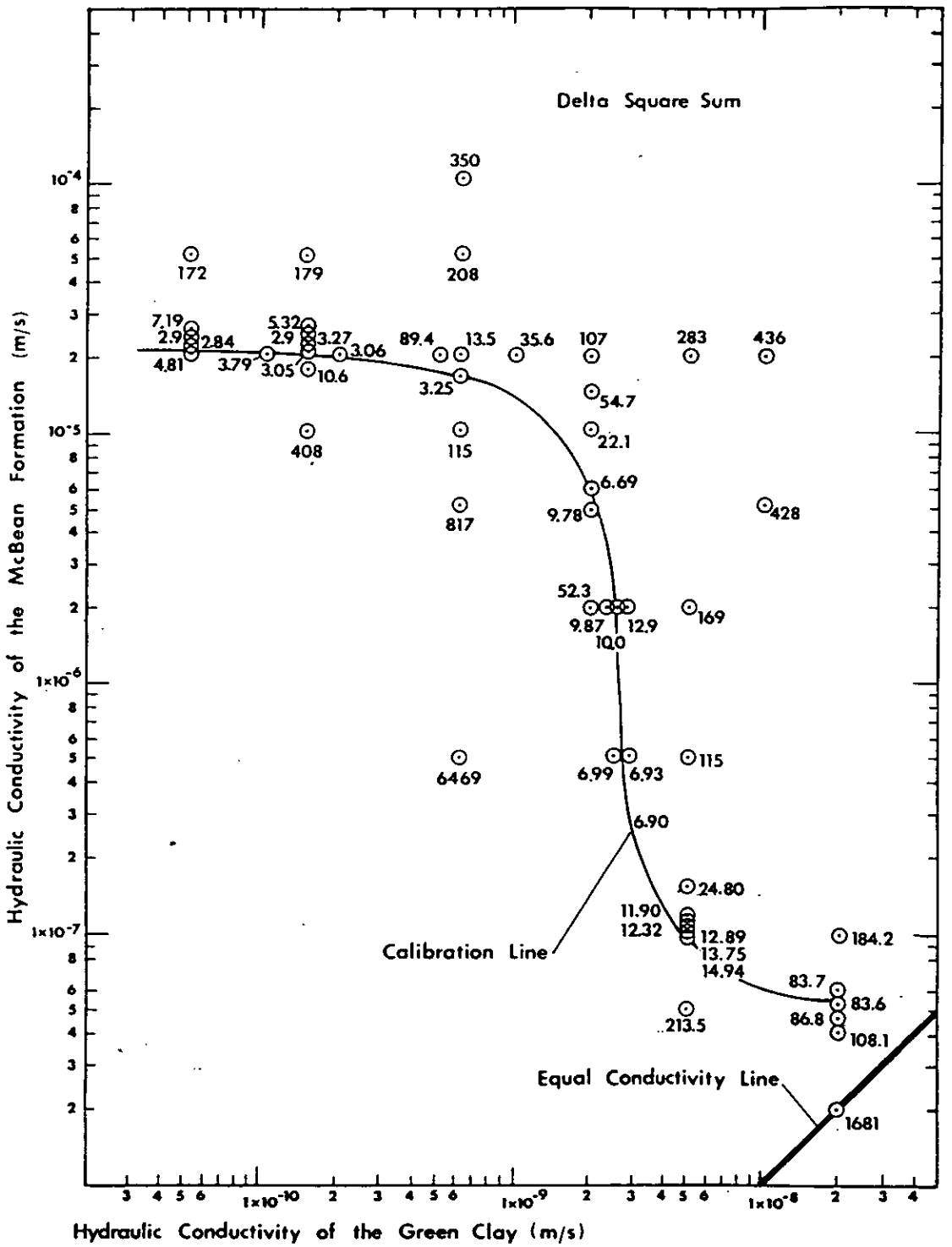

Figure 9-7 Parameter Variation McBean Formation - Green Clay: Delta Square Sum.

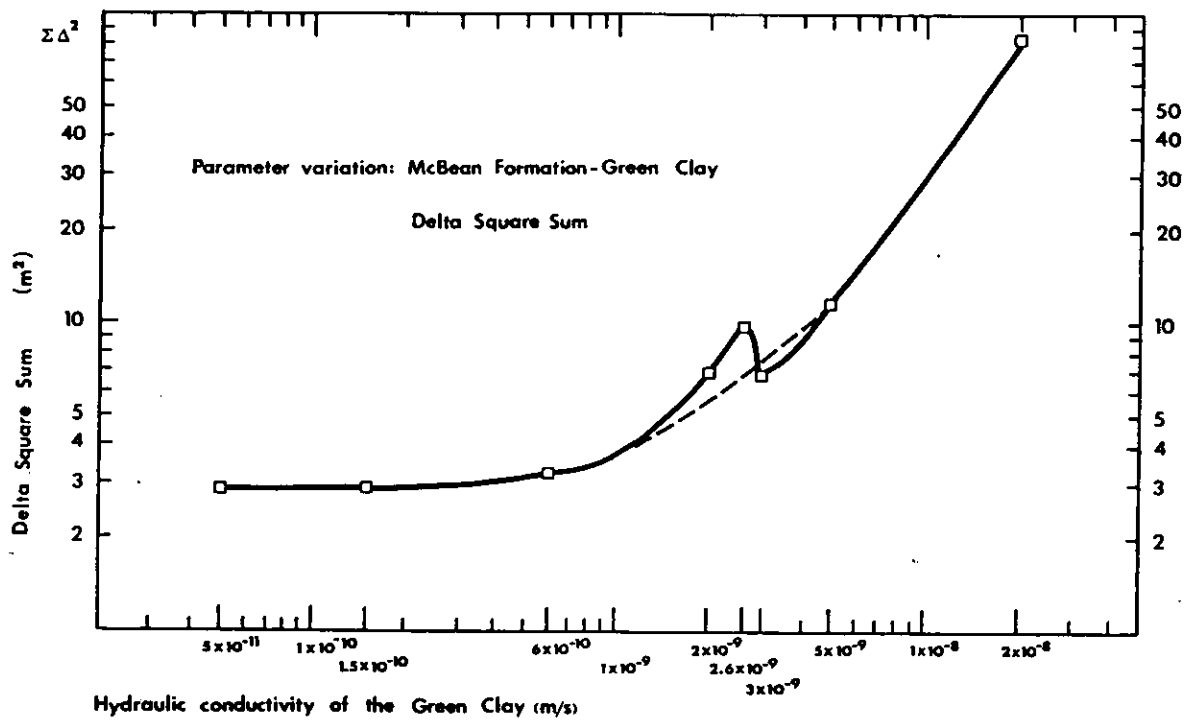

Figure 9-8 Parameter Variation McBean Formation - Green Clay: Delta Square Sum.

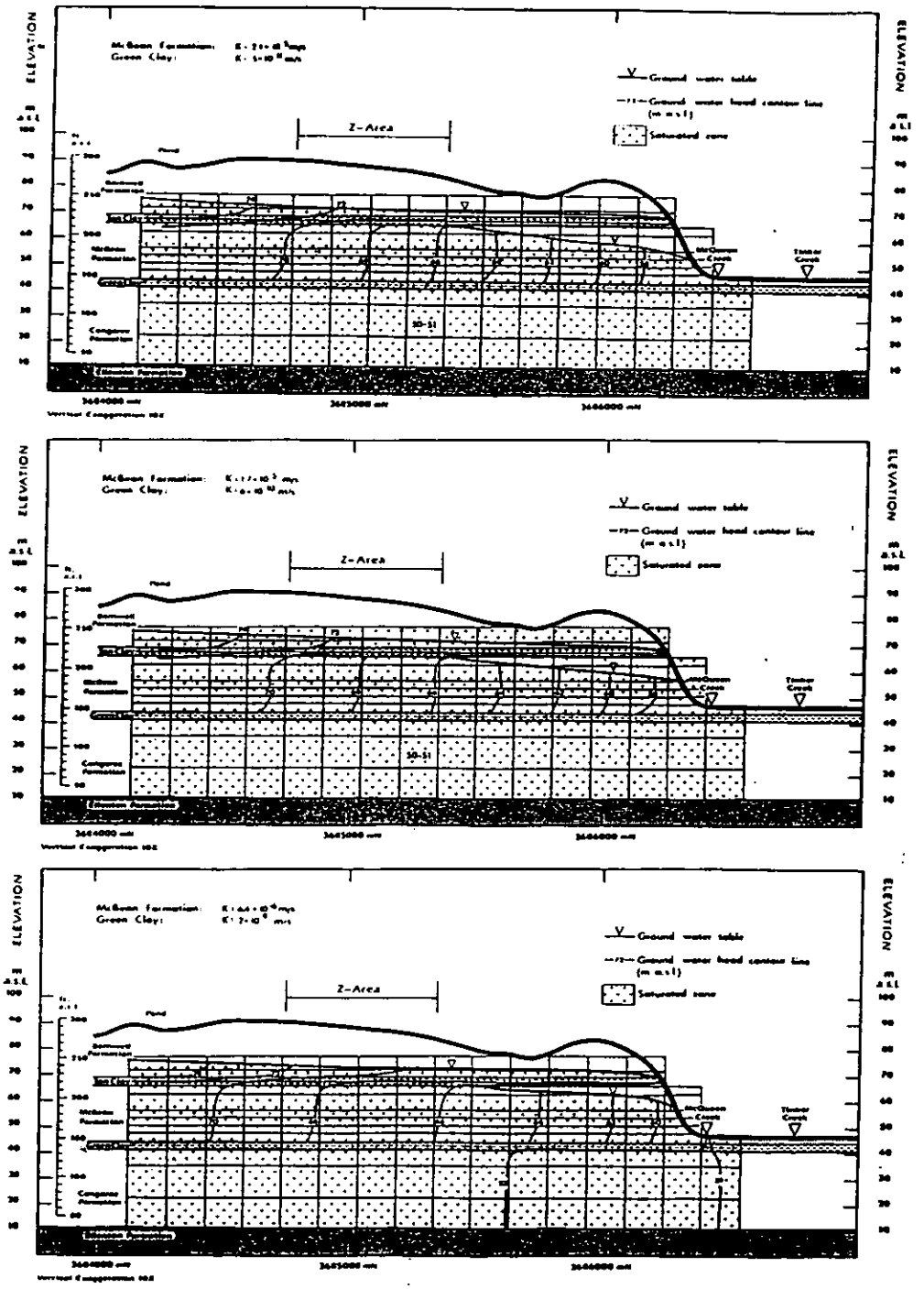

Figure 9-9 Parameter Variation McBean Formation - Green Clay: Ground Water Head Distribution (South-North-Cross-Section).

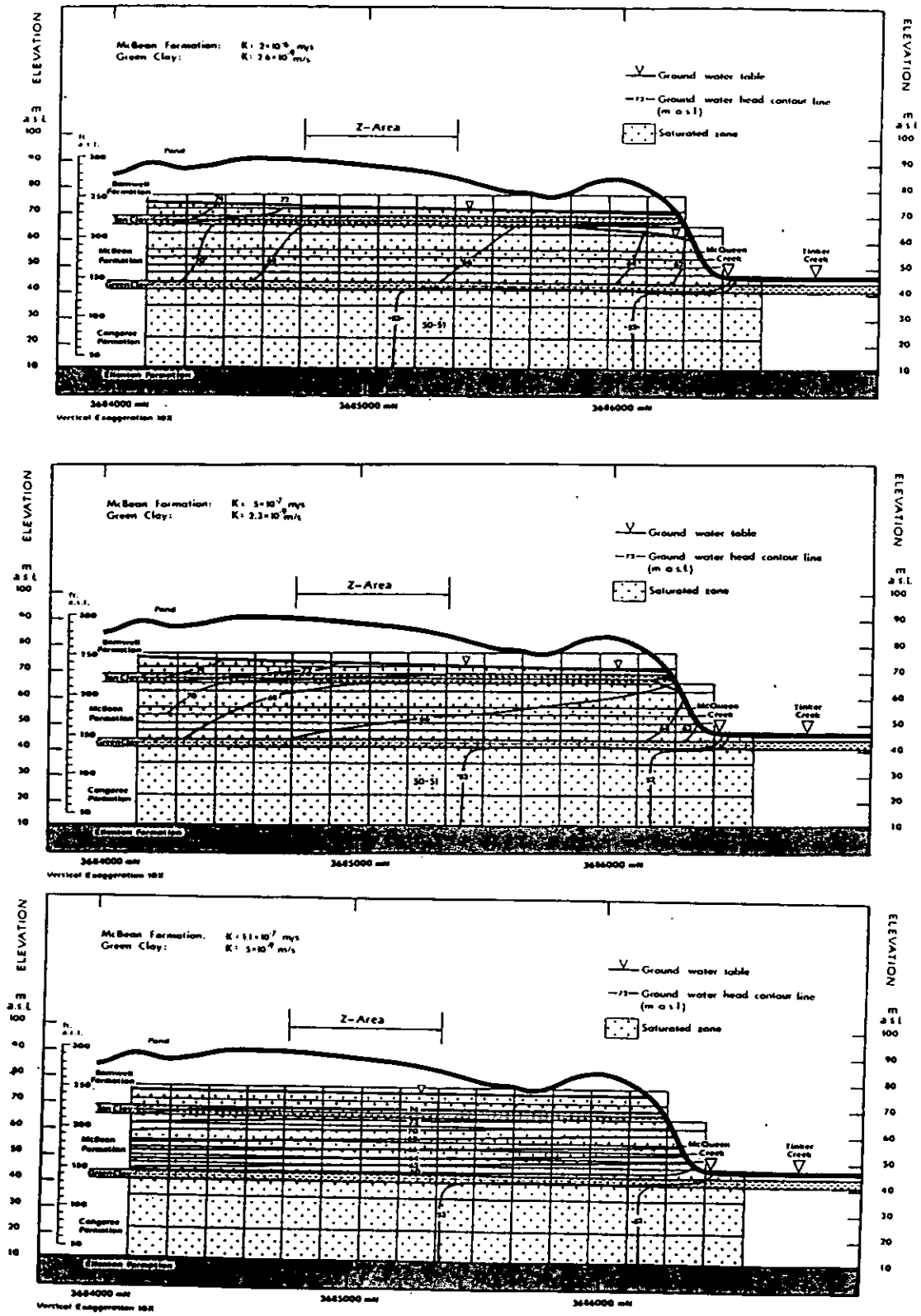

Figure 9-9 Parameter Variation McBean Formation - Green Clay: Ground Water Head Distribution (South-North-Cross-Section).

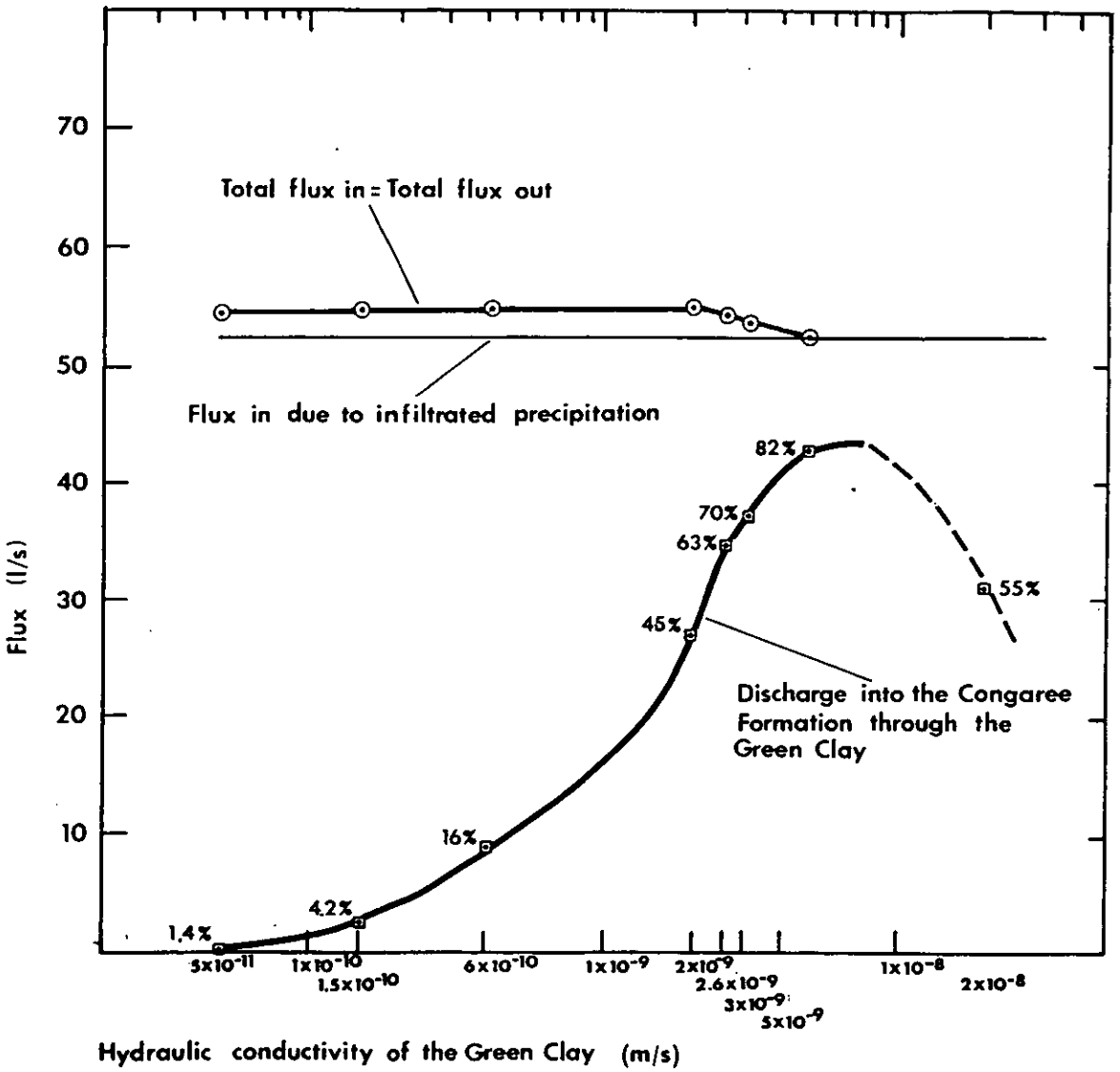

Figure 9-10 Parameter Variation McBean Formation - Green Clay: Material Balance.

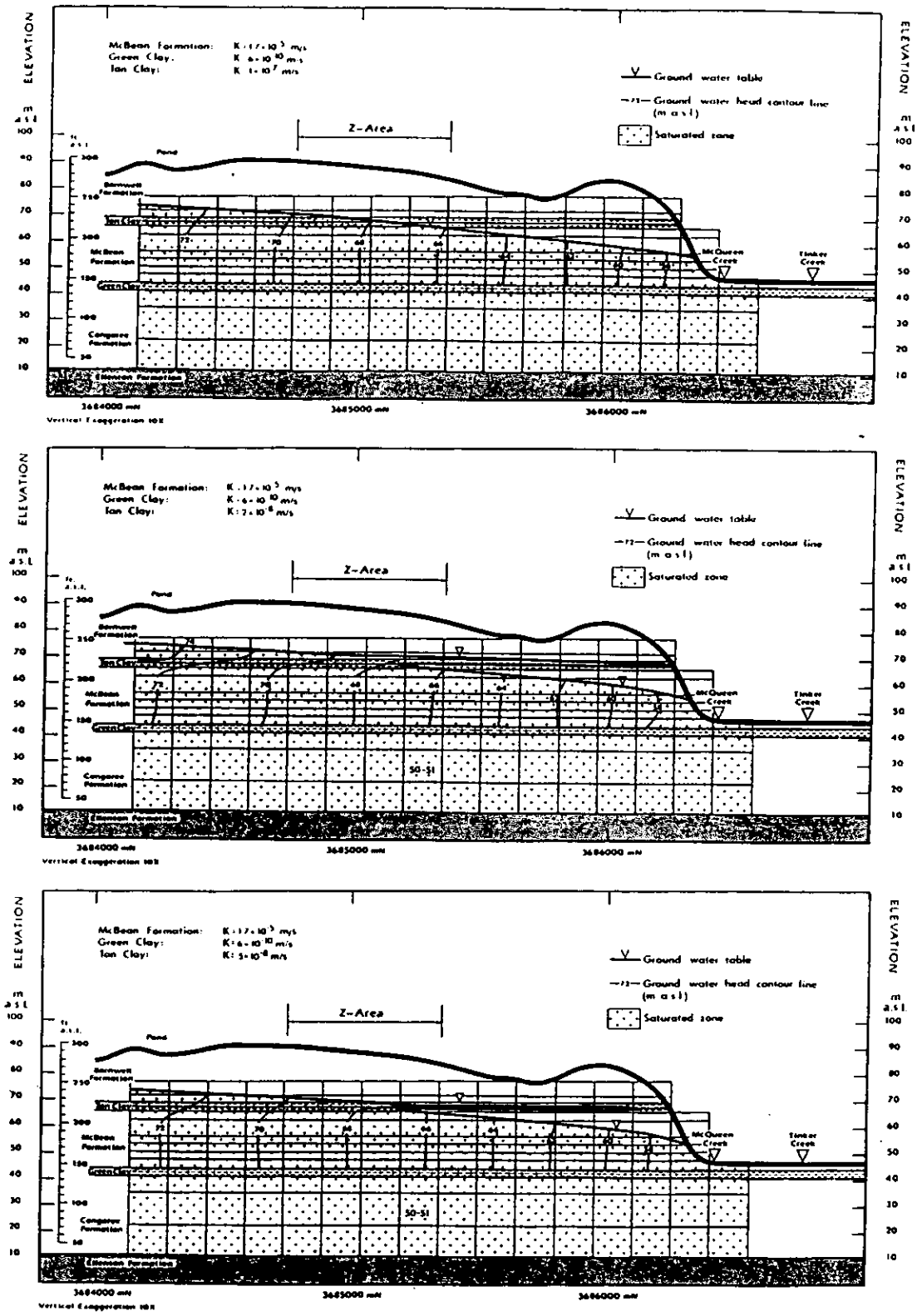

Figure 9-11 Parameter Variation Tan Clay: Ground Water Head Distribution (South-North-Cross-Section).

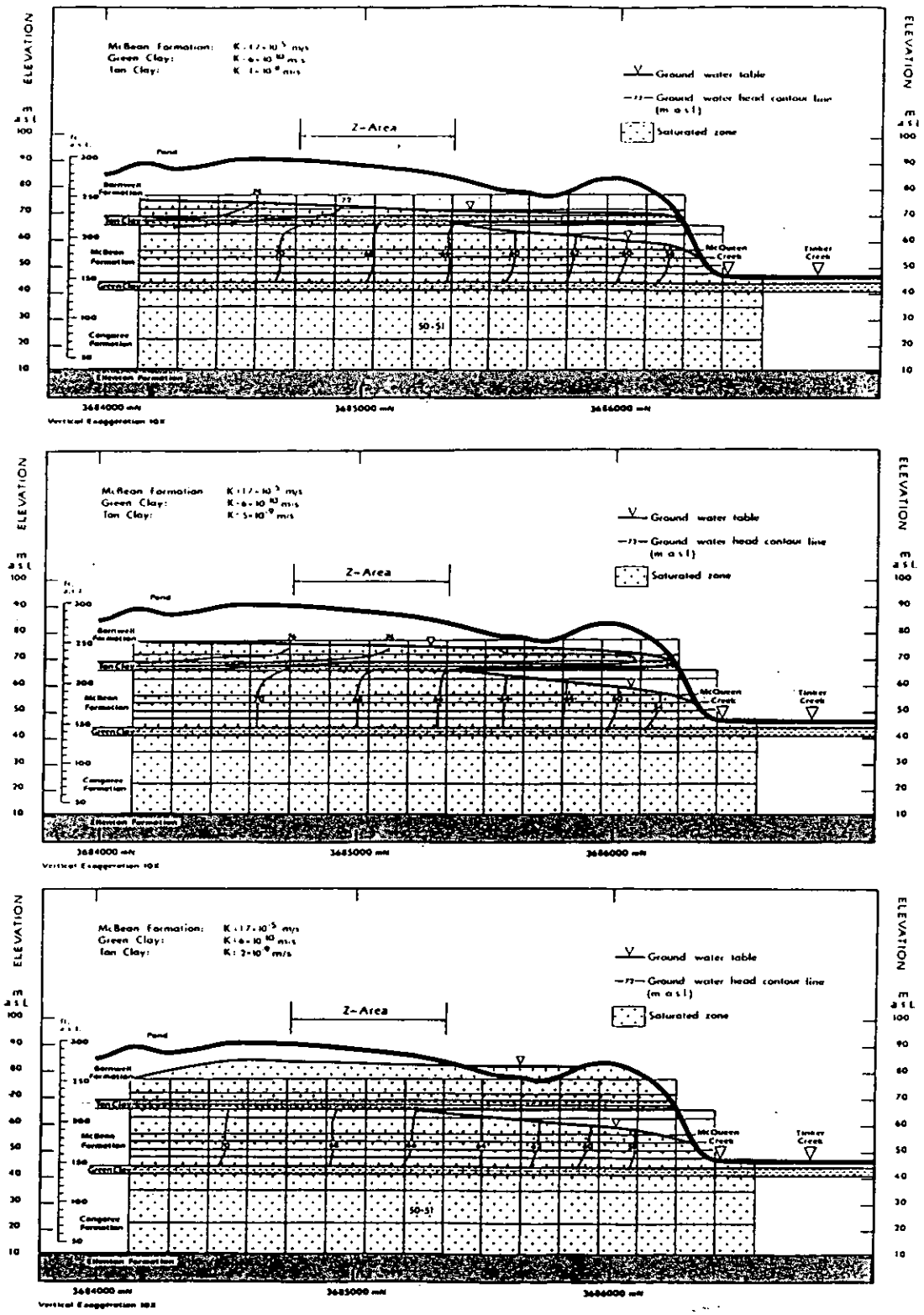

Figure 9-11 Parameter Variation Tan Clay Hydraulic Conductivity: Ground Water Head Distribution (South-North-Cross-Section).

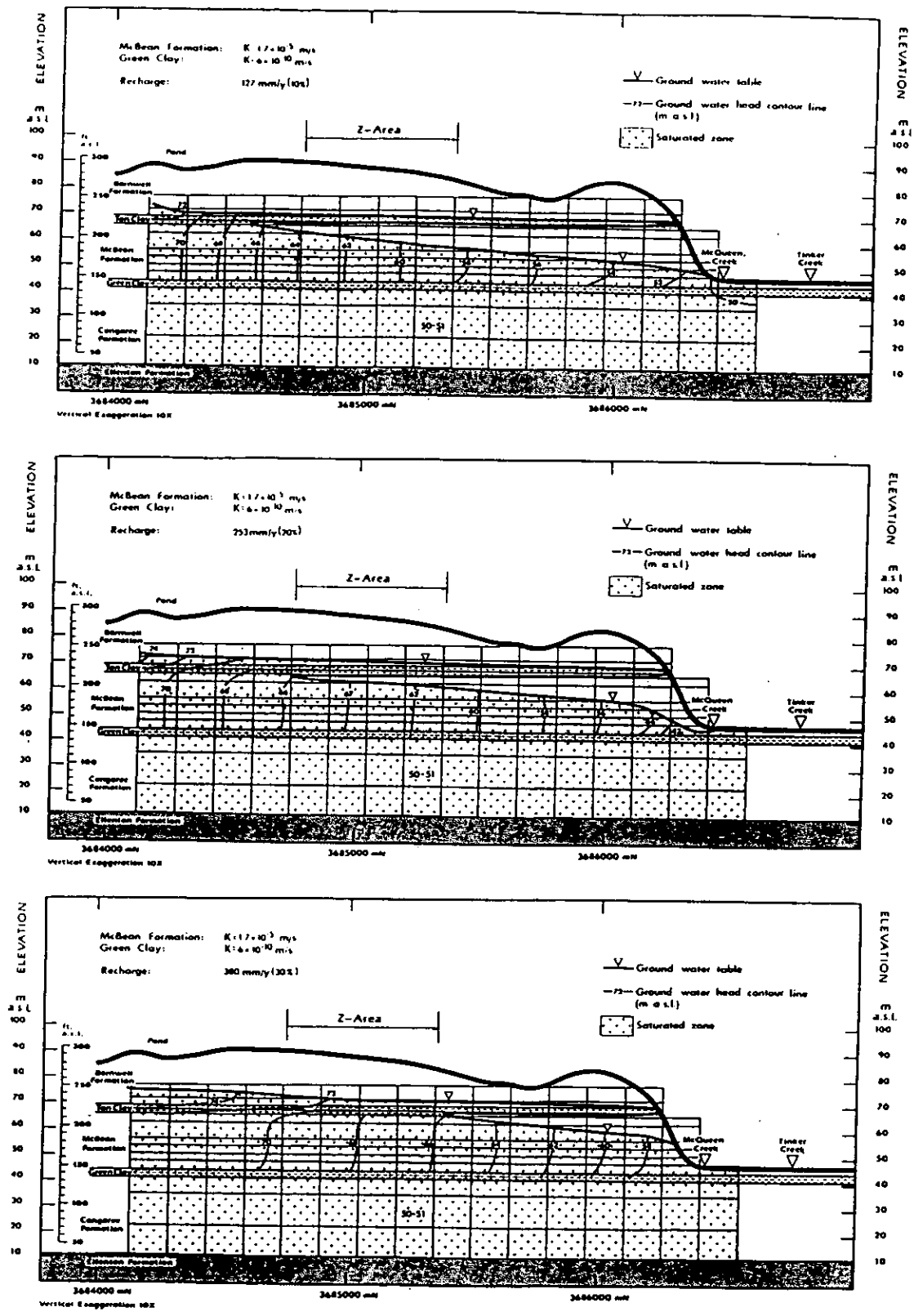

Figure 9-12 Parameter Variation Recharge (Infiltration): Ground Water Head Distribution (South-North-Cross-Section).

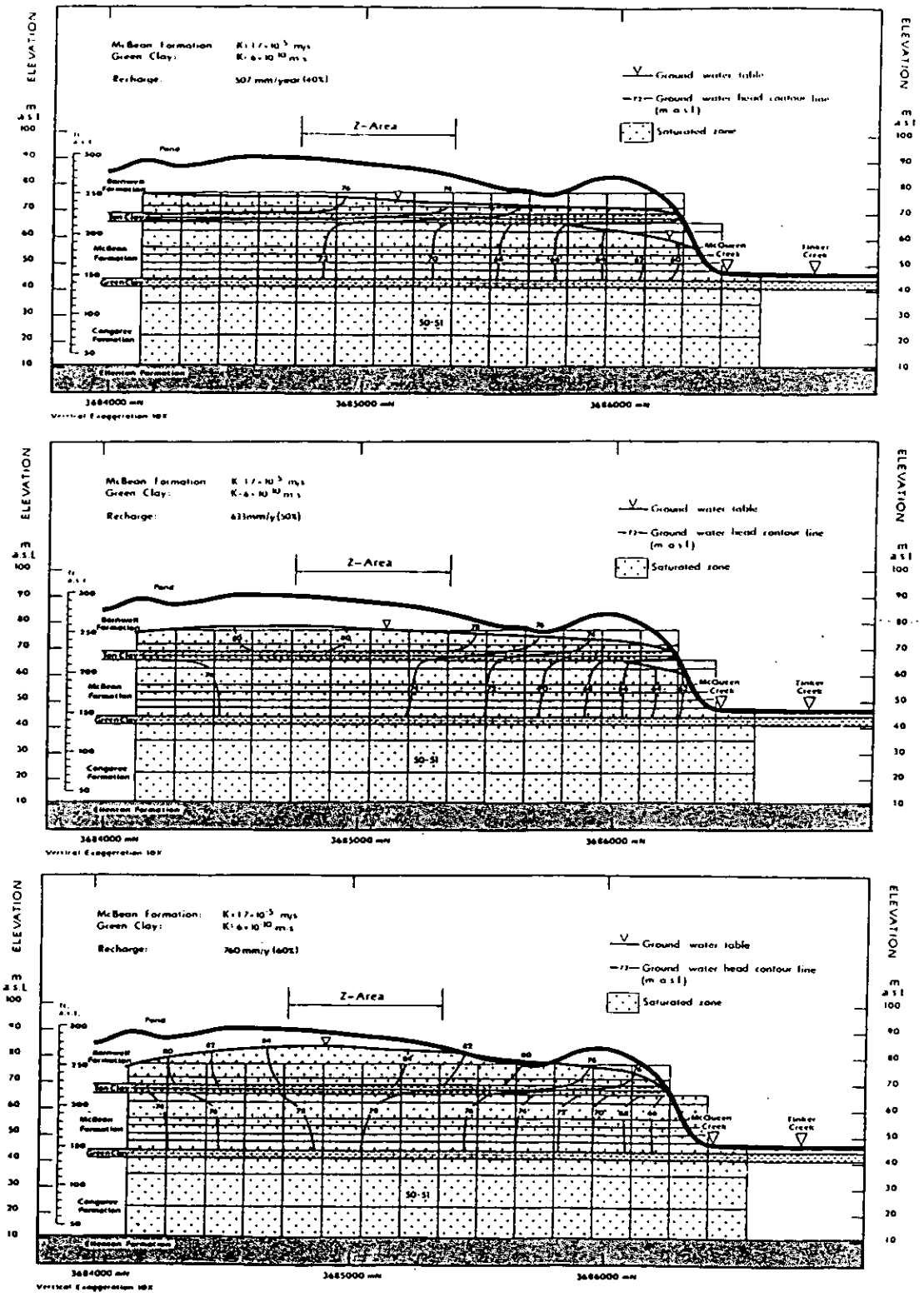

Figure 9-12 Parameter Variation Recharge (Infiltration): Ground Water Head Distribution (South-North-Cross-Section).

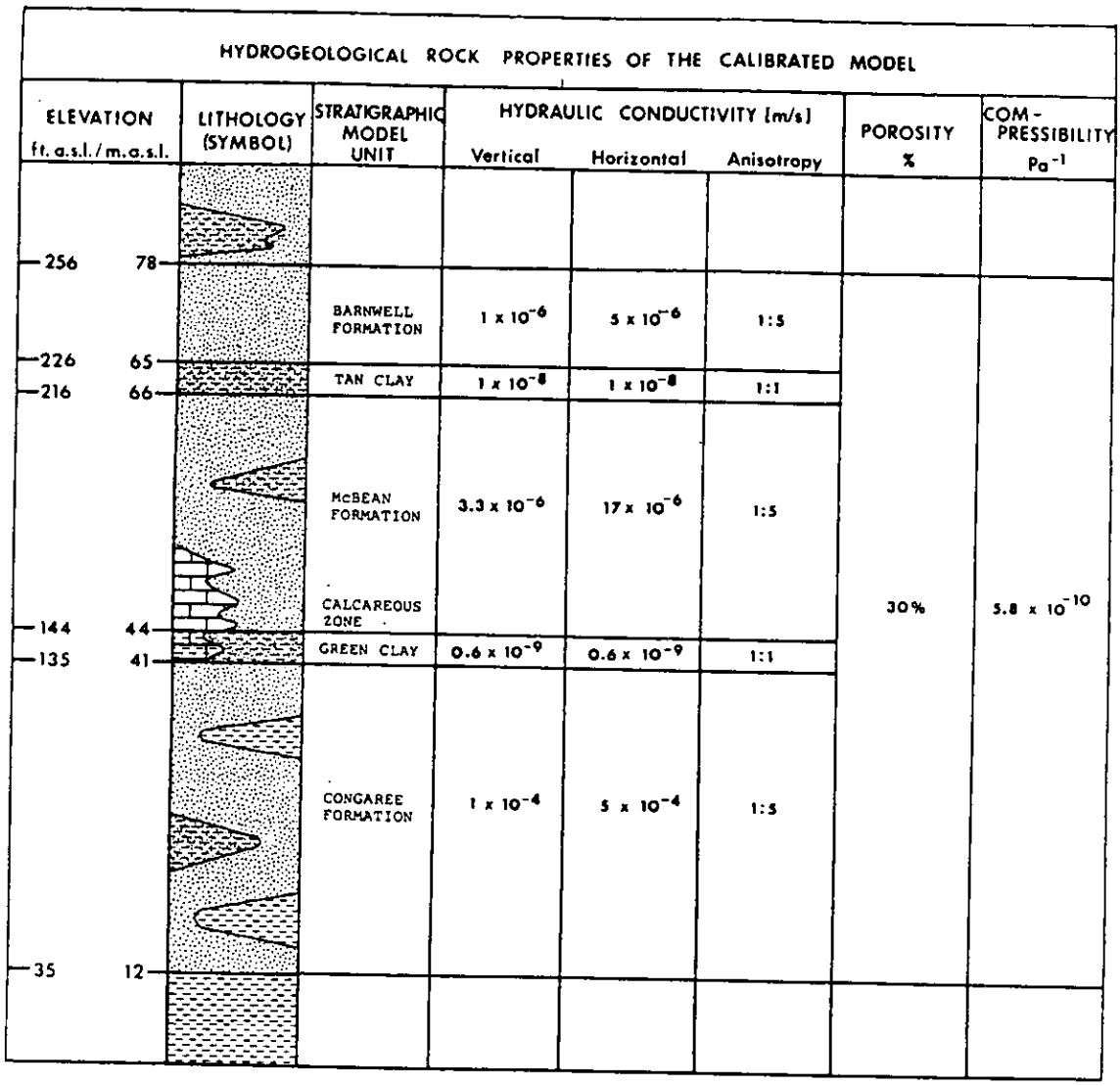

Figure 9-13 Hydrogeologic Rock Properties of the Calibrated Model.

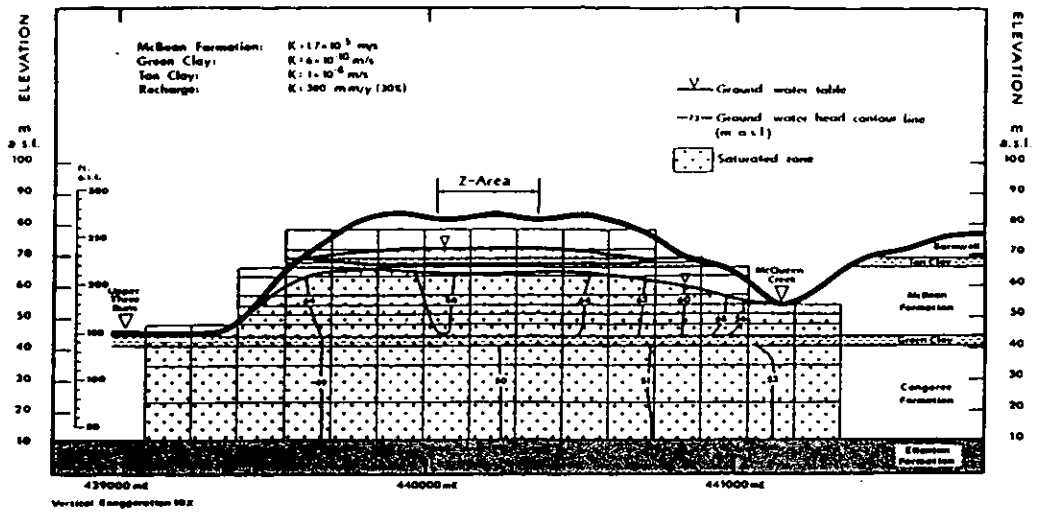

Figure 9-14 Calibrated Flow Model: West-East-Cross-Section.

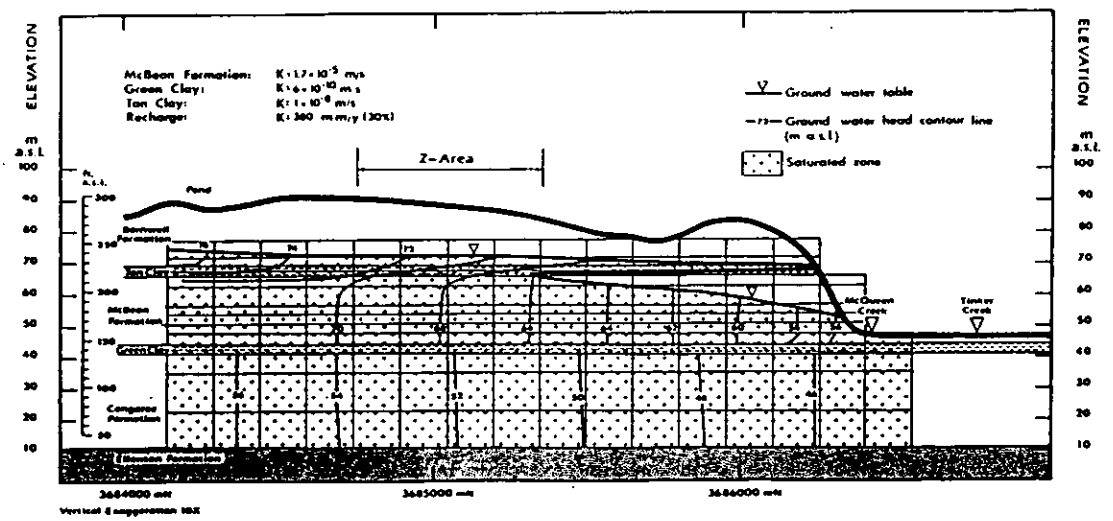

Figure 9-15 Calibrated Flow Model: South-North-Cross-Section.

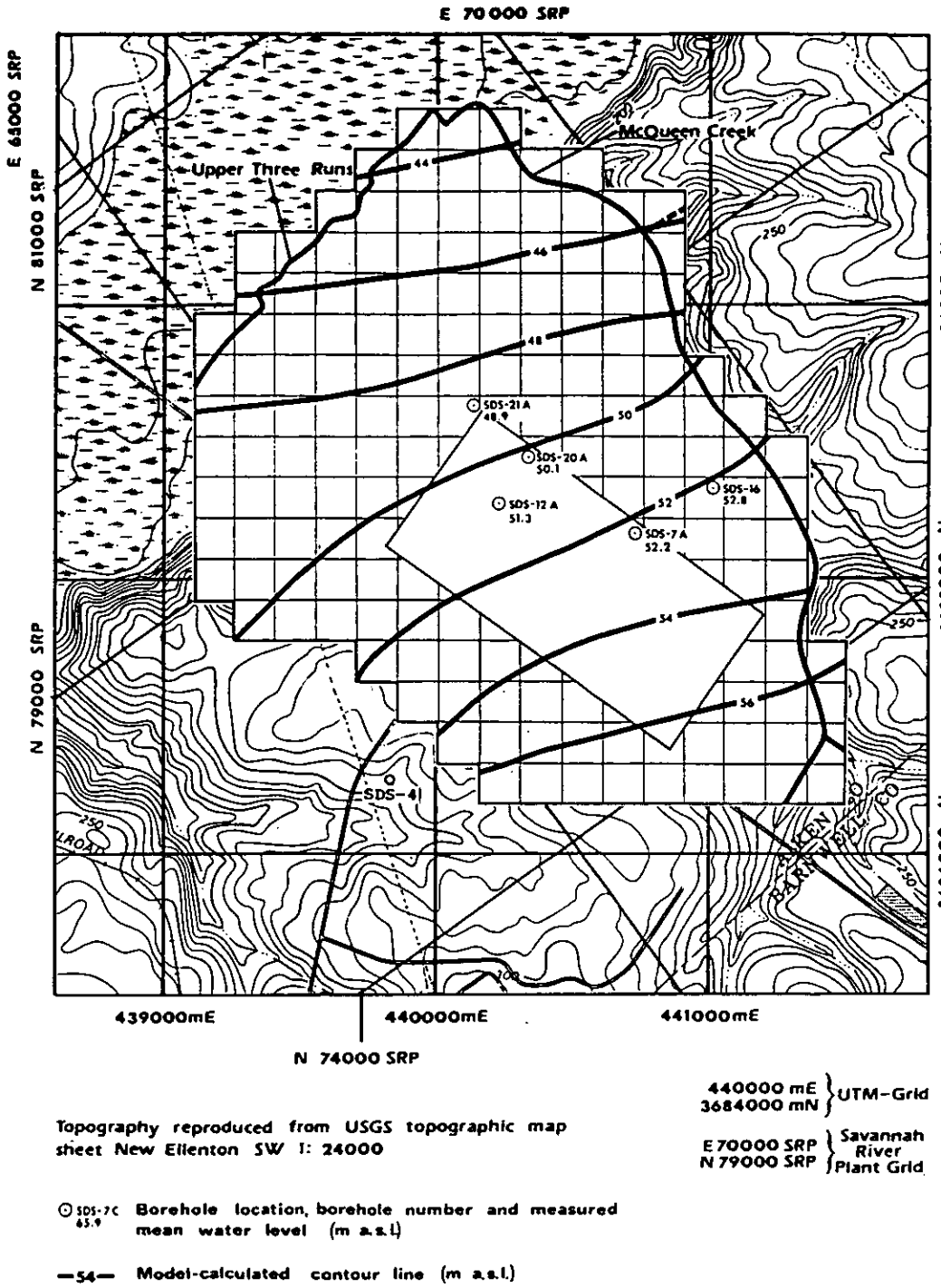

Figure 9-16 Calibrated Flow Model: Calculated Piezometric Surface in the Congaree Formation

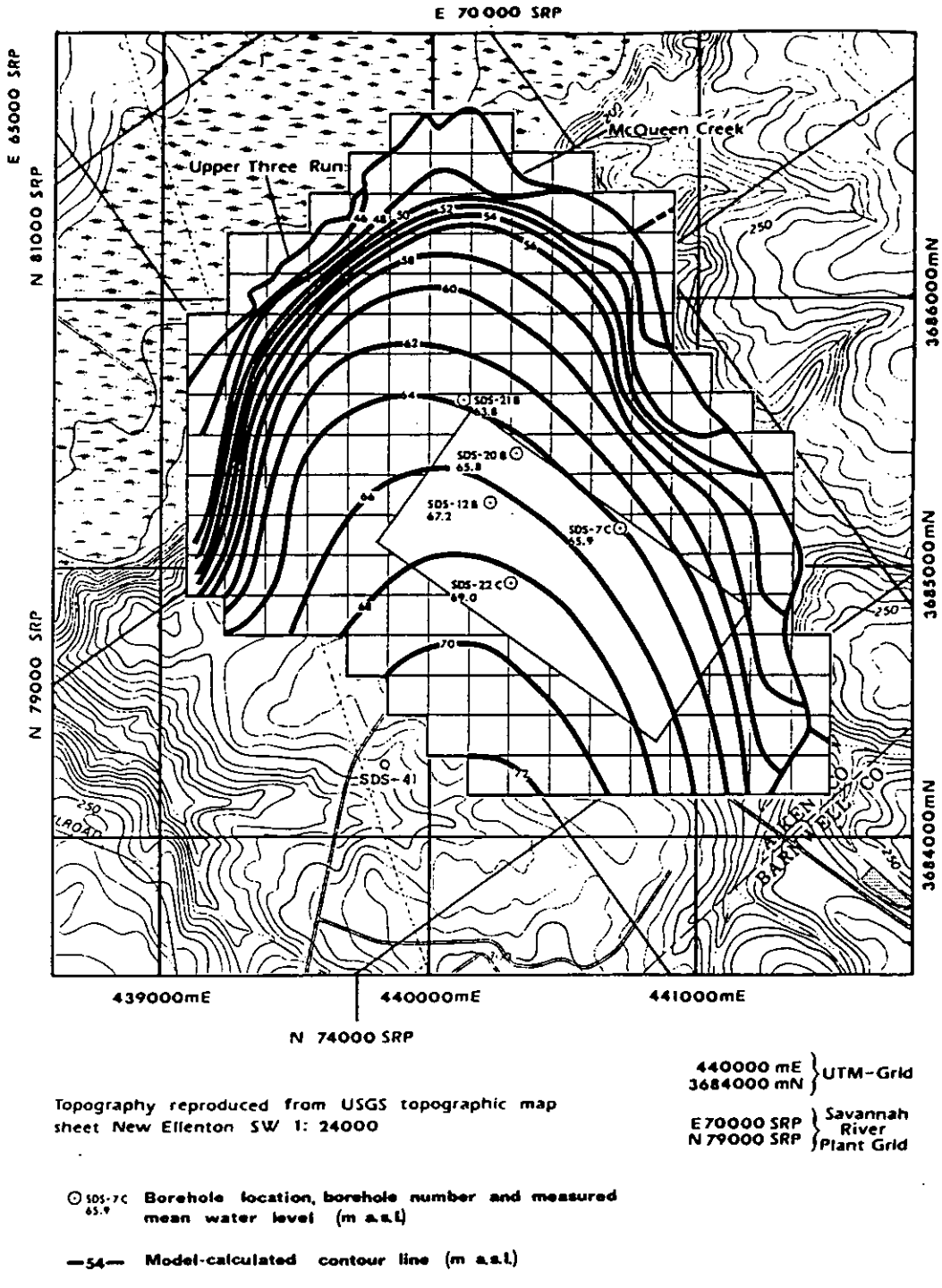

Figure 9-17 Calibrated Flow Model: Calculated Piezometric Suface in the McBean Formation

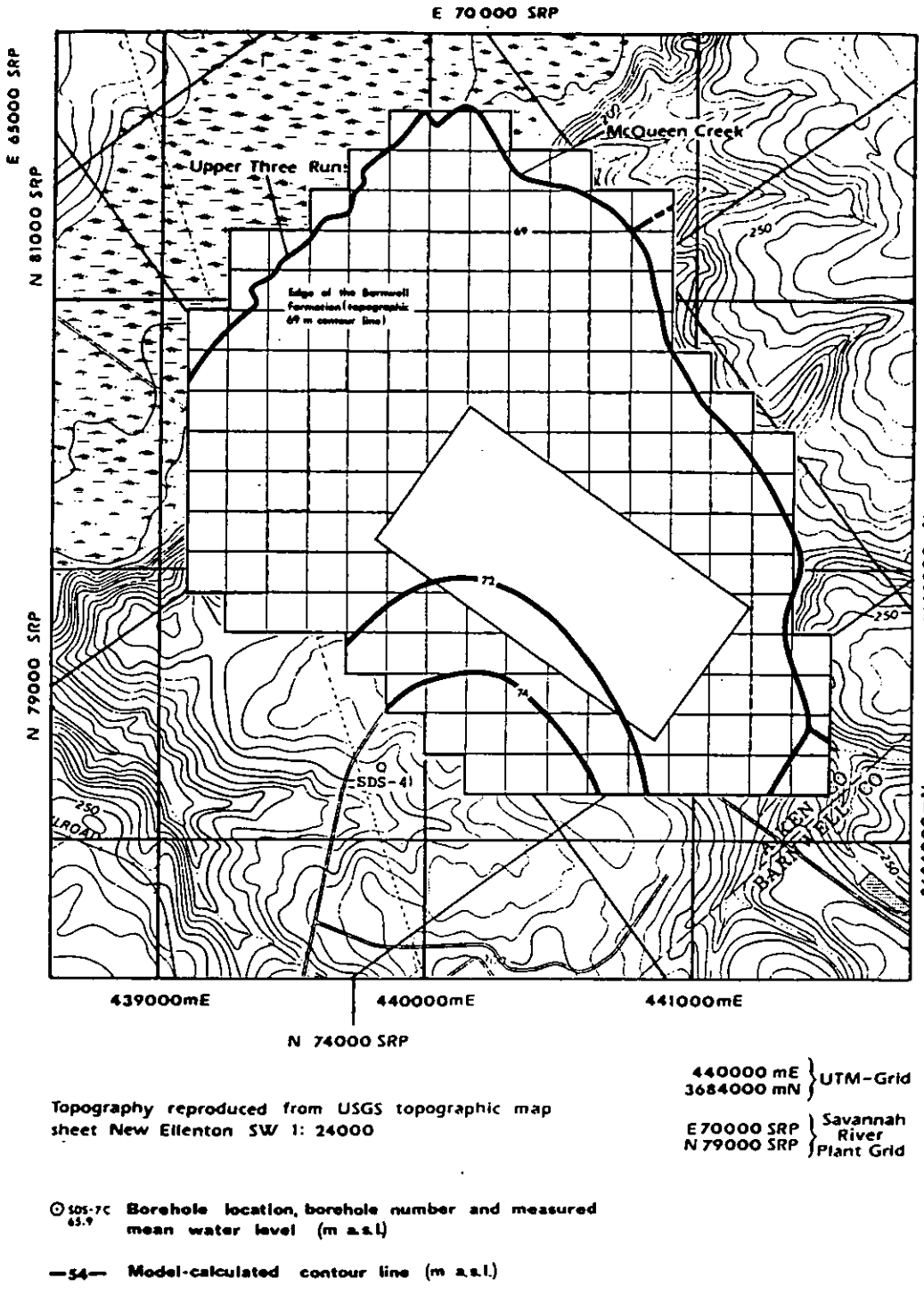

Figure 9-18 Calibrated Flow Model: Calculated Piezometric Surface in the Barnwell Formation

Boreholes Screened in the Congaree Formation	Measured Mean Water Levels (m a.s.l.)	Initial Flow Model Calculated Heads for Borehole Locations (m a.s.l.)	Δ Head (m)
SDS-7A	52.2	52.4	0.2
SDS-12A	51.3	50.7	-0.6
SDS-16A/B	52.8	52.3	-0.5
SDS-20A	50.1	50.3	+0.2
SDS-21A	48.5	49.0	+0.1

Average Δ Head: -0.12 m

Sum (Δ Head)^2: 0.7 m^2

Table 9-1 Initial Flow Model: Calculated Congaree Heads Versus Measured Mean Congaree Water Levels.

Boreholes Screened in the McBean Formation	Measured Mean Water Levels (m a.s.l.)	Initial Flow Model Calculated Heads for Borehole Locations (m a.s.l.)	Δ Head (m)
SDS-7C	65.9	63.2	-2.7
SDS-12B	67.2	64.0	-3.2
SDS-20B	65.8	62.4	-3.4
SDS-21B	63.8	61.9	-1.9
SDS-22C	65.0	66.3	-3.7

Average Δ Head: -3.0 m

Sum (Δ Head)^2: 46.4 m^2

Table 9-2 Initial Flow Model: Calculated McBean Heads Versus Measured Mean Water Levels.

Boreholes Screened in the Congaree Formation	Measured Mean Water Levels (m a.s.l.)	Initial Flow Model Calculated Heads for Borehole Locations (m a.s.l.)	Δ Head (m)
SDS-7A	52.2	52.4	0.2
SDS-12A	51.3	50.7	-0.6
SDS-16A/B	52.8	52.2	-0.6
SDS-20A	50.1	50.2	+0.1
SDS-21A	48.9	48.9	0.0

Average Δ Head: -0.18 m

Sum (Δ Head)^2: 0.77 m^2

Table 9-3 Calibrated Flow Model: Calculated Congaree Heads Versus Measured Mean Congaree Water Levels.

Boreholes Screened in the McBean Formation	Measured Mean Water Levels (m a.s.l.)	Initial Flow Model Calculated Heads for Borehole Locations (m a.s.l.)	Δ Head (m)
SDS-7C	65.9	65.4	-0.4
SDS-12B	67.2	66.9	-0.3
SDS-20B	65.8	65.1	-0.7
SDS-21B	63.8	64.9	+1.1
SDS-22C	6.0	68.8	-0.2

Average Δ Head: -0.1 m

Sum (Δ Head)^2: 1.99 m^2

Table 9-4 Calibrated Flow Model: Calculated McBean Heads Versus Measured McBean Water Levels

10.0 CONTAMINANT TRANSPORT

After completion of the flow analysis the contaminant transport parameters (Section 8.4.3 and 8.4.6) were incorporated into the calibrated steady state flow model (Section 9.3). As mentioned before, the period of interest for the transient modeling was considered to be between 50 and 200 years (Section 7.5).

10.1 Time Step Considerations

Using the method of characteristics ("point tracking method") in the HCTM code, the time steps should be chosen such that the distance the particles move within one time step is not larger than the dimension of the grid block which is parallel to the direction of flow (Appendix B-4.4.3). This general rule of thumb prevents errors which occur when particles, moving in a very heterogeneous flow field, move more than one grid block in a time step.

In the actual model, the restricting grid block dimension is the vertical dimension (3 m) of the thin layers in the Barnwell Formation and the Tan Clay. There the ground water flow is almost perpendicular to the horizontal layers. The vertical component of ground-water flow in the Barnwell Formation or the Tan Clay is about 1.2 m/y, which is essentially the applied recharge (380 mm/year) divided by the pore volume (0.3). Thus the maximum time step allowed by the above rule would be about 2.5 years. However, it was empirically established during the modeling study with the actual flow field that the time step could be increased to 5 years without affecting the modeling results. Therefore a time step of 5 years was selected for the actual contaminant transport modeling. With the upper limit for the time period of interest (200 years) a full contaminant transport simulation comprised 40 time steps.

10.2 Transport Modeling Base Case

The results of the contaminant transport modeling using the calibrated flow field and the previously mentioned transport parameters are displayed in sections through the model area (Figure 10-1 and 10-2). The cross-sections illustrate the transient development of the contaminant concentrations within the model area.

During the first 20 years (after the first contaminants reach the upper model boundary) a contaminant plume develops beneath Z-Area. Due to dispersion and diffusion, the relative contaminant concentrations in the center of the plume are only 0.5 and 0.75 after 10 and 20 years, respectively. Due to dispersion, the lower concentration areas of the contaminant plume extend somewhat further from the source. The 0.1 contour line is in the middle of the McBean Formation after 10 years and reaches the Green Clay within 20 years. The 0.01 contour line reaches the Green Clay within 10 years and the bottom of the model after 15 years. However, the 0.01 contour line represents only the fastest moving particles. More representative for the movement of the contaminant front beneath Z-Area is the 0.5 contour line. Outside Z-Area the 0.1 contour line can be considered to be representative of the contaminant front, because there the contaminants become more diluted by uncontaminated recharge, the further they travel.

Using the 0.1 contour line as an indicator for the contaminant front, the contaminants reach McQueen Creek (at the position of the West-East cross-section) within 50 years. At this time, the 0.5 contour line beneath Z-Area has almost reached the Green Clay and the concentrations in the Congaree Formation range from 0.1 to 0.25. At the same time relatively high concentrations (up to 0.9) occur in the center of the contaminant plume directly beneath Z-Area.

At 100 years the contaminant concentrations within the model area have reached an apparent "steady state". Small variations in the contaminant concentrations after 100 years are insignificant.

The concentrations at 200 years are also shown in three areal concentration maps, one for each aquifer (Figure 10-3, 10-4, and 10-5). These maps, together with the cross-sections at 100 and 200 years, reveal the three dimensional contaminant distribution.

The apparent "steady state" contaminant distribution is characterized by a stable center with high contaminant concentrations (0.75 and greater) in the Barnwell Formation, the Tan Clay and the upper part of the McBean Formation directly beneath Z-Area. In the lower part of the McBean Formation beneath Z-Area the concentrations are between 0.75 and 0.45. The "steady state" concentrations in the Congaree Formation beneath Z-Area range between 0.1 and 0.25.

Outside Z-Area and upstream with respect to the ground water flow, i.e., to the south and the west of Z-Area, the concentrations are zero within 100 to 200 m. Downstream, i.e., to the east in the McBean Formation and to the north in the Congaree Formation, the contaminant plume reaches McQueen Creek and the northern model boundary, respectively. The steady state contaminant concentrations in the McBean Formation at McQueen Creek range between 0 and about 0.2. Thus the ground water discharged from the McBean Formation into McQueen Creek has contaminant concentrations up to 0.2. As Figure 10-4 shows, ground water with concentrations between 0.1 and 0.2 enters McQueen Creek along approximately 500 m (between 3,685,000 mN and 3,685,000 mN). The total discharge over that length is about 6.4 L/s. The base flow of McQueen Creek, measured at a weir about 500 m downstream, is about 87 L/s (Parizek and Root, 1984). Thus the contaminated discharge entering McQueen Creek will be diluted by a factor of 10.

In the Congaree Formation, the contaminant concentrations are generally lower than in McBean Formation. As Figure 10-3 shows, the concentrations in the center of the plume (beneath Z-Area) range between 0.15 and 0.2 (at the elevation of the grid block centers of the upper-most Congaree grid block). The plume reaches the northern boundary, after 200 years, where the contaminant concentrations are about 0.05. Thus

ground water with that contaminant concentration is leaving the model area via flow in the Congaree.

It is possible to set-up an overall material balance for the apparent "steady state" of the contaminant transport model (Table 10-1). The total flux into the model is about 182 L/s, with 54.3 L/S of that total into the upper aquifers. The contaminated recharge is 4.68 L/s with a normalized concentration of 1.0. This is about one tenth of the flux into the Barnwell and the McBean Formations. Therefore the contaminant recharge from the planned disposal site area can be diluted by, at best, a factor of 10. Because there is no homogeneous dilution within the entire model area, concentrations between 0 and 0.2 were calculated.

About 90% of the contaminant input discharges from the upper aquifers into the creeks. The base flow of Upper Three Runs Creek downstream of Z-Area (between Road F and Road C bridges) is about 425 L/s (Parizek and Root, 1984). Thus the overall dilution of the contaminants released by the planned landfill disposal site can be expected to be about 100, resulting in relative concentrations of about 0.01 in Upper Three Runs Creek.

Part of the McBean ground water discharges through the Green Clay into the Congaree Formation (9.0 L/s). About 10% of the contaminant input is transported to the ground water through the Green Clay into the Congaree Formation. Thus the average concentration of the contaminants entering the Congaree Formation is about 5.5%. This is about the same concentration at which the contaminants leave the model area after 200 years through the central part of the northern boundary. Within the Congaree Formation, the contaminants will be further diluted before they are discharged into the Savannah River some 15 to 20 km distant.

10.3 Variation of the Infiltration Rate at Z-Area

The contaminant modeling as described in the previous section (base case) is based on the assumption that the infiltration rate is constant over the entire model area. However, it is possible that the design of the planned landfill disposal (see Section 2) will affect the infiltration rate at Z-Area. In order to evaluate the effect on contaminant concentrations in the ground water, caused by an increased or decreased infiltration rate (representing diffenrent disposal designs), three additional contaminant transport simulations with different infiltration rates were performed.

10.3.1 Contaminant Concentrations With a 0.3% Infiltration Rate

The first additional contaminant transport simulation was conducted for a substantially reduced infiltration rate at Z-Area. A very low infiltration rate might be representative of a landfill disposal design which comprises an impermeable layer (e.g., clay cap) completely covering the disposal area, collection of the run-off and drainage of that run-off to one of the creeks. With such a design, it should be possible to reduce the infiltration rate to about 1% of the normal infiltration rate. Thus the resulting infiltration rate at Z-Area would be 0.3% of the average rainfall.

Using the same model parameters as for the base case, except for the 0.3% infiltration rate at Z-Area, the contaminant transport modeling was conducted over a time period of 200 years. The results, i.e., the long term ("steady state") contaminant concentrations in the ground water, are shown in the Figures 10-6 through 10-10 (2 cross-sections and 3 areal concentration maps).

The cross-sections demonstrate also the effect of the reduced recharge of Z-Area on the ground water tables in the Barnwell and McBean Formations. At Z-Area, the thickness of the saturated zone in the Barnwell Formation is drastically reduced, thus the perched

water table is barely existent. Also the water table in the McBean Formation is considerably lower (about 2 m) at Z-Area than in the base case model. This is because the overall flux into the upper most aquifers is reduced by 3.9 L/s from 52.65 L/s (base case) down to 48.75 L/s. The reduced infiltration rate alone would cause a drop of 4.8 L/s, but part of that loss is compensated by a higher flux into the McBean Formation through the southern model boundary (the boundary conditions were not altered during the infiltration rate analyses).

As far as the contaminant concentrations are concerned, they are considerably lower (with respect to a source term concentration of 1.0) than in the base case. As Figures 10-2 through 10-3 show, the concentrations in the saturated zone in the Barnwell Formation are about 0.05 at the maximum. In the lower part of the McBean Formation, the concentrations are below 0.03, and in the Congaree Formation the concentrations are less than 0.01. These low relative contaminant concentrations are caused by a dilution of a relatively small amount of contaminants (0.95 L/s) in a comparatively large amount of uncontaminated recharge (48.75 L/s) which enters the model outside of Z-Area.

However, the calculated concentrations are relative concentrations with respect to the concentration (1.0) of the source term. It cannot be expected that the source term concentrations are independent of the disposal design site. Thus it is very likely that a reduction of the infiltration rate at the landfill disposal site will cause higher contaminant concentrations in the remaining recharge. This must be taken into account when comparing the concentrations calculated by the contaminant transport simulations with different infiltration rates.

10.3.2 Contaminant Concentrations With a 3% Infiltration Rate

The second additional contaminant transport simulation was performed with a 3% infiltration rate. This infiltration rate might be representative of a disposal design which is similar to the one described in Section 10.3.1, but which has a somewhat more permeable cover.

Again, the contaminant transport modeling was conducted for a time period of 200 years, using the same model parameters as for the base case, but with a 3% infiltration rate at Z-Area. The results, i.e., the long term ("steady state") contaminant concentrations in the ground water are shown in Figures 10-11 through 10-15, (2 cross-sections and 3 areal concentration maps).

The thickness of the perched ground water table in the McBean Formations is significantly reduced, as with the 0.3% case. The overall flux into the two upper aquifers (Barnwell and McBean Formations) is reduced by 3.0 L/s from 52.65 L/s (base case) down to 45.65 L/s. As in the previous modeling variant, the reduced infiltration alone would result in 4.3 L/s less recharge to the upper aquifers, but part of this is compensated by a higher flux into the McBean Formation through the southern model boundary.

The long term contaminant concentrations in the ground water are lower (with respect to the source term concentration of 1.0) than with 30% infiltration (base case), but higher than with 0.3% infiltration. As Figures 10-11 and 10-15 show, the concentrations in the saturated part of the Barnwell Formation are as high as 0.75 in the center of Z-Area, but do not exceed 0.25 outside Z-Area. In the lower part of the McBean Formation the concentrations are generally below 0.1, although in the center of Z-Area concentrations of 0.25 occur. In the Congaree Formation the concentrations are generally low (0.025 or less) except in the center of the plane directly below the Green Clay where concentrations of 0.15 to 0.1 were calculated.

As pointed out in the previous section, the resulting long term relative concentrations depend on the ratio of the contaminant inflow (at Z-Area) to the uncontaminated recharge, which essentially restricts the possible dilution factor for the contaminants within the model area. Thus, with 3% infiltration, the relative concentrations (as related to an input concentration of 1.0) are generally higher than with 0.3% but lower than with 30%. However, as mentioned in the previous section, the absolute source term concentration depends on the actual disposal design. Thus the relative concentrations of simulations with different infiltration rates cannot be compared directly.

10.3.3 Contaminant Concentrations With a 90% Infiltration Rate

The last additional contaminant transport simulation was performed with a 90% infiltration rate at Z-Area, which is three times the assumed average infiltration rate for the model area. Such an infiltration rate might be representative of a disposal design which comprises many small saltstone blocks, arranged in a large array, with a separate impermeable layer (e.g., a clay cap) above each saltstone block and a drainage system for the run-off between the blocks. Such a design might cause a relatively high infiltration rate at Z-Area, because the surficial run-off can infiltrate at Z-Area itself.

The additional contaminant transport modeling was performed with a 90% infiltration rate at Z-Area, while the other model parameters were left unchanged as compared to the base case. The time period covered by the simulation was 200 years. The results, i.e., the long term ("steady state") contaminant concentrations in the ground water are shown in Figures 10-16 through 10-20 (2 cross-sections and 3 areal concentration maps).

The cross-sections demonstrate also the effect of the increased recharge at Z-Area on the ground water tables in the Barnwell and

McBean Formations. At Z-Area, the perched water table is as high as 78 m a.s.l., which is about 6 m higher than in the base case. In the McBean Formation, the water table is about 3 to 4 m higher than in the base case. Consequently, the unsaturated zone in the McBean Formation is considerably smaller.

The overall flux into the two upper aquifers (Barnwell and McBean Formations) is increased by 8.0 L/s, from 52.65 L/s (base case) up to 60.65 L/s. The additional recharge at Z-Area alone would cause an increase of 9.0 L/s, but due to the higher water tables in the upper two aquifers, the flux into the model through the southern model boundaries is somewhat reduced. Thus an initial increase of 8.0 L/s results from the three times higher (than base case) infiltration rate.

The contaminant concentrations in all three aquifers are considerably higher than in the base case. As Figure 10-20 shows, the contaminant concentrations are as high as 0.9 within most parts of Z-Area and the low concentration contour lines (0.05 and 0.1) are significantly further away from Z-Area than in the base case. The concentrations in the lower McBean Formation are 0.7 and higher beneath Z-Area as compared to 0.5 for the base case. At the creeks, the concentrations in the McBean Formation are only slightly higher than in the base case (less than 0.25), but ground water with contaminant concentrations of 0.2 and more discharge into a longer part of McQueen Creek. In the Congaree Formation contaminant concentrations of 0.35 and more (in the upper part of the Congaree Formation) occur in the center of the plane beneath the Green Clay. The concentrations in the Congaree Formation at the northern boundary are about 0.1.

Generally, the higher contaminant concentrations (as compared to the base case) obtained with the 90% infiltration rate at Z-Area reflect one fact; more contaminated recharge (14.6 L/s instead of 4.5 L/s) is diluted in about the same uncontaminated recharge. However, the

absolute source term concentrations depends on the actual disposal design. For the 90% infiltration rate case at Z-Area it can be assumed that the absolute concentration of the recharge at Z-Area is lower than the source term concentration of the base case. Therefore, again a direct comparison of the relative concentrations of the simulation with different infiltration rates is not possible.

10.4 Site Assessment

The purpose of this section is to briefly review the results of the study in the context of nitrate water quality standards and to present in summary, the predictions of ground water quality at the Z-Area boundary and throughout the ground water system by presenting the travel paths and travel time of nitrate in the system. The eventual discharge of nitrate to surface waters is also presented and the resultant surface water nitrate concentrations are quantified.

The drinking water quality standard for nitrate is the World Health Organization recommended maximum permissible concentration in drinking water of 45 mg/L. The travel times and travel paths are presented below in terms of predicted concentrations (in each formation) at times up to 200 years after disposal using a realistic dispersion coefficient (longitudinal dispersivity = 10 m). In this section the development of the contaminated zones is presented by taking the "front" position calculated using a dispersivity of 0, thereby allowing molecular diffusion as the only dispersive mechanism. In this instance, the resultant is a very sharp contamination front where the 0.1 and 0.9 concentration contour lines are virtually indistinguishable. In essence, the travel paths and travel times are those associated with the average ground water velocity.

Figure 10-21 shows the development of the front in the Barnwell Formation over a period of 200 years. The horizontal component of ground water flow at the center of each grid block is also shown. With reference also to Figure 10-5, it can be seen that without dispersion the

"source" concentration reaches the Z-Area boundary within about 10 years. However, the expected relative concentration at the Z-Area boundary with a realistic dispersivity is of the order of 0.3 to 0.4. The development of a nondispersed contaminant front in the McBean Formation is presented in Figure 10-22. Full source concentration is reached at the Z-Area boundary within 10 years, while full concentration discharge begins to develop over a limited reach (about 300 m) of McQueen Creek within 40 years. However, actual observed relative concentrations are more likely to be with the order of 0.2 (see Figure 10-4). The front in the underlying Congaree Formation reaches the northern extremes of the modeled area between 75 and 100 years after disposal. The concentrations which would be observed in the Congaree Formation at the northern extremes are of the order of 0.05 or less.

The travel times and travel paths for nitrate in the ground water system are presented in Sections 10.1 through 10.3 in terms of predicted relative concentrations in each formation at times up to 200 years after disposal. It is concluded that nitrate concentrations in the ground water at the Z-Area boundary will not exceed 50% of the source concentration. Nitrate concentrations in McQueen Creek will not exceed 10% of the source concentration, while concentrations in Upper Three Runs Creek will be likely less than 1% of the source concentration.

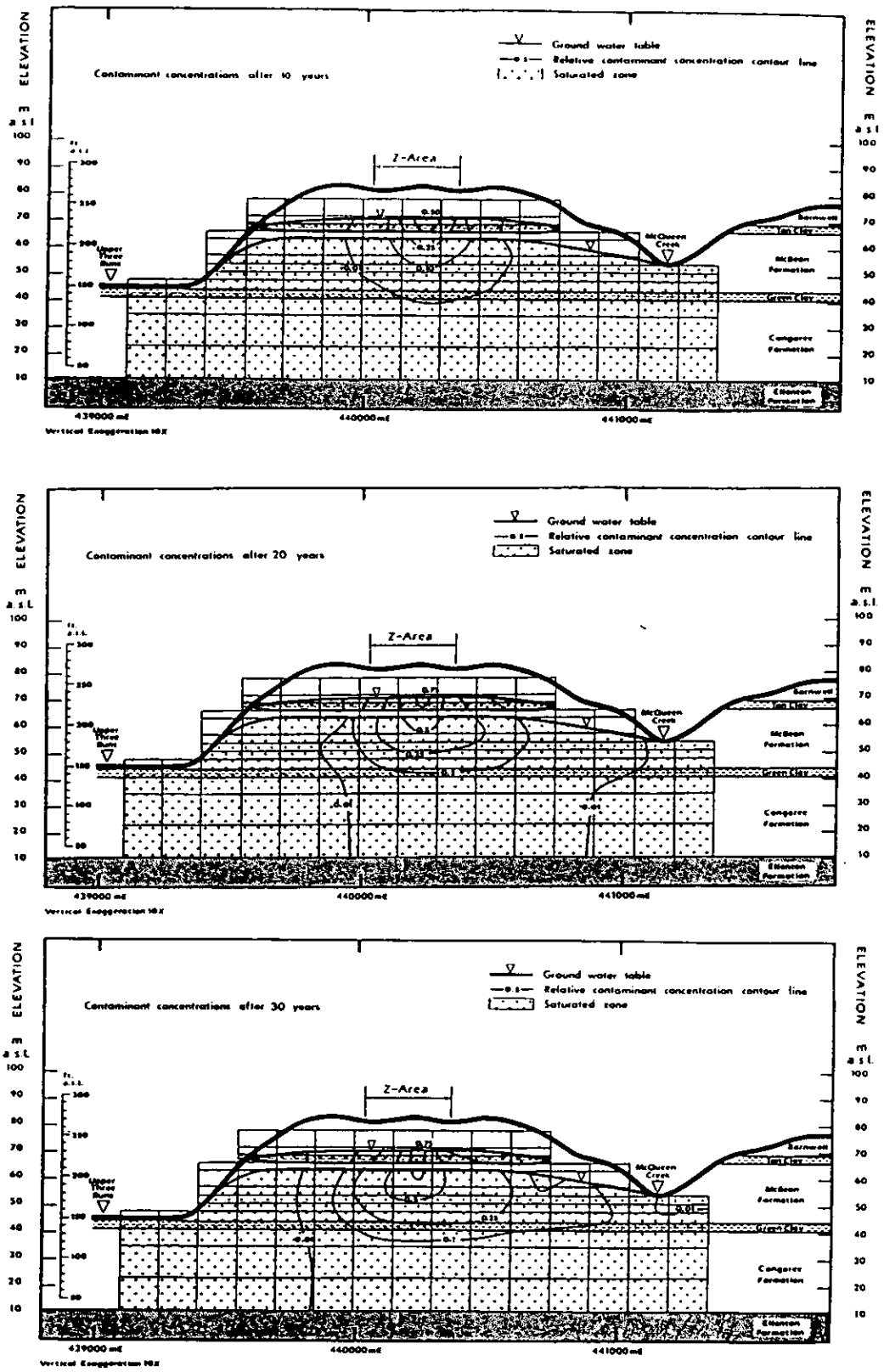

Figure 10-1 Contaminant Concentrations (West-East Cross-Section).

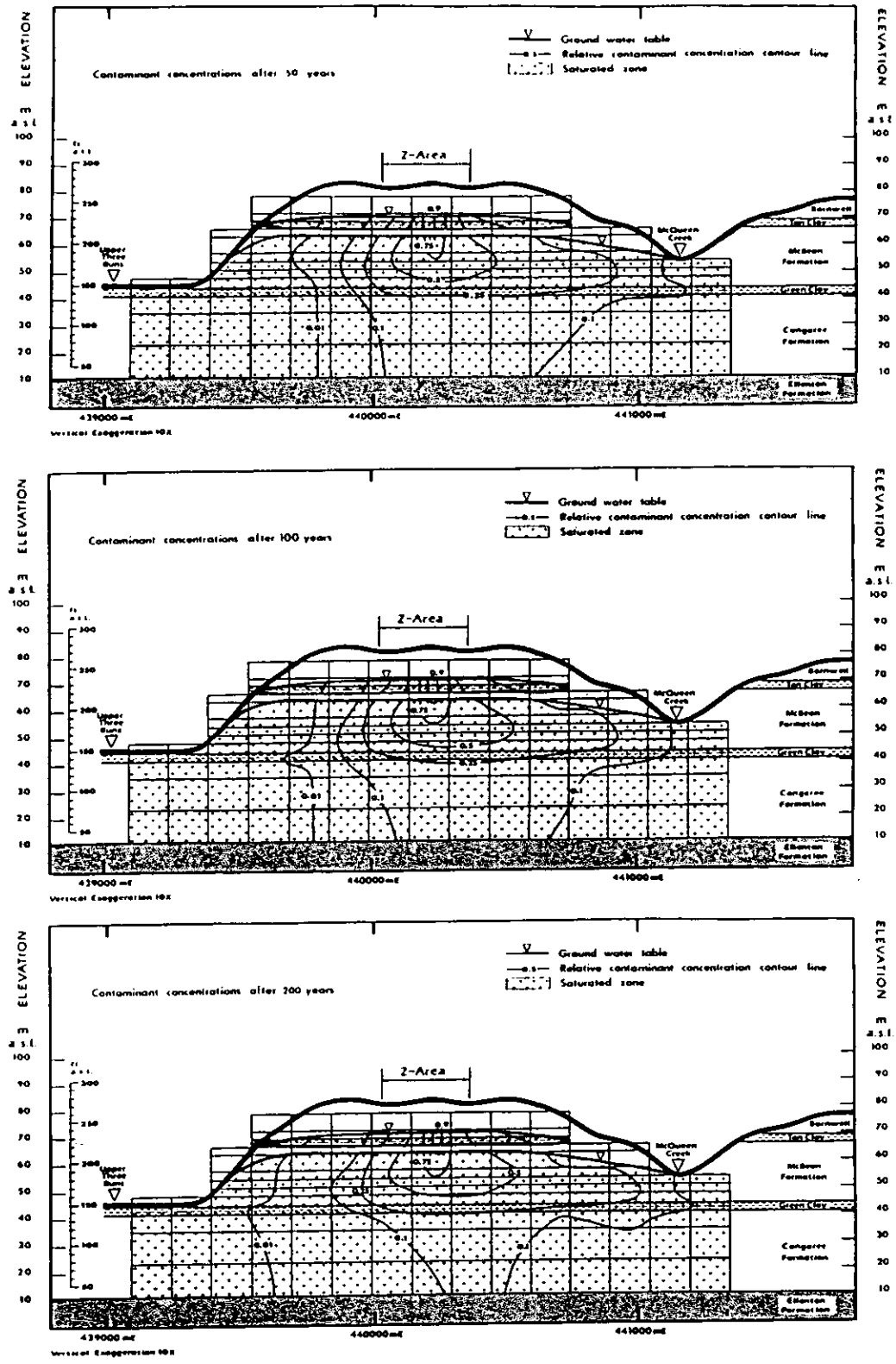

Figure 10-1 Contaminant Concentrations (West-East Cross-Section).

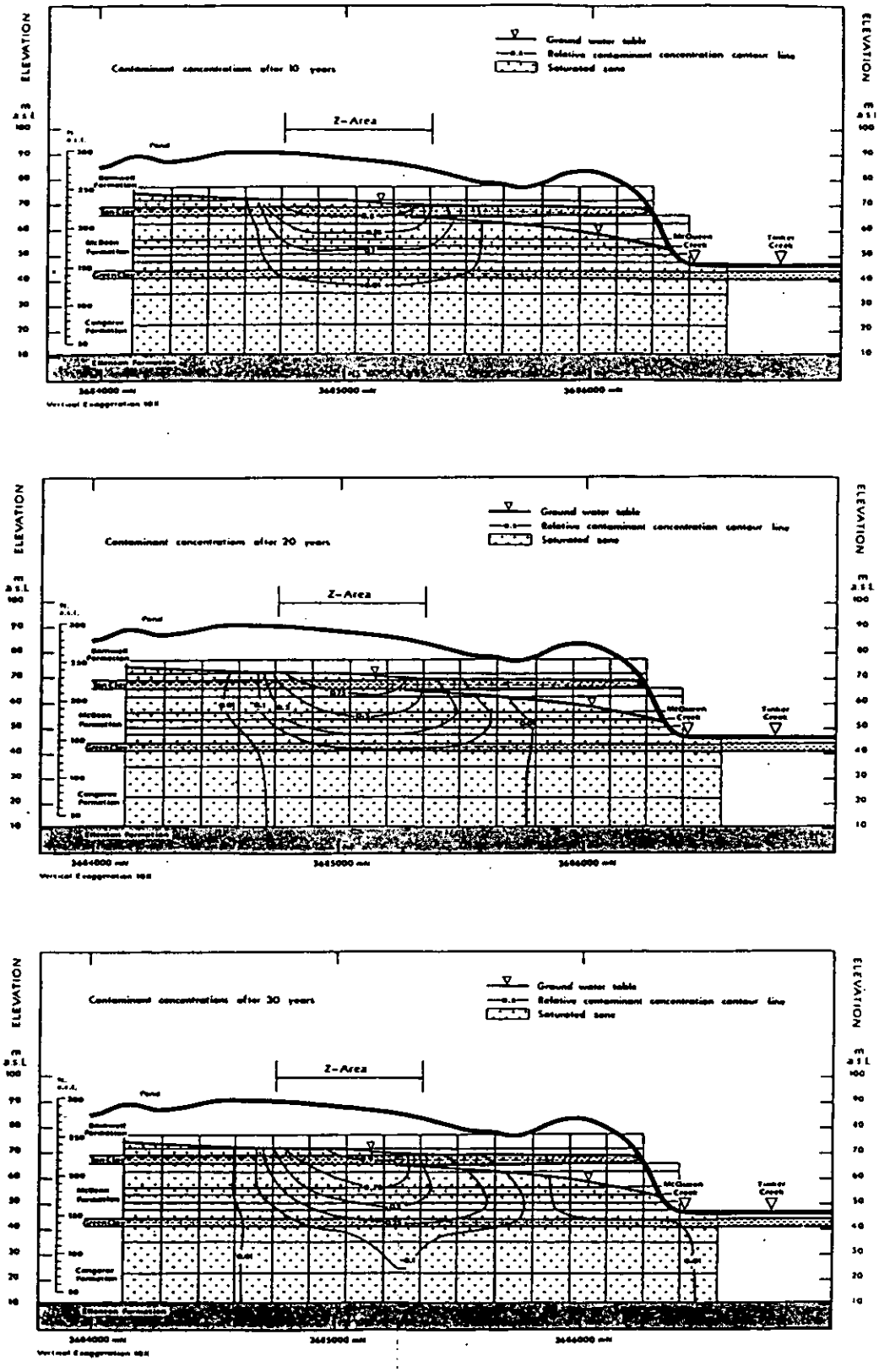

Figure 10-2 Contaminant Concentrations (South-North Cross-Sections).

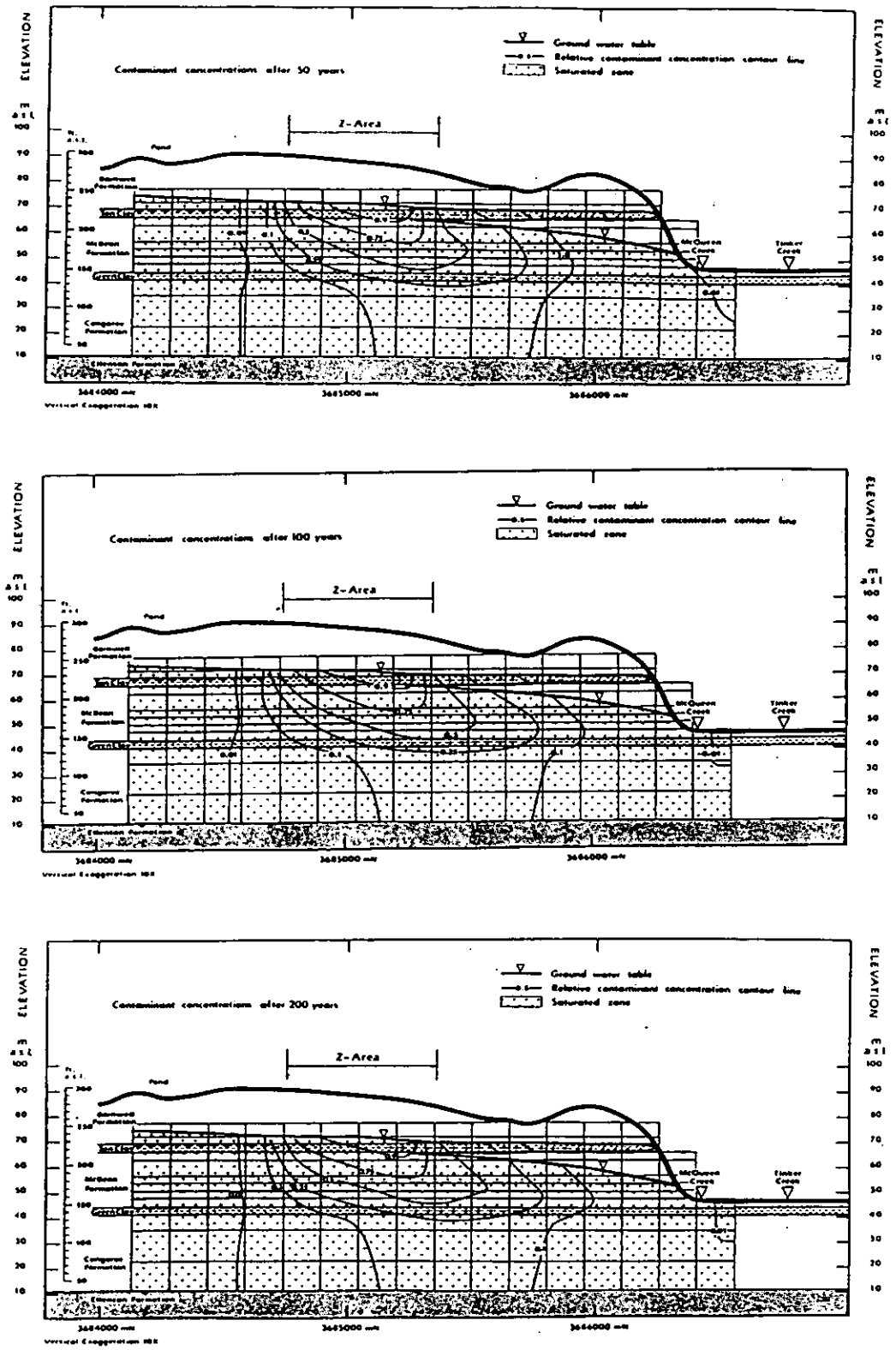

Figure 10-2 Contaminant Concentrations (South-North Cross-Sections).

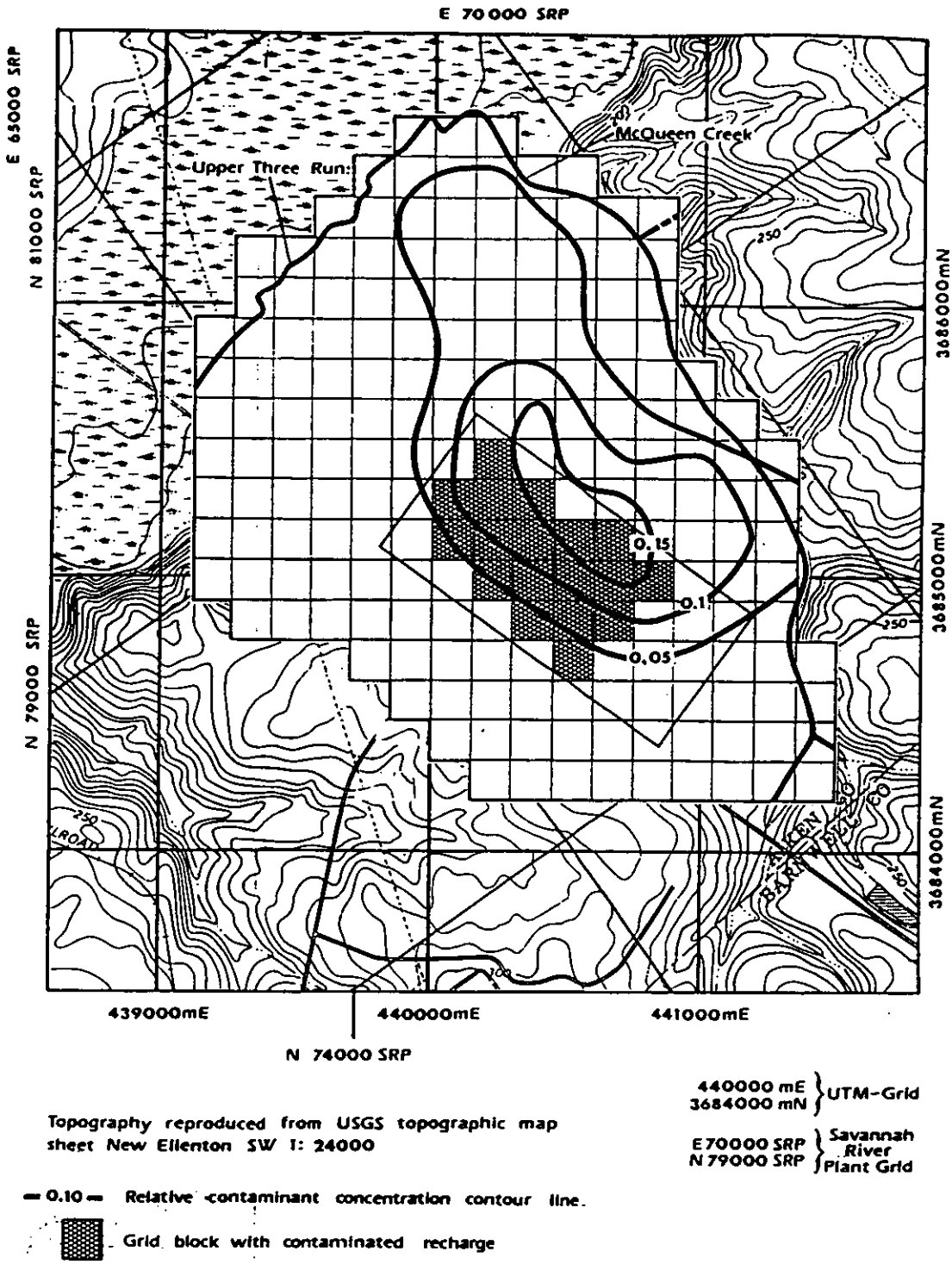

Figure 10-3 Contaminant Concentrations in the Congaree Formation (Upper Part) After 200 Years.

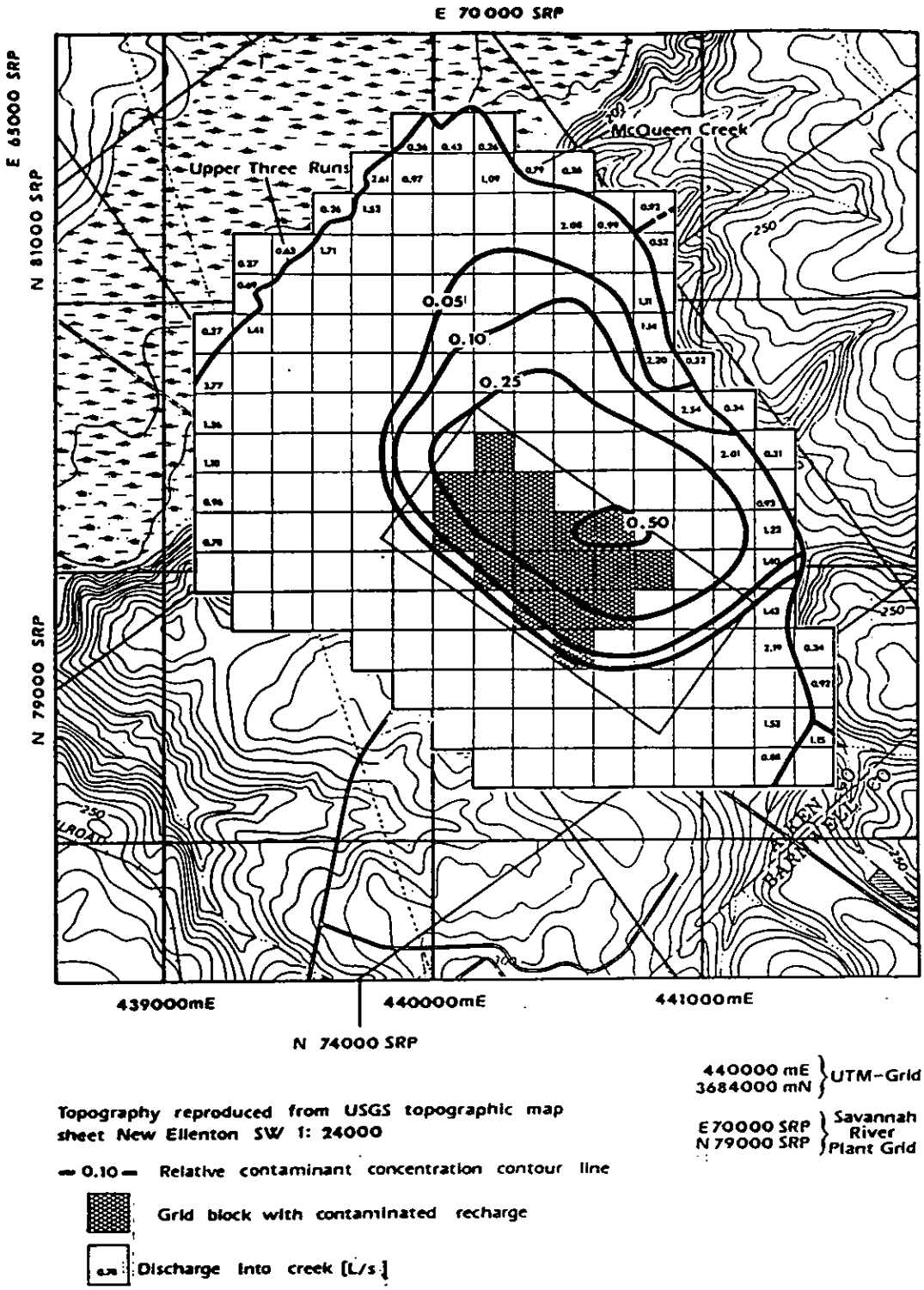

Figure 10-4 Contaminant Concentrations in the McBean Formation (Lower Part) After 200 Years.

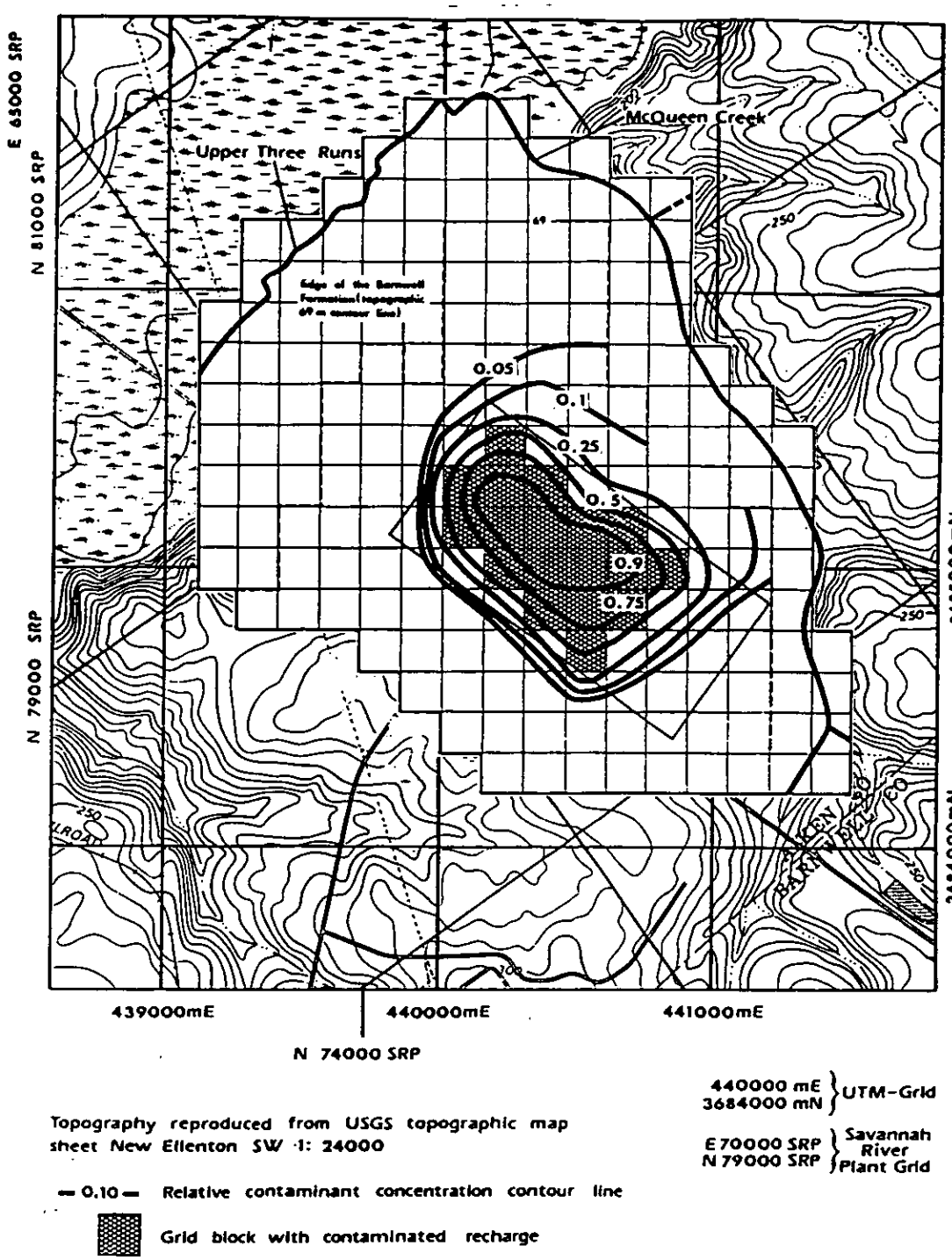

Figure 10-5 Contaminant Concentrations in the Barnwell Formation After 200 Years.

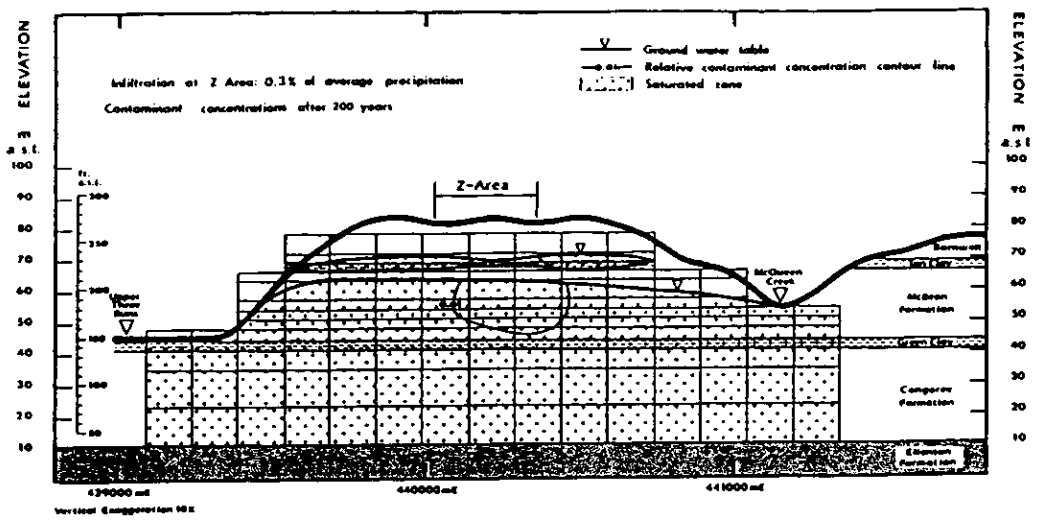

Figure 10-6 Contaminant Concentrations With 0.3% Infiltration at Z-Area After 200 Years (West-East Cross-Section).

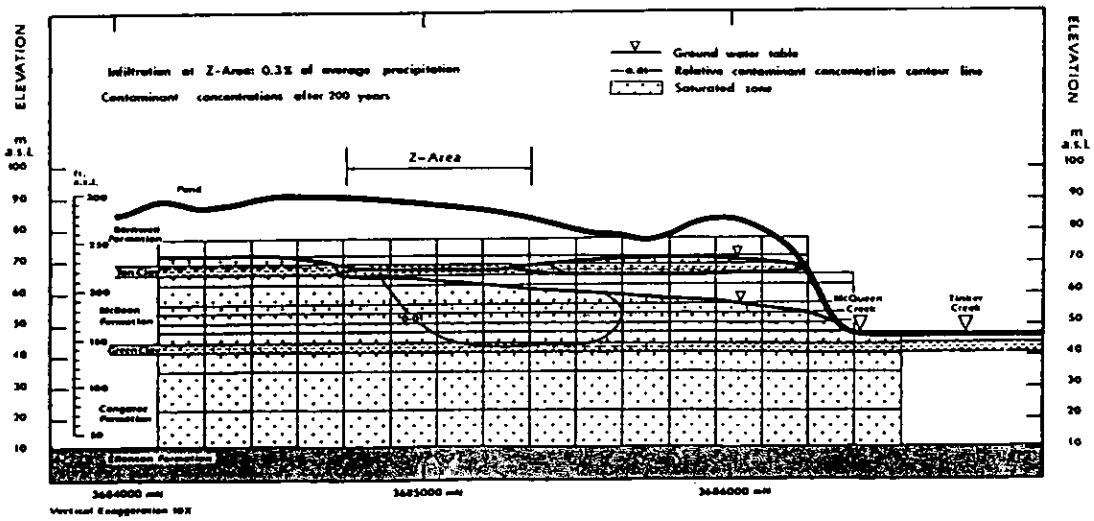

Figure 10-7 Contaminant Concentrations With 0.3% Infiltration at Z-Area After 200 Years (South-North Cross-Section).

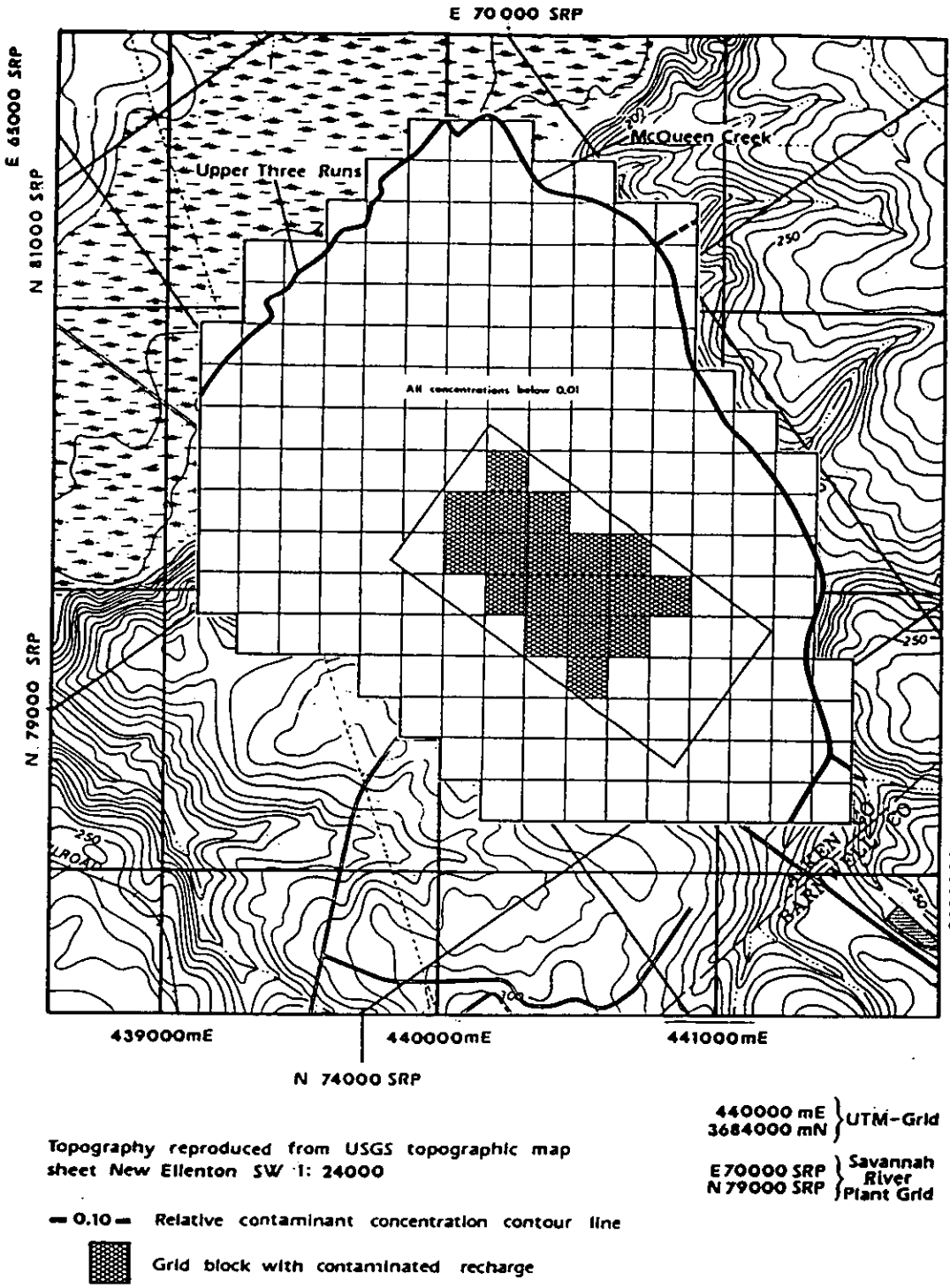

Figure 10-8 Contaminant Concentrations in the Congaree Formation (Upper Part) With 0.3% Infiltration at Z-Area After 200 years.

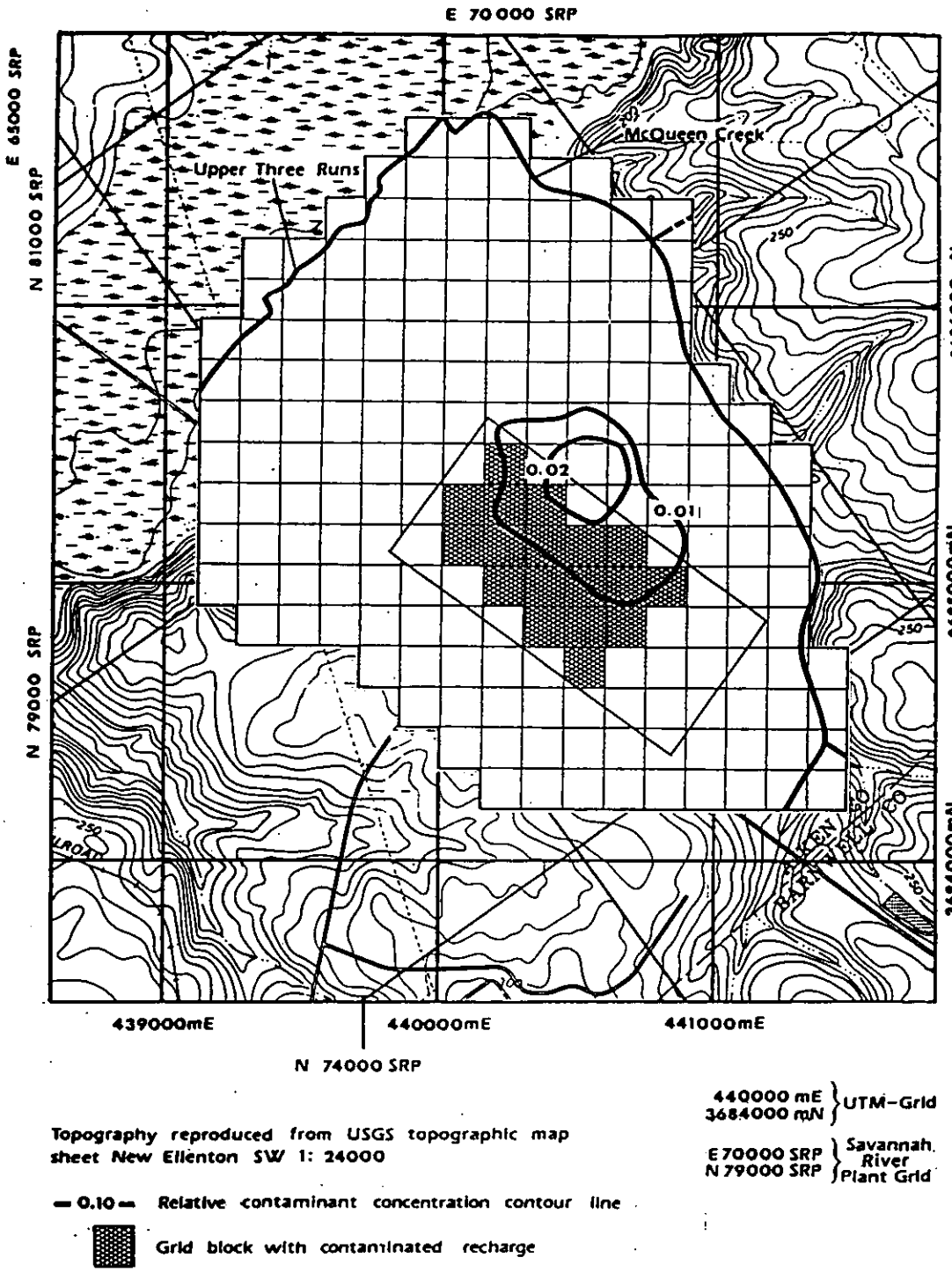

Figure 10-9 Contaminant Concentrations in the McBean Formation (Lower Part) With 0.3% Infiltration at Z-Area After 200 Years.

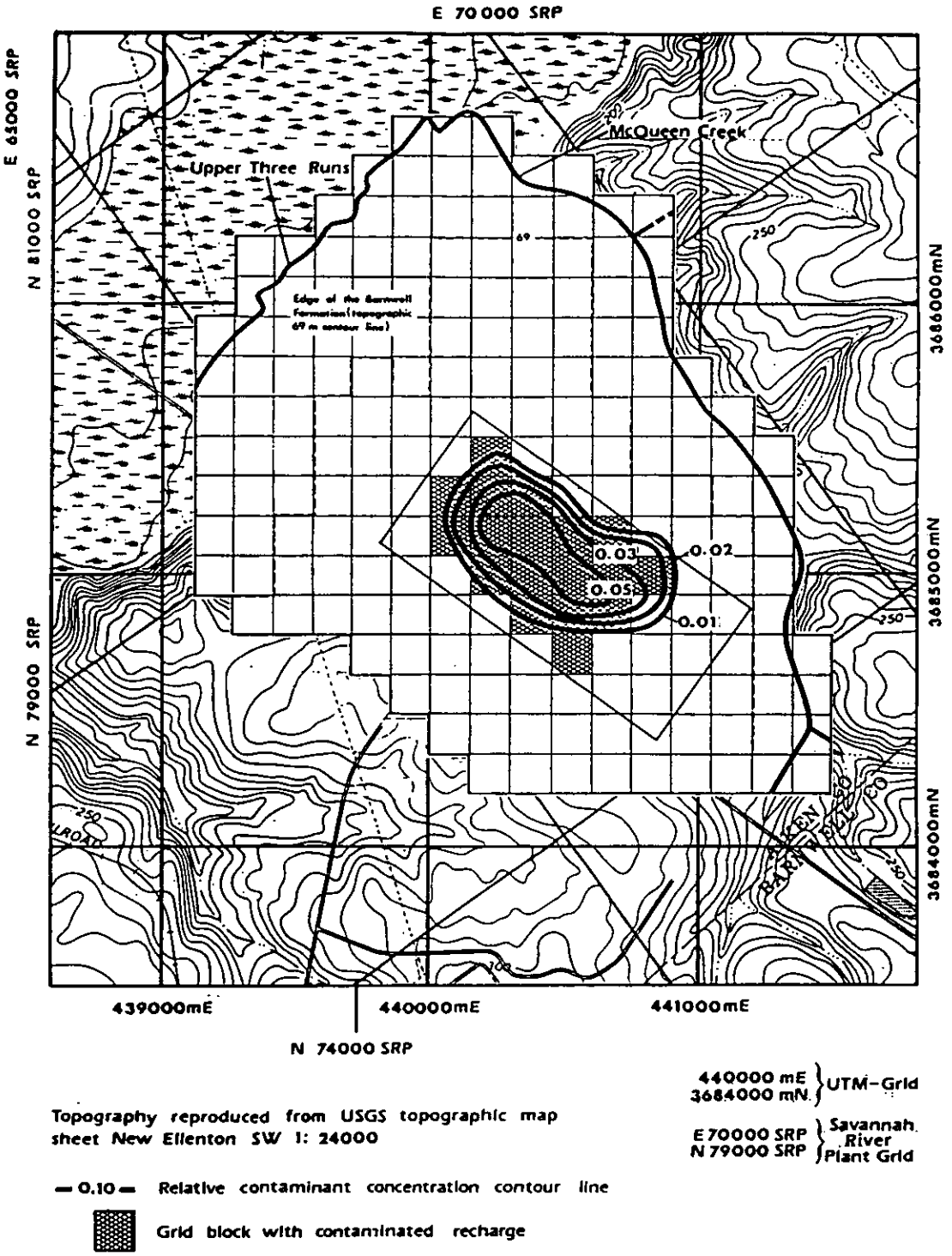

Figure 10-10 Contaminant Concentrations in the Barnwell Formation With 0.3% Infiltration at Z-Area After 200 years.

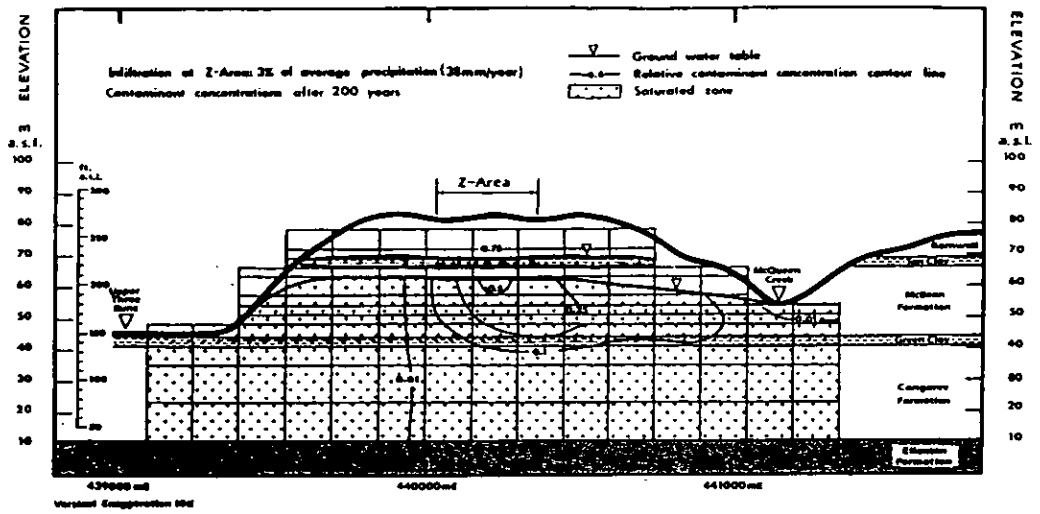

Figure 10-11 Contaminant Concentrations With 3% Infiltration at Z-Area After 200 Years (West-East Cross-Section).

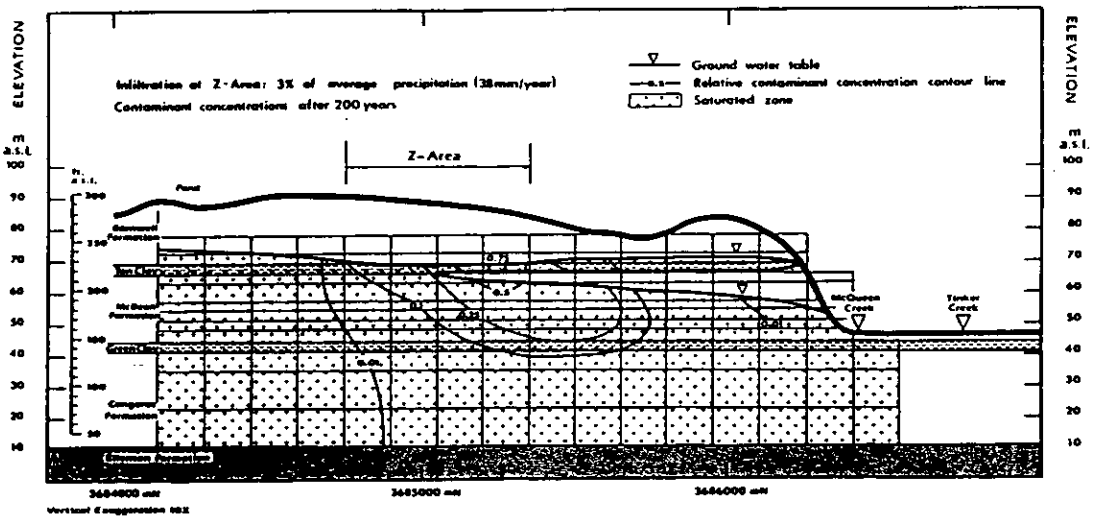

Figure 10-12 Contaminant Concentrations With 3% Infiltration at Z-Area After 200 Years (South-North Cross-Section).

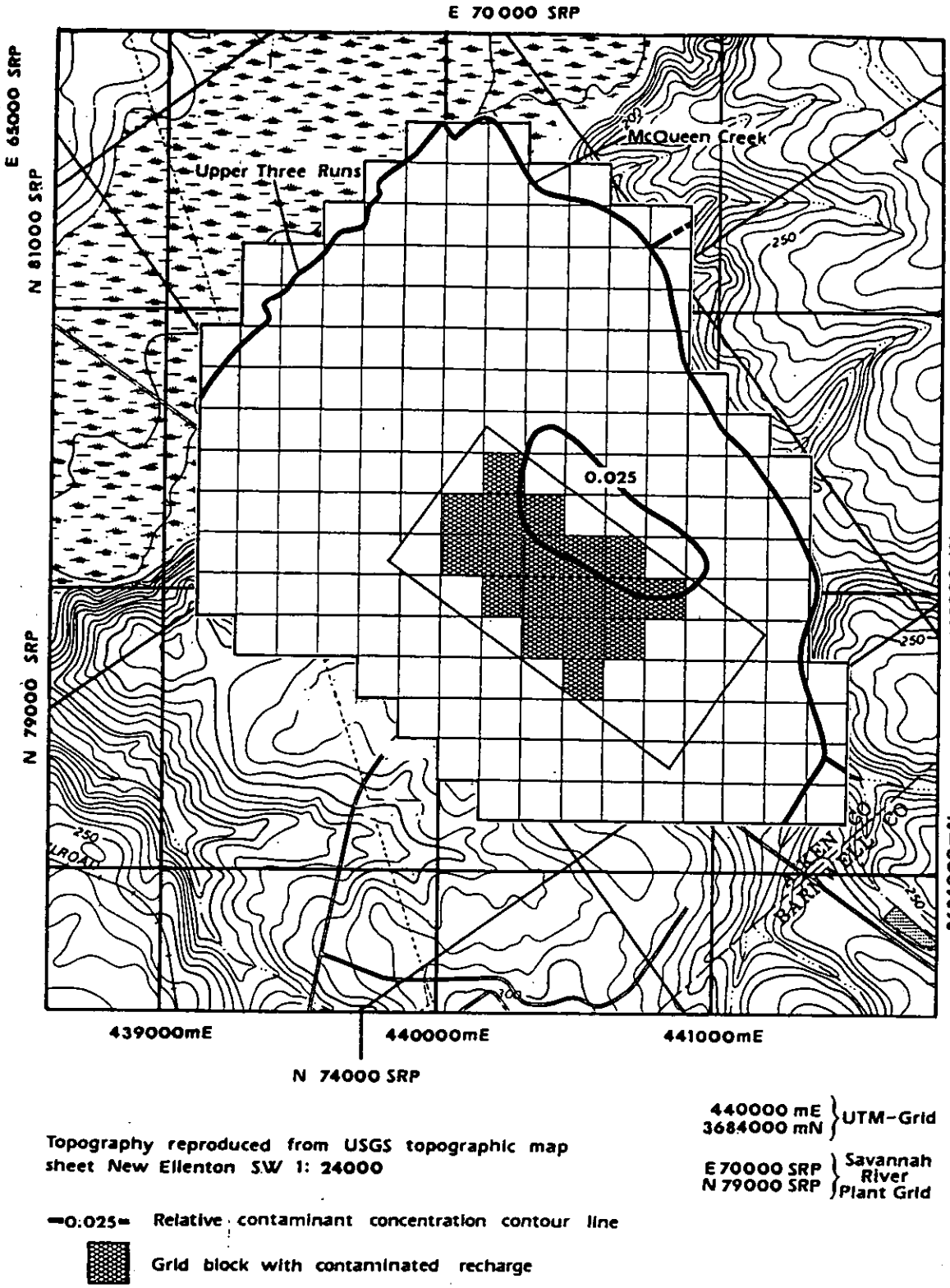

Figure 10-13 Contaminant Concentrations in the Congaree Formation (Upper Part) With 3% Infiltration at Z-Area After 200 Years.

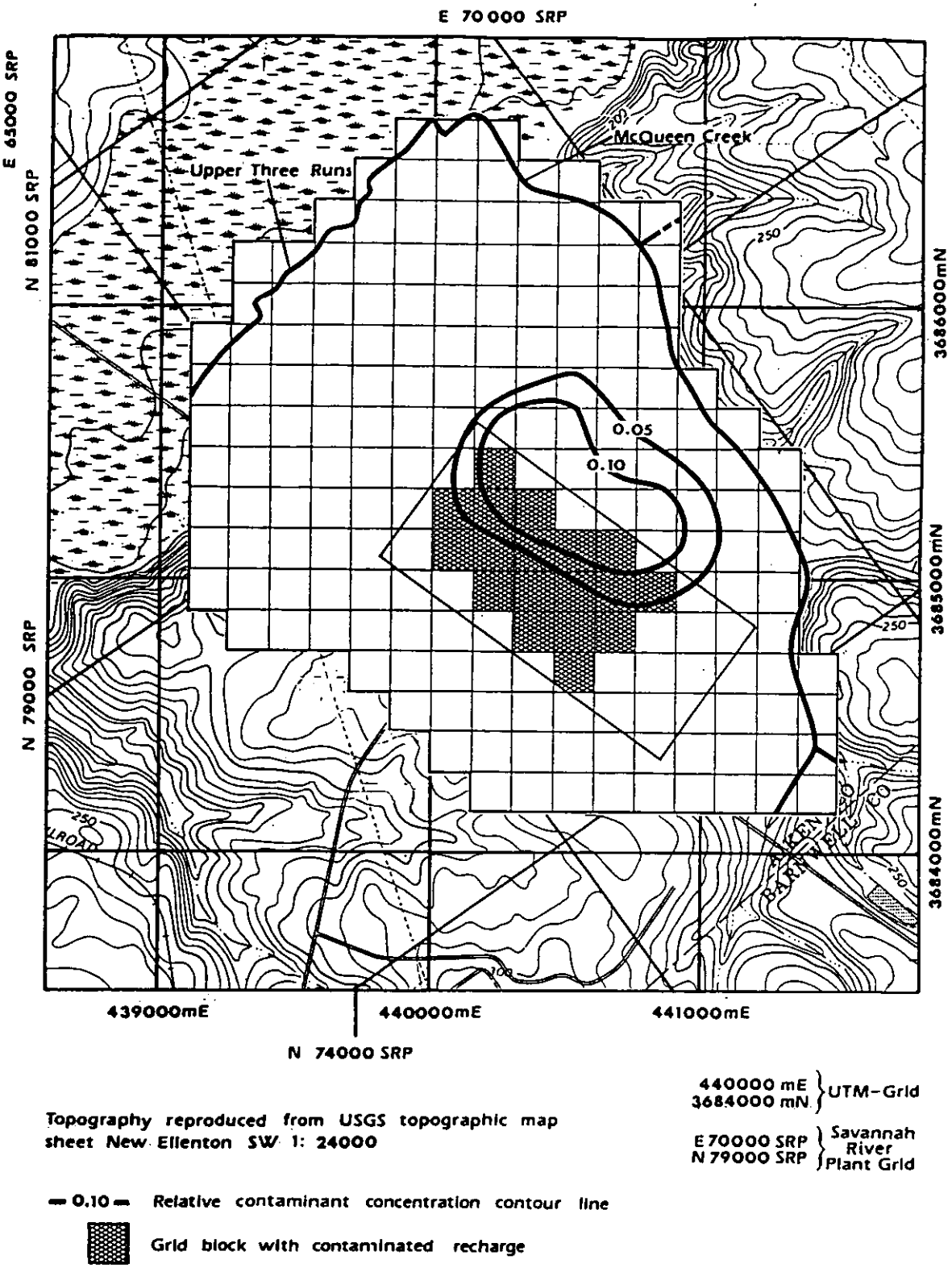

Figure 10-14 Contaminant Concentrations in the McBean Formation (Lower Part) With 3% Infiltration at Z-Area After 200 Years.

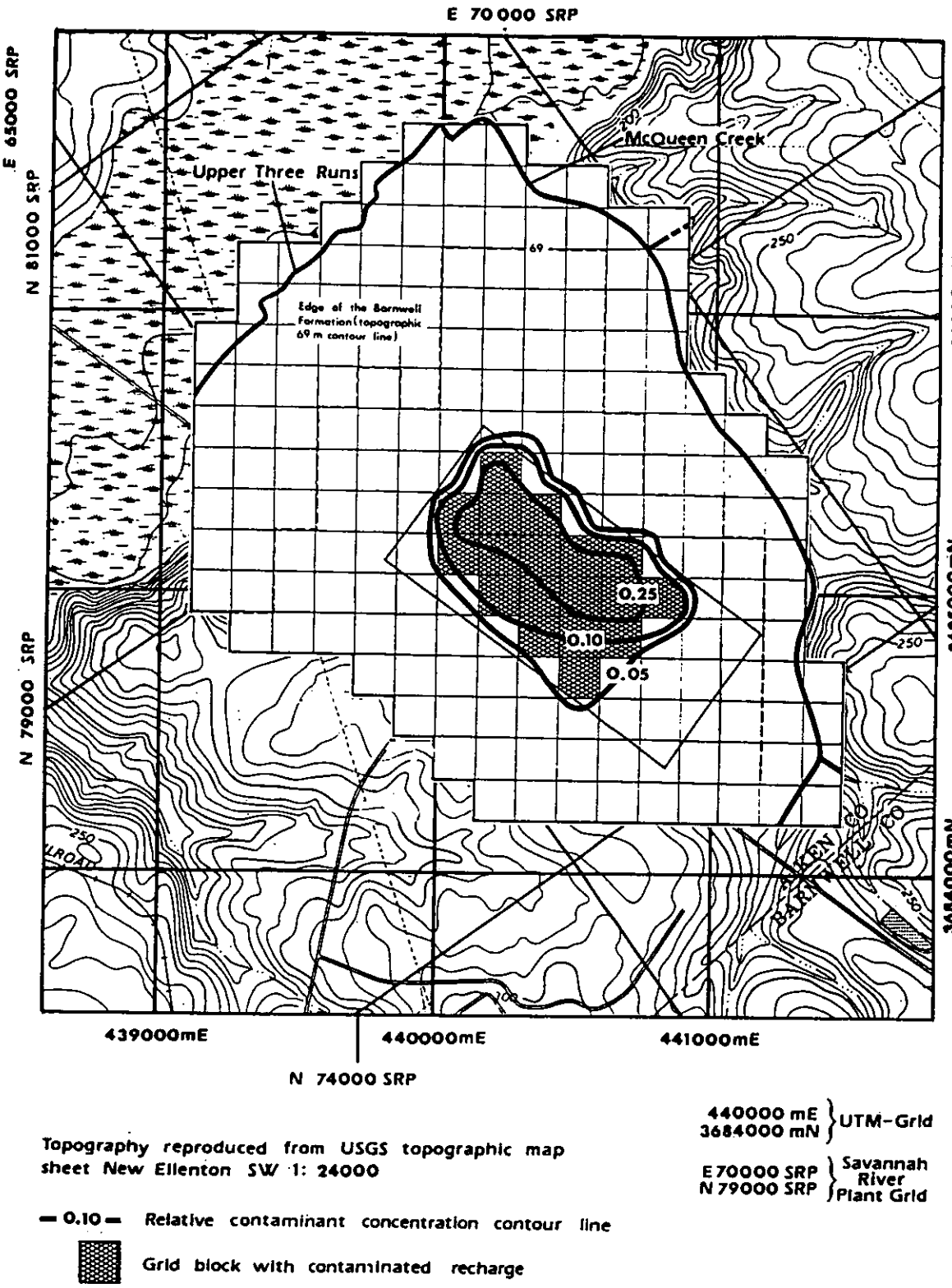

Figure 10-15 Contaminant Concentrations in the Barnwell Formation With 3% Infiltration at Z-Area After 200 Years.

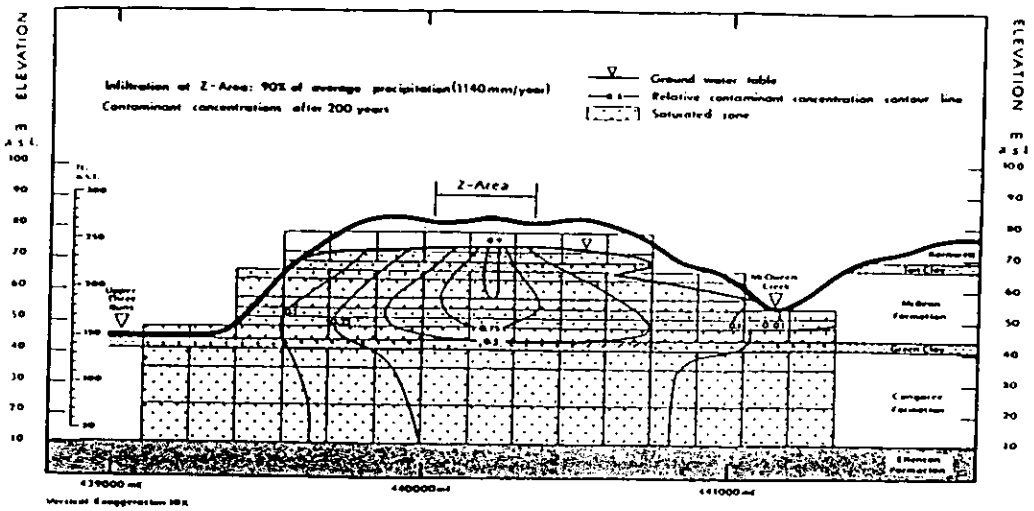

Figure 10-16 Contaminant Concentrations With 90% Infiltration at Z-Area After 200 Years (West-East Cross-Section).

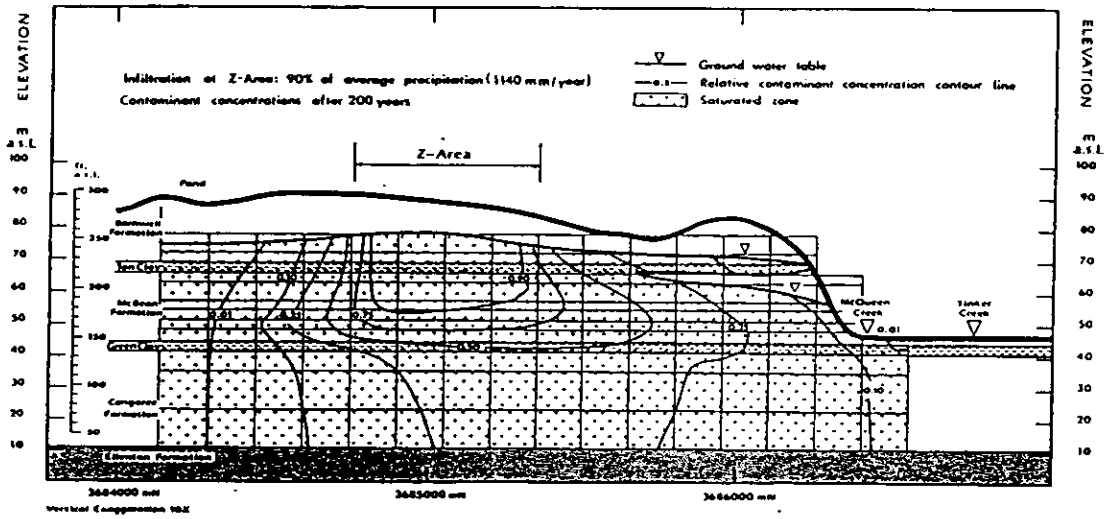

Figure 10-17 Contaminant Concentrations With 90% Infiltration at Z-Area After 200 Years (South-North Cross-Section).

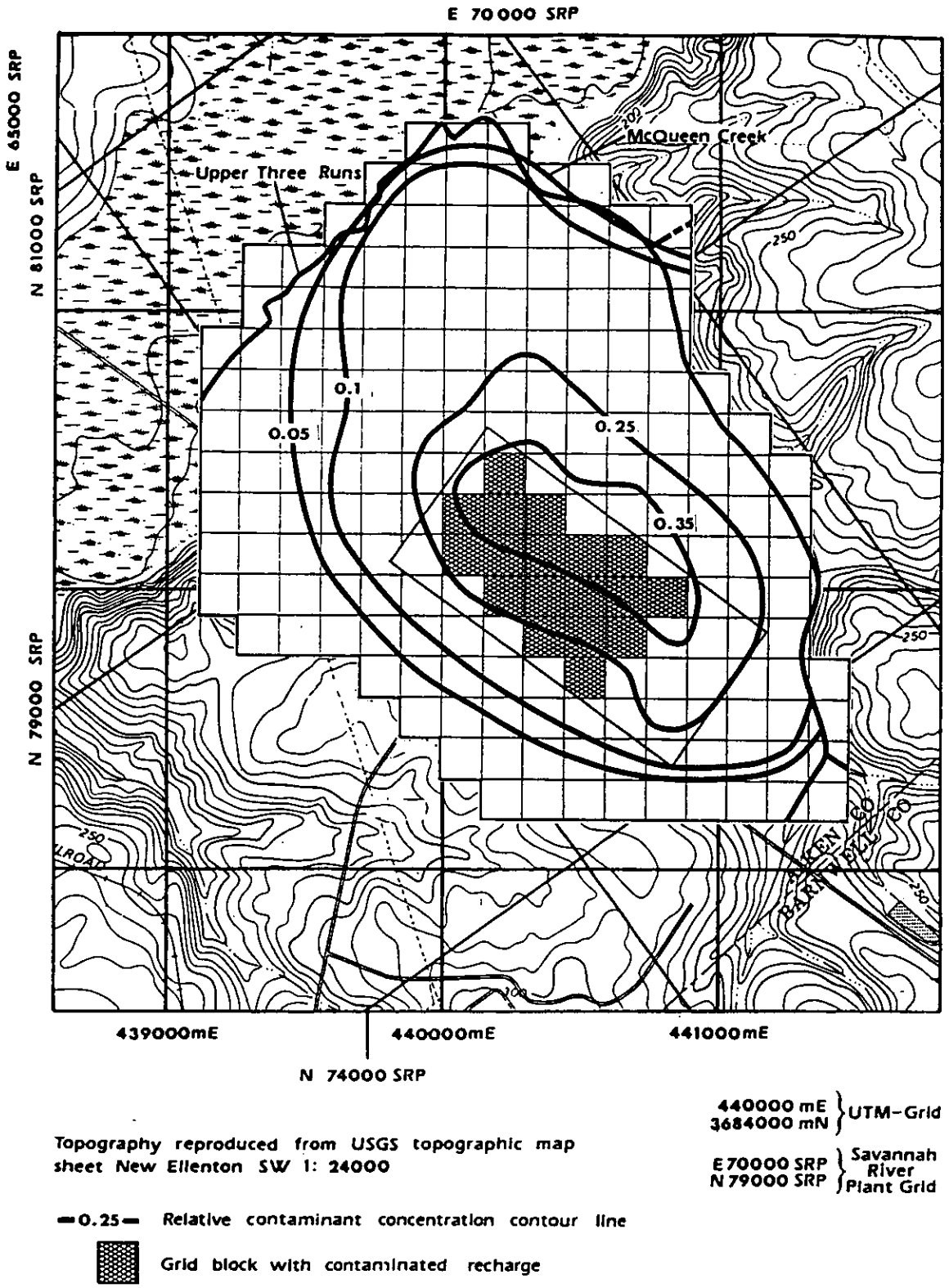

Figure 10-18 Contaminant Concentrations in the Congaree Formation (Upper Part) With 80% Infiltration at Z-Area After 200 Years.

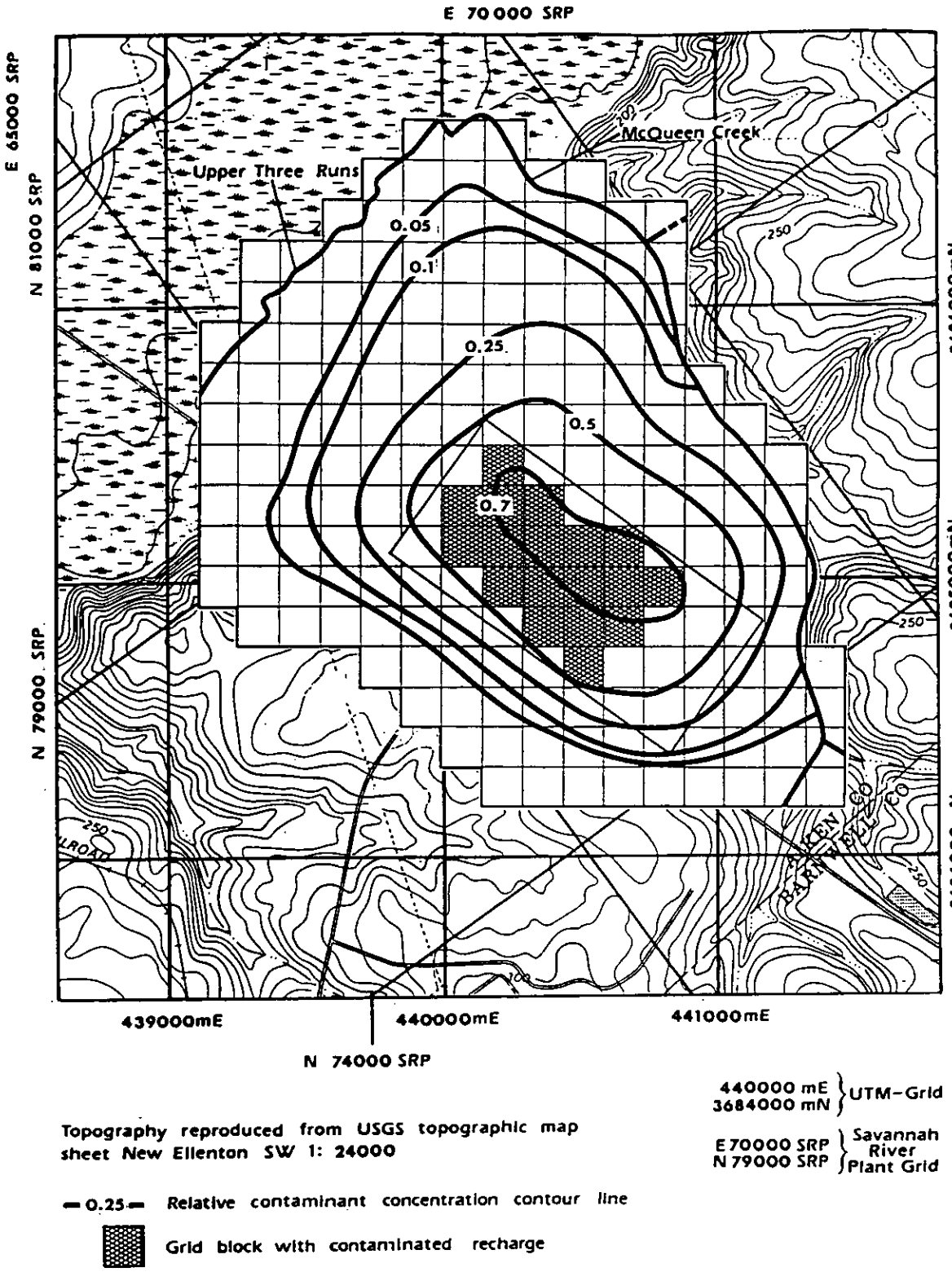

Figure 10-19 Contaminant Concentrations in the McBean Formation (Lower Part) With 90% Infiltration at Z-Area After 200 Years.

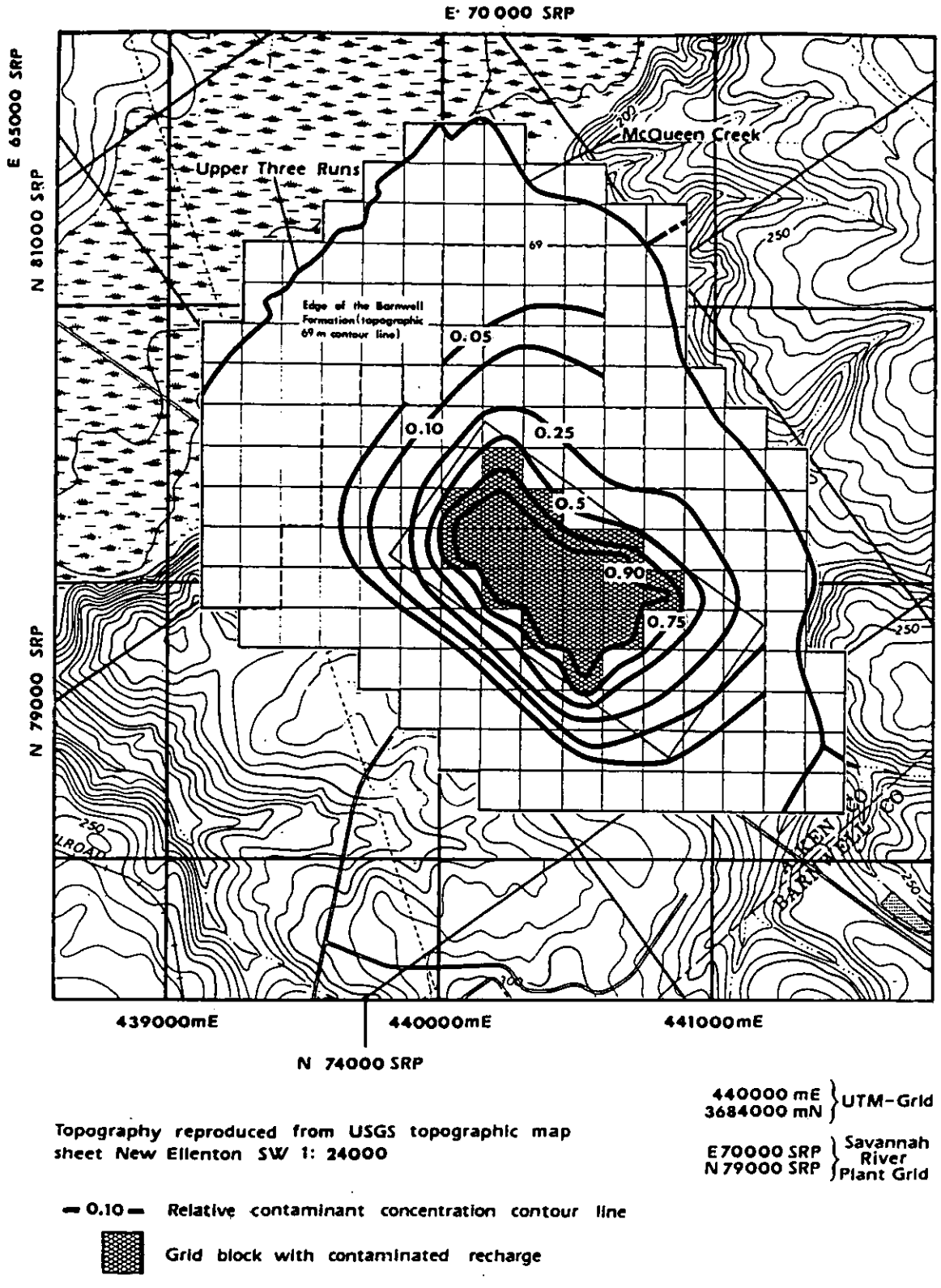

Figure 10-20 Contaminant Concentrations in the Barnwell Formation With 90% Infiltration at Z-Area After 200 Years.

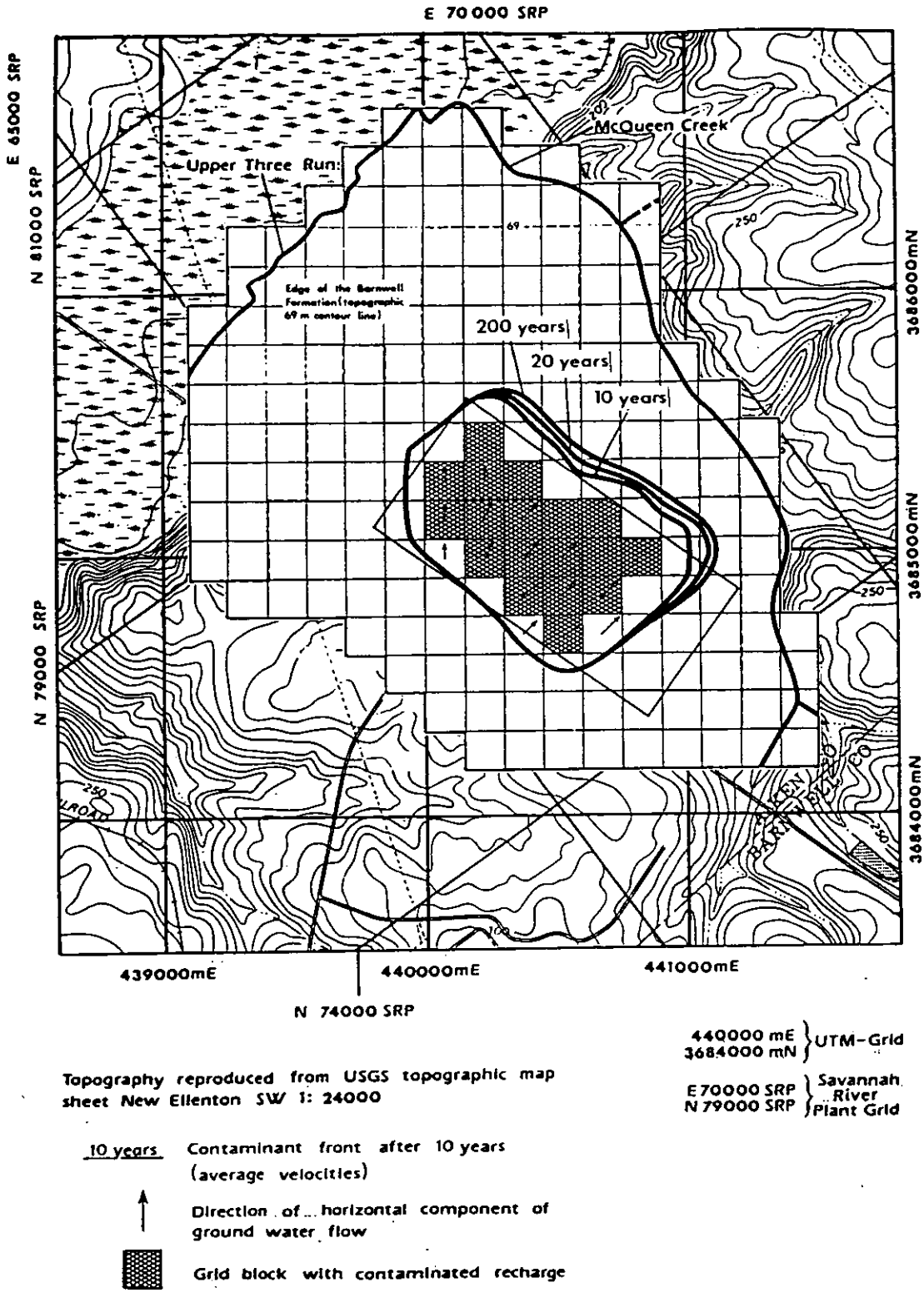

Figure 10-21 Transient Contaminant Front in the Barnwell Formation.

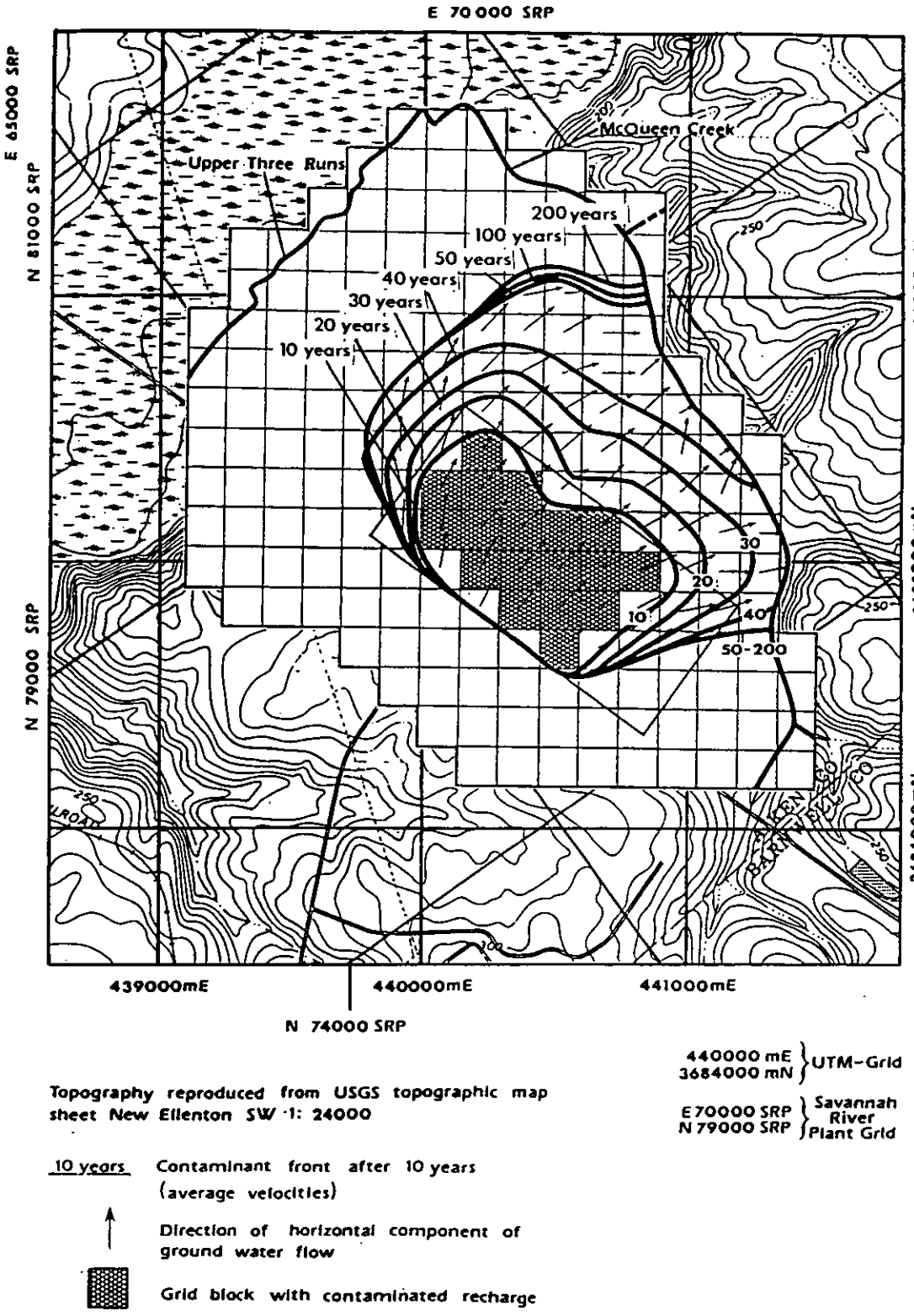

Figure 10-22 Transient Contaminant Front in the McBean Formation.

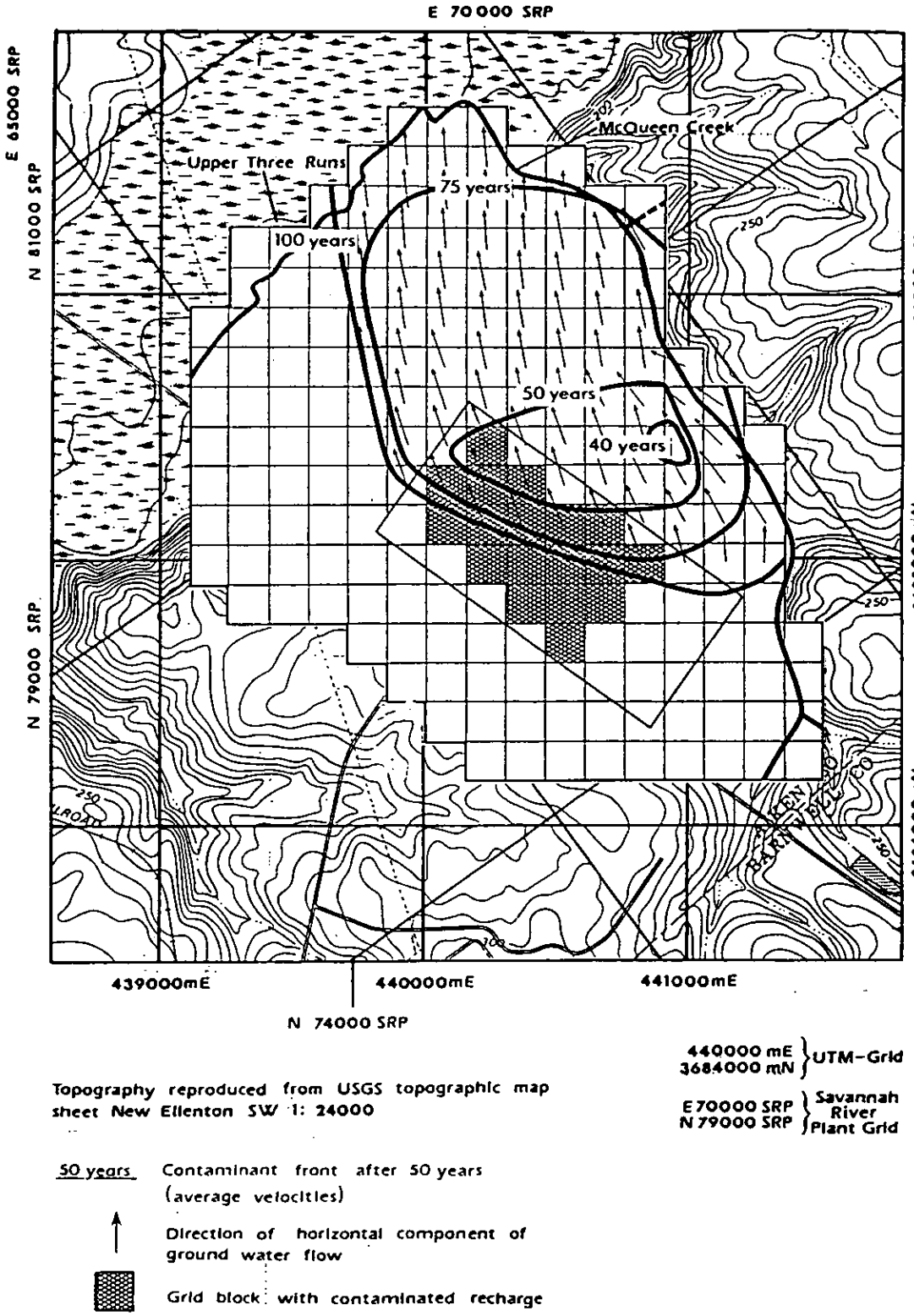

Figure 10-23 Transient Contaminant Front in the Congaree Formation.

Ground Water Balance

Flux into Barnwell and McBean Formation through Southern constant head boundary	1.67	L/s
Recharge (infiltrated precipitation)	52.65	L/s
Flux into Congaree Formation through Southern constant head boundary	128.1	L/s
Total Flux In	182.4	L/s
Flux out of the McBean Formation into Upper Three Runs and McQueen Creeks	45.3	L/s
Flux out of the Congaree Formation through the Northern constant head boundary	137.1	L/s
Total Flux Out	182.4	L/s

Contaminant Balance

Material input: (Recharge with contaminant concentration = 1.0)	4.8	L/s
Material output: From McBean Formation into creeks	4.2	L/s*
Material output: From Congaree Formation through constant head boundary	0.5	L/s*
	4.7	

* - Calculated for contaminant concentration = 1.0, although the actual concentrations are much lower.

Table 10-1: Contaminant Transport Modeling: Material Balance

REFERENCES

Christensen, E. J. and Gordon, D. E., 1983. Technical Summary of Groundwater Quality Protection Program at Savannah River Plant, DPST-83-829, E. I. du Pont de Nemours & Co., Savannah River Laboratory, Aiken, SC.

Cook, J. R., 1983. Estimation of High Water Table Levels of the Saltstone Disposal Site (Z-Area), DPST-83-609, E. I. du Pont de Nemours & Co., Savannah River Laboratory, Aiken, SC.

Cooke, C. W., 1936. "Geology of the Coastal Plain of South Carolina", U.S. Geological Survey Bulletin 867.

Cooke, C. W. and MacNeil, F. S., 1952. "Tertiary Stratigraphy of South Carolina", U.S. Geological Survey Professional Paper 243-B, pp. 19-29.

d'Appolonia, 1981. Boring and Instrument Installation, DWFP Salt Disposal Site, E. I. du Pont Nemours & Co., Savannah River Laboratory, Aiken, SC.

INTERA, 1982. Hydrology Contaminant Transport Model, Theory, Implementation, and User Input, INTERA Technologies, Austin, TX.

INTERA, August 1985. An evaluation of the Leaching of Saltstone Due Both to Convection and Diffusion.

INTERA, January 1986. Validation of Unsaturated Flow Models Using Tank 24 Lysimeter Data.

Fenimose, J. W. and Hooker, R. L., 1977. The Assessment of Solid Low-Level Waste Management at the Savannah River Plant, E. I. du Pont de Nemours and Co., Savannah River Laboratory, Aiken, SC.

Freeze, R. A., and Cherry, J. A., 1979. GROUNDWATER, Prentice-Hall, Englewood Cliffs, NJ.

Garden, A. O., Jr., , Peaceman, D. W., Possi, A. L., Jr. Numerical Calculation of Multidimensional Miscible Displacement by the Methods of Characteristics, Society of Petroleum Engineers Journal, March 1964, pp. 26-36.

Gruber, Paul, 1983. P.G.: A Hydrologic Study of the Unsaturated Zone Adjacent to a Radionuclide Waste Disposal Site at the Savannah River Plant, Aiken, South Carolina in James W. Mercer, R.S.C. Rao & I. Wendell Maxine: Role of the Unsaturated Zone in Radioactive and Hazardous Waste Disposal, Ann Arbor Science Publishers, Collingwood, MI.

Huddleston, P., 1982. "The Development of the Stratigraphic Terminology of the Claibornian and Jacksonian Marine Deposit in Western South Caroling and Eastern Georgia", Geological Investigations Related to the Stratigraphy in the Kaolin Mining District, Aiken County, South Carolina - Carolina Geological Society Field Trip Guidebook, pp. 21-33.

Kuckling, H., 1982. Taschenbuck der Physik, VerlagHerri Deutsch, Frankfurt, West-Germany.

Lantz, R. B., "Quantitative Evaluation of Numerical Diffusion (Truncation Error)", SPE Jr., September 1971.

Marine, I. W., and Siple, G. E., 1974. Buried Triassic Basin in Central Savannah River Plant Area, South Caroling and Georgia, Geological Society of American Bulletin, Vol. 85, pp. 311-320.

Marine, I. Wendell, 1974. Geohydrology of the Buried Traissic Basin at the Savannah River Plant, Ground Water, Volume 12, No.2, pp. 84-96.

Marine, I. W., 1976. Structural and Sedimentational Model of the Buried Dunbarton Triassic Basin, South Carolina and Georgia. DP-MS-74-39, E. I. du Pont de Nemours & Co., Savannah River Laboratory, Aiken, SC.

Mittwede, S.K., "Stratigraphy of the Jackson Area, Aiken County, South Carolina", Geological Investigations Related to the Stratigraphy in the Kaolin Mining District, Aiken County, South Carolina - Carolina Geological Society Field Trip Guidebook, pp. 65-78.

Parizek, Richard R. & Root, Robert W., Jr., 1984. Progress Toward the Development of a Ground-Water Velocity Model for the Radioactive Waste Management Facility Savannah River Plant, South Carolina. Quarterly Report, July 15, 1984, The Pennsylvania State University.

Quisenberry, V., 1985. Hydraulic Properties of Saltcrete and Z-Area Soil.

Rankin, D. W., 1977. "Studies Related to the Charleston South Carolina Earthquake of 1886", U. S. Geological Survey Professional Paper 1028, pp. 1-15.

Root, R. W., Jr., 1982. Numerical Modeling of Ground-Water Flow at the Savannah River Plant, E. I. du Pont de Nemours & Co., Savannah River Laboratory, Aiken, SC.

Sargent, Kenneth A., 1984. Study of a Perched Condition in the DWPF Saltstone Disposal Site, E. I. du Pont de Nemours & Co., Savannah Rivers Laboratory, Aiken, SC.

Siple, G. E., 1967. "Geology and Ground Water of the Savannah River Plant and Vicinity, South Carolina", U. S. Geological Survey Water Supply Paper 1841.

Toulocikian, Y. S. and Ho, C. Y., 1981. Physical Properties of Rocks and Minerals, McGraw Hill, CINDAS Data Series on Material Properties, Volume II-2, 548 p.

REFERENCES FOR APPENDIX A

d'Appolonia, 1981. Boring and Instrument Installation, DWFP Salt Disposal Site, E . I. du Pont Nemours & Co., Savannah River Laboratory, Aiken, SC.

Christensen, E. J. and Gordon, D. E., 1983. Technical Summary at Groundwater Quality Protection Program at Savannah River Plant, DPST-83-829, E. I. du Pont de Nemours & Co., Savannah River Laboratory, Aiken, SC.

Cooper, H. H., Jr., Bredehoeft, J. D., and Papadopoulos, I. S., 1967. Response of a Finite-Diameter Well to an Instantaneous Charge of Water. Water Resources Res., 3, pp 263-269.

Gelhar, L. W. and Axness, C. L., 1983. Three-Dimensional Stochastic Analysis on Microdispersion in Aquifers. Water Resources Research, Vol. 15, No. 1, pp. 161-180.

Hvorslev, M. J., 1951. Time Lag and Soil Permeability in Groundwater Observations. U. S. Army Corps Engrs. Waterways Exp. Sta. Bull. 36, Vicksburg, Miss.

Neuman, S. P., 1982. Statistical Characterization of Aquifer Heterogeneities: An Overview, Geological Society of American, Special Paper, 189.

REFERENCES FOR APPENDIX B

Lantz, R. B., 1971. "Quantitative Evaluation of Numerical Diffusion (Truncation Error)", SPE Jr., September 1971.

Price, H. S. and Coats, K. H., 1973. "Direct Methods in Reservoir Simulation", SPE 4278 presented at the 3rd SPE Symposium on January 1973, Houston, Texas.

Scheidegger, A. E., 1961. "General Theory of Dispersion in Porous Media", Geophys. Res. Jour., October 1961.

Van Genuchten et al, 1979. "Movement of Solutes in Soil: Computer-Simulated and Laboratory Results", presented in Soil Chemistry.

APPENDIX A

Field Hydraulic Measurements at Z-Area
in June 1985

A-1 INTRODUCTION

The general geology and hydrologeology of the region in general and the Savannah River Plant area in particular are fairly well known (Christensen and Gordon, 1983). However very little detailed hydrologic information about the Z-Area itself is available. Most of the existing hydrogeologic information was derived from the field and laboratory investigation program conducted by d'Appolonia in 1981. This program included drilling (25 locations, 25 boreholes) sampling, and geophysical borehole logging at and around Z-Area (Figure A-1).

The boreholes were completed with piezometers for measurement of ground water levels and hydrochemical sampling (d'Appolonia, 1981). During 1984 some additional boreholes were drilled and piezometers installed (J. Cook, pers. comm.).

Thus the existing hydrogeologic information about the Z-Area itself consisted essentially of:

- ground water level measurements performed in the above mentioned boreholes since 1982.
- results of laboratory tests performed on 'undisturbed' samples obtained during the above mentioned drilling, i.e., estimates about formation properties such as grain size distribution, horizontal and vertical permeabilities and both total and effective porosities.
- some hydraulic conductivity measurements conducted in boreholes at or adjacent to the Z-Area.

In an attempt to determine in more detail the spatial variability of the hydraulic conductivity across Z-Area a series of slug withdrawal tests were conducted by INTERA Technologies in the above mentioned piezometers in June 1985. Prior to these hydraulic conductivity tests water level measurements in all boreholes were attempted.

The results of the hydraulic measurements performed in June 1985 are summarized in the following sections.

A-2 WATER LEVEL MEASUREMENTS IN JUNE 1985

Initially, in about 40 wells (Figure A-1) the water levels were to be measured prior to the slug withdrawal tests. However, all shallow wells which were screened in the Barnwell Formation were found to be dry (June 18-20, 1985). This appears to result from the fact that precipitation at the Savannah River Region was about 400-500 mm below normal for the period September 1984 to June 1985. This unusually low precipitation rate has also resulted in the drying of McQueen Creek, which flows along the east side of the Z-Area hill north to Upper Three Runs Creek.

The results are summarized in Table A-2. This table also shows some of the piezometer specifications (d'Appolonia, 1981), the formation in which the piezometer is screened, and a summary (minimum, maximum, mean) of the water level data from du Pont.

The water level data from June 18-20 are reviewed together with the water table data by du Pont within the frame work of the general data review (see Section 6.7).

A-3 HYDRAULIC TESTING IN JUNE 1985

Initially about 40 wells were to be tested by slug withdrawal tests. However, most shallow wells were found to be dry. Thus, only 15 hydraulic tests were performed between June 18 and June 20, 1985. These tests consisted of the withdrawal of a known volume of fluid from the wells and

measurements of water level recovery over time. Using the techniques of Hvorslev (1951) and Cooper et al. (1967), the hydraulic conductivities were calculated. A brief introduction to both methods is given in Freeze and Cherry (1979, pp 339 ff). The difference between both methods derives from emphasizing different aspects of the well configuration. The Hvorslev method is best suited for point piezometers that are open only over a short interval at their base, while the Cooper et al. method is suitable for screened piezometers that are open over the entire thickness of a confined aquifer.

As far as the methodology is concerned, the initial analytical method of Hvorslev assumes a homogeneous, isotropic, infinite medium in which both soil and water are incompatible. Hvorslev reasoned that the rate of inflow (q) at the piezometer tip at any time (t) is proportional to the hydraulic conductivity (K) of the soil or rock and to the unrecovered water level difference H-h, so that

$$q(t) = \pi r^2 \frac{dh}{dt} = FK(H-h)$$

where F is a factor that depends on the shape and dimension of the piezometer intake. To interpret field data, the data are plotted in semilogarithmic form with logarithmic normalized recovery $(H-h)/(H-H_o)$ against linear time t (Figure A-2). The basic time lag, T_o, at $(H-h)/(H-H_o) = 0.37$ is read out graphically and the hydraulic conductivity calculated by

$$K = \frac{\pi r^2}{T_o F}$$

Hvorslev has also presented formulas for anisotropic conditions and for a wide variety of shape factors that treat such cases as a piezometer open only at its basal cross section and a piezometer that just encounters a permeable formation underlying an impermeable one.

The analysis of Cooper et al. (1967) is subject to the same assumptions as the Theis solution for pumping from a confined aquifer. Contrary to the Hvorslev method of analysis, it includes consideration of both formation

and water compressibilities. It utilizes a type curve matching procedure to determine the aquifer coefficients T and S (Figure A-3). The hydraulic conductivity K can then be determined on the basis of the relation, K = T/b, where b is the aquifer thickness. Like the Theis solution, the method is based on the solution to a boundary-value problem that involves the transient equation for ground water flow.

For field test data evaluation, the method requires that the plot is prepared on semilogarithmic paper with the reverse format to that of the Hvorslev test; the $H - h/H - H_o$ scale linear, while the t scale is logarithmic. The field curve is then superimposed on the type curves shown in (Figure A-3). With the axes coincident, the data plot is translated horizontally into a position where the data best fit one of the type curves. A matchpoint is chosen (or rather, a vertical axis is matched) and values of t and W are read off the horizontal scales at the matched axis of the field plot and the type plot, respectively. For ease of calculation it is common to choose a matched axis at W = 1.0. The transmissivity T is then given by

$$T = \frac{Wr^2}{t}$$

where the parameters are expressed in any consistent set of units.

In principle, the storativity S can be determined from the a value of the matched curve and the expression shown on Figure A-3. In practice, since the slopes of the various a lines are very similar, the determination of S by this method is unreliable.

As already mentioned, the test data obtained by INTERA Technologies in June 1985 were evaluated using both the Hvorslev method and the Cooper et al. method. The data plots are shown in Figures A4a-f, while the results are summarized in Table A-3. A comparison shows that the results from both methods are fairly consistent. Generally the Cooper et al.

method provides higher conductivity values than the Hvorslev method. The ratio of the two types of values ranges from 1.1 to 3.8 with a mean at 2.4.

Using the mean calculated from the results of both evaluation methods, the measured conductivities range as follows:

McBean Formation: $1.1 \times 10^{-8} - 1.8 \times 10^{-4}$ m/s
Congaree Formation: $2.0 \times 10^{-7} - 1.8 \times 10^{-4}$ m/s

The large range covered by the test results (4 orders of magnitude in the McBean Formation, 3 orders of magnitude in the Congaree Formation) may reflect the heterogeneity of both formations. In heterogeneous formations, the representative hydraulic conductivity depends on the size of volume, for which it shall be representative and on the direction of the flow in relation to the heterogeneities (Neuman 1982; Gelhar and Axness, 1983).

At Z-Area it can be assumed, that the heterogeneities consist in horizontally layered lenses of clay, clayey sand, and sand. Thus the horizontal hydraulic conductivity corresponds to a ground water flow parallel to the heterogeneities or lenses. For this case, the arithmetic mean is best suited to derive a representative value from a given data set (Neuman, 1982; Gelhar and Axness, 1983).

The arithmetic mean values of the measured conductivities for both formations are:

McBean Formation: 2.89×10^{-5} m/s
Congaree Formation: 6.05×10^{-5} m/s

For the vertical flow, which in the actual case is a flow across and around the clay and sand lenses, the effective vertical hydraulic conductivity is likely lower than the horizontal hydraulic conductivity. If the clay and sand lenses were continuous strata throughout the area in

consideration, it would be possible to use the harmonic mean of the field test results as an estimate for the effective vertical hydraulic conductivity (Neuman, 1982; Gelhar and Axness, 1983). But at Z-Area, the clay and sand lenses within the individual hydrostratigraphic units are not continuous over the entire site area (see borehole logs in d'Appolonia, 1981). Thus it is not possible to calculate the vertical hydraulic conductivity from INTERA's field test results.

The hydraulic conductivity data obtained from INTERA's field tests are reviewed with the conductivity values taken from the literature within the context of the general data review (see Section 6.6).

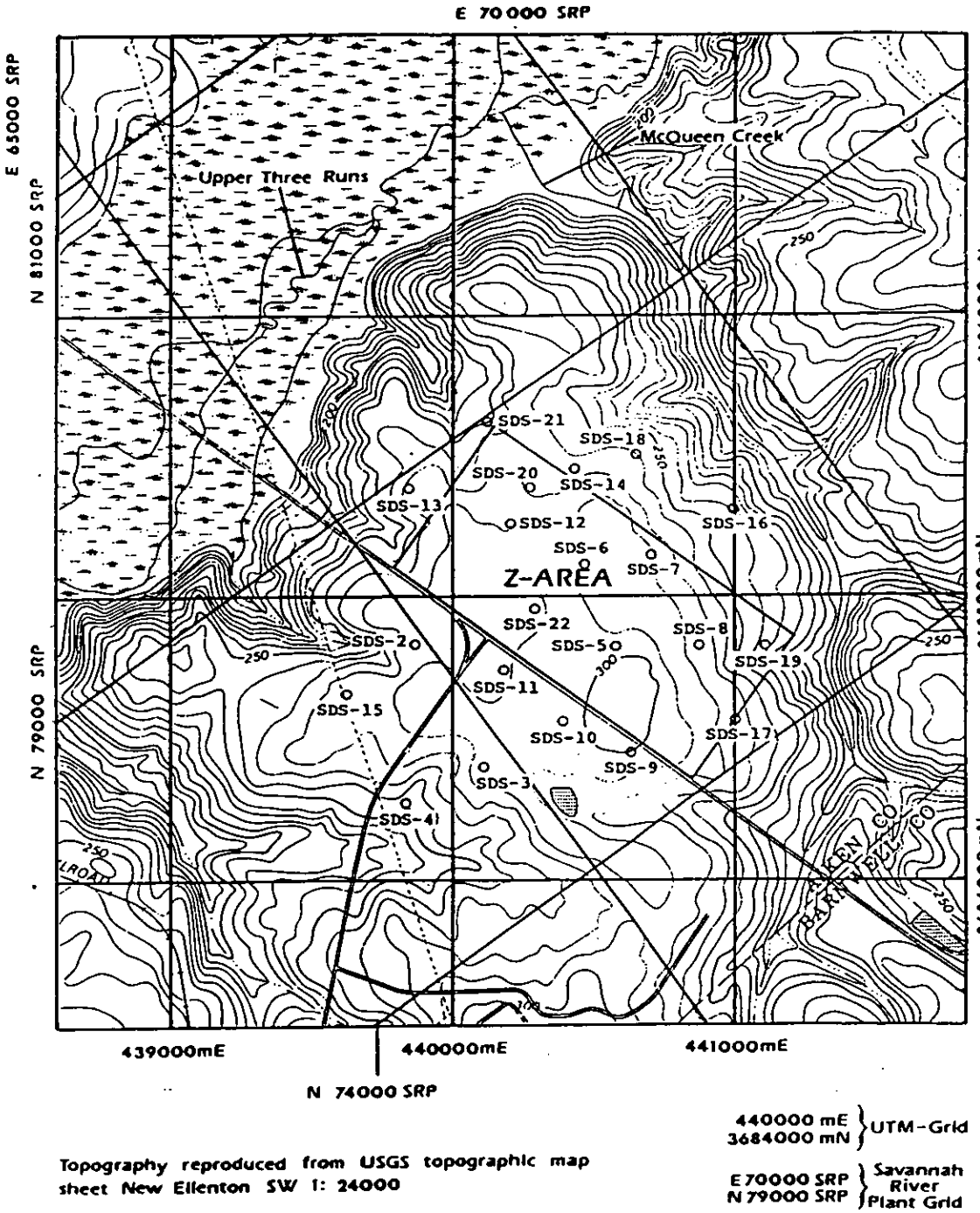

Figure A-1 Borehole locations at Z-Area

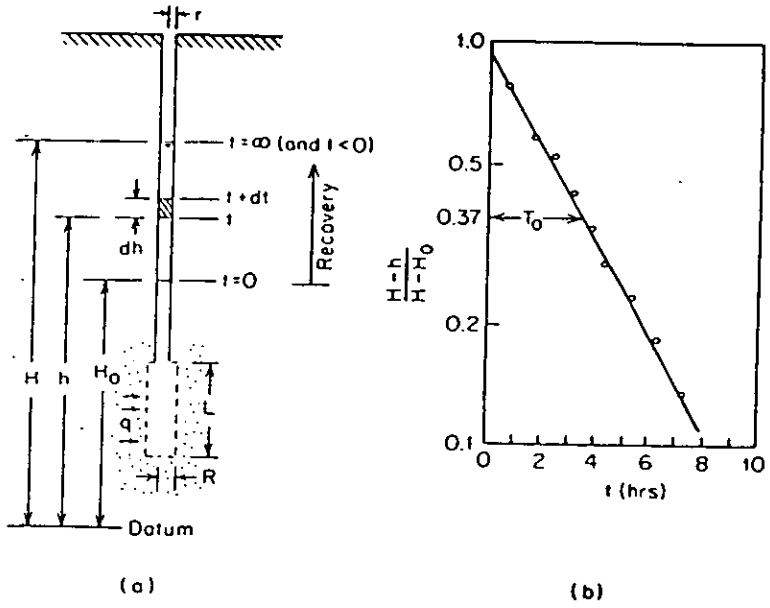

Figure A-2 Hvorslev Piezometer test. (a) Geometry; (b) method of analysis. (from Freeze and Cherry, 1979)

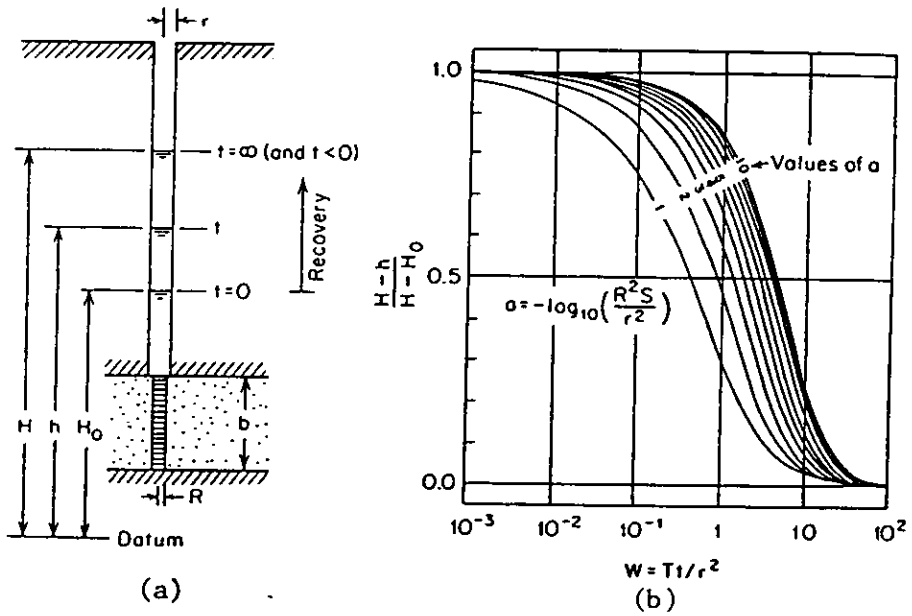

Figure A-3 Piezometer test in a confined aquifer (Cooper et al.) (a) Geometry; (b) type curves (from Freeze and Cherry, 1979)

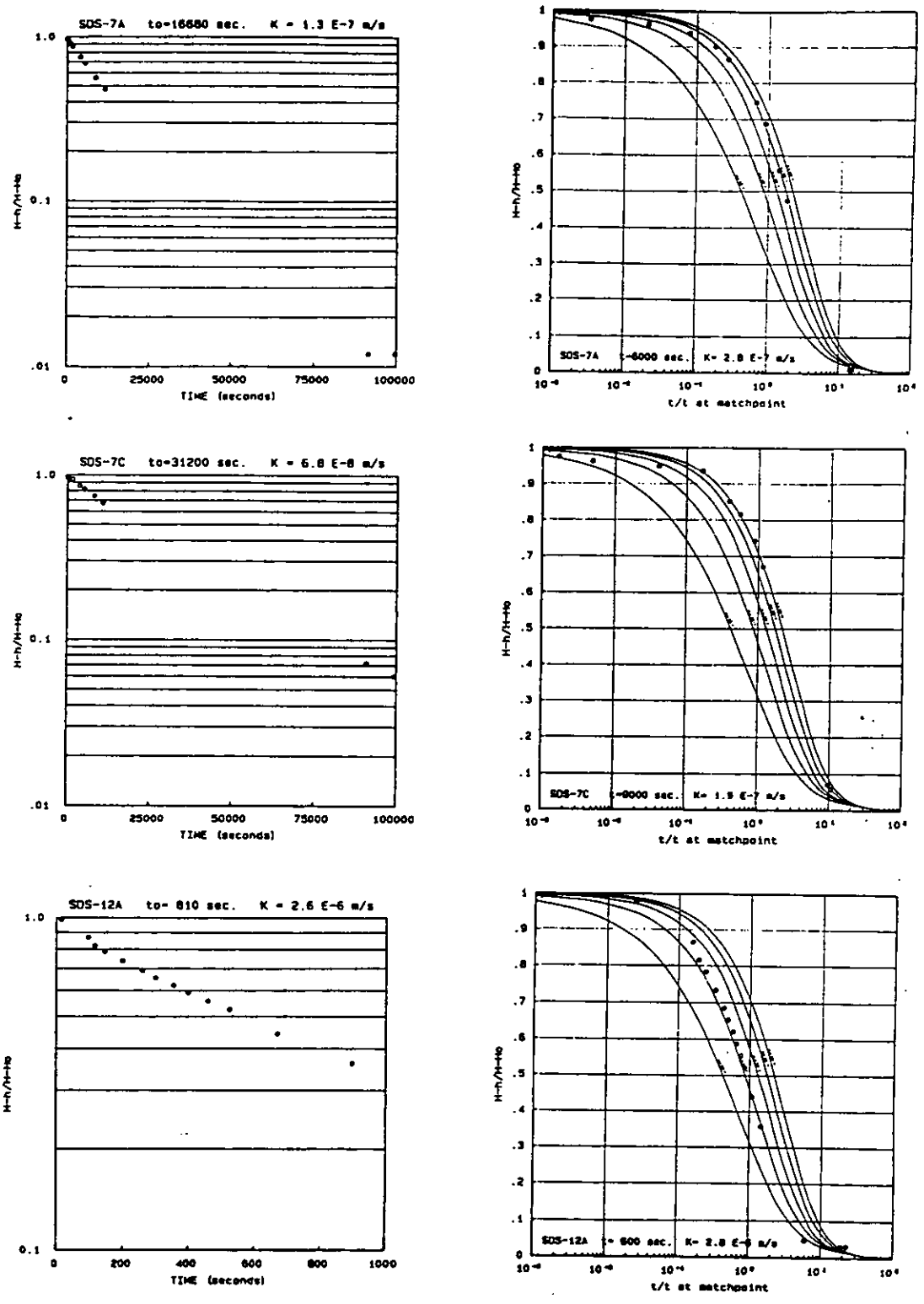

Figure A-4a Field Hydraulic Measurements (INTERA, June 1985 Data Plots)

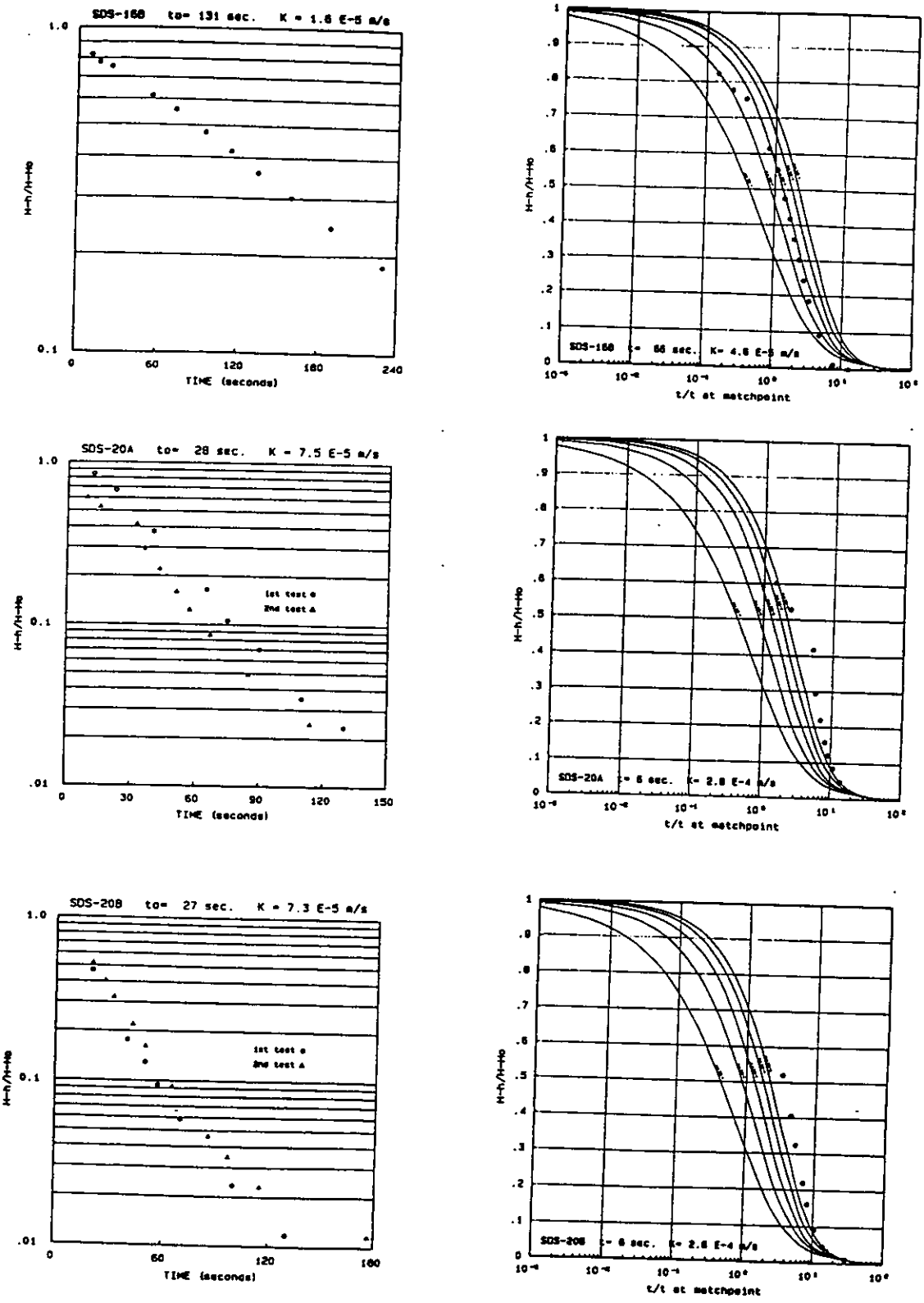

Figure A-4b Field Hydraulic Measurements (INTERA, June 1985 Data Plots)

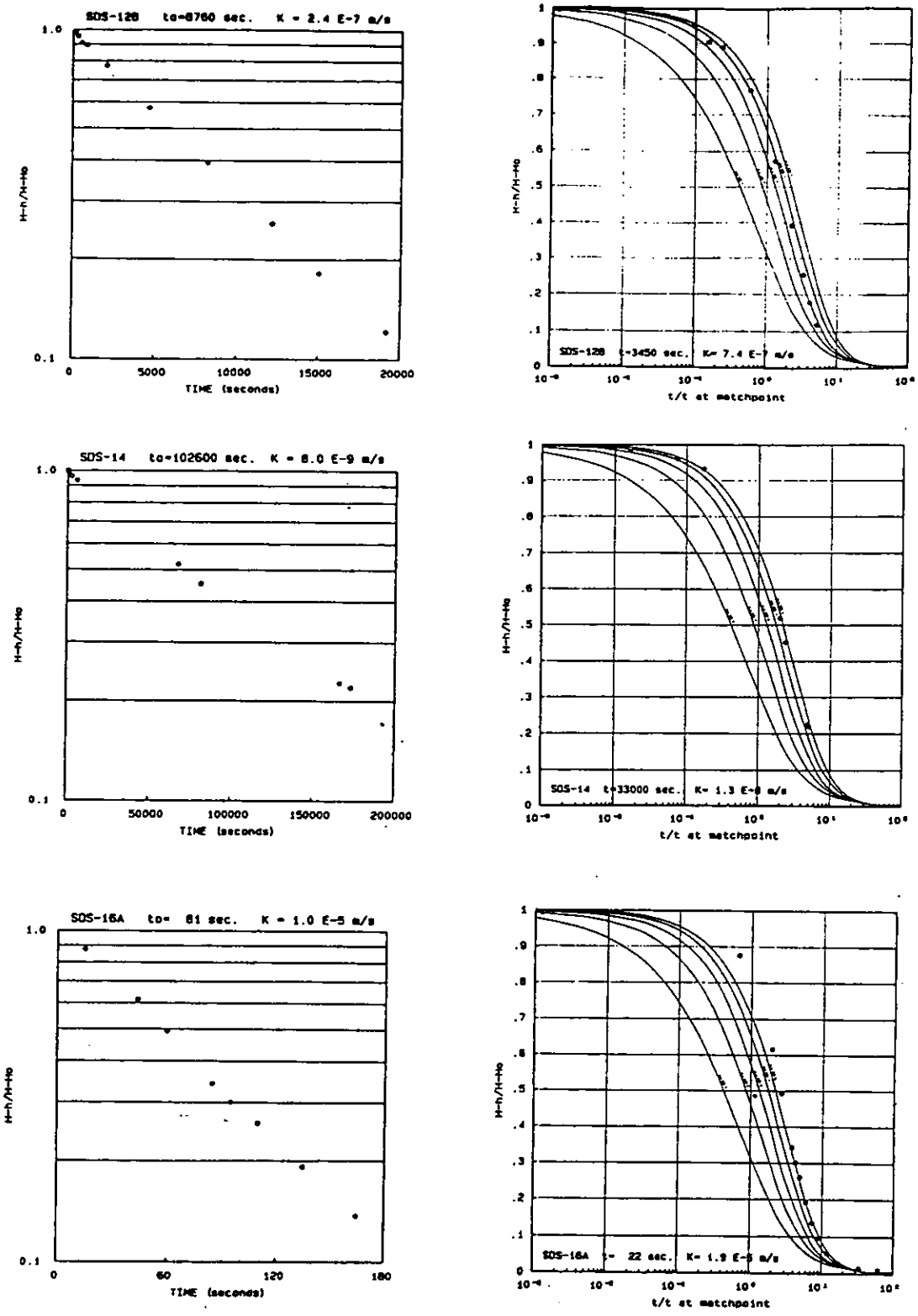

Figure A-4c Field Hydraulic Measurements (INTERA, June 1986 Data Plots)

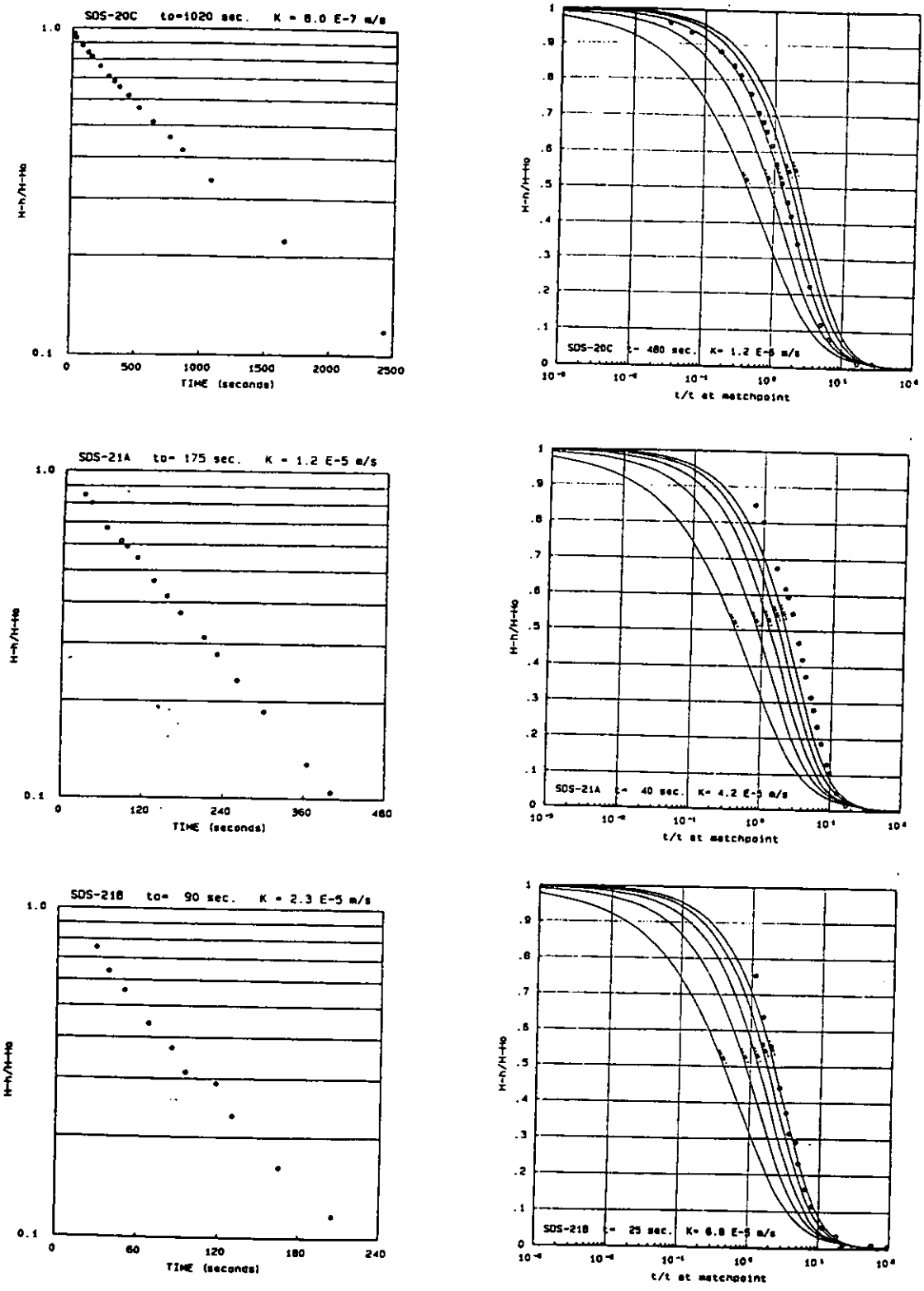

Figure A-4d Field Hydraulic Measurements (INTERA, June 1985 Data Plots)

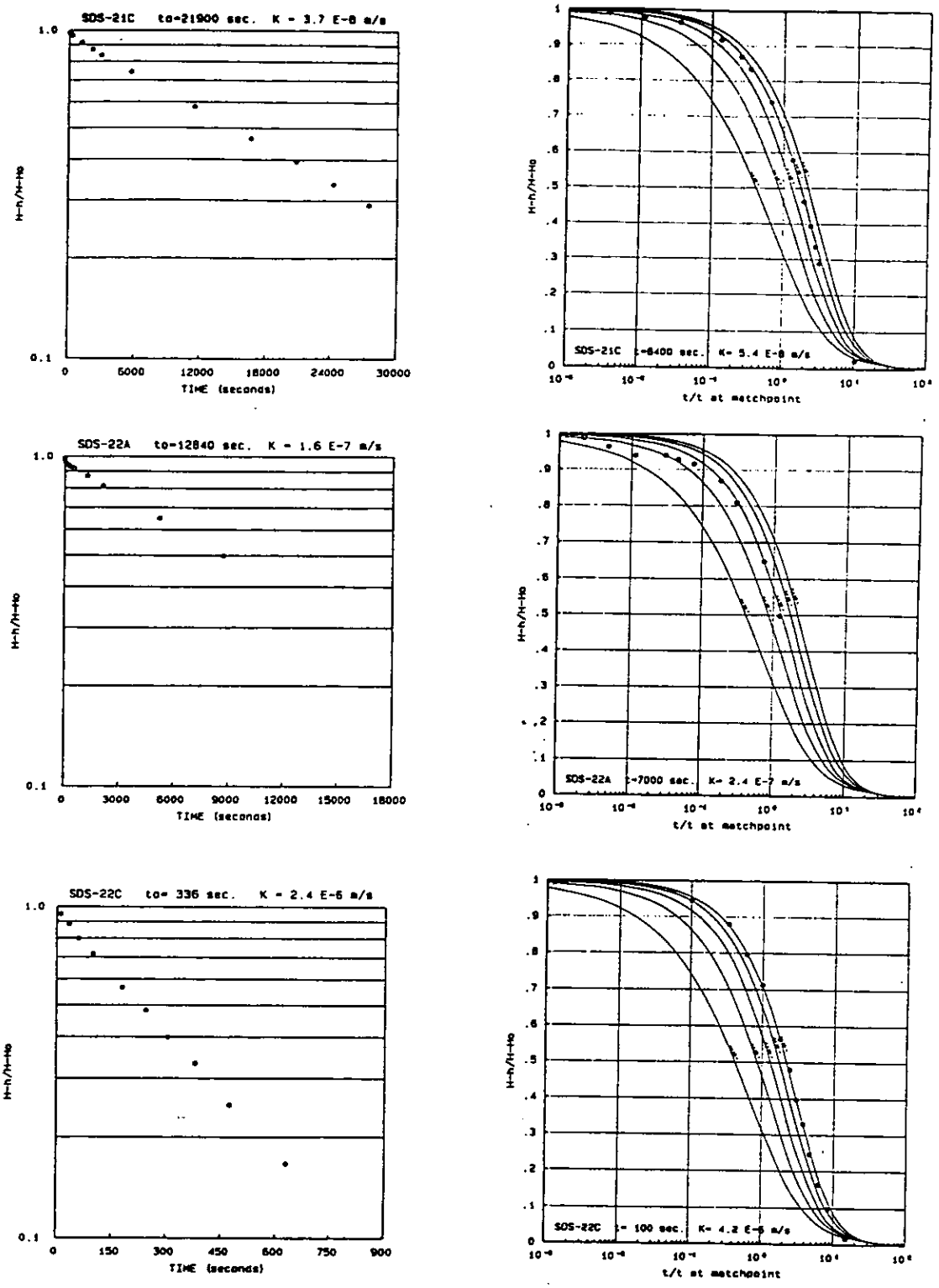

Figure A-4e Field Hydraulic Measurements (INTERA, June 1985 Data Plots)

BOREHOLE NUMBER	FORMATION SCREENED	ELEVATION TOP CASING (m asl)	SCREEN BOTTOM (m asl)	SCREEN LENGTH (m)	FEBRUARY 1982 (ft bs)	MARCH 1982 (ft bs)	APRIL 1982 (ft bs)	JULY 1982 (ft bs)	AUGUST 1982 (ft bs)	SEPTEMBER 1982 (ft bs)	OCTOBER 1982 (ft bs)	DECEMBER 1982 (ft bs)
SDS-1	Barnwell ?	90.00	63.7 ?	6.1 ?	67.85	68.20	68.01	67.57	67.20	66.75	66.34	65.95
SDS-2	Barnwell	88.27	65.71	6.1	61.26	61.25	61.15	60.86	60.59	60.44	60.21	60.00
SDS-3	Barnwell	89.15	64.16	6.1	57.57	57.26	57.03	56.70	56.45	56.08	55.77	55.85
SDS-4	McBean	78.45	56.51	6.1	26.11	25.96	26.82	26.01	25.55	25.22	25.25	25.50
SDS-4A	Barnwell	78.52	69.62	1.5	25.99	25.67	26.58	26.02	25.82	25.21	25.25	25.46
SDS-5	Barnwell	88.33	66.91	6.1	56.02	56.05	55.75	55.50	55.18	54.71	54.42	54.45
SDS-6	Barnwell	88.39	66.11	6.1	62.97	63.25	63.36	62.97	62.82	62.27	62.02	61.60
SDS-7A	Congaree	84.99	22.86	1.5	107.70	107.70	107.50	108.21	107.90	108.18	108.55	108.15
SDS-7B	McBean	84.73	41.24	1.5	71.60	71.36	71.39	71.15	71.15	70.41	70.49	70.80
SDS-7C	McBean	84.48	56.14	1.5	64.68	64.66	64.60	64.16	63.86	63.29	62.98	62.64
SDS-7D	McBean	84.49	62.67	1.5	62.70	62.96	62.82	62.30	62.10	61.52	61.06	61.10
SDS-8	McBean	82.94	61.54	1.5	55.51	55.56	55.49	55.00	54.96	54.27	54.45	53.52
SDS-9	Barnwell	90.13	68.00	1.5	58.84	58.85	58.61	58.07	57.74	57.74	57.03	56.99
SDS-10	Barnwell	89.98	68.79	6.4	59.45	59.57	59.36	58.81	58.40	58.10	57.86	57.34
SDS-11	Barnwell	88.97	64.84	6.1	58.81	58.92	58.76	58.47	58.12	57.81	57.40	57.38
SDS-12A	Congaree	84.91	41.57	1.5	110.62	110.66	110.58	111.00	111.43	111.46	111.73	111.45
SDS-12B	McBean	84.94	56.91	1.5	61.16	61.22	61.12	60.85	60.70	60.35	60.09	60.08
SDS-12C	McBean	84.16	62.82	1.5	60.92	60.96	60.80	60.28	60.22	60.01	59.85	59.70
SDS-13	McBean ?	84.57	62.30	6.1	68.33	68.28	68.21	68.05	68.00	67.79	67.73	67.77
SDS-14	McBean ?	81.47	61.17	6.1	11.13	11.16	11.23	18.35	10.00	10.82	13.05	25.93
SDS-14A	Barnwell	82.60	77.05	6.1	10.40	10.54	10.83	12.40	9.65	10.61	11.90	13.40
SDS-15	Barnwell	86.84	64.62	6.1	60.31	60.25	60.20	59.91	59.23	59.48	59.28	59.16
SDS-16A	Congaree	71.41	?	1.5								
SDS-16B	Congaree	71.41	?	1.5								
SDS-16C	McBean	71.41	56.52	6.1	34.83	34.70	34.72	34.88	34.49	34.20	34.24	34.44
SDS-17	McB./Bw.	82.69	59.92	6.1	48.77	48.72	48.51	48.07	47.86	47.65	47.75	47.35
SDS-18	Barnwell	78.91	68.7 ?	6.1	dry	dry	dry	dry	dry	dry	dry	dry
SDS-18A	McBean	78.91	62.79	6.1								
SDS-19	McBean	71.96	58.77	6.1	29.08	28.05	28.91	29.22	29.08	28.57	28.75	29.02
SDS-20A	Congaree	79.80	?	?								
SDS-20B	McBean	79.80	?	?								
SDS-20C	McBean	79.81	?	?								
SDS-21A	Congaree	76.50	?	?								
SDS-21B	McBean	76.44	?	?								
SDS-21C	McBean	76.44	?	?								
SDS-22A	McBean ?	86.35	?	?								
SDS-22B	McBean	86.32	?	?								
SDS-22C	McBean	86.29	?	?								

m asl : Meters above mean sea level
ft bs : feet below surface

Table A-1a Water Level Measurements at Z-Area (in feet below top of casing, 1985)

BOREHOLE NUMBER	FORMATION SCREENED	ELEVATION TOP CASING (m asl)	SCREEN BOTTOM (m asl)	SCREEN LENGTH (m)	MARCH 1984 (ft bs)	APRIL 1984 (ft bs)	MAY 1984 (ft bs)	JUNE 1984 (ft bs)	JULY 1984 (ft bs)	AUGUST 1984 (ft bs)	SEPTEMBER 1984 (ft bs)	OCTOBER 1984 (ft bs)	NOVEMBER 1984 (ft bs)	DECEMBER 1984 (ft bs)
SDS-1	Barnwell ?	90.00	63.7 ?	6.1 ?	44.45	44.15	42.28	60.70	60.25	59.50	59.23	59.62	59.74	59.75
SDS-2	Barnwell	89.37	65.71	6.1	59.00	58.86	57.97	57.12	56.85	56.23	56.28	55.90	56.05	56.28
SDS-3	Barnwell	89.15	64.16	6.1	54.06	53.43	52.08	51.52	51.39	51.23	51.33	51.82	52.10	52.39
SDS-4	McBean	78.45	56.51	6.1	22.89	22.50	21.20	21.62	21.45	21.58	22.02	22.60	23.16	23.67
SDS-4A	Barnwell	78.52	69.62	1.5	23.06	22.41	21.05	21.52	21.40	21.45	21.98	22.54	23.20	23.70
SDS-5	Barnwell	88.33	66.51	6.1	54.05	53.28	51.70	51.78	51.42	51.00	50.87	51.08	51.27	51.63
SDS-6	Barnwell	88.39	66.11	6.1	60.63	60.52	58.60	57.85	57.51	57.14	57.00	57.05	57.22	57.28
SDS-7A	Congaree	84.99	22.86	1.5	107.53	107.73	107.55	107.25	107.81	107.28	107.67	107.65	106.80	106.25
SDS-7B	McBean	84.73	41.24	1.5	76.28	64.06	67.25	66.15	66.23	65.80	65.91	66.33	66.22	66.88
SDS-7C	McBean	84.48	56.14	1.5	61.75	61.56	59.10	57.72	57.02	56.82	56.85	57.23	57.36	58.05
SDS-7D	McBean	84.49	62.67	1.5	60.25	60.00	57.45	55.25	55.00	54.87	54.98	55.35	55.41	55.95
SDS-8	McBean	82.94	61.54	1.5	52.56	51.05	48.10	50.50	49.16	48.08	48.13	48.55	48.84	47.20
SDS-9	Barnwell	90.13	68.00	1.5	55.03	54.75	53.70	53.05	52.95	52.15	52.18	52.26	52.75	53.33
SDS-10	Barnwell	89.98	68.79	6.4	55.94	55.71	54.75	53.90	53.40	52.24	52.28	52.95	53.30	53.82
SDS-11	Barnwell	88.97	66.84	6.1	55.51	55.15	54.10	53.35	53.13	52.35	52.38	52.42	53.05	53.43
SDS-12A	Congaree	84.91	41.57	1.5	110.58	110.79	110.37	110.61	110.35	110.00	110.13	110.22	109.36	109.34
SDS-12B	McBean	84.94	56.91	1.5	58.67	58.23	56.72	55.28	54.78	54.05	54.03	54.18	54.24	54.70
SDS-12C	McBean	84.16	62.82	1.5	58.76	57.89	56.41	55.00	54.55	53.60	53.60	54.58	53.75	54.15
SDS-13	McBean ?	84.57	62.30	6.1	67.08	66.75	65.55	64.30	64.10	64.03	64.07	64.50	64.30	64.55
SDS-14	McBean ?	81.47	61.17	6.1	14.15	12.30	?	36.40	36.05	36.13	37.09	37.77	37.97	39.54
SDS-14A	Barnwell	82.60	77.05	6.1	8.85	8.85	8.00	10.30	10.08	11.30	13.15	18.52	18.55	18.43
SDS-15	Barnwell	86.84	64.62	6.1	58.28	58.05	56.86	55.91	55.74	55.46	55.52	55.56	55.70	56.05
SDS-16A	Congaree	71.41	?	1.5										
SDS-16B	Congaree	71.41	?	1.5										
SDS-16C	McBean	71.41	56.52	6.1	12.83	33.72	32.78	32.75	31.02	31.40	31.71	32.24	32.12	32.20
SDS-17	McB./Bw.	82.69	59.92	6.1	44.55	45.04	44.93	44.19	44.07	42.00	42.10	43.22	42.78	43.10
SDS-18	Barnwell	78.91	66.7 ?	6.1	dry	dry	dry	dry	dry	dry	dry	dry	dry	dry
SDS-18A	McBean	78.91	61.79	6.1										
SDS-19	McBean	72.96	56.77	6.1	26.40	25.50	23.85	23.85	23.78	24.10	24.37	24.66	25.35	25.66
SDS-20A	Congaree	79.80	?	?										
SDS-20B	McBean	79.80	?	?										
SDS-20C	McBean	79.83	?	?										
SDS-21A	Congaree	76.50	?	?										
SDS-21B	McBean	76.44	?	?										
SDS-21C	McBean	76.44	?	?										
SDS-22A	McBean ?	86.35	?	?										
SDS-22B	McBean	86.33	?	?										
SDS-22C	McBean	86.29	?	?										

m asl : meters above mean sea level
ft bs : feet below surface

Table A-1b Water Level Measurements at Z-Area (in feet below top of casing, 1984)

BOREHOLE NUMBER	FORMATION SCREENED	ELEVATION TOP CASING (m asl)	SCREEN BOTTOM (m asl)	SCREEN LENGTH (m)	FEBRUARY 1985 (ft bs)	MARCH 1985 (ft bs)	APRIL 1985 (ft bs)	MAY 1985 (ft bs)	JUNE 1985 (ft bs)	JULY 1985 (ft bs)	OCTOBER 1985 (ft bs)
SDS-1	Barnwell ?	90.00	63.7 ?	6.1 ?	61.28	61.80	62.48	63.46	64.45	65.45	66.20
SDS-2	Barnwell	88.27	65.71	6.1	57.28	57.78	58.20	58.44	58.68	58.95	60.34
SDS-3	Barnwell	89.15	64.16	6.1	53.94	54.85	54.90	55.10	55.50	55.80	57.31
SDS-4	McBean	78.45	56.51	6.1	23.96	24.42	24.70	24.97	25.21	25.50	26.48
SDS-4A	Barnwell	78.52	69.62	1.5	24.13	24.45	24.75	24.96	25.16	25.40	26.70
SDS-5	Barnwell	88.33	66.51	6.1	53.00	53.35	53.60	54.10	54.55	55.05	56.17
SDS-6	Barnwell	88.39	66.11	6.1	58.20	58.25	58.98	59.60	60.20	60.80	61.90
SDS-7A	Congaree	84.99	22.86	1.5	106.93	106.70	107.00	107.15	107.28	107.45	108.09
SDS-7B	McBean	84.73	61.24	1.5	67.70	68.30	68.48	68.78	69.05	69.38	71.12
SDS-7C	McBean	84.48	56.14	1.5	59.60	59.85	60.25	60.80	61.30	61.84	63.85
SDS-7D	McBean	84.49	62.67	1.5	57.55	58.20	58.50	58.95	59.43	59.95	61.90
SDS-8	McBean	82.94	61.54	1.5	48.90	49.40	49.85	50.37	50.87	51.42	53.92
SDS-9	Barnwell	90.13	68.00	1.5	54.52	55.16	55.70	56.50	56.62	56.75	58.47
SDS-10	Barnwell	89.98	68.79	6.4	55.02	55.55	56.08	56.40	56.95	57.30	58.80
SDS-11	Barnwell	88.97	66.84	6.1	54.43	54.95	55.45	56.05	56.33	56.42	57.88
SDS-12A	Congaree	84.91	41.57	1.5	109.30	109.32	109.48	109.65	109.75	109.50	110.48
SDS-12B	McBean	84.94	56.91	1.5	56.10	65.42	57.00	57.40	57.80	58.22	60.06
SDS-12C	McBean	84.16	62.82	1.5	55.60	55.98	56.45	56.85	57.25	57.70	59.60
SDS-13	McBean ?	84.57	62.30	6.1	65.53	65.70	65.75	66.09	66.40	66.78	67.67
SDS-14	McBean ?	81.47	61.17	6.1	39.95	38.80	38.80	41.75	43.95	46.15	47.97
SDS-14A	Barnwell	82.60	77.05	6.1	11.25	11.88	13.00	15.80	17.15	18.40	18.70
SDS-15	Barnwell	86.84	64.62	6.1	56.85	57.47	57.25	15.58	58.35	58.58	59.80
SDS-16A	Congaree	71.41	?	1.5	60.00	59.85	59.80	60.00	60.23	60.50	61.20
SDS-16B	Congaree	71.41	?	1.5	62.30	62.30	62.20	62.30	62.50	62.85	63.30
SDS-16C	McBean	71.41	56.52	6.1	32.96	33.20	33.35	33.60	33.80	34.00	33.40
SDS-17	McB./Bw.	82.69	59.92	6.1	44.22	44.75	45.25	45.58	45.90	46.25	48.00
SDS-18	Barnwell	78.91	68.7 ?	6.1	dry	dry	dry	dry	dry	dry	dry
SDS-18A	McBean	78.91	62.79	6.1	50.90	51.27	51.55	51.60	52.05	52.38	54.24
SDS-19	McBean	71.96	58.77	6.1	26.03	26.40	26.75	27.38	28.00	28.65	29.19
SDS-20A	Congaree	79.80	?	?	97.28	97.48	97.25	97.40	97.32	97.65	98.22
SDS-20B	McBean	79.80	?	?	44.42	44.91	45.20	45.50	45.85	46.24	49.26
SDS-20C	McBean	79.83	?	?	45.20	46.05	46.50	46.55	46.95	47.50	47.95
SDS-21A	Congaree	76.50	?	?	90.35	90.38	90.40	90.50	90.81	91.15	91.22
SDS-21B	McBean	76.44	?	?	40.48	40.80	40.95	41.15	41.45	41.78	43.75
SDS-21C	McBean	76.44	?	?	41.38	41.45	41.60	41.80	42.05	42.35	42.82
SDS-22A	McBean ?	86.35	?	?	97.03	95.20	94.70	94.10	93.15	93.68	89.61
SDS-22B	McBean	86.32	?	?	50.85	51.30	51.60	51.95	52.27	52.68	60.22
SDS-22C	McBean	86.29	?	?	55.75	56.15	56.50	57.00	57.45	58.00	54.48

m asl : meters above mean sea level
ft bs : feet below surface

Table A-1c Water Level Measurements at Z-Area (in feet below top of casing, 1982)

BOREHOLE NUMBER	FORMATION SCREENED	ELEVATION TOP CASING (m asl)	SCREEN BOTTOM (m asl)	SCREEN LENGTH (m)	FEBRUARY 1982 (m asl)	MARCH 1982 (m asl)	APRIL 1982 (m asl)	JULY 1982 (m asl)	AUGUST 1982 (m asl)	SEPTEMBER 1982 (m asl)	OCTOBER 1982 (m asl)	DECEMBER 1982 (m asl)
SDS-1	Barnwell ?	90.00	61.7 ?	6.1 ?	69.32	69.21	69.27	69.40	69.52	69.65	69.81	69.90
SDS-2	Barnwell	88.27	65.71	6.1	69.60	69.60	69.63	69.73	69.80	69.85	69.92	69.98
SDS-3	Barnwell	89.15	64.16	6.1	71.60	71.70	71.77	71.87	71.94	72.06	72.15	72.13
SDS-4	McBean	78.45	56.51	6.1	70.49	70.54	70.37	70.52	70.66	70.76	70.75	70.68
SDS-4A	Barnwell	78.52	69.62	1.5	70.60	70.63	70.42	70.59	70.74	70.84	70.83	70.76
SDS-5	Barnwell	88.33	66.51	6.1	71.26	71.25	71.34	71.41	71.51	71.65	71.74	71.73
SDS-6	Barnwell	88.39	66.11	6.1	69.20	69.11	69.08	69.20	69.33	69.41	69.49	69.61
SDS-7A	Congaree	84.99	22.86	1.5	52.16	52.16	52.33	53.01	52.10	52.02	51.90	52.03
SDS-7B	McBean	84.73	41.24	1.5	62.91	62.98	62.97	62.98	63.04	63.27	63.24	63.24
SDS-7C	McBean	84.48	56.14	1.5	64.77	64.77	64.79	64.92	65.02	65.19	65.28	65.33
SDS-7D	McBean	84.49	62.67	1.5	65.58	65.50	65.34	65.50	65.56	65.74	65.88	65.87
SDS-8	McBean	82.94	61.54	1.5	66.02	66.01	66.03	66.18	66.31	66.40	66.34	66.63
SDS-9	Barnwell	90.13	68.00	1.5	72.20	72.19	72.26	72.43	72.53	72.53	72.75	72.76
SDS-10	Barnwell	89.98	68.79	6.4	71.86	71.82	71.89	72.05	72.18	72.25	72.34	72.50
SDS-11	Barnwell	88.97	66.84	6.1	71.04	71.01	71.06	71.15	71.26	71.35	71.47	71.48
SDS-12A	Congaree	84.91	61.57	1.5	51.19	51.18	51.21	51.08	50.95	50.94	50.85	50.94
SDS-12B	McBean	84.94	56.91	1.5	66.29	66.28	66.31	66.39	66.44	66.55	66.62	66.61
SDS-12C	McBean	84.16	62.82	1.5	65.59	65.58	65.63	65.79	65.77	65.87	65.92	65.96
SDS-13	McBean ?	84.57	62.30	6.1	63.74	63.76	63.78	63.83	63.84	63.91	63.93	63.91
SDS-14	McBean ?	81.47	61.17	6.1	78.08	78.07	78.05	75.88	78.42	78.17	77.80	73.57
SDS-14A	Barnwell	82.60	77.05	6.1	79.43	79.39	79.30	78.82	79.66	79.37	79.09	78.52
SDS-15	Barnwell	86.84	64.62	6.1	68.46	68.48	68.49	68.56	68.79	68.71	68.77	68.81
SDS-16A	Congaree	71.41	?	1.5								
SDS-16B	Congaree	71.41	?	1.5								
SDS-16C	McBean	71.41	56.52	6.1	60.79	60.83	60.83	60.78	60.90	60.99	60.97	60.91
SDS-17	McB./Bw.	82.69	59.92	6.1	67.82	67.84	67.90	68.04	68.10	68.17	68.14	68.29
SDS-18	Barnwell	78.91	68.7 ?	6.1	dry	dry	dry	dry	dry	dry	dry	dry
SDS-18A	McBean	78.91	62.79	6.1								
SDS-19	McBean	71.96	58.77	6.1	63.10	63.41	63.15	63.05	63.10	63.25	63.20	63.11
SDS-20A	Congaree	79.80	?	?								
SDS-20B	McBean	79.80	?	?								
SDS-20C	McBean	79.83	?	?								
SDS-21A	Congaree	76.50	?	?								
SDS-21B	McBean	76.44	?	?								
SDS-21C	McBean	76.44	?	?								
SDS-22A	McBean ?	86.35	?	?								
SDS-22B	McBean	86.32	?	?								
SDS-22C	McBean	86.29	?	?								

m asl : meters above mean sea level
ft bs : feet below surface

Table A-1d Water Level Measurements at Z-Area (in meters above sea level, 1982)

BOREHOLE NUMBER	FORMATION SCREENED	ELEVATION TOP CASING [m asl]	SCREEN BOTTOM [m asl]	SCREEN LENGTH [m]	MARCH 1984 [m asl]	APRIL 1984 [m asl]	MAY 1984 [m asl]	JUNE 1984 [m asl]	JULY 1984 [m asl]	AUGUST 1984 [m asl]	SEPTEMBER 1984 [m asl]	OCTOBER 1984 [m asl]	NOVEMBER 1984 [m asl]	DECEMBER 1984 [m asl]
SDS-1	Barnwell ?	90.00	83.7 ?	6.1 ?	70.36	70.45	71.02	71.50	71.64	71.86	71.95	71.83	71.79	71.79
SDS-2	Barnwell	88.27	85.71	6.1	70.29	70.33	70.60	70.86	70.94	71.13	71.13	71.23	71.19	71.13
SDS-3	Barnwell	89.15	84.16	6.1	72.67	72.86	73.28	73.45	73.49	73.54	73.50	73.38	73.27	73.13
SDS-4	McBean	78.45	56.51	6.1	71.47	71.59	71.59	71.86	71.91	71.87	71.74	71.56	71.39	71.24
SDS-4A	Barnwell	78.52	69.62	1.5	71.49	71.69	72.10	71.96	72.00	71.98	71.82	71.65	71.45	71.30
SDS-5	Barnwell	88.33	66.51	6.1	71.86	72.09	72.27	72.55	72.66	72.79	72.82	72.76	72.70	72.59
SDS-6	Congaree	88.39	66.11	6.1	69.91	69.94	70.47	70.76	70.86	70.97	71.02	71.00	70.95	70.93
SDS-7A	McBean	84.99	22.86	1.5	52.21	52.15	52.21	52.30	52.13	52.29	52.17	52.18	52.44	52.60
SDS-7B	McBean	84.73	41.24	1.5	61.48	65.20	64.23	64.57	64.34	64.67	64.64	64.51	64.55	64.34
SDS-7C	McBean	84.48	56.14	1.5	65.66	65.72	66.47	67.01	67.10	67.16	67.15	67.06	67.00	66.79
SDS-7D	McBean	84.49	62.67	1.5	66.13	66.20	66.98	67.62	67.73	67.77	67.74	67.62	67.60	67.44
SDS-8	Barnwell	82.84	61.54	1.5	66.82	66.20	66.28	67.55	68.07	68.89	68.88	68.75	68.66	68.55
SDS-10	Barnwell	90.13	68.00	1.5	73.36	67.39	68.28	67.55	68.89	74.23	74.23	74.20	74.05	73.88
SDS-11	Barnwell	89.98	68.79	6.4	72.93	73.44	73.76	73.96	73.99	74.06	74.05	73.84	73.73	73.58
SDS-12A	Congaree	88.97	66.84	6.1	72.05	73.00	73.39	73.55	73.70	73.01	73.00	72.99	72.80	72.66
SDS-12B	McBean	84.91	41.57	1.5	51.21	72.16	73.48	72.71	72.78	73.01	73.00	72.99	72.80	72.66
SDS-12C	McBean	84.84	56.91	1.5	67.06	51.14	51.27	51.20	51.28	51.38	51.34	51.31	51.58	51.58
SDS-13	McBean	84.16	62.82	1.5	66.25	67.19	67.65	68.09	68.24	68.47	68.47	68.43	68.41	68.27
SDS-14	McBean ?	84.57	62.30	6.1	64.13	66.52	66.97	67.40	67.53	67.82	70.87	67.52	67.74	67.66
SDS-14A	Barnwell	81.47	61.17	6.1	77.16	64.22	64.59	64.97	65.03	65.05	65.04	64.91	64.97	64.90
SDS-15	Barnwell	82.60	77.05	6.1	78.90	78.90	80.16	70.38	70.48	70.46	70.16	69.96	69.90	69.43
SDS-16A	Congaree	86.84	64.63	6.1	69.06	69.15	69.51	69.80	79.53	79.16	78.59	76.96	76.95	76.98
SDS-16B	Congaree	71.61	?	1.5					69.84	69.94	69.92	69.91	69.86	69.76
SDS-16C	McBean	71.41	?	1.5										
SDS-17	McB./Bw.	82.69	56.52	6.1	61.40	61.13	61.42	61.43	61.96	61.84	61.74	61.58	61.62	61.60
SDS-18	Barnwell	78.81	59.92	6.1	69.11	68.96	69.00	69.22	69.26	69.89	69.86	69.82	69.65	69.55
SDS-18A	McBean	78.91	69.7 ?	6.1	dry	dry	dry	dry	dry	dry	dry	dry	dry	dry
SDS-19	McBean	71.96	62.79	6.1										
SDS-20A	Congaree	79.80	58.77	6.1	63.91	64.19	64.69	64.69	64.71	64.61	64.53	64.44	64.23	64.14
SDS-20B	McBean	79.80	?	?										
SDS-20C	McBean	79.83	?	?										
SDS-21A	Congaree	76.50	?	?										
SDS-21B	McBean	76.44	?	?										
SDS-21C	McBean	76.44	?	?										
SDS-22A	McBean ?	86.35	?	?										
SDS-22B	McBean	86.32	?	?										
SDS-22C	McBean	86.29	?	?										

m asl : meters above mean sea level
ft bs : feet below surface

Table A-1e Water Level Measurements at Z-Area (in meters above sea level, 1984)

BOREHOLE NUMBER	FORMATION SCREENED	ELEVATION TOP CASING [m asl]	SCREEN BOTTOM [m asl]	SCREEN LENGTH [m]	FEBRUARY 1985 [m asl]	MARCH 1985 [m asl]	APRIL 1985 [m asl]	MAY 1985 [m asl]	JUNE 1985 [m asl]	JULY 1985 [m asl]	OCTOBER 1985 [m asl]
SDS-1	Barnwell ?	90.00	61.7 ?	6.1 ?	71.32	71.16	70.96	70.66	70.36	70.05	69.82
SDS-2	Barnwell	88.27	65.71	6.1	70.81	70.66	70.53	70.46	70.38	70.30	69.88
SDS-3	Barnwell	89.15	64.16	6.1	72.71	72.52	72.42	72.33	72.23	72.14	71.68
SDS-4	McBean	78.45	56.51	6.1	71.14	71.01	70.92	70.84	70.77	70.68	70.38
SDS-4A	Barnwell	78.52	69.62	1.5	71.17	71.07	70.98	70.91	70.85	70.78	70.38
SDS-5	Barnwell	88.33	66.51	6.1	72.18	72.07	71.99	71.84	71.70	71.55	71.21
SDS-6	Barnwell	88.39	66.11	6.1	70.65	70.64	70.41	70.22	70.04	69.86	69.64
SDS-7A	Congaree	84.99	22.86	1.5	52.40	52.47	52.38	52.33	52.29	52.34	52.04
SDS-7B	McBean	84.73	41.24	1.5	64.10	63.94	63.86	63.77	63.68	63.58	63.05
SDS-7C	McBean	84.48	56.14	1.5	66.31	66.24	66.12	65.95	65.80	65.63	65.11
SDS-7D	McBean	84.49	62.67	1.5	66.95	66.75	66.66	66.52	66.38	66.22	65.62
SDS-8	McBean	82.94	61.54	1.5	68.04	67.68	67.75	67.59	67.43	67.27	66.51
SDS-9	Barnwell	90.13	68.00	1.5	73.31	73.32	73.15	72.91	72.87	72.83	72.31
SDS-10	Barnwell	89.98	68.79	6.4	73.21	73.05	72.89	72.79	72.62	72.51	72.06
SDS-11	Barnwell	88.97	66.84	6.1	72.38	72.22	72.07	71.89	71.83	71.77	71.33
SDS-12A	Congaree	84.91	41.57	1.5	51.60	51.62	51.54	51.49	51.46	51.53	51.24
SDS-12B	McBean	84.94	56.91	1.5	67.84	65.00	67.57	67.44	67.32	67.19	66.61
SDS-12C	McBean	84.16	61.82	1.5	67.21	67.10	66.95	66.83	66.71	66.57	65.93
SDS-13	McBean ?	84.57	62.30	6.1	64.60	64.54	64.53	64.43	64.33	64.22	63.88
SDS-14	McBean ?	81.47	61.17	6.1	69.29	69.64	69.64	68.74	68.07	67.40	66.85
SDS-14A	Barnwell	82.60	77.05	6.1	79.17	78.98	78.64	77.78	77.37	76.93	76.90
SDS-15	Barnwell	86.84	64.62	6.1	69.51	69.32	69.39	82.09	69.05	68.98	68.61
SDS-16A	Congaree	71.41	?	1.5	53.12	53.17	53.18	53.12	53.05	52.97	52.76
SDS-16B	Congaree	71.41	?	1.5	52.42	52.45	52.45	52.42	52.36	52.25	52.12
SDS-16C	McBean	71.41	56.52	6.1	61.36	61.29	61.24	61.17	61.11	61.05	60.62
SDS-17	McB./Bw.	82.69	59.93	6.1	69.21	69.05	68.90	68.80	68.70	68.59	68.06
SDS-18	Barnwell	78.91	68.7 ?	6.1	dry	dry	dry	dry	dry	dry	dry
SDS-18A	McBean	78.91	62.79	6.1	63.40	63.28	63.20	63.12	63.05	62.94	62.36
SDS-19	McBean	71.96	58.77	6.1	64.03	63.81	63.81	63.61	63.43	63.23	63.06
SDS-20A	Congaree	79.80	?	?	50.15	50.09	50.16	50.11	50.14	50.04	49.86
SDS-20B	McBean	79.80	?	?	66.26	66.11	66.02	65.93	65.82	65.71	64.79
SDS-20C	McBean	79.83	?	?	66.05	65.79	65.66	65.44	65.32	65.35	65.21
SDS-21A	Congaree	76.50	?	?	48.96	48.95	48.95	48.92	48.82	48.72	48.70
SDS-21B	McBean	76.44	?	?	64.10	64.00	63.96	63.90	63.81	63.71	63.10
SDS-21C	McBean	76.44	?	?	63.83	63.81	63.76	63.70	63.62	63.53	63.39
SDS-22A	McBean ?	86.35	?	?	56.78	57.33	57.49	57.67	57.96	57.80	59.04
SDS-22B	McBean	86.32	?	?	70.82	70.68	70.59	70.49	70.39	70.26	67.96
SDS-22C	McBean	86.29	?	?	69.30	69.18	69.07	68.92	68.78	68.61	68.48

m asl : meters above mean sea level
ft bs : feet below surface

Table A-1f Water Level Measurements at Z-Area (in meters above sea level, 1985)

BOREHOLE NUMBER	FORMATION SCREENED	ELEVATION TOP CASING [m asl]	SCREEN BOTTOM [m asl]	SCREEN LENGTH [m]	NUMBER OF READINGS	MINIMUM [ft bs]	MAXIMUM [ft bs]	MINIMUM [m asl]	MAXIMUM [m asl]	MEAN [m asl]	DIFFERENCE MAX.-MIN. [m]	INTERA JUNE 85 [m asl]
SDS-1	Barnwell	90.00	83.7 ?	6.1	25	68.20	59.23	69.21	71.95	70.58	2.73	
SDS-2	Barnwell	88.37	65.71	6.1	25	61.26	55.90	69.60	71.33	70.40	1.63	
SDS-3	Barnwell	89.15	64.16	6.1	25	57.57	51.23	71.60	73.54	72.55	1.93	dry
SDS-4	McBean	78.45	56.51	6.1	25	26.52	21.20	70.37	71.99	71.09	1.62	dry
SDS-4A	Barnwell	78.52	69.42	1.5	25	26.70	21.05	70.38	72.10	71.16	1.72	dry
SDS-5	Barnwell	88.33	66.51	6.1	25	56.17	50.87	71.21	72.82	71.98	1.62	dry
SDS-6	Barnwell	88.39	66.11	6.1	25	63.36	57.00	69.08	71.02	70.11	1.94	dry
SDS-7A	Congaree	84.89	23.86	1.5	26	108.55	106.25	51.90	52.60	52.22	0.70	52.28
SDS-7B	McBean	84.73	41.24	1.5	25	76.28	64.06	61.48	65.20	63.73	3.72	
SDS-7C	McBean	84.48	56.14	1.5	26	64.68	56.82	64.77	67.16	65.93	2.40	65.75
SDS-7D	McBean	84.49	62.67	1.5	25	62.98	54.87	65.30	67.77	66.50	2.47	dry
SDS-8	McBean	82.94	61.54	1.5	25	55.36	46.08	66.01	68.89	67.40	2.89	dry
SDS-9	Barnwell	90.13	68.00	1.5	25	58.83	52.15	72.19	74.23	73.19	2.04	dry
SDS-10	Barnwell	89.98	68.79	6.4	25	59.57	52.24	71.82	74.06	72.87	2.23	dry
SDS-11	Barnwell	88.97	66.84	6.1	25	58.92	52.35	71.01	73.01	72.00	2.00	dry
SDS-12A	Congaree	84.91	41.57	1.5	26	111.73	109.22	50.85	51.62	51.29	0.77	51.49
SDS-12B	McBean	84.94	56.91	1.5	26	63.42	54.03	65.00	68.47	67.23	3.47	67.28
SDS-12C	McBean	84.16	62.62	1.5	25	60.96	43.60	65.58	70.87	66.79	5.29	dry
SDS-13	McBean ?	84.57	62.30	6.1	25	68.32	64.03	63.74	65.05	64.36	1.31	dry
SDS-14	McBean ?	81.47	61.17	6.1	25	47.97	10.00	66.85	78.42	72.82	11.57	77.20
SDS-14A	Barnwell	82.60	77.05	6.1	25	18.70	8.00	76.90	80.16	78.68	3.26	dry
SDS-15	Barnwell	86.84	64.62	6.1	25	60.31	15.58	69.46	82.09	69.71	13.63	
SDS-16A	Congaree	71.41	?	1.5	0	61.20	59.80	52.76	53.18	53.04	0.43	52.98
SDS-16B	Congaree	71.41	?	1.5	8	63.38	62.20	52.13	52.45	52.35	0.34	52.32
SDS-16C	McBean	71.41	56.53	6.1	25	35.40	31.02	60.62	61.96	61.22	1.34	dry
SDS-17	McB./Bw.	82.69	59.92	6.1	25	48.77	42.00	67.82	69.89	68.80	2.06	dry
SDS-18	Barnwell	78.91	68.7 ?	6.1	0							
SDS-18A	McBean	78.91	62.79	6.1	7	54.24	50.90	62.38	63.40	63.05	1.02	dry
SDS-19	McBean	71.96	56.77	6.1	25	29.22	23.78	63.05	64.71	63.78	1.66	dry
SDS-20A	Congaree	79.80	?	?	8	98.22	97.25	49.86	50.16	50.07	0.30	50.05
SDS-20B	McBean	79.80	?	?	8	49.26	44.42	64.79	66.26	65.80	1.48	65.75
SDS-20C	McBean	79.83	?	?	8	47.95	45.20	65.21	66.05	65.58	0.84	65.41
SDS-21A	Congaree	76.50	?	?	8	91.22	90.35	48.70	48.96	48.86	0.27	48.84
SDS-21B	McBean	76.44	?	?	8	43.75	40.48	63.10	64.10	63.80	1.00	63.79
SDS-21C	McBean	76.44	?	?	8	42.82	41.38	63.39	63.83	63.65	0.44	63.56
SDS-22A	McBean ?	86.35	?	?	8	97.03	89.61	56.78	59.04	57.79	2.26	58.23
SDS-22B	McBean	86.32	?	?	7	60.22	50.85	67.96	70.82	70.17	2.86	
SDS-22C	McBean	86.29	?	?	8	58.00	54.48	68.61	69.68	69.03	1.07	68.71

m asl : meters above mean sea level
ft bs : feet below surface

Table A-2 Water Level Measurements at Z-Area Summary and Data from INTERA (June, 1985)

Well Identifier	Screened Formation	Bottom of the Screen [m.a.s.l.]	Screen Length [m]	Hydraulic Conductivity [m/s] Cooper et al. (a)	Hvorslev (b)	Ratio a/b	Mean (a*b)x0.5
SDS-7A	Congaree	22.86	1.52	2.8×10^{-7}	1.3×10^{-7}	2.15	2.1×10^{-7}
SDS-7C	McBean	56.14	1.52	1.9×10^{-7}	6.8×10^{-8}	2.78	1.3×10^{-7}
SDS-12A	Congaree	41.57	1.52	2.8×10^{-6}	2.6×10^{-6}	1.08	2.7×10^{-6}
SDS-12B	McBean	56.91	1.52	7.4×10^{-7}	2.4×10^{-7}	3.08	4.9×10^{-7}
SDS-14	McBean (?)	61.17	6.10	1.3×10^{-8}	8.0×10^{-9}	1.63	1.1×10^{-8}
SDS-16A	Congaree (?)	?	1.52(?)	1.9×10^{-5}	1.0×10^{-5}	1.9	1.8×10^{-4}
SDS-16B	Congaree (?)	?	1.52(?)	4.6×10^{-5}	1.6×10^{-5}	2.88	3.1×10^{-5}
SDS-20A	Congaree (?)	?	1.52(?)	2.8×10^{-4} *	7.5×10^{-5}	3.73	1.8×10^{-4}
SDS-20B	McBean (?)	?	1.52(?)	2.8×10^{-4} *	7.3×10^{-5}	3.83	1.8×10^{-4}
SDS-20C	McBean (?)	?	6.10(?)	1.2×10^{-6}	8.0×10^{-7}	1.50	1.0×10^{-6}
SDS-21A	Congaree (?)	?	1.52(?)	4.2×10^{-5}	1.2×10^{-5}	2.50	2.7×10^{-5}
SDS-21B	McBean (?)	?	1.52(?)	6.8×10^{-5}	2.3×10^{-5}	2.96	4.6×10^{-5}
SDS-21C	McBean (?)	?	6.10(?)	5.4×10^{-8}	3.7×10^{-8}	1.46	4.6×10^{-8}
SDS-22A	Congaree (?)	?	1.52(?)	2.4×10^{-7}	1.6×10^{-7}	1.50	2.0×10^{-7}
SDS-22C	McBean (?)	?	6.10(?)	4.2×10^{-6}	2.4×10^{-6}	1.75	3.3×10^{-6}
					mean ratio =	2.38	

* indicates that type curve match was not highly reliable.

Table A-3 Hydraulic Conductivities Measured June 18-20 by INTERA Technologies (Piezometer data taken from d'Appolonia, 1981)

APPENDIX B

HCTM Documentation

B-1 THEORY AND TECHNICAL APPROACH

The Hydrology Contaminant Transport Model (HCTM) is intended to be a user-oriented, comprehensive tool for calculating ground water flow and transport of a contaminant dissolved in ground water and adsorbed on rock mass. The model consists basically of two parts. The first calculates the single phase flow of a slightly compressible liquid in a porous medium. The second part calculates movement and hydrodynamic dispersion of a contaminant flowing in the calculated velocity field.

Three-dimensional, rectangular cartesian grid (x,y,z) and two-dimensional, cylindrical grid (r,z) systems are provided as user options. The code can be used for one-dimensional linear or radial, and two-dimensional areal (horizontal) or cross-sectional (vertical) problems as well. One-dimensional radial and two-dimensional cylindrical coordinate systems are extremely well suited to single well interpretive or predictive calculations.

Major assumptions contained in the model are:

(a) Laminar flow. Darcy's law is satisfied.
(b) Single phase fluid.
(c) Constant fluid viscosity.
(d) Fluid density is a function of fluid pressure only.
(e) Hydrodynamic dispersion proportional to fluid velocity.
(f) System properties (porosity, permeability, thickness and elevation) vary with position. These properties can be specified for each grid block in the model.
(g) Boundary conditions allow natural water movement, recharge, and the location of injection, production and observation points anywhere within the system.

B-1.1 Model Equations

Let x, y, z be a Cartesian coordinate system and let z be the depth of a point below a horizontal reference plane. Then, the basic equation describing single-phase flow in a porous medium results from a combination of the continuity equation

$$- \nabla \cdot \rho \underline{u} - q' = \frac{\partial(\Phi\rho)}{\partial t} \qquad (1)$$

and Darcy's law in three dimensions

$$\underline{u} = - \frac{\underline{\underline{k}}}{\mu} \left(\nabla p - \frac{\rho g}{g_c} \nabla z\right) \qquad (2)$$

where g = acceleration due to gravity;
g_c = gravitational conversion factor;
k = permeability;
q' = fluid withdrawal rate per unit medium volume;
$\underline{u}$ = Darcy velocity vector;
μ = fluid viscosity;
Φ = porosity;
and ρ = fluid density.

The result is the basic flow equation

$$\nabla \cdot \frac{\rho \underline{\underline{k}}}{\mu} \left(\nabla p - \frac{\rho g}{g_c} \nabla z\right) - q' = \frac{\partial(\Phi\rho)}{\partial t} \qquad (3)$$

Fluid potential can be defined by

$$\Phi = \int_{p_d}^{p} \frac{dp}{\rho g} - z \qquad (4)$$

Now, assuming that $\Phi = \Phi(p)$ only, and $\rho = \rho(p)$ only, Equation (3) can be combined with Equation (4) and rewritten as

$$\nabla \cdot \frac{\underline{\underline{k}}\rho g}{\mu} \cdot \rho \nabla \Phi - q' = g\Phi\rho^2(c_w + c_R) \frac{\partial \Phi}{\partial t} \qquad (5)$$

where $c_w = \frac{1}{\rho} \frac{d\rho}{dp}$ - fluid compressibility

$c_R = \frac{1}{\Phi} \frac{d\Phi}{dp}$ - rock compressibility

or $$\nabla \cdot \underline{\underline{K}} \cdot \nabla \Phi - \left(\frac{q'}{\rho}\right) = s \frac{\partial \Phi}{\partial t} \qquad (6)$$

where $\underline{\underline{K}}$ = hydraulic conductivity tensor;
s = storage coefficient

A material balance for the dissolved contaminant results in the solute or concentration equation

$$-\bar{\nabla}.(\rho C\underline{u}) + \nabla.\rho \underline{\underline{E}} \nabla C - q'C - \Phi\lambda C\rho - \rho R_a' = \frac{\partial(\Phi\rho C)}{\partial t} \qquad (7)$$

where C = concentration;
$\underline{\underline{E}}$ = dispersivity tensor, includes hydrodynamic dispersion and molecular diffusion;

R_a' = rate of adsorption of contaminant

λ = rate of decay (reaction)

Since the fluid density is not a function of concentration, the concentration equation becomes

$$- \nabla.C\underline{u} + \nabla.\underline{\underline{E}}.\nabla C - \frac{q'}{\rho} C - \lambda\Phi C - R_a' = \Phi \frac{\partial C}{\partial t} \qquad (8)$$

An equation for the contaminant adsorbed on rock mass is

$$-\lambda\rho_R(1-\Phi)S + R_a' = \rho_R(1-\Phi) \frac{\partial S}{\partial t} \qquad (9)$$

where S = contaminant concentration on rock;
(contaminant adsorbed/mass of rock)

The term R_a' in Equations (8) and (9) is the rate of contaminant adsorption on rock and can be written as:

$$R_a' = \rho_R (1-\Phi) k_r (S_e-S) \qquad (10)$$

where k_r is the adsorption rate constant and S_e is the equilibrium concentration on rock. In this model, it is expressed as:

$$S_e = k_1 C^{k_2} \qquad (11)$$

where k_1 and k_2 are equilibrium constants. For an equilibrium sorption case, $k_r = \infty$. For a linear sorption case, $k_2 = 0$.

In the present model, the concentration S is expressed in terms of a pseudo-fluid concentration, C_s, as follows:

$$C_s = \frac{\rho_R(1-\phi)}{\phi} S \qquad (12)$$

and therefore

$$R_a' = k_r (C_{s_e} - C_s) \qquad (13)$$

Equations (6), (8) and (9) are the basic set of model equations, and they are subject to the following boundary conditions and constraints:

(a) Specified pressure and concentration at specified locations $p = p_b$ and $C = C_b$;
(b) Fluid injection and withdrawal wells at specified locations;
(c) Specified areally distributed recharge.

This set is a non-linear system of equations which must be solved numerically. These equations are solved by dividing the region of interest into a three-dimensional grid and developing finite-difference approximations for this grid. Once the region of interest is divided into grid blocks, finite-difference equations are developed whose solution closely approximates the solution of Equations (6), (8), and (9).

B-1.2 Finite-Difference Approximations

The finite-difference forms of the basic set of partial differential equations are:

Basic Flow Equation

$$\Delta T_w \Delta \Phi - q = \frac{sV}{\Delta t} \delta\Phi \qquad (14)$$

Dissolved Contaminant Equation

$$\Delta T_w C \Delta \Phi + \Delta T_E \Delta C - qC - \lambda VC - R_a = \frac{V}{\Delta t} \delta C \qquad (15)$$

Sorbed Contaminant Equation

$$-\lambda \rho_R (1-\Phi) S + k_r \Phi (C_{s_e} - C_s) = \rho_R (1-\Phi) \frac{\delta S}{\delta t} \qquad (16)$$

where the difference operators are defined by

$$\Delta T_w \Delta \Phi = \Delta_x (T_{wx} \Delta_x \Phi) + \Delta_y (T_{wy} \Delta_y \Phi) + \Delta_z (T_{wz} \Delta_z \Phi) \qquad (17)$$

with

$$\begin{aligned} \Delta_x (T_{wx} \Delta_x \Phi) = {} & T_{w,i+1/2,j,k} (\Phi_{i+1,j,k} - \Phi_{i,j,k}) \\ & - T_{w,i-1/2,j,k} (\Phi_{i,j,k} - \Phi_{i-1,j,k}) \end{aligned} \qquad (18)$$

and

$$\delta_x = x^{n+1} - x^n \qquad (19)$$

For a Cartestian geometry, the transmissibilities are defined as follows:

$$T_{w,i+1/2,j,k} = \frac{2\Delta y_j \Delta z_k}{(\frac{\Delta x}{k_x})_i + (\frac{\Delta x}{k_x})_{i+1}} \tag{20}$$

and

$$T_{E,i,j+1/2,k} = \frac{2\Delta x_i \Delta z_k}{(\frac{\Delta y}{E})_j + (\frac{\Delta y}{E})_{j+1}} \tag{21}$$

For radial geometry, the term

$$\frac{2\Delta y_i \Delta z_k}{\Delta x_i + \Delta x_{i+1}} \tag{22}$$

becomes

$$\frac{2\pi \Delta z_k}{\ln (\frac{r_{i+1}}{r_i})} \tag{23}$$

and the volume term in Equations (14) and (15) is written as $\pi \Delta r_i^2 z_k$.

The constituent dispersion tensor E, needs additional description. It is taken in the present model as dependent upon the hydrodynamic dispersivity. This dispersivity is a function of the local fluid velocity. Scheidegger (1961) has shown that for an isotropic porous medium, there can be no more than, two independent dispersivity factors. This requirement is essential so that the dispersion tensor is invariant under coordinate transformations. These two dispersivities are longitudinal, in the direction of flow, and transverse, perpendicular to flow. Generally, both are functions of the magnitude of the flow velocity. These values can be expressed as:

$$D_l = \alpha_l \underline{u}$$

and (24)

$$D_t = \alpha_t \underline{u}$$

When the velocity vector is divided into components along the coordinate axes, nine components of the dispersivity tensor occur. In the present model, the off-diagonal components of the hydrodynamic dispersivity tensor are neglected. The three diagonal components can be expressed as follows:

$$\begin{aligned} E_{xx} &= D_l \cos^2\theta\cos^2\psi + D_t \sin^2\theta\cos^2\psi + D_t \sin^2\psi \\ E_{yy} &= D_l \cos^2\theta\sin^2\psi + D_t \sin^2\theta\sin^2\psi + D_t \cos^2\psi \\ E_{zz} &= D_l \sin^2\theta + D_t \cos^2\theta \end{aligned} \qquad (25)$$

where

$$\theta = \tan^{-1} \frac{u_y}{u_z} \qquad (26)$$

and

$$\psi = \tan^{-1} \frac{u_z}{u_x^2 + u_x^2} \qquad (27)$$

The more general expressions for the dispersivity tensor, including the molecular diffusion, can be written as:

$$\underline{\underline{E}} = \underline{\underline{D}} + D_m \underline{\underline{I}} \qquad (28)$$

where D_m is the molecular diffusivity and $\underline{\underline{I}}$ is the unit tensor.

B-1.3 Point Tracking Method

The original contaminant transport equation, Equation (8), can be replaced as five ordinary differential equations given by:

$$\frac{dx}{dt} = \frac{u}{\Phi R_d} \tag{29}$$

$$\frac{dy}{dt} = \frac{v}{\Phi R_d} \tag{30}$$

$$\frac{dz}{dt} = \frac{w}{\Phi R_d} \tag{31}$$

$$\frac{dC}{dt} = -\lambda C \tag{32}$$

and $$\Phi \frac{dC}{dt} = \nabla \cdot \Phi E \nabla C \tag{33}$$

The above written equations and the decay are solved as follows:

(1) Initialize an array of points throughout the subregion of the grid system. Each point has the property of position (x,y,z) and concentration, C.

(2) Move the points over the time step, Δt, given by Equations (29), (30), and (31). The fluid velocity components come from the flow equation solution.

(3) Decay each particle concentration according to Equation (32).

(4) Calculate the grid block concentration from

$$\overline{C} = \Sigma C_{ijk}/n \quad \text{where } n = \text{number of points in grid block } ijk.$$

(5) Using this grid block concentration distribution, solve for the concentration change due to diffusion:

$$\delta C_{ijk} = \frac{\Delta t}{\Phi} \cdot \nabla \cdot \Phi E \nabla C$$

(6) Adjust each point concentration within a grid block by this δC.

(7) Repeat steps 2 through 6.

Step (5) above is always solved by a line-successive-overrelaxation (LSOR) technique.

B-2 CODE VERIFICATION

Several calculational tests were performed to verify the model. These tests are outlined as follows:

(1) Flow model tests
   (a) Cartesian coordinates
   (b) Radial coordinates

(2) Contaminant transport model tests
   (a) Linear equilibrium adsorption
      (i) Finite difference method
      (ii) Point tracking method
   (b) Non-linear equilibrium adsorption
   (c) Non-equilibrium kinetic adsorption

The results of these tests were compared with calculations from known analytical solutions to the model equations and/or previous work. This section includes details of the tests.

B-2.1 Flow Model Tests

Since the model has the option of using both cylindrical (r-z) and rectangular Cartesian (x,y,z) coordinates, both grid systems were checked. These runs were compared with the Ei - function (exponential integral) analytical solution to radial flow subject to a specified rate by letting the wellbore radius approach zero.

This solution has the form

$$p = \frac{g\mu}{4\pi kh}\left[-Ei\left(-\frac{\mu c r^2}{4kt}\right)\right] \qquad (34)$$

where $-Ei(y) = \int_y^{\infty} \frac{e^{-x}}{x}\, dx.$

Table B-1 gives the aquifer and fluid properties used in the tests. Table B-2 gives the two grid systems used in terms of block-centered positions where, in the rectangular system, $y_j = x_i$. The test was injection at $1.84 \times 10^{-4} m^3/sec$ of water for a one day period followed by a shut-in period of one day.

Table B-1 Aquifer and Fluid Properties for Flow Model Test

Aquifer

Conductivity	6.31×10^{-8} m/sec
Porosity	0.03
Compressibility	5.8×10^{-10}/Pa
Thickness	30.48 m
Initial Potential	20.3 m

Water

Viscosity	1.0×10^{-3} Pa-s
Compressibility	4.35×10^{-10}/Pa
Specific Weight	9800 Pa/m

Table B-2 Flow Test Grid Systems

Block i	Radial (r_i, m)	Rectangular (x_i, m)
Wellbore	.11	.11
1	.61	.61
2	.95	1.22
3	1.49	2.44
4	2.32	4.88
5	3.62	9.75
6	5.65	19.51
7	8.82	39.01
8	13.76	78.03
9	21.47	106.70
10	33.51	152.40
11	52.30	213.40
12	81.63	304.80
13	127.39	457.20
14	198.82	
15	310.30	
16	484.28	

Each grid system was compared with the analytical solution at two distances from the well. The first comparison was at the wellbore ($r = 0.114$ m) and the second at a distance of 13.7 m. Observation wells were placed in the appropriate blocks to make the comparison at 13.7 m. Since the well rates for these blocks are zero, no additional pressure drop from the grid block average is present and the well index calculation is not essential. However, this calculation is quite important for the injection well during the injection phase.

For the radial geometry, the additional pressure drop from the block center of 0.61 m down to the wellbore of .11 m requires a well index of $(6.28)(6.31 \times 10^{-8})(30.48)/\ln\ (.61/.11)$ or 7.05×10^{-6} m^2/sec. Since the problem is symmetrical, the well was placed in block (1,1,1) for the rectangular geometry and one-fourth of the injection rate was used. Also, one-fourth of the well index calculation for rectangular geometry was used.

Figures B-1 and B-2 plot the comparisons between the calculated and analytical solutions results at the two distances.

B-2.2 Contaminant Transport Model Tests

Three different sets of test runs were made to verify the contaminant transport model. The tests were designed to exercise the three different options the user has for modeling chemical adsorption.

B-2.2.1 Linear Equilibrium Adsorption Tests

As a user option, a finite-difference or a particle tracking method of solving the transport equation may be selected when a linear adsorption isotherm is being used. Each of these methods were tested and compared with each other as well as with the analytical solution by Lester et al. (1975) given below as

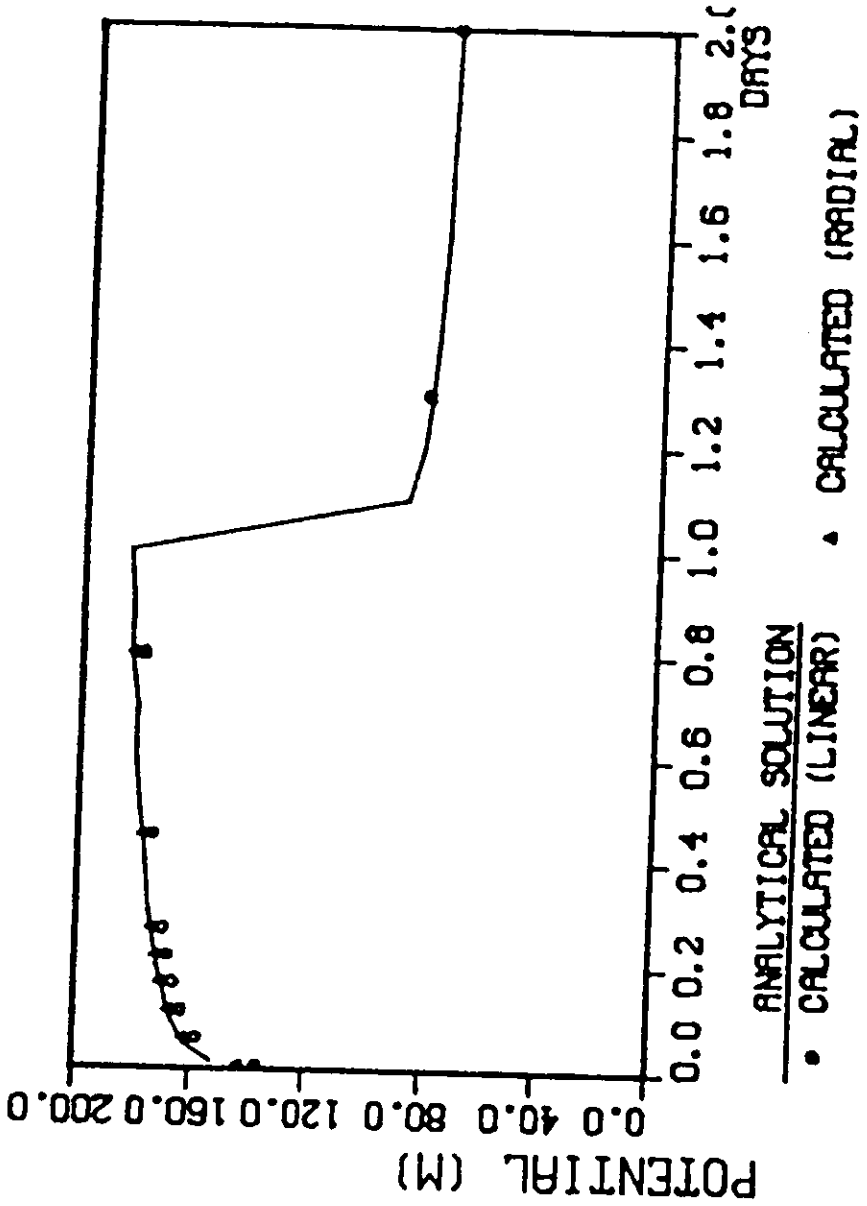

Figure B-1 Flow Model Test

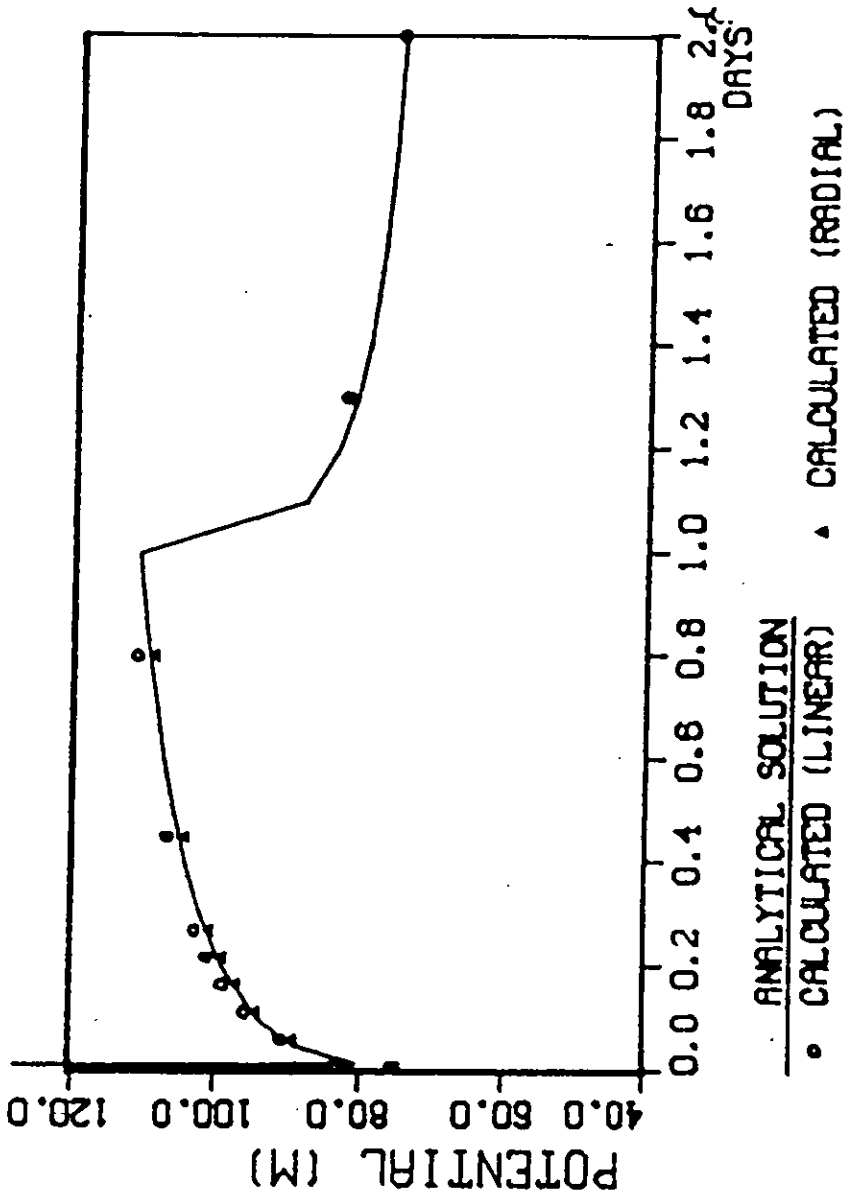

Figure B-2 Flow Model Test (R=13.7 M)

$$\frac{C}{Co} = \frac{1}{2} \exp(R\theta) \left[\operatorname{erfc}\left(\frac{\eta}{2}\frac{KP}{\theta} - \frac{P\theta}{4K}\right) + \exp(P\eta) \operatorname{erfc}\left(\frac{\eta}{2}\frac{KP}{\theta} + \frac{P\theta}{4K}\right)\right] \quad (35)$$

with boundary conditions of

$C = C_o \exp(-t)$	for $0 \leq t < T$	at $x = 0$
$C = 0$	for $t = 0$	at all x
$C = 0$	for $t > T$	at $x = 0$

where

- T = leach time
- P = VL/D
- R = L/V
- η = Z/L
- θ = tV/L

The source boundary is approximately the same as that in HCTM provided that the contaminant half life $T_{1/2} >> T$.

Table B-3 gives the data used as input to the model for this test. Fifty grid blocks were used with injection and production wells in grid blocks one and fifty, respectively. The flow rate was 3.5×10^{-5} m^3/sec.

Figure B-3 compares the breakthrough curves at 1000 m as calculated by each method of solution (finite-difference and point tracking) with the analytical solution.

Table B-3 Data for Linear Contaminant Transport Test

Aquifer

Length	1000 m
Porosity	.3
Compressibility	1.0×10^{-9}/Pa
Conductivity	1.76×10^{-4} m/sec

Fluid

Viscosity	.001 Pa-sec
Compressibility	1.0×10^{-9}/Pa
Specific Weight	9800 Pa/m

Contaminant

Dispersivity	10 m
Half Life	∞
Adsorption Coefficient, K_d	7.05×10^{-5} m^3/kg

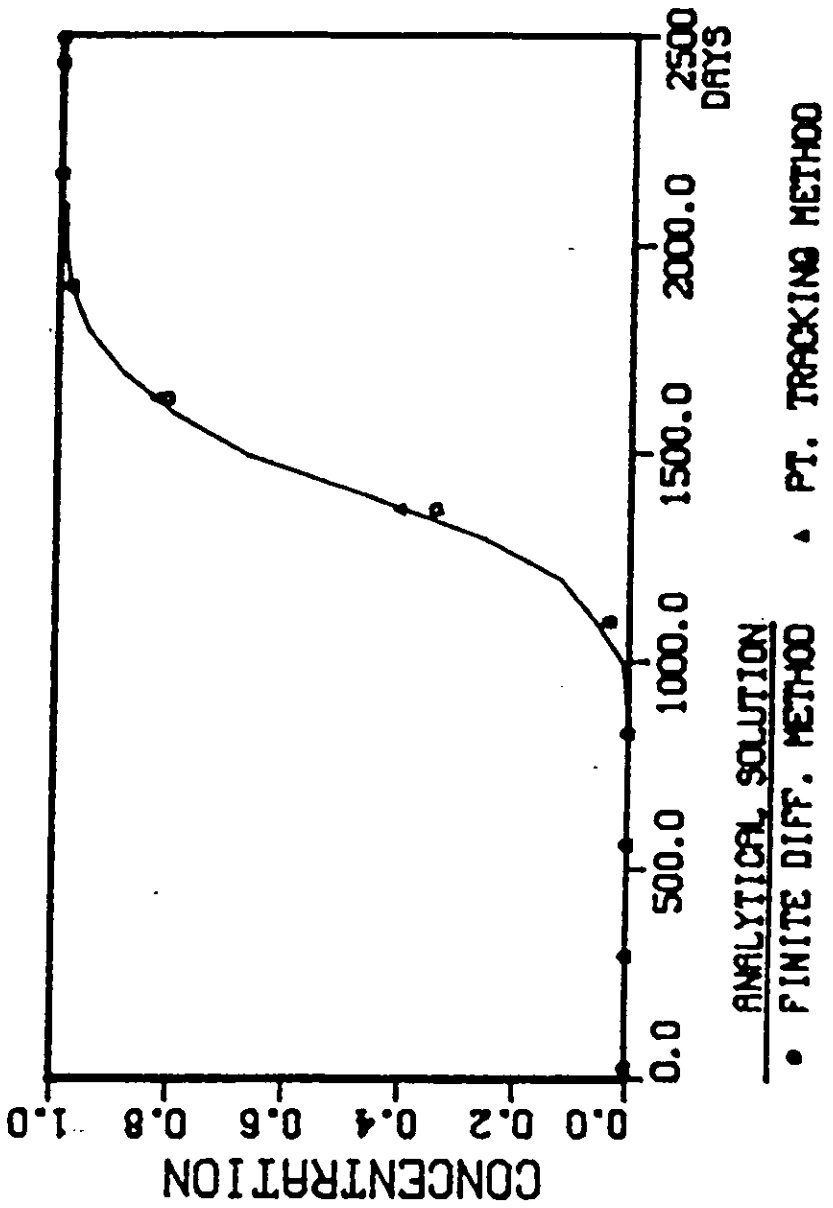

Figure B-3 Linear Adsorption Test

B-2.2.2 Non-linear Equilibrium Adsorption Tests

For the non-linear (Freundlich) adsorption isotherm of the form $C_{se} = k_1 C^{k_2}$, a series of tests were run varying the exponential coefficient, k_2. Since no analytical solutions are available for comparison when the adsorption isotherm is non-linear, these tests were designed to:

(1) reproduce the results obtained by previous investigators (Van Genuchten et al., 1979) and,
(2) observe the influence of varying the exponential coefficient on the slope of a solute pulse traveling through a soil column.

Table B-4 gives the pertinent physical data used for the test. A Darcy velocity of 1.85×10^{-6} m/sec was established again by using an injection and production well in the one-dimensional system. A contaminant concentration of 1.0 was maintained in the injected fluid for 1.25 days. A series of four test runs were made, varying the exponential (Freundlich) coefficient from 0.4 to 1.5.

Figure B-4 plots the results of the tests after a simulation time of 3 days. The results agree well with those obtained by the work previously referenced. As can be seen in the figure, the shape of the pulse is nearly symmetrical when the adsorption isotherm is linear (i.e., $k_2 = 1$). However, the more the exponential coefficient varies from unity, the more asymmetrical the solute distribution becomes. Since, when $k_2 < 1$, the rate of adsorption at lower concentrations is higher than at higher concentration, more material will be drawn from the soil solution towards the downstream adsorption sites. As the solution concentration increases and the rate of adsorption decreases, this causes the solution concentration to increase even faster, leading to the observed steep front. The reverse effect occurs when $k_2 > 1$, as can be seen from the test results.

Table B-4 Data for Non-linear Adsorption Tests

Soil Bulk Density	1.4×10^{3} kg/m^3
Porosity	0.4
K_d	1.43×10^{-4} m^3/kg
Diffusivity	3.47×10^{-8} m^2/sec

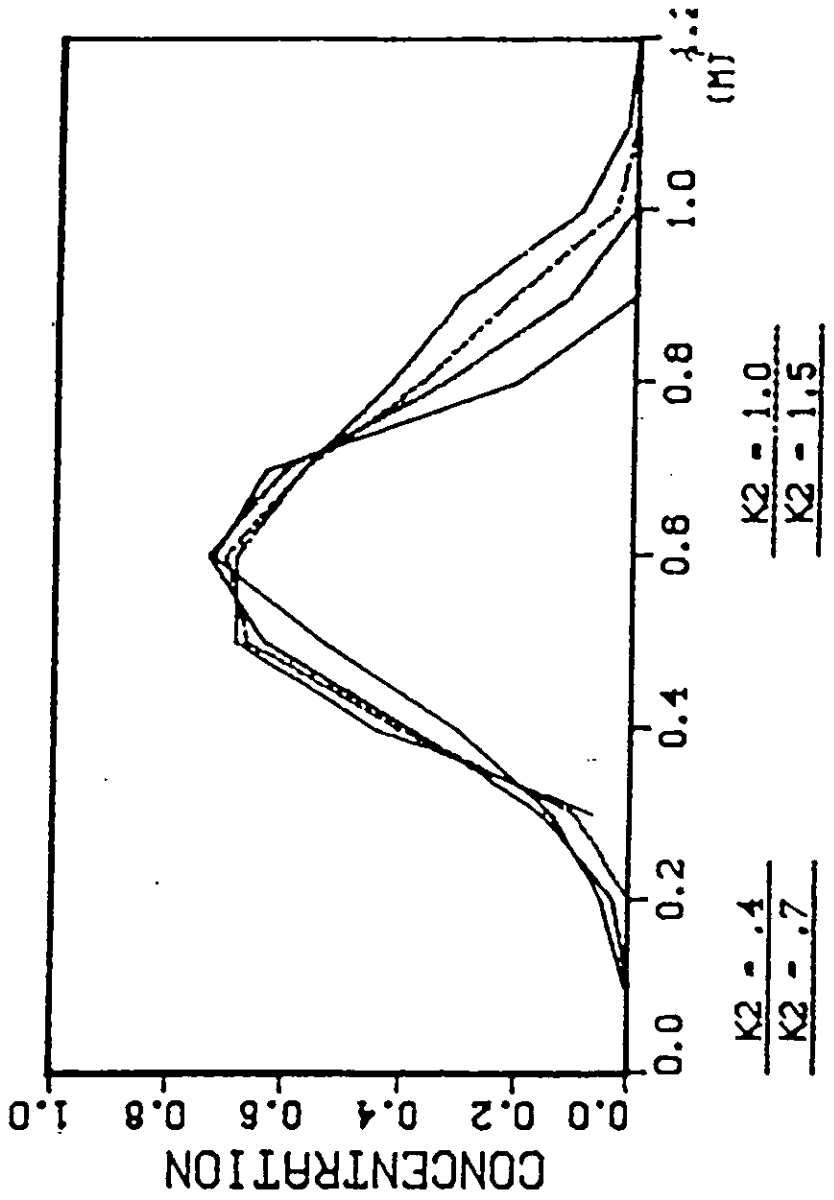

Figure B-4 Non-Linear Equilibrium Adosorption

B-2.2.3 Non-equilibrium Adsorption Tests

The test performed for non-equilibrium kinetic adsorption was taken from Van Genuchten et al., (1979). The analytical solution given there is for a linear adsorption isotherm and is expressed as follows:

$$\frac{C}{C_1} = \begin{cases} C_1(s,t) & 0 < t \leq t_o \\ C_1(s,t) - C_1(s,t-t_o) & t > t_o \end{cases} \qquad (36)$$

with:

$$C_1(s,t) = G(s,t)\exp(-rR_D t) + r_o \int^t G(s,\tau)[R_D I_o(\zeta) + R_D/(t-\tau) I_1(\zeta)] \exp[-r(R_D\tau + t-\tau)]d\tau \qquad (37)$$

$$G(s,t) = \frac{1}{2}\,\mathrm{erfc}\,\frac{s(1-t)^2}{4t} + \left(\frac{st}{\pi}\right)\exp\frac{-s(1-t)^2}{4t} - \frac{1}{2}(1 + s + st)e^s \mathrm{erfc}\,\frac{s(1+t)^2}{4t} \qquad (38)$$

$$\zeta = 2r\,R_D\tau\,(t-\tau); \qquad R_D = \frac{\rho b^k}{0}; \qquad r = \frac{k_r x}{v}$$

$$s = \frac{vx}{D}; \qquad t = \frac{vt}{x}; \qquad t_o = \frac{vt_o}{x}$$

where I_o and I_1 are modified Bessel functions of the first kind and of order 0 and 1, respectively.

Table B-5 gives the physical data used in the test. A Darcy flow rate was established at 5.9×10^{-7} m/sec again by using wells. The source concentration was maintained at 1.0 for 7.6 days. The concentration at L = 30 cm. was observed for a simulating period of 15 days.

Several runs were made using different values of the kinetic rate coefficient (k_r) and comparisons made with the analytic solution. Figure B-5 is a plot of the calculated concentration and the analytic solution for a rate coefficient of 2.91×10^{-6}/sec. Similar agreement was achieved with the different rate coefficients used.

Table B-5 Non-Equilibrium Adsorption Test

Soil Bulk Density	136 kg/m^3
Porosity	0.47
Diffusivity	9.7×10^{-9} m^2/sec
Freundlich coefficient	3.13×10^{-4} m^3/kg
Freundlich exponent	1.0

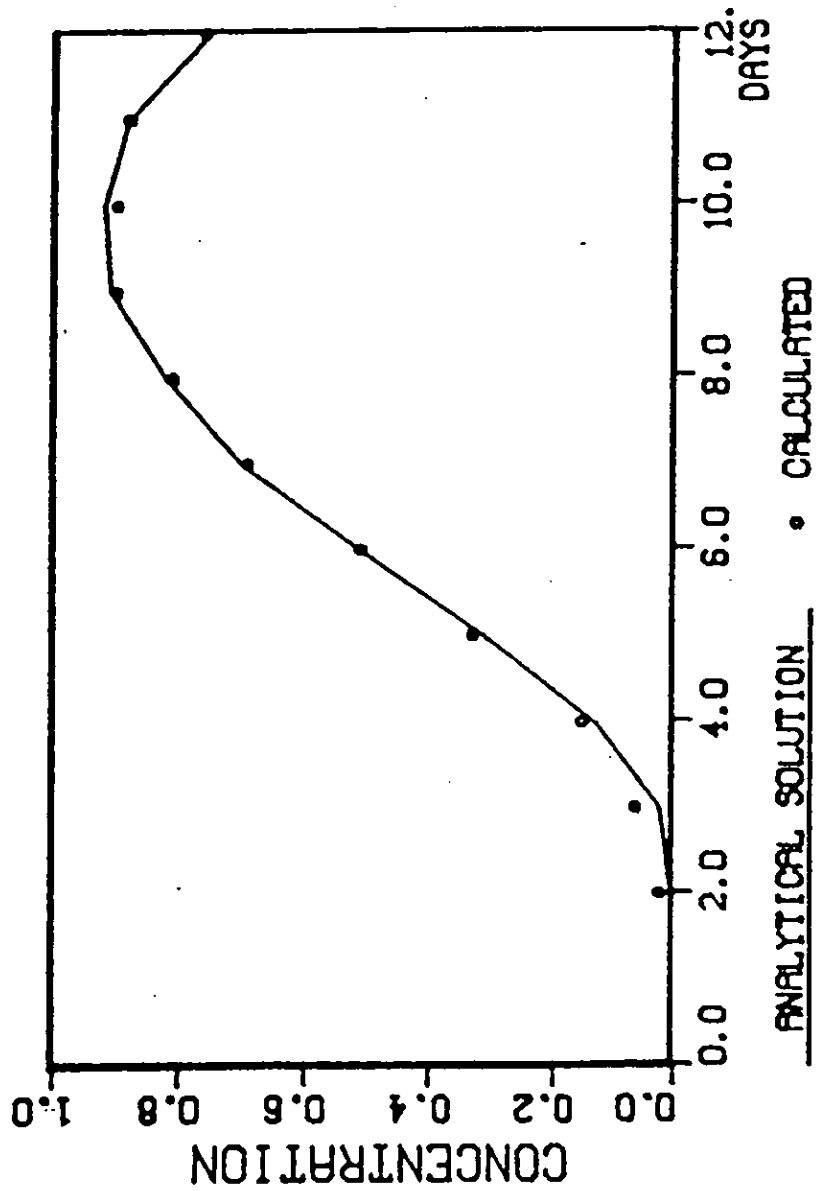

Figure B-5 Kinetic Adsorption Test

B-3 COMPUTER ASPECTS

B.3.1 Program Organization

The program is organized as a main routine which simply controls flow between various calculational subroutines. Many features are included to enhance program efficiency and user applicability. These include:

(a) Three-dimensional arrays are stored in singly subscripted arrays with subscripts computed at execution time.

(b) The dimensional common area is organized so that only one routine need be recompiled if dimensions are not sufficient for the problem to be solved.

(c) The user has the option of choosing a reduced bandwidth direct solution method, GAUS3D, or a line-successive, overrelaxation, iterative method, LSOR, in solving the finite-difference matrix equations.

(d) Visual aids of plots and contour maps of pressure and concentration are available as a user option.

B-3.2 Program Dimensions

All arrays that depend on problem size are stored in one large array, A, in blank common. Depending upon the specifications of a particular problem, e.g., grid dimensions, number of wells, number of boundary conditions, the position of each needed dimensional array within this overall array is computed in the main program. These individual array addresses are then passed to the various subroutines as arguments. The advantage is that only the main program needs to be recompiled in order to redimension for a particular problem.

The dimension of the array, A, may be determined as follows:

IG + IL for LSOR solution

IG + IA + ICfor direct solution

where

$IG = 7*NX + 3*NY + 2*NZ + 4*NX*NY + 21*NB + NX*NWMAX + 3*MAXRCH + 4*NRT + 7*MAXBC + 3*NMAX + 5$

$IL = 3*NB$

$IA = [NB(2NS + 1) + NS^2 + NS(2NS^2 + 1)/3]/2*1.02$ or $7*NB$, whichever is larger

$IC = 10(NB + NZ) + 6(NB/2 + 1)$

NX,NY,NZ = Number of grid blocks in the x, y, and z directions, respectively.

$NB = NX*NY*NZ$

NMAX = Maximum of NX, NY, or NZ

NS = Product of the two smaller dimensions

NWMAX = Maximum number of wells

MAXRCH = Maximum number of recharge blocks

NRT = Number of adsorbing regions

MAXBC = Maximum number of boundary condition blocks

B-3.3 Truncation Error as Relaced to Block Size and Time-Step-Restrictions

The contaminant transport equations which contain convective terms are largely responsible for numerical dispersion. The pressure or flow equation, since it does not contain a convective term, has truncation error which is much less significant.

Basically, the problem can be described as..

(1) A first order correct finite-difference approximation to the time or convective (first order) space derivative results in second order truncation error which is virtually identical to the physical dispersion.

(2) A second order correct finite-difference approximation eliminates the term identical to physical dispersion, but introduces a time step and block size restriction for obtaining valid results, i.e., results which are free of over/undershoot.

In HCTM, the user has the option to choose from among several forms of the finite-difference approximation to the transport equation. These are:

(1) Backward-in-space, backward-in-time
(2) Backward-in-space, central-in-time
(3) Central-in-space, backward-in-time
(4) Central-in-space, central-in-time

Table B-6 summarizes the stability considerations and numerical diffusivity introduced by these various forms. Equivalent truncation error forms or stability criteria can be derived for a radial system by substituting in the Table

$$v = b/2\pi r\Delta z$$

and

$$\Delta x = \Delta r = \frac{1}{r}\,\Delta 1nr$$

Table B-6 Summary of Numerical Diffusion and Stability

Difference Term		Numerical	Stability
Spatial	Time	Diffusivity	Criteria
BIS	BIT	$\frac{v\Delta x}{2} + \frac{v^2\Delta t}{2}$	None
CIS	BIT	$\frac{v^2\Delta t}{2}$	$\frac{v\Delta x}{2} \leq E$
BIS	CIT	$\frac{v\Delta x}{2}$	$\frac{v\Delta t}{2\Phi\Delta x} \leq 1$
CIS	CIT	None	$\frac{v\Delta t}{2\Phi\Delta x} \leq 1$

B-4 USER OPTIONS

B-4.1 Equations and Numerical Considerations

B-4.1.1 Equations

The model contains two basic partial differential equations, one for conservation of total fluid mass and the other for conservation of contaminant mass. As described in Section B.1, the general forms of the equations are transient. For the sake of efficiency, a user option has been provided to solve the equations in the following 4 modes:

(1) steady-state solution of the flow equation, no contaminant transport
(2) transient solution of the flow equation, no contaminant transport
(3) steady-state flow solution with contaminant transport
(4) transient solution of the flow and contaminant transport equation

Under the first two options, the concentration equation is not solved. Under the third and fourth options, transient solution of the concentration equation is obtained.

B-4.1.2 Confined/Unconfined Aquifers

The model can be used for a confined as well as an unconfined aquifer system. The form of flow equation given by Equation (7) is applicable to both confined and unconfined systems. However, the storage coefficient being related to the rock and fluid and rock compressibilities, as shown in Equation (6), is correct only for confined systems. For unconfined aquifers, the storage coefficient is porosity divided by aquifer thickness (ϕ/b). The accumulation term is still

$$s\frac{\partial \phi}{\partial t}$$

In an unconfined aquifer, as the water level changes, horizontal aquifer transmissivity also changes. This change is taken into account when the unconfined aquifer option is selected.

B-4.1.3 Method of Solution for the Contaminant Transport Equation

The model includes a user option to solve the concentration equation by a finite-difference method or by a point tracking (method of characteristics) method. For a non-retarded and non-decaying contaminant (inert), the characteristics equations are given in Section B.1.3. For linear adsorption isotherms (constant retardation factor), the characteristics equations remain virtually the same; the only difference being that the velocities are retarded by the retardation factor. The dispersion part of the equation is solved by finite-difference. The decay or the reaction term could be included in the finite-difference equation but it would control time step selection or introduce numerical truncation error. Therefore, the decay portion is superimposed analytically during convection. This method should be used whenever the numerical criteria for finite-difference becomes restrictive.

The finite-difference method can introduce numerical truncation error or show overshoot/undershoot in the results if both time steps and block sizes are not controlled, as described in Section B.3.3. Theoretically, method of characteristics does not introduce any truncation error and has no time step, block size restrictions. It is recommended to choose the size of a time step that particle movement is restricted to between one-half and one block per time step.

B-4.1.4 Solution Techniques

There are two methods provided to solve the finite-difference equations. Each involves solving a number of algebraic equations simultaneously, where the number of equations equals the number of grid blocks. For a typical problem, it is of the order of a few hundred. The two methods included in the model are:

(1) Direct-alternating diagonal direction Gaussian elimination (ADGAUSS) method

(2) Iterative-line successive overrelaxation (LSOR) method

The direct method included here is the reduced band width method of Price and Coats (1973). This method is considerably more efficient relative to computing time and storage requirements as compared to a non-ordered matrix inversion. In the same paper, Price and Coats presented a comparison of work requirements for ADGAUSS and LSOR for parabolic equations similar to the ones solved in this model. Their conclusion was that for nominal band widths of 40, the ADGAUSS method requires the same amount of computing time as the LSOR method with 44 iterations. Up to band widths of roughly 80, they found ADGAUSS to be quite competitive.

In the direct solution option, the model includes an optimum ordering scheme of the alternating diagonal type. This ordering routine is called only once when the direct method is selected. In the LSOR method, the rate of convergence can be enhanced by selecting the acceleration or overrelaxation parameter properly. The model includes a scheme to calculate the optimum parameter. The acceleration parameter is calculated at the first time step and every time the time step changes by a factor of two or more from the time step at which the previous value of the parameter was calculated.

The iterative method should be selected whenever core storage is a consideration. We have found that the LSOR method does not always converge. For computationally difficult problems, such as large contrasts in transmissibility, poor convergence of the LSOR method may necessitate use of the direct method.

B-4.1.5 Finite-Difference Approximations

As discussed in Section B.3.3, approximating the convective term in the contaminant transport equation can introduce numerical truncation error which is virtually identical to the physical dispersion (numerical dispersion). The flow equation does not contain a first-order spatial derivative term and,

therefore, has relatively insignificant truncation error. Second order truncation error (numerical dispersion) in the concentration equation can be eliminated by using central-difference approximations in space and time. A user option has been provided to select central or backward-difference approximations in space and time.

B-4.2 Geometry

B-4.2.1 Coordinate System

The model user is provided with options to run the model in one, two, or three-dimensional cartesian coordinate system or in one or two-dimensional axi-symmetric cylindrical coordinate system. For cartesian systems, the x-direction must always be used. For one-dimensional problems, the single direction must be the x-direction. Two-dimensional problems can be x-y (areal) or x-z (vertical). The axi-symmetric problems can be described by a single layer (r-direction only) or by a multi-layer system (r-z).

B-4.2.2 Block Sizes

The model provides for use of variable size blocks in any one of 3 dimensions. There are no model restrictions as to the variability in block sizes. However, using variable block sizes can introduce slight truncation error at the blocks where the sizes change. A good rule of thumb is to try to keep the ratio of adjacent blocks within a factor of 2.

In addition to the above, two options are included to vary the block thickness on a block-by-block basis. The first option is for problems where the blocks in the uppermost and the lowermost layers can be adjusted to model structural variations. This option should be used carefully. Individual blocks in the intermediate layers should not be varied as this could lead to a physically unrealistic description. The second option is for one and two-dimensional areal problems (single layer) where the thickness of the single layer can be adjusted from block to block.

B-4.2.3 Structure

The aquifer structure can be described in one of three different ways. These are as follows:

(1) A uniform, strictly horizontal structure
(2) A uniform, inclined structure with a constant dip angle
(3) Enter vertical variability on each vertical column by column basis (each areal block)

B-4.3 Heterogeneities

B-4.3.1 Retardation Parameters

Rock types are used to describe heterogeneities in sorption or retardation parameters. There is no restriction to the number of rock types.

B-4.3.2 Transport Properties

Heterogeneities in permeability values and porosity can be described on a regional basis. A region could be as small as a single block. Fluid flow transmissibilities, as given by Equation (20), correspond to block edges. These edge transmissibilities can be modified independently. An application of this option may be the description of a fault.

B-4.4 Initial and Boundary Conditions

B-4.4.1 Initial Conditions

For the flow equation, initially the system is assumed to be in hydrostatic equilibrium. This means that the potentials are constant everywhere in the system. For steady-state flow problems, initial potential is of no real significance.

For the concentration equation, the user may initialize concentrations on a regional or block-by-block basis.

B-4.4.2 Injection/Withdrawal Wells

The wells can be used not only to describe real wells but also other types of source and sink terms. The wells may be an injection, withdrawal or observation well. An observation well is described by entering a zero withdrawal rate. For injection wells, a specified concentration fluid is injected, and, for production wells, the concentration of the produced fluid is the grid block concentration. Generally, the fluid rate would be a user-specified rate. To make the model more useable, however, an option has been included to specify bottom-hole potential conditions. A simplified wellbore model is used to calculate the pressure drop between the wellbore and the center of the numerical grid block in which the well is located.

Pressure drop between the grid block and the wellbore is important in using the model to obtain bottom-hole potential (or water level). Often, it is impractical to refine the grid to the extent necessary to make this pressure drop negligible. In this model, we have used the concept of adding on the steady-state radial flow pressure drop from the average block pressure down to the wellbore pressure. This expression takes the form of

$$q = WI \, \Delta \, \Phi$$

where WI is well index. In radial coordinates, the well index can be approximated by

$$WI = \frac{2 \, K \, \Delta z_k}{\ln (r_i / r_w)}$$

and in Cartesian coordinates by

$$WI = 2\pi K \; z_k \left(\frac{\bar{r}-r_w}{r_w}\right) \left[\frac{1}{1-\frac{\bar{r}}{r_w}\left(1-\ln\frac{\bar{r}}{r_w}\right)}\right]$$

$$\text{with } \bar{r} = \frac{\Delta x_i \Delta y_j}{\pi}$$

There are two well specification options provided in the model. Under the first option, the total well rate is specified and, for a multi-layer completion, it is allocated between different layers based upon permeability x thickness values of different layers. The specified well potential is not used. Under the second option, a rate and a wellbore potential are specified. Using the well index, a rate is calculated that corresponds to the specified potential. The lower of the specified and calculated rates is then used.

The well data is part of the recurrent data and any portion, or all, of it can be changed as the simulation progresses.

B-4.4.3 Constant Potential, Concentration Boundaries

Constant potential and concentration values can be specified along the edges of certain blocks. These values may vary spatially but cannot be changed with time.

B-4.4.4 Vertical Recharge

The model provides an option to include vertical recharge of fluid into the aquifer at specified concentration values.

B-4.5 Simulation Restart

The program includes an optional restart feature which, for long operational runs, should reduce the total computing time and expense. By retaining intermediate results and data from the computer core, a problem may be interrupted and restarted at specified convenient times in the simulation run. Thus a long simulation may be divided into several shorter runs. Such a procedure reduces the risk of not being able to use a complete run because of data errors over a small portion of the run. Also, this option does not require repeating calculations for the common history period for several prediction runs.

B-4.6 Printer Outputs

B-4.6.1 Tables of Values

The amount of output generated can be controlled by the user. This applies to material balance summaries, well summaries, transmissibilities, velocities, and grid block values of potentials and concentration. These options can be summarized as follows:

(1) Material balance summary printout can be completely suppressed, printed at selected time intervals, or printed at every time step.
(2) Well summary printout can be completely suppressed, printed at selected time intervals, or printed at every time step.
(3) For the grid block potentials, pressures, and flow transmissibilities, the available options are:

    (a) suppress all print out
    (b) print initial potentials only
    (c) print flow transmissibilities and initial potentials only
    (d) print potentials at selected time intervals only or with options (b) or (c)
    (e) print fluid potentials and pressures at selected time intervals only, or with options (b) or (c)

(f) print potentials at every time step only or with options (b) or (c)

(g) print potentials and pressures at every time step only or with options (b) or (c)

(4) Dispersion (including diffusion) transmissibilities printout can be suppressed or printed at selected time intervals.

(5) Grid block concentrations printout can be suppressed, printed at selected time intervals, or printed at every time step.

(6) Darcy velocities printout can be suppressed or printed at selected time intervals.

B-4.6.2 Contour Maps

At times, numerical model results can be made more comprehensible by generating contour maps of potential and/or concentration. These maps can be generated at selected time intervals during the simulation. Since the model employs both cartesian and cylindrical coordinates, cross-sections of horizontal or vertical planes can be obtained.

The mapping program prints a contour diagram of the dependent variable, Φ or C, and twenty contour intervals are described with different characters. The specific character to be mapped at each point is evaluated by bilinear interpolation between the four nearest grid point values.

Arbitrary dimensions of the map width and scale can be chosen. Often, it is convenient to map areal planes to scale, e.g., 1 inch = 100 m in each direction. However, cross-sectional planes generally are better displayed by a distorted scale, e.g., 1 inch = 20 m vertical versus 1 inch = 100 m in the horizontal. If dimensions larger than a single page width or length are chosen, multiple printer pages are used.

B-4.6.3 Time Plots

This portion of the model enables the user to plot (1) calculated potential and concentration versus time for any specified well or (2) plot comparative values of observed pressure or concentration with calculated values of the same variable as a function of time. This feature is especially useful for well test or tracer test analysis.

The plotting program presents basically an x, y plot with the exception that two ordinates (observed and calculated dependent variables) are plotted versus the abscissa value (time). Two different characters are used to identify the two different ordinate values with a third character specifying coincident values. Variable spacing along the time axis is used in the plot.